SERUM MARKERS OF ATHEROGENESIS

IN

APOE*3 LEIDEN MICE

NUALA MURPHY

DOCTOR OF PHILOSOPHY

DEPARTMENT OF BIOCHEMISTRY AND MOLECULAR BIOLOGY
ROYAL FREE AND UNIVERSITY COLLEGE MEDICAL SCHOOL
ROYAL FREE CAMPUS
ROWLAND HILL STREET
LONDON NW3 2PF

SEPTEMBER 2001

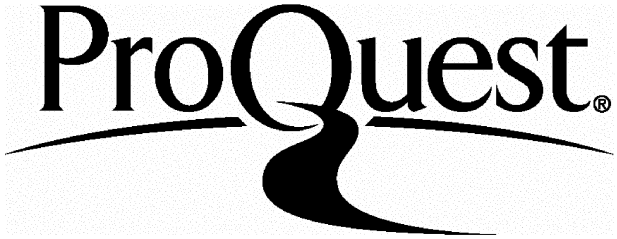

Abstract

Atherosclerosis is a major cause of morbidity and mortality in Westernised societies. Unfortunately, the disease remains largely silent until clinical symptoms ensue. Secreted chemokines and shed forms of adhesion molecules are found in the circulation, and it was hypothesized that systemic levels of these molecules could prove useful 'markers' of the monocyte recruitment that characterises atheroma development.

Serum concentrations of CC (JE/Monocyte Chemotactic Protein-1 [MCP-1]) and CXC (KC, Macrophage Inflammatory Protein-2 [MIP-2]) chemokines, and/or soluble adhesion molecules, Vascular Cell Adhesion Molecule-1 [VCAM-1] and Intercellular Adhesion Molecule-1 [ICAM-1], were measured during development of atherosclerosis in apoE*3 Leiden mice and their non-transgenic littermates, fed diets high in fat and cholesterol containing sodium cholate (HFC/C), deficient (HFC/LAO) or supplemented with (HFC/HAO) antioxidant vitamins.

ApoE*3 Leiden mice developed marked hypercholesterolaemia and lesions that progressed from early Type I 'fatty streaks' to more complex fibrous plaques; by contrast, their non-transgenic littermates (C57BL/6J) exhibited a much less pronounced hypercholesterolaemia, and developed small fatty streak lesions, after consuming the same HFC/C diet. Interestingly, antioxidant vitamins signally failed to reduce atheroma development in either apoE*3 Leiden or non-transgenic mice fed HFC/HAO compared with HFC/LAO.

Rapid increases in serum concentrations of KC appeared to be associated with early development of atheroma in apoE*3 Leiden mice fed diet HFC/C, compared with their non-transgenic littermates. By contrast, circulating levels of JE/MCP-1 were elevated to a similar degree in both groups of mice consuming the HFC/C diet, and coincided with development of hypercholesterolaemia. However, systemic JE and KC levels were unaffected by consumption of either HFC/HAO or HFC/LAO forms of this diet.

Circulating levels of sICAM-1 were elevated in both apoE*3 Leiden mice, and the non-transgenic controls consuming HFC/C diet. Systemic levels of these molecules were sensitive to the presence of dietary antioxidants, with high levels of sVCAM-1 and sICAM-1 noted in non-transgenic mice consuming the HFC/LAO diet.

Hepatic expression of JE and KC mRNA were detected by *in-situ* hybridisation in both groups of animals fed HFC/C diet. Aortic expression of JE mRNA, but not KC, mRNA was seen within macrophage-rich atherosclerotic lesions in apoE*3 Leiden mice. However, RT-PCR detected the presence of both JE and KC mRNA in aortic and hepatic tissues.

In summary, it is clear that the systemic markers investigated in this thesis were not specific to atheroma and did not provide greater predictive value, in terms of lesion progression, than measurement of more established 'risk factors' such as serum cholesterol. The results suggest that multiple inflammatory sites may be involved in their production, consequent to the atherogenic diet and the development of gross hyperlipidaemia. Indeed, the atherogenic diet used may have masked any subtle differences in systemic chemokine and adhesion molecule concentrations that were caused directly by the atherosclerotic lesions.

Acknowledgements

I would especially like to thank my PhD supervisor, Dr Annette Graham, for her constant guidance, support and encouragement throughout this project. The present state of this thesis owes much to her incredible generosity with time and patience. I would also like to thank Prof. Richard Bruckdorfer and my industrial supervisors, Dr Martin Benson and Dr Pieter Groot.

I am grateful for the help of my colleagues in the Dept. Biochemistry & Molecular Biology (Royal Free & University College Medical School) and the Dept. Vascular Biology (GlaxoSmithKline). A special thank-you goes to Dr Alex Robertson, Dr Sylvia Low, Dr Anna Palmer, Philip Overend, David Grimsditch and Martin Vidgeon-Hart.

Finally, I am indebted to both the BBSRC and GlaxoSmithKline for their generous financial support of this studentship.

Abbreviations

-/-	Homozygous knockout
ACAT	AcylCoA: Cholesterol Acyltransferase
ANOVA	Analysis of Variance
Apo	Apolipoprotein
APP	Acute Phase Protein(s)
APR	Acute Phase Response
APRF	Acute Phase Response Factors
ATBC	Alpha-Tocopherol, Beta-Carotene Cancer Prevention Study
bp	base pair
BSA	Bovine Serum Albumin
CAD	Coronary Artery Disease
CAM	Cell Adhesion Molecule
CC	β-Chemokines
CCR	CC-Chemokine Receptor
CD	Cluster of Differentiation antigen/Cluster Designation
CE	Cholesteryl Ester
CETP	Cholesteryl Ester Transfer Protein
CHAOS	Cambridge Heart Antioxidant Study
CHD	Coronary Heart Disease
CRP	C-Reactive Protein
C_t	Threshold cycle
CTAP 111	Connective Tissue Activating Peptide 111
CVD	Coronary Vascular Disease
CXC	α-Chemokines
CXCR	CXC-Chemokine Receptor
DAB	3,3'-Diaminobenzidine
DAG	Diacylglycerol
DARC	Duffy Antigen Receptor Complex
DEPC	Diethylpyrocarbonate
DMEM	Dulbecco's Modified Eagle Medium
dNTPs	Deoxynucleotide Triphosphates
DTT	Dithiothreitol
EDTA	Ethylenediaminetetraacetic Acid
ELAM	Endothelial Leukocyte Adhesion Molecule-1/ E-selectin/CD62E
ELISA	Enzyme-Linked Immunoabsorbent Assay
ELR	Glutamate-Leucine-Arginine
ENA-78	Endothelial Cell Derived Neutrophil Activating Peptide-78
FAM	6-carboxyl-fluorescein
FC	Free Cholesterol
FD	Familial Dysbetalipoproteinaemia

FPLC	Fast Performance Liquid Chromatography
GCP-2	Granulocyte Chemotactic Protein-2
GDP	Guanosine Diphosphate
GISSI	Gruppo Italiano per lo Studio della Sopravvivenza nell'Infarto Miocardico
GPI	Glycophosphatidylinositol
GRO-α	Growth Related Oncogene-α/ murine KC
GRO-β	Growth Related Oncogene-β/ murine MIP-2α
GRO-γ	Growth Related Oncogene-γ/ murine MIP-2β
GSK	GlaxoSmithKline
GTP	Guanosine Triphosphate
h	hour(s)
HBSS	Hanks Balanced Salt Solution
HDL	High Density Lipoprotein
HFC/C	High Fat/High Cholesterol/Sodium Cholate Diet
H_2O_2	Hydrogen Peroxide
HOPE	Heart Outcomes Prevention Evaluation Study
Hp	Haptoglobin
HPETE	Hydroperoxyeicosatetraenoic acid
HMG-CoA	3-Hydroxy-3-Methylglutaryl Coenzyme A
ICAM-1	Intercellular Adhesion Molecule-1, CD54
IDL	Intermediate Density Lipoprotein
IHC	Immunohistochemistry
IκB	Inhibitor of NF-κB
IgSF	Immunoglobulin Gene SuperFamily
IKK	IκB Kinase
IPTG	Isopropyl-thiogalactoside
IL-1α	Interleukin-1α
IL-1β	Interleukin-1β
IL-4	Interleukin-4
IL-8	Interleukin-8
IP_3	Inositol 1,4,5-triphosphate
IP-10	Interferon-Inducible Protein of 10kd
JE	Murine homologue of MCP-1
kb	kilobase
KC	Murine Ligand for the IL-8RH
LB	Luria-Bertani
LB_{AMP}	Luria-Bertani agar or broth containing ampicillin (50 μg/ml)
LCAT	Lecithin: Cholesterol Acyltransferase
LDL	Low-Density Lipoprotein
LDLR	Low-Density Lipoprotein Receptor
LFA-1	Leukocyte Function Associated molecule-1, CD11a/CD18, αLβ2
LFC	Low Fat/Cholesterol diet

Lp(a)	Lipoprotein(a)
LPS	Bacterial endotoxin / Lipopolysaccharide
LOX-1	Endothelial oxidised LDL receptor
LRP	LDL receptor Related Protein
Mac-1	CD11b/CD18, $\alpha_M\beta_2$
MCP-1/2/3/4	Monocyte Chemotactic Protein-1/2/3/4
M-CSF	Macrophage Colony Stimulating Factor
MIG	Monokine Induced by Interferon-γ
mIL-8RH	Murine homologue CXCR2
min	minute(s)
MIP-1α	Macrophage Inflammatory Protein-1α
MIP-1β	Macrophage Inflammatory Protein-1β
MIP-2	Macrophage Inflammatory Protein-2, Murine Ligand for mIL-8RH
mmLDL	minimally modified LDL
MONICA	MONItoring trends and determinants of CArdiovascular disease
mRNA	Messenger Ribonucleic Acid
NAP-2	Neutrophil Activating Peptide-2
NHANES	First National Health and Nutrition Examination Survey
NIK	NF-κB Inducing Kinase
NK	Nuclear Factor
NF-κB	Nuclear Factor-Kappa B
NTG	Non-Transgenic
ORO	Oil-Red-O
oxLDL	Highly oxidised LDL
PAF-AH	Platelet Activating Factor-Acetyl Hydrolase
PBP	Platelet Basic Protein
PBS	Phosphate Buffered Saline
PCR	Polymerase chain reaction
PECAM	Platelet Endothelial Cell Adhesion Molecule-1
PEIPC	1-Palmitoyl-2(5,6-EpoxyisoprostaneE_2)-*sn*-Glycero-3-Phosphorylcholine
PF-4	Platelet Factor-4
PGPC	1-Palmitoyl-2-Glutaroyl-*sn*-Glycero-3-Phosphorylcholine
PIP_2	Phosphatidyl Inositol 4,5 Bisphosphate
PKC	Protein Kinase C
PNPP	disodium P-NitroPhenyl Phosphate
PON1	Paraoxonase 1
POVPC	1-Palmitoyl-2(5-Oxovaleroyl)-*sn*-Glycero-3-Phosphorylcholine
P-selectin	PADGEM, CD62P
PSGL-1	P-Selectin Glycoprotein Ligand-1
PTCA	Percutaneous Transluminal Coronary Angioplasty
RANTES	Regulated on Activation Normal T-cell Expressed and Secreted
RT	Room Temperature

s	second
SAA	Serum Amyloid A
SAP	Serum Amyloid P
SCR	Short Consensus Repeat domains
SSC	Sodium chloride/Sodium citrate
sICAM-1	Soluble ICAM-1
sVCAM-1	Soluble VCAM-1
SDF-1	Stromal Cell-Derived Factor-1
SPACE	Secondary Prevention with Antioxidants of Cardiovascular Disease in Endstage Renal Disease
SRA	Scavenger Receptor A
SR-AI/II	Scavenger Receptor-AI/II
SR-B1	Scavenger Receptor-B1
SSC	Saline Sodium Citrate
TAE	Tris/Acetate buffer
TAMRA	6-carboxyl-tetramethyl-rhodamine
Taq	*Thermus aquaticus*
TBST	Tris-buffered saline/Tween
β-TG	β-Thromboglobulin
t.l.c	thin layer chromatography
TMB	3,3', 5,5'-tetramethylbenzidine
TNF-α	Tumour Necrosis Factor-α
TRL	Triglyceride Rich Lipoproteins
VCAM-1	Vascular Cell Adhesion Molecule-1, CD106
VLA-4	Very Late Antigen-4, CD49/CD29, $\alpha_4\beta_1$
VLDL	Very Low Density Lipoprotein
X-gal	5-bromo-4-chloro-3-indolyl-B-D-galactopyranoside

Table of Contents

List of Figures

List of Tables

Chapter 1

Introduction

1 Introduction

1.1 Atherosclerosis

Atherosclerosis is the main cause of coronary heart disease (CHD), cerebral ischaemia and gangrene of the lower extremities [1]. It is presently the leading cause of morbidity and mortality in Western society and contributes globally to a third of all mortalities (www.who.ch). The disease develops progressively over a period of years, and involves the formation of increasingly complex vascular lesions, which protrude into the lumen of the artery and impede blood flow [1]. Plaque rupture can result by occlusive thrombosis and as a consequence the clinical symptoms of angina, myocardial infarction or stroke ensue. Unfortunately, the disease advances silently until a late stage of progression, making early diagnosis and treatment difficult. The search for an early and reliable indicator of atherosclerosis is ongoing and provides the rationale for the work contained in this thesis.

1.1.1 Risk factors for atherosclerosis

Many risk factors for atherosclerosis have been identified by epidemiological studies. These can be grouped under two sub-headings: factors with a genetic component, and those that are largely environmental [1]. Risk factors containing a strong genetic component include hyperlipidaemia, hypertension, diabetes, obesity, elevated levels of lipoprotein(a) (Lp(a)) and male gender [1]. Environmental factors may include diet, cigarette smoking, lack of physical exercise and possibly exposure to infectious microorganisms such as *Chlamydia pneumoniae* [1].

1.1.2 Hyperlipidaemia, a major risk factor for atherosclerosis

Studies have shown that raised plasma low-density lipoprotein (LDL) cholesterol is a significant risk factor for the development of atherosclerosis [2]. Population, migration and epidemiological studies have all indicated a strong association between eating a 'Western diet' (a high fat, high cholesterol diet) and the development of atherosclerosis [1]. Indeed, similar diets are usually required in experimental animals to induce the development of atherosclerosis [3-6].

Hyper or dyslipidaemia refers to a derangement in plasma lipid profiles, such as hypercholesterolaemia and/or hypertriglyceridaemia, that predisposes individuals to atherosclerosis. The relative abundance of particular 'atherogenic' lipoproteins in the plasma appears to be a significant risk factor in the development of atherosclerosis. In particular, elevated levels of apolipoprotein B (apoB) containing lipoproteins, such as

LDL, very low-density lipoproteins (VLDL) and chylomicron remnants are associated with an increased incidence of CHD [2]. To understand the significance of hyperlipidaemia it is necessary to look briefly at lipid transport mechanisms.

1.1.2.1 Lipoproteins

Blood lipids, due to their insolubility in water, are carried in specialised structures known as lipoproteins. These typically consist of a highly hydrophobic core of triglyceride and cholesteryl ester, with a hydrophilic outer surface monolayer of phospholipid and free cholesterol. Associated with each particle are one or more proteins termed apolipoproteins (apo). These proteins have hydrophobic domains, which anchor the protein to the particle, and hydrophilic domains, which are exposed on the surface. Some of the apolipoproteins have a largely structural role within lipoproteins while others direct the metabolism and clearance of lipoproteins within the circulation [7].

Lipoproteins are divided into several classes that can be distinguished by composition, size and density. These are chylomicrons, VLDL, intermediate density lipoproteins (IDL), LDL and high-density lipoproteins (HDL). Lipoprotein fractions can be separated by ultracentrifugation on the basis of their density and flotation values, by electrophoresis on the basis of their mobility in an electric current, and by column chromatography (Section 2.3.3) on the basis of their size. The characteristics of the major lipoprotein fractions are listed in Table 1-1. Each class has a specific role in the transport of lipid, but all act in a concerted manner to control lipid flux throughout the body [7]. In addition, enzymes are found associated with lipoproteins. For example, lecithin: cholesterol acyltransferase (LCAT), an enzyme that esterifies free cholesterol is located on HDL as well as paraoxonase (PON1), which has a less, defined physiological role (Section 1.9.5).

The transport of lipids around the body can be divided into three major pathways: the exogeneous pathway, the endogenous pathway and the reverse cholesterol transport pathway. The exogenous pathway (Figure 1-1) is associated with the transport of dietary lipids in the form of chylomicrons (Section 1.1.2.1.1), from the intestine to other tissues. In contrast, the endogenous pathway (Figure 1-2) distributes lipids of hepatic origin as VLDL (Section 1.1.2.1.2). The reverse cholesterol transport pathway (Figure 1-3) is involved in the transport of cholesterol from peripheral tissues to the liver (Section 1.1.2.1.6).

The realisation of the importance of lipoproteins with regard to atherosclerosis began with the observation that elevated LDL cholesterol levels are characterised by an increased incidence of atherosclerosis and its clinical consequences [8]. In contrast, elevated HDL levels are associated with a decreased risk of atherosclerosis and CHD [9]. Furthermore, individuals with elevated postprandial triglyceridaemia, a condition characterised by elevated levels of triglyceride rich lipoproteins (TRL) such as chylomicrons and their remnants, also have increased risk of CHD [10].

Lipoprotein	Main source	Main apolipoproteins	Density range g/ml	Electrophoretic mobility
Chylomicron	Small intestine	B-48, A-I, E, C	<0.950	Origin
VLDL	Liver + intestine	B-100, E, A-I, C	0.950-1.006	Pre-β
LDL	In the circulation from IDL	B-100	1.019-1.063	β
HDL	Liver + intestine	A-I, A-II	1.063-1.21	α

Table 1-1 Characteristics of the major lipoprotein classes.
Adapted from [7,11]

1.1.2.1.1 Chylomicrons

Dietary triglycerides and cholesterol are absorbed and re-esterified by enterocytes in the intestinal wall and secreted as chylomicron particles [10]. Chylomicrons consist of a core of triglyceride and cholesteryl ester, with a surface of free cholesterol and phospholipids, and the apolipoproteins, apoB-48 and apoA-I [7]. The newly secreted or nascent chylomicrons reach the plasma via the lymphatic system and acquire apoC-II and apoE from HDL [10].

In the circulation, chylomicrons are hydrolysed by lipoprotein lipase, perhaps the most important enzyme in triglyceride metabolism [11]. Lipoprotein lipase is found bound to proteoglycans on the surface of capillary endothelial cells of adipose tissue, cardiac and skeletal muscle [10]. The lipolysis of the chylomicron particle by lipoprotein lipase is dependent on the presence of apoC-II [10]. As the triglyceride is hydrolysed, the particle shrinks and becomes known as the chylomicron remnant. During this process the chylomicron loses its A- and C- apolipoproteins, which are transferred to HDL together with excess phospholipid and free cholesterol [10]. The chylomicron is now

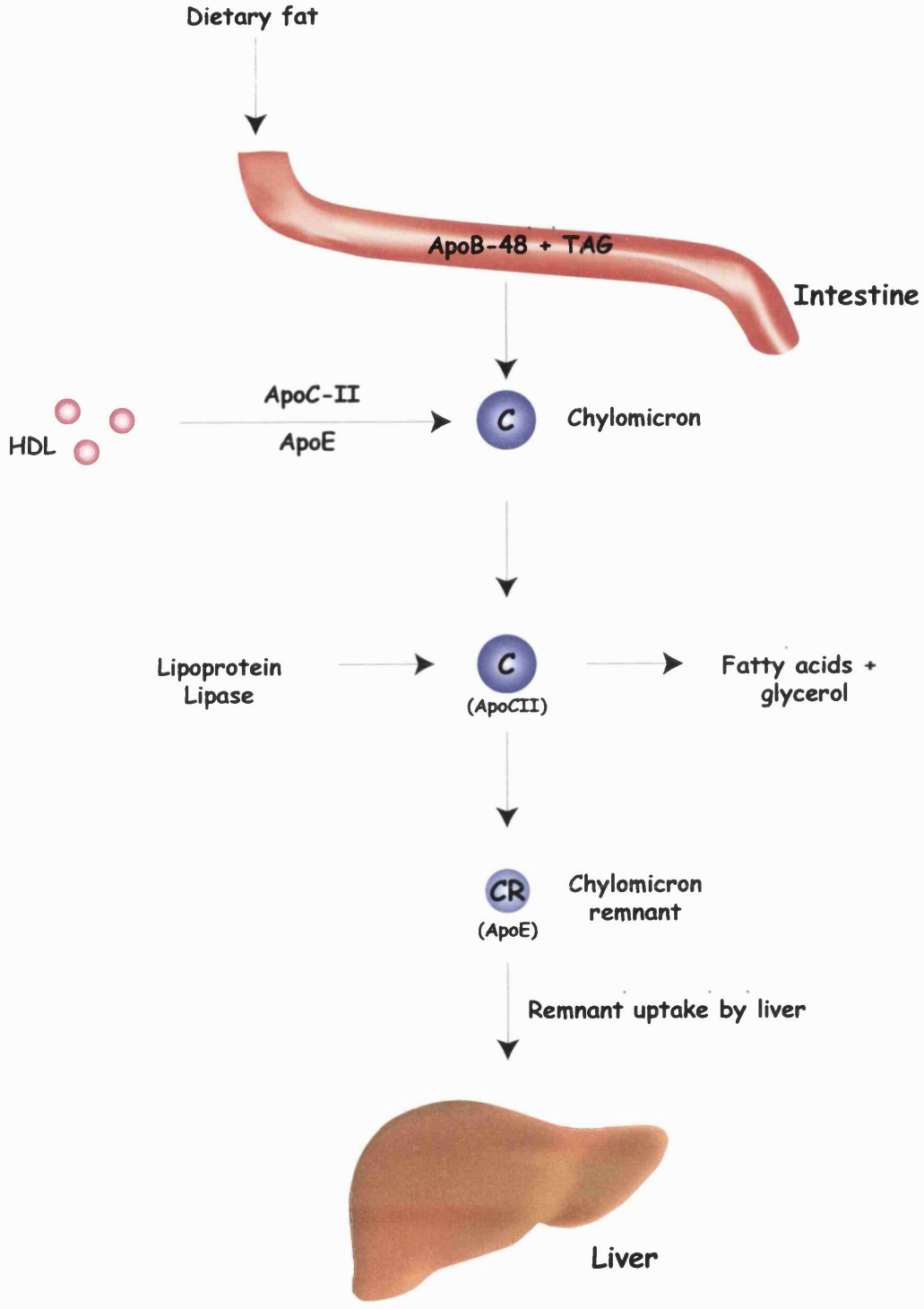

Figure 1-1 Overview of the exogenous lipoprotein pathway

Chylomicrons are synthesised in intestinal epithelial cells, secreted into the lymph and pass into the blood. Once in the bloodstream, chylomicrons undergo metabolism. Their function is to deliver dietary triacylglycerol to peripheral tissues, like adipose tissue and skeletal muscle (not shown). Nascent chylomicrons pick up apoE and apoC-II from HDL. The triacylglycerol core of the chylomicron is hydrolysed to fatty acids and glycerol by the action of lipoprotein lipase. This causes the chylomicron particle to become much smaller until it is termed a chylomicron remnant. It is then recognised by means of apoE, via members of the LDL receptor family such as the LDL receptor related protein (LRP) or the LDL receptor (LDLR).

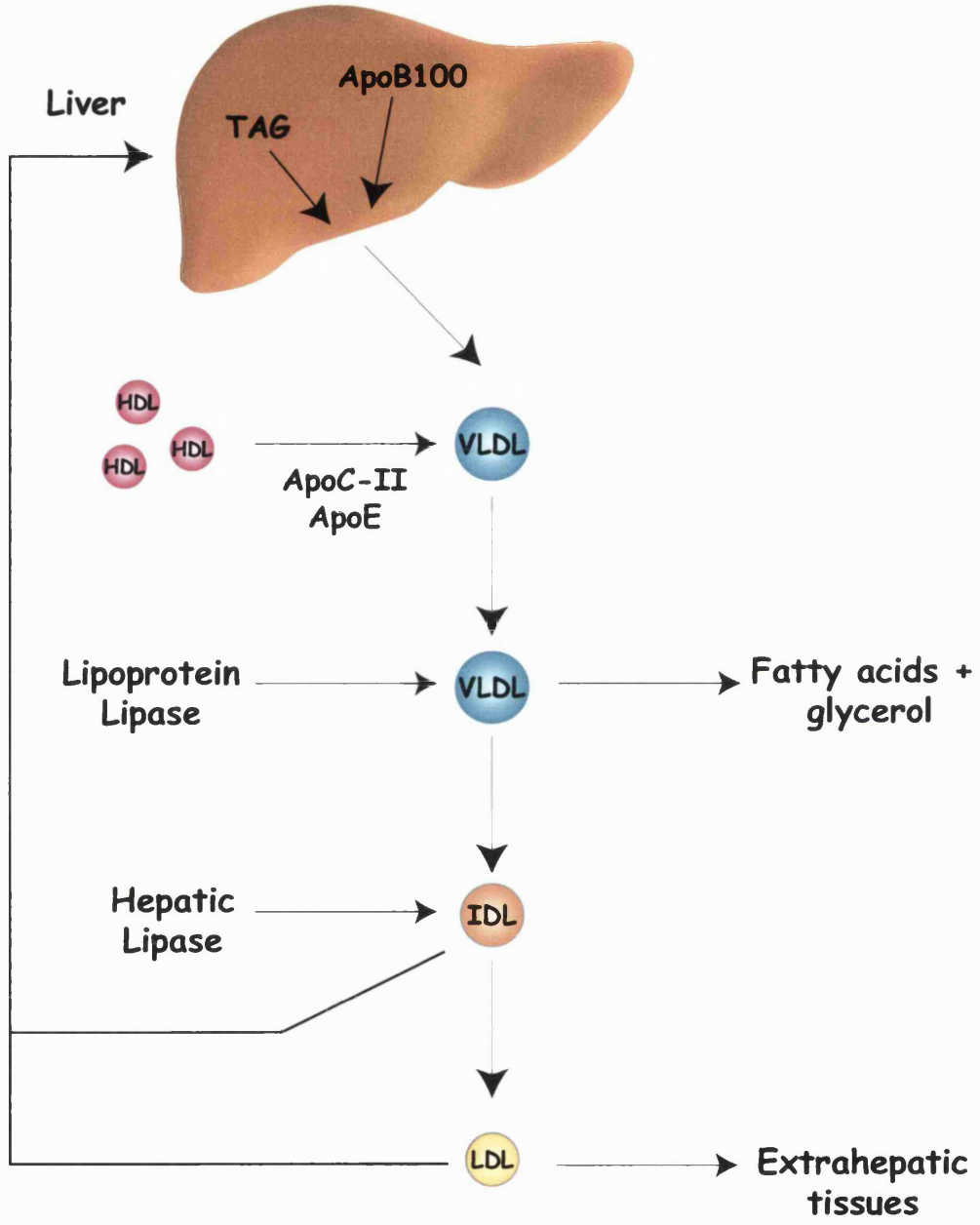

Figure 1-2 Overview of the endogenous lipoprotein pathway

VLDL metabolism is very similar to that of the chylomicron: the VLDL particles gain apoE and apoC-II from HDL. The triacylglycerol is again hydrolysed by lipoprotein lipase, expressed on skeletal muscle, or adipose tissue, and the particle shrinks as the core is removed. The ultimate remnant generated from VLDL metabolism is termed LDL. This particle contains only apoB-100, and is recognised by the LDLR in the liver and other tissues.

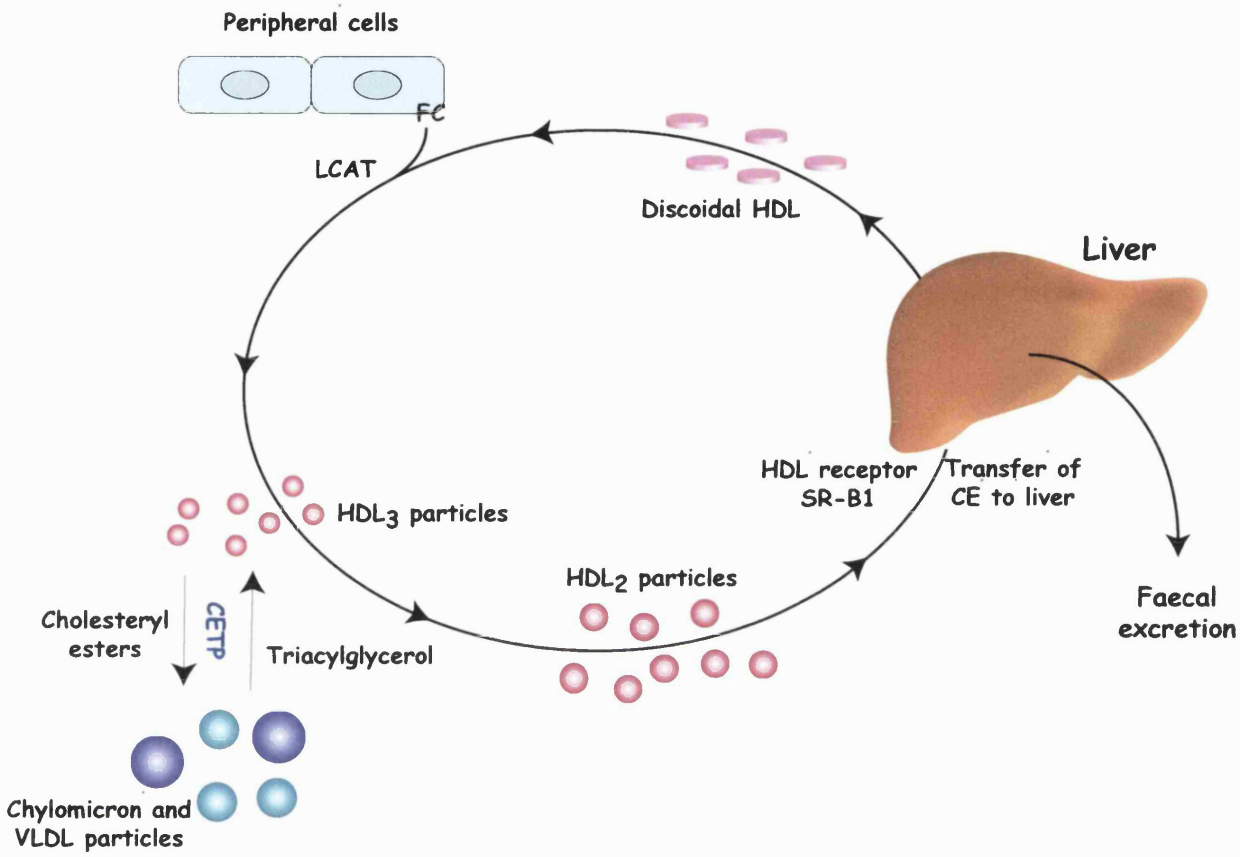

Figure 1-3 Overview of the reverse cholesterol transport pathway

Discoidal HDL is secreted from the liver and acquires free cholesterol (FC) from peripheral cells. The cholesterol is esterified by the action of LCAT to a spherical particle, now termed HDL_3. Some of the cholesteryl ester (CE) in the core of the HDL_3 particle is exchanged for some of the triacylglycerol core in the VLDL/chylomicrons, this process is mediated by cholesteryl ester transfer protein (CETP). The acquired triacylglycerol increases the size of the HDL particle, now termed HDL_2. The HDL_2 is now metabolised by the liver – the CE is delivered to the liver via the HDL receptor (scavenger receptor-B1 [SR-B1]), and the triacylglycerol is hydrolysed by hepatic lipase.

relatively enriched in cholesteryl ester and is transported to the liver where, via apoE it is recognised and taken up by members of the LDL receptor family, including the LDL receptor related protein (LRP) or the LDL receptor (LDLR) [10].

1.1.2.1.2 Very low density lipoproteins

In the liver, exogenous and endogenous lipids are assembled with apoB-100, as well as small amounts of apoE and apoC, to form VLDL [7]. As these particles are synthesised in the liver, their lipid content tends to reflect that of the hepatocyte [7].

In the circulation, the content of apoE and apoC on the VLDL particle increases due to the transfer from other lipoproteins, in particular HDL [7]. The triglycerides present in VLDL are hydrolysed in the same way as chylomicrons, by the action of lipoprotein lipase [10,12]. The remaining remnant is known as IDL and can be cleared from the circulation by the liver in the same way as chylomicron remnants [10].

1.1.2.1.3 Intermediate density lipoproteins

Intermediate density lipoproteins are also known as VLDL remnants, as they can be generated from VLDL by the action of lipoprotein lipase [11]. Intermediate density lipoproteins contain apoB-100 and apoE and can be cleared from the circulation by the liver or further catabolised by hepatic lipase to LDL [11]. Compared with other species, such as the rabbit, humans have relatively low levels of this lipoprotein fraction [13].

1.1.2.1.4 Low density lipoproteins

The majority of cholesterol in the plasma is carried in LDL [7]. It has a role in the delivery of dietary cholesterol to extrahepatic organs [14], although the majority of LDL is cleared from the circulation by the liver. Elevated plasma LDL is a major risk factor for atherosclerosis [1,8,15] and much evidence has accumulated to explain its atherogenic effects *in vivo* [16-20].

Low-density lipoprotein is generated by the hydrolysis of IDL by hepatic lipase activity. The only apolipoprotein present in this particle is apoB-100 [7]. Subclasses of LDL exist that appear to possess differing atherogenic potential. In normolipidaemic subjects, 3 subclasses can be readily identified: LDL I, LDL II and LDL III [21]. Of these, small dense LDL III is thought to be the most atherogenic and is associated with increased risk of CHD [22,23]. However, the reason why this is more atherogenic than the other subclasses of LDL has yet to be established. One possible explanation is given by the 'response-to-retention' hypothesis [24-26]. This states that once in the

subendothelial space, atherogenic lipoproteins are retained by extracellular matrix molecules leading to prolonged residence time of these particles in the intima. In turn, this may lead to their oxidative modification, generating biological responses that promote lesion formation. Small dense LDL binds more readily to proteoglycans on the arterial wall and is better retained than normal buoyant LDL [27]. It is also more susceptible to oxidation than native LDL [28]. These factors when taken together may enhance its atherogenicity (Section 1.9.2).

Native LDL is taken up by LDLR in the plasma membrane and internalised. This process is mediated by apoB-100, however, the LDLR will also bind apoE containing ligands such as chylomicron remnants [11]. Once in the cell, lipoproteins are delivered to lysosomes where they are degraded and the receptor is recycled back to the plasma membrane. The lysosomes break down the cholesteryl ester core of the lipoprotein into free cholesterol, which is subsequently released into the cytosol triggering cellular cholesterol homeostasis mechanisms [11]. Firstly, the cell can store excess free cholesterol as cholesteryl ester, by activating the enzyme Acyl CoA: Cholesterol AcylTransferase (ACAT) [7]. Secondly, the over accumulation of cholesterol leads to the down regulation of LDLR gene expression, so that the uptake of any further lipoprotein derived cholesterol is prevented [7]. Finally, the cell limits any further endogenous biosynthesis of cholesterol by repressing expression of the gene encoding the enzyme 3-Hydroxy-3-MethylGlutaryl Coenzyme A reductase (HMG-CoA reductase) [7]. Thus, cholesterol uptake into the cell via the LDLR is tightly regulated, and cannot result in excessive lipid accumulation.

1.1.2.1.5 Lipoprotein(a)

Lipoprotein(a) is an LDL-sized cholesterol rich lipoprotein particle. It contains apoB-100 which is linked via a disulphide bond to apo(a). Lp(a) has been identified in atherosclerotic tissue [29,30] and studies have indicated that elevated levels of Lp(a) are associated with increase risk of CHD and stroke [31,32]. Lp(a) is retained in the artery wall more avidly than LDL possibly because it can bind to extracellular matrix molecules by both its apo(a) and apoB component [33]. Mice overexpressing human apolipoprotein (a) and liver apoB-100 develop high circulating levels of Lp(a) and develop 8-fold greater aortic fatty streak lesions compared with their non-transgenic controls [34].

1.1.2.1.6 High density lipoproteins

HDL is synthesised by the liver and small intestine and is the smallest and most dense of the plasma lipoproteins [7]. It contains apoA-I as the predominant protein constituent and has associated with it a number of enzymes including LCAT, platelet activating factor acetyl hydrolase (PAF-AH) and PON1. [7,13]. Classically, HDL can be separated into two major subfractions: HDL_2 and HDL_3 (Figure 1-3).

HDL is involved in reverse cholesterol transport, a role that is believed to explain the strong inverse correlation between plasma HDL levels and CHD observed in many studies [35,36]. HDL particles begin life as a discoidal particle consisting mainly of apoA-I and phospholipid [7]. These particles 'pick up'/accept free cholesterol from cells, and from the surface layer of triglyceride rich lipoproteins, which are subsequently esterified by the action of LCAT. The particle, therefore, acquires a core of cholesteryl ester and becomes spherical rather than discoidal. Cholesteryl esters in HDL are then either taken to the liver or exchanged for triglyceride in VLDL by the action of CETP [7].

Recently, studies in transgenic mice overexpressing human apoA-I, the apolipoprotein present in most subfractions of HDL, have confirmed the anti-atherogenic role of HDL. These animals have increased HDL-cholesterol and resist atherosclerosis induced by diet [37], apoE deficiency [38] or the human Lp(a) transgene [39]. Other athero-protective effects of HDL may be associated with its antioxidant properties (Section 1.9.5) [40,41].

1.1.2.1.7 Remnant lipoproteins

Remnant lipoproteins are produced when chylomicrons and VLDL are catabolised by lipoprotein lipase. Compared with their nascent forms, TRL remnants are depleted of triglyceride, A- and C-apolipoproteins and relatively enriched in cholesteryl esters, apoB and apoE, reviewed in [12,42]. Transfer proteins such as CETP, which moves cholesteryl ester to TRL from HDL, may enrich the cholesteryl ester content of TRL, particularly in hypertriglyceridaemic patients [12,42]. Such remnants are smaller and denser than their nascent precursors and have slower electrophoretic mobility [12,42]. For example, normal VLDL has a pre-β electrophoretic mobility whereas its remnant has β electrophoretic mobility and is known as β-VLDL [12,42]. However, β-VLDL can be secreted directly from the liver, particularly from mice fed high fat/high cholesterol diets (Section 1.2.1) [43] and are implicated in the pathogenesis of atherosclerosis [10,12].

1.1.2.1.8 Remnant lipoproteins and atherosclerosis

In healthy individuals remnant lipoproteins are rapidly cleared from the circulation by the liver [12,42]. However, individuals with type III hyperlipoproteinaemia have impaired apoE-mediated clearance of partially hydrolysed TRL, a marked accumulation of remnant lipoproteins such as β-VLDL, and are at increased risk of coronary and carotid atherosclerosis and peripheral vascular disease, reviewed in [10,12]. Experimental mice fed atherogenic diets enriched in cholesterol have increased circulating levels of β-VLDL [43,44], and this is believed to be responsible for their accelerated development of atherosclerosis. Indeed, β-VLDL has been shown to heighten monocyte adhesion to endothelial cells, increase endothelial production of Monocyte Chemoattractant Protein (MCP-1) and Macrophage Colony-Stimulating Factor (M-CSF) and promote foam cell formation, reviewed in [10,12]

Smaller partially catabolised TRL (TRL remnants) are believed to be more atherogenic than their nascent forms [12,42]. Evidence linking remnant lipoproteins to the development of atherosclerosis is increasing: (i) remnant TRL due to their small size are more likely to penetrate the endothelium compared with their larger nascent forms [45]; (ii) due to their small size, enriched apoE content and association with lipoprotein lipase, TRL remnants are more likely to be retained within the arterial intima by proteoglycans (Section 1.1.2.1.4) [46]; (iii) TRL remnants from hypertriglyceridaemic patients, have been shown to induce cholesteryl ester accumulation in macrophages [47].

1.1.2.2 Apolipoproteins

Apolipoproteins are the protein component of lipoproteins. They confer functional specificity and help solubilise cholesterol and triglyceride for transport [7]. Some apolipoproteins serve to define the type of receptor with which the lipoprotein may bind, while other apolipoproteins activate lipoprotein-specific enzymes (Table 1-2). Five broad groups of apolipoproteins have been described [7]. According to current nomenclature, group A are found in the highest amounts in HDL, while group B are associated with VLDL, LDL and chylomicrons. Members of group C and E exchange between several classes of lipoprotein with HDL acting as the distributor. ApoD acts to facilitate the transfer of esters of cholesterol between lipoproteins.

Apolipoprotein	Function
A-I	Activates LCAT
A-II	Enhances hepatic lipase activity
B-I00	Directs binding of LDL particles to the LDL receptor
B-48	Structural component of chylomicrons and their remnants
C-I	Activates LCAT
C-II	Activates lipoprotein lipase and LCAT
C-III	Inhibits lipoprotein lipase
D	Acts on cholesteryl ester transfer protein to facilitate the movement of cholesteryl esters from HDL_3 to other lipoproteins
E	Directs binding of chylomicron remnants to hepatic lipoprotein receptors

Table 1-2 Apolipoproteins: their functions.

Adapted from reference 7.

1.1.2.2.1 Apolipoprotein A

There are three main isoforms of apoA: apoA-I, apoA-II and apoA-IV. These apolipoproteins are not related, however, they often occur together in lipoprotein fractions. The intestine is capable of synthesising all the apoA proteins but only apoA-I and apoA-II are synthesised in the liver. ApoA-I is the main apolipoprotein on HDL and has been shown to be important in reverse cholesterol transport [7]. Like apoA-I, apoA-II is also found on HDL and both these proteins act as cofactors for LCAT. The majority of apoA-IV is free in plasma, however it is also found on chylomicrons and in small amounts on HDL. Its function is not entirely clear, but may also act as an activator of LCAT.

1.1.2.2.2 Apolipoprotein B

ApoB is predominantly found on chylomicrons, VLDL and LDL. There are two isoforms: apoB-48 and B-100 [10]. ApoB-48 is produced by intestinal cells and incorporated into chylomicrons [10]. In contrast, apoB-100 is produced by the liver and incorporated into VLDL [10]. Both isoforms are products of the apoB-100 gene; apoB-48 is produced by a specific enzyme, apo Bec, which edits the messenger RNA to introduce a stop codon [10]. Unlike the other apolipoproteins, apoB is not exchanged between lipoproteins. ApoB is an integral component of VLDL, IDL and LDL, and functions as a ligand for the LDLR and LRP [10]. Both apoB isoforms are essential for plasma triglyceride and cholesterol metabolism [48].

1.1.2.2.3 Apolipoprotein C

There are three main forms of apoC: apoC-I, apoC-II and apoC-III [7]. They are present on HDL from where they can be transferred to VLDL and chylomicrons. ApoC-I is an activator of LCAT and also binds phospholipid [7], while apoC-II is an essential activator of lipoprotein lipase [7]. ApoC-III is the most abundant of the C-apolipoproteins, and appears to have an inhibitory effect on the hydrolysis and clearance of chylomicrons and VLDL via lipoprotein lipase [7].

1.1.2.2.4 Apolipoprotein D

ApoD acts on CETP to facilitate the movement of cholesteryl esters from HDL to other lipoproteins [7].

1.1.2.2.5 Apolipoprotein E

ApoE is predominantly synthesised by hepatocytes and intestinal cells; however, it is also synthesised by a wide range of peripheral cells including brain and macrophages [49]. It exists in three major isoforms apoE2, apoE3 and apoE4, and is involved in the hepatic uptake of chylomicron and VLDL remnants via members of the LDL receptor family. The different isoforms have different affinities for the receptors and contribute to variations in lipoprotein levels within a population [49]. The most common phenotype is apoE3; apoE3 is therefore considered to be the wild-type form of the protein, with apoE2 and E4 as variants [49]. ApoE2 is the rarest variant and is associated with recessive forms of type III hyperlipoproteinaemia due to defective receptor binding [50]. ApoE4 displays normal receptor binding but is a risk factor for restenosis [51] and is implicated in the pathogenesis of Alzheimer's disease [52].

1.1.3 Basic structure of blood vessels

All blood vessel walls except for the very smallest (capillaries) are composed of three concentric layers or tunics of tissues. These surround the vessel lumen and have different functions, which shall be briefly explained. A typical diagram of a large artery is shown in Figure 1-4.

1.1.3.1 Tunica intima

The innermost layer is known as the tunica intima. This layer is in intimate contact with circulating blood contained in the lumen of the artery. The intima contains a continuous layer of squamous endothelial cells, the endothelium, which forms a smooth surface reducing friction as blood flows through the vessel. A subendothelial layer is also present in blood vessels greater than 1 mm in diameter. The

subendothelium is a layer composed of loose connective tissue and smooth muscle cells, both of which are arranged longitudinally. Beneath the subendothelium is the internal elastic lamina, which separates the tunica intima from the tunica media [53].

1.1.3.2 Tunica media

The central or middle layer is known as the tunica media, which consists of circularly arranged smooth muscle cells and a stromal network of elastic fibres, collagen and proteoglycans. Large muscular arteries such as the aorta have an external elastic lamina, which separates this layer from the tunica adventitia [53]

1.1.3.3 Tunica adventitia

The outermost layer of the blood vessel wall is called the tunica adventitia. This layer is composed of fibroblasts, collagen fibres and longitudinally arranged elastic fibres. The adventitia is penetrated by nerve fibres and, in larger blood vessels, a system of tiny capillaries known as vasa vasorum, which literally translated means 'vessels of the vessel'. The vasa vasorum function to nourish the cells located in the media and adventitia, whilst the intima obtains nutrients directly from circulating blood [53].

Atherosclerosis affects all layers of the vessel wall, the intima most severely and the adventitia least. This suggests that the intima has greater exposure to initiating factors. It is therefore pertinent to look at the endothelium in more detail.

1.1.4 The endothelium

The entire circulatory system is lined with a continuous single cell thick membrane, known as the endothelium. This is made up of a layer of flattened, elongated tear shaped cells with oval nuclei. The long axes of these cells are arranged parallel to the direction of blood flow. The endothelium was once believed to be a functionally inert semi-permeable membrane; however, this is far from the truth.

In health, the vascular endothelium forms a multifunctional interface between circulating blood and various body organs/tissues. It provides a selectively permeable barrier for macromolecules, as wells as a non-thrombogenic and non-adhesive container that actively maintains the fluidity of the blood and the vessel tone [54]. As endothelial activation is thought to be an important primary event in atherogenesis it will be discussed in more detail below.

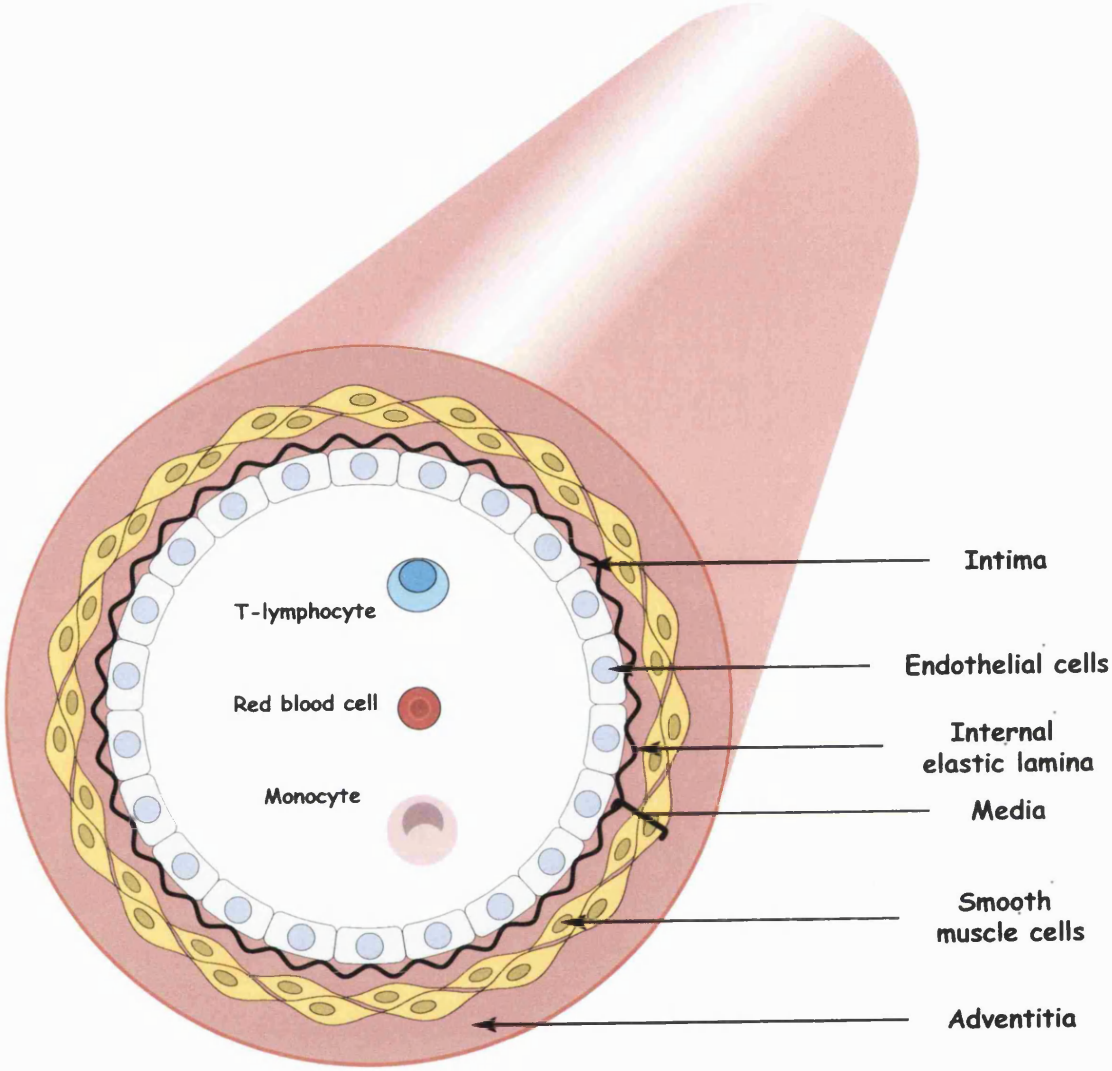

Figure 1-4 A schematic diagram of a normal large artery

A large artery consists of three concentric layers of tissue. The intima, the innermost layer is composed of a monolayer of endothelial cells. The media, the middle layer, consists of smooth muscle cells. The adventitia, the outermost layer, consists of fibroblasts, collagen fibres and longitudinally arranged elastic fibres.

1.1.4.1 Endothelial activation

Endothelial activation is a pivotal process in the chronic inflammation that typifies atherogenesis, as it modulates mononuclear cell adhesion and plays an important role in the initiation, progression and clinical emergence of the disease. The progression of atherosclerosis or atherogenesis may be viewed as a 'response to injury' [55]. It must be noted that the word 'injury' does not necessarily imply physical damage to the endothelium. Rather, the endothelium becomes 'primed' by activating species [15]. Elevated plasma lipoproteins and other components associated with coronary artery disease (CAD) risk may be considered putative 'activating species' [15,55]. Examples of potential atherogenic activating species include hypercholesterolaemia, by-products of cigarette smoke, glycosylated products associated with diabetes or ageing, altered blood dynamics, oxidative stress (including oxygen species, free radicals and oxidised lipids) and infection with viruses or bacteria (Figure 1-5) [1,15]. Indeed, *in vivo* and *in vitro* studies have observed that all of these factors can increase the expression of adhesion molecules (Section 1.4) [56-60] and chemokines (Section 1.6) [61-63] necessary for leukocyte recruitment (Section 1.3) and may enhance the permeability of the endothelium to macromolecules such as LDL. Furthermore, the 'injury' also induces the endothelium to have pro-coagulant rather than anti-coagulant properties and to produce cytokines and growth factors [1]. If the injurious agent is not effectively removed, then the inflammatory response continues unabated and atherogenesis is initiated [15]. Equally, monocytes once in the subendothelial space can produce cytokines, matrix degrading enzymes and oxidising species, which can maintain/exacerbate the inflammatory response (Section 1.1.5).

1.1.5 Pathogenesis of atherosclerosis

The formation of atherosclerotic plaque involves the focal accumulation of lipids, macrophages, T-lymphocytes, smooth muscle cells and extracellular matrix in the intima of large arteries [15]. Table 1-3 illustrates the classifications of the various types of lesions found during the progression of atherosclerosis. One of the earliest detectable events in human and experimental atherosclerosis is the increased expression of adhesion molecules by the 'activated' endothelium (Section 1.1.4.1). This is followed by the accumulation of macrophages in the arterial wall [56,64], a process that involves adhesion of circulating monocytes (Section 1.3) to the endothelium, their transendothelial migration, and differentiation into tissue macrophages [15]. Once in the subendothelial space, the macrophages ingest modified LDL via scavenger receptors (Section 1.9.2) [65]. Lipid uptake via this route is not regulated, the macrophage accumulates excessive amounts of lipoprotein cholesterol, and is transformed into

lipid-laden macrophage foam cells (Section 1.9.2) [15]. Macrophage derived foam cells can produce cytokines, growth factors and matrix metalloprotease enzymes contributing to the development of the lesion. Monocyte/macrophages are, therefore, considered to have a central role in atherogenesis.

Each characteristic atherosclerotic lesion (Table 1-3) represents a different stage in a chronic inflammatory process in the artery and, that will if unabated and excessive, result in advanced complicated lesions [15]. The fatty streak is the earliest lesion of atherosclerosis and consists of areas of focal intimal thickening produced by the accumulation of lipid-laden macrophage foam cells, surrounded by the extracellular matrix and containing a variable number of T-lymphocytes (Figure 1-6). These lesions are not clinically significant but are the precursors of more advanced lesions. Fatty streaks are predominantly localised to the aorta in the first decade of life, in the coronary arteries in the second decade and the cerebral arteries in the third or fourth decade [1]. They tend to develop in specific arterial sites, at regions of low shear stress, especially in areas of arterial branching or curvature where blood flow is disturbed [66]. Fatty streaks have the potential to progress into fibrous lesions. Foam cells die and release their lipid content and smooth muscle cells migrate into the intima and enclose the lipid rich necrotic core to form a fibrous cap (Figure 1-7). Fibrous lesions can become increasingly complex, with calcification and haemorrhage from small neovessels that grow into the lesion from the media of the blood vessel wall (Figure 1-8) [1].

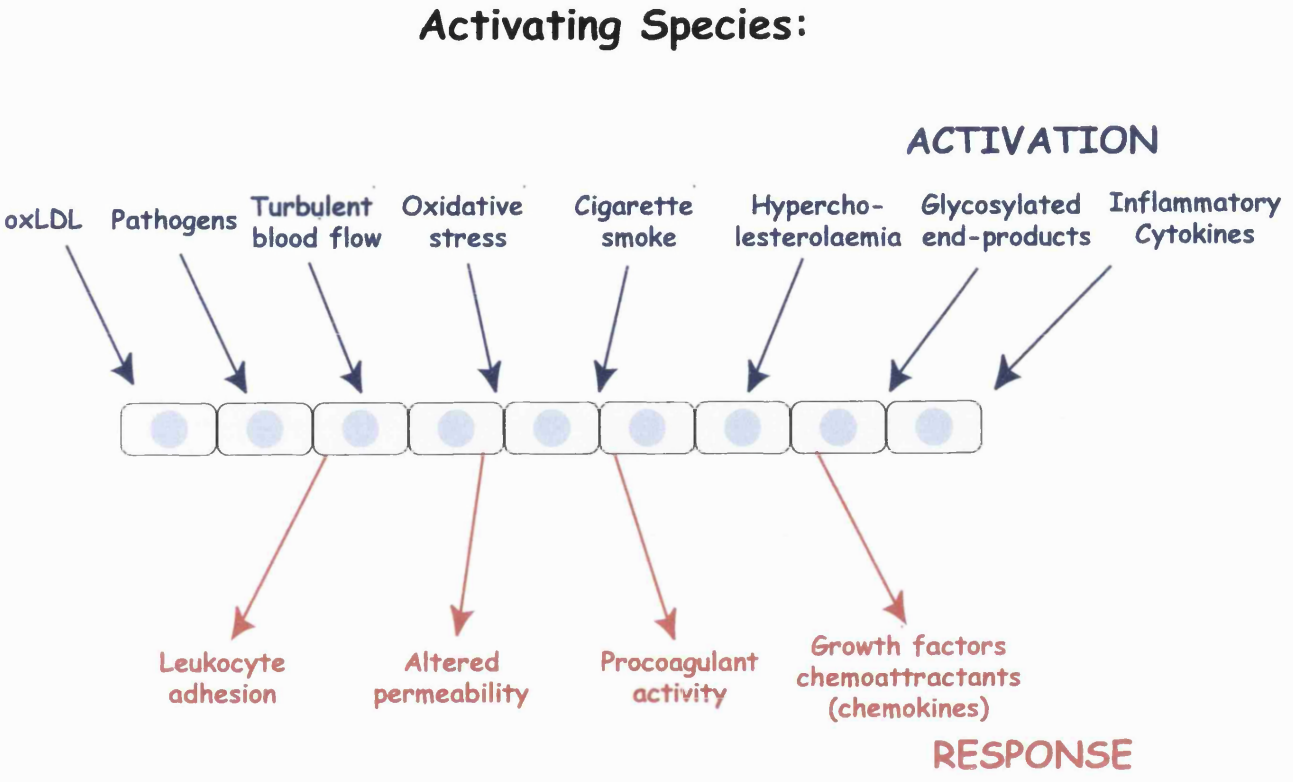

Figure 1-5 Inflammation in atherogenesis: Endothelial activation

Nomenclature and main histology	Sequences in progression	Main growth mechanism	Earliest Onset	Clinical Correlation
Type I (initial) lesion isolated macrophage foam cells.	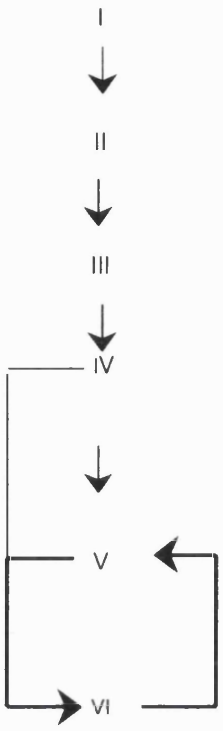		from first decade	clinically silent
Type II (fatty streak) lesion mainly intracellular lipid accumulation.				
Type III (intermediate) lesion. Type II changes and small extracellular lipid pools.			from third decade	
Type IV (atheroma) lesion, Type II changes & core of extracellular lipid				clinically Silent or overt
Type V (fibroatheroma) lesion, lipid core & fibrotic layer, or multiple lipid cores & fibrotic layers, or mainly calcific, or mainly fibrotic		Accelerated smooth muscle and collagen increase	from fourth decade	
Type VI (complicated) lesion, surface defect, haematoma-haemorrhage, thrombus		Thrombosis Haematoma		

Table 1-3 Lesion pathology and classification.

Figure adapted from reference 67.

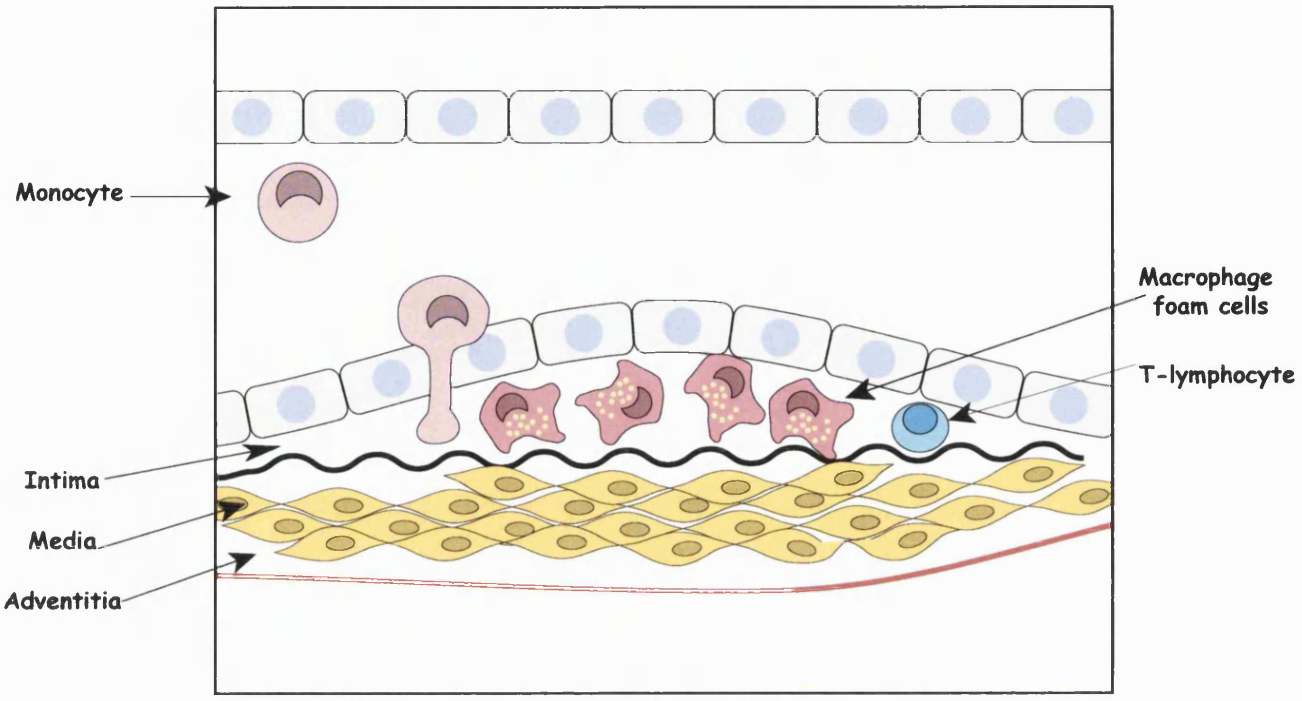

Figure 1-6 A schematic diagram of a fatty streak lesion

The fatty streak initially consists of lipid-laden macrophage foam cells together with T-lymphocytes. Later, smooth muscle cells migrate from the media and join the inflammatory cells in the intima.

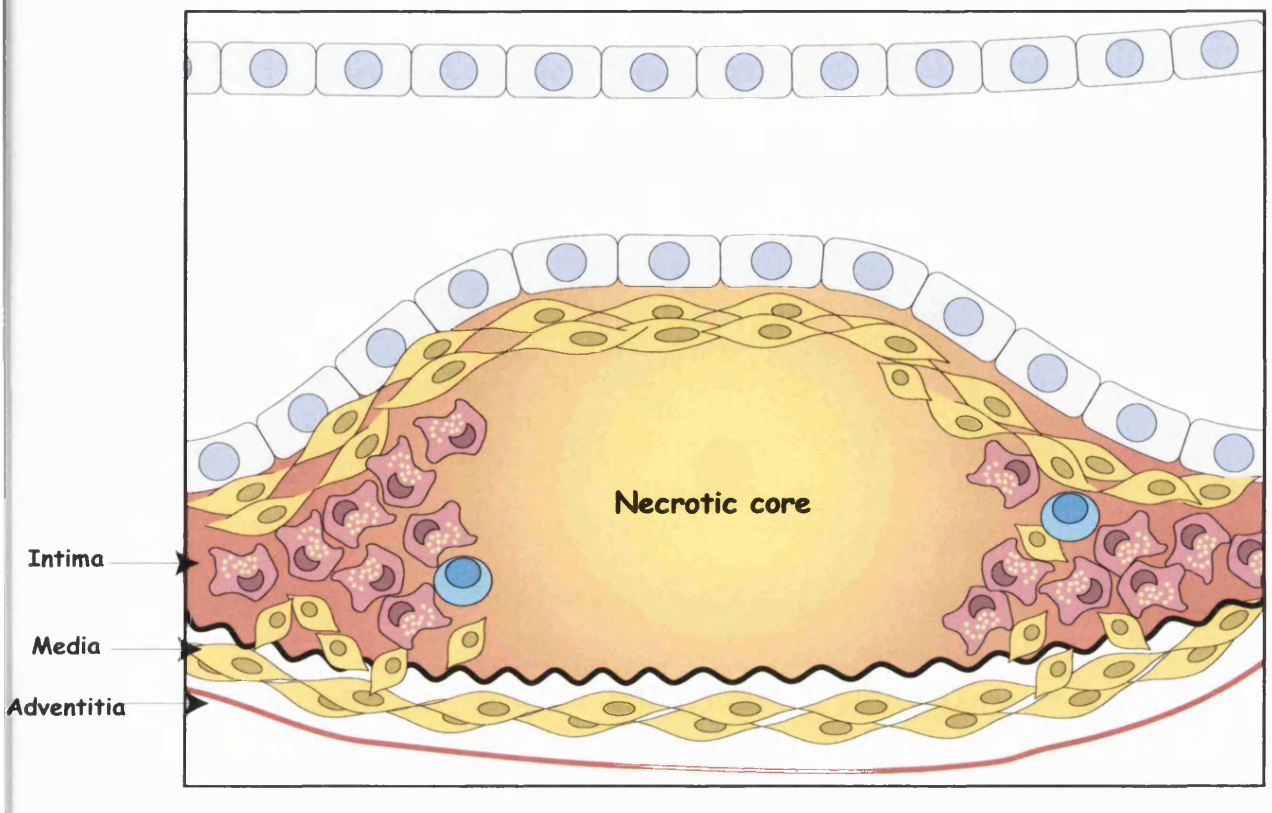

Figure 1-7 A schematic diagram of a fibrous plaque

As fatty streaks progress to intermediate and advanced lesions, they form fibrous caps that 'wall off' the lesion from the vessel lumen. This is composed of smooth muscle cells, which migrate into the intima and secrete extracellular matrix. Monocytes continue to enter the subendothelial space and eventually become lipid-laden foam cells. The death of macrophage foam cells leaves behind a growing mass of extracellular lipid and other cellular debris (necrotic core). The size of the lipid pool in the core of the lesion and the thickness of the fibrous cap relates directly to the stability of the atherosclerotic plaque. Lipid rich plaques with thin fibrous caps, containing an increased number of inflammatory cells are known as vulnerable plaques. Plaques can become weakened or vulnerable to rupture by the action of matrix metalloproteases, especially in the shoulder regions.

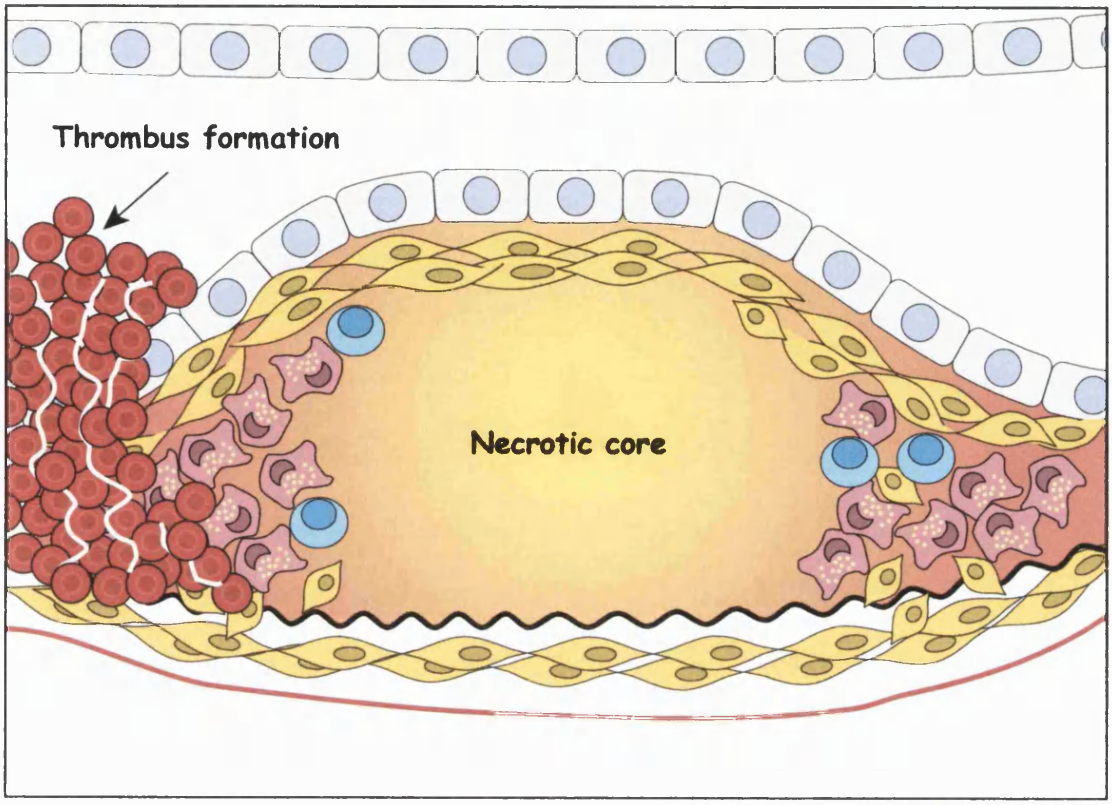

Figure 1-8 A schematic diagram of a complex lesion

The fibrous cap can rupture exposing tissue factor and collagen in the necrotic core leading to thrombus formation and obstruction of the artery. Thinning of the fibrous cap is usually apparent at the shoulder regions of the lesion. This is due to the continuing influx and activation of macrophages, which release matrix metalloprotease enzymes at these sites. These enzymes degrade extracellular matrix and can cause haemorrhage from the vasa vasorum or from the lumen of the artery leading to thrombus formation. Acute myocardial infarctions and strokes are usually due to the rupture of an atherosclerotic lesion in a coronary or carotid artery.

1.2 Mouse models of atherosclerosis

Mice are useful experimental animals because of their small size, short generation time, large litter size, easy maintenance and potential for genetic manipulation. The main disadvantage of the mouse with regard to the study of atherosclerosis is that they do not readily develop the disease: wild-type mice on a chow (non-atherogenic) diet do not develop atherosclerosis [43,68]. This is thought to be a consequence of their low plasma cholesterol concentrations and protective lipoprotein profile, which consists mainly of anti-atherogenic HDL [43]. However, the mouse has two unique advantages compared to other mammals. Firstly, many inbred strains exhibit genetic variations relevant to lipoprotein metabolism and altered susceptibility to atherosclerosis e.g. C57BL/6J (Section 1.2.2) [69]. Secondly, the construction of transgenic and gene targeted (knockout) animals is more advanced in the mouse than in any other animal [69]. This allows the genes involved in lipoprotein metabolism and disease pathogenesis (Section 1.1.5) to be manipulated. At present, mice have been generated with a wide range of lipid profiles, which mimic normal and abnormal human lipoprotein profiles, and these have been widely adopted as useful models of atherosclerosis. Genetically modified mice, such as the apoE$^{-/-}$, apoE*3 Leiden transgenic and LDL receptor$^{-/-}$, develop lesions which are histologically similar to those found in human coronary arteries (Table 1-6). Indeed, these mice have been used for exploring the role of other genes implicated in atherosclerosis [70-75]. Table 1-4 outlines the major differences and similarities in atherogenesis and lipoprotein metabolism in humans and mice.

Mice	Humans
On a normal chow diet, the majority of plasma cholesterol is transported in HDL [43] (mice lack CETP [76]). On an atherogenic diet, the majority of plasma cholesterol is contained in the VLDL fraction – generation of β-VLDL.	The majority of plasma cholesterol is carried in the LDL fraction (HDL exchanges CE for TG in VLDL).
Liver and intestine can edit apoB100 to apoB48 [77].	Editing of apoB100 only occurs in the intestine.
Most murine models develop atherosclerosis due to hyperlipidaemia.	Hyperlipidaemia is only one of the many risk factors for atherosclerosis.
Extreme cholesterol levels seen in apoE$^{-/-}$, LDLR$^{-/-}$ and apoE*3 Leiden mice fed atherogenic diets. Mouse knockout experiments are the genetic equivalent of recessively inherited conditions in humans.	Extreme cholesterol levels would be rarely observed in humans. Also being completely null for the apoE or LDLR gene is rare and therefore these types of conditions only make a small contribution to total human burden of atherosclerosis.
Mutations in single genes can cause atherosclerosis in mice e.g. apoE*3 Leiden mice	Pattern of inheritance of atherosclerosis in humans is more compatible with polygenic inheritance - a combination of multiple small changes in gene function.
Lesion distribution is predominantly in the aortic arch where particular haemodynamic conditions may exist (mice use 4 legs) [78].	The distribution of lesions in humans is predominantly in the abdominal aorta.
Development of lesions can be mapped from initial insult to fibro-fatty lesion	Biopsy and autopsy material used. Initiating factors are therefore difficult to determine.
Plaque rupture and thrombosis is not a common feature of mouse atherosclerosis. This feature is only observed after extended feeding of atherogenic diets to apoE$^{-/-}$ and LDLR$^{-/-}$ mice [81,82].	Plaque rupture and thrombosis are major problems in human atherosclerosis leading to myocardial infarction and stroke.
Mice and humans are genetically quite similar, since they carry, with few exceptions, the same set of genes to control lipoprotein metabolism [43].	
Rubin and Smith compared the results of various genetic manipulations on atherosclerosis in mice to see what would be predicted to occur in humans. They found complete agreement between the observed mouse result and the predicted human result [83].	

Table 1-4 Comparison of mice and human atherosclerosis and lipoprotein metabolism

1.2.1 Diets

Prior to the development of atherosclerosis prone genetically modified mice, many studies were performed using in-bred mice fed chow-based diets supplemented with varying amounts of saturated fats, cholesterol and sodium cholate [84-86]. Of these, the semi-synthetic diet developed by Beverley Paigen and colleagues [3,4,87] is frequently used to accelerate lesion development in in-bred mice, and genetically modified strains. The diet typically contains cholesterol (usually 1%) and cocoa butter (15%) as the major fat source as well as sodium cholate (0.5%). The high levels of cholesterol and sodium cholate are primarily required to accelerate disease development [4]. Although fatty streak lesions still occur if lower cholesterol and sodium cholate levels are used, however, the feeding period must be extended considerably [4].

Before the Paigen diet was developed, non-defined diets were used in laboratory mice. Commercial pelleted rat chow (4% fat) served as the low fat control diet and a mixture of the Thomas-Hartroft diet (30% cocoa butter, 5% cholesterol & 2% sodium cholate) and the rat chow, served as the atherogenic diet (1 part Thomas-Hartroft diet and 3 parts breeder chow; 15% fat, 1.25% cholesterol & 0.5% sodium cholate) [3]. As the chow was made from natural products, the exact amount and the source of the fat, carbohydrate and protein was undefined. Therefore, the composition from batch to batch varied markedly. These differences could affect experimental results and so Paigen's group set out to formulate a diet of defined composition that would produce aortic lesions [3].

Paigen's group compared 8 synthetic diets [3]. They investigated the effects by varying the concentration of cocoa butter or cocoa oil, glucose or sucrose whilst keeping the cholesterol (1.25%) and sodium cholate (0.5%) levels constant. These experimental diets were compared with the control atherogenic diet (Thomas-Hartroft diet and breeder chow; 1:3). A combination of cocoa butter (15%) and sucrose (50%) was found to be the most effective. Only mice receiving this diet had lesion development, depressed HDL-C and elevated VLDL/LDL levels similar to those fed the control atherogenic diet [3].

Importantly, Nishina *et al* observed that these semi-synthetic diets produced fewer pathological changes in the liver and decreased gallstone formation [4,88]. Many investigators have based the composition of their atherogenic diets on the Paigen diet, but have varied the amount of cholesterol and sodium cholate present (Table 1-5). For example, Groot *et al* [44] used a low fat/cholesterol diet (6.2% fat, 0.01% cholesterol), a

high fat/cholesterol diet (15% fat, 0.25% cholesterol), and a severely atherogenic diet (15% fat, 1% cholesterol and 0.5% sodium cholate) to investigate lesion development in apoE*3 Leiden mice (Section 1.2.5).

Nishina *et al* [4] also observed that the type of saturated fat included in the diet markedly influenced lesion development. Diets rich in monounsaturated and polyunsaturated fats decreased plasma cholesterol whereas diets high in saturated fat were positively correlated to plasma cholesterol levels [4].

Diet	% Fat (w/w)	% Cholesterol (w/w)	% Cholate (w/w)
Low fat/low cholesterol (LFC)	4 to 6.2%	0.01%	-
'Western' type diet	21%	0.25%	-
High fat/cholesterol (HFC)	15%	0.25 to 1.25%	-
High fat/high cholesterol/cholate (HFC/C)	15%	1%	0.5%

Table 1-5 Typical compositions of experimental diets

1.2.2 C57BL/6J mouse

The inbred mouse strain, C57BL/6J develops hypercholesterolaemia, and aortic and coronary fatty streak lesions, when maintained on a HFC/C diet (Table 1-6) [69,88,89]. In general, lesion development in this model occurs first at the base of the aortic sinus and then progresses upwards towards the valve attachments (type I) and free aortic wall (type II). After 5 to 7 week of diet challenge, type I fatty streaks are evident at the base of the aortic sinus [69,78] and after 9 to 11 weeks type II lesions have developed [89]. After 12 months consumption of this diet, sizeable fatty streak lesions have developed, but remain confined to the aortic origin [78]. Fatty streaks have also been observed, but to a lesser extent, in the ascending aorta [78,89]

Although C57BL/6J mice have been widely used in atherosclerosis research and initially provided promising results, there are a number of disadvantages inherent to this model. Firstly, atherosclerosis is limited to the fatty streak stage and therefore it can only be viewed as a model for the very early events in atherosclerosis [43]. Secondly, extended periods of time (> 3 months) are required for the development of these small lesions.

1.2.3 LDL receptor knockout mouse (LDL receptor$^{-/-}$)

The LDL receptor provides cells with lipoprotein cholesterol, especially hepatocytes, and cells within the adrenal glands, ovaries and testes. These cells require large amounts of cholesterol for the synthesis of bile acids and steroid hormones. The LDL receptor plays an essential role in cholesterol homeostasis (Section 1.1.2.1.4). Both IDL and LDL accumulate in the plasma of patients with familial hypercholesterolaemia, who have dysfunctional LDL receptors [7].

LDL receptor-deficient mice consuming a non-atherogenic diet have elevated levels of plasma IDL and LDL [68]. These changes are not sufficient to cause atherosclerosis, however, when fed a 'Western' type diet (Table 1-5) these mice develop lipid-rich, necrotic lesions [68]. LDL receptor$^{-/-}$ mice are mainly used to study atherosclerosis in the context of hyperlipidaemia. This condition can be reversed in mice by inoculating them with an adenovirus containing the LDL receptor gene [90].

1.2.4 ApoE knockout mouse (apoE$^{-/-}$)

ApoE is a component of chylomicrons and very low-density lipoprotein remnants and functions as a ligand for receptor-mediated uptake of these particles from the blood by the liver [49]. In mice and humans, the apoE gene is one of the major genes determining plasma lipid levels and the importance of this apolipoprotein is well illustrated in familial dysbetalipoproteinaemia (FD), whose underlying cause is one of the several mutations in the apoE gene (usually apoE2) resulting in the production of dysfunctional apoE or its absence from plasma [49]. Individuals with FD are characterised by marked increases in remnant lipoproteins, the presence of β-VLDL and develop premature atherosclerosis [42,91].

Mice deficient in apoE have a severely altered lipoprotein profile showing a very high level of atherogenic VLDL, which induces extreme susceptibility to atherosclerosis (Table 1-6). When fed a normal chow diet, fatty streak lesions develop after 10 weeks of age and by 15 week old complex lesions characterised by a fibrous cap and necrotic core can be seen [78,92-94]. Qiao *et al* [69] noted that aortic lesions in apoE knockout mice after twenty weeks on a normal diet were more than ten times larger than those seen in C57BL/6J mice maintained for thirty weeks on an HFC/C diet. ApoE$^{-/-}$ mice develop extensive lesions throughout the aortic tree, at similar atherosclerosis prone sites as observed in human atherosclerosis [79]. Furthermore, lesions in the apoE$^{-/-}$ mice appear to resemble human lesions, in that they progress from fatty streaks through to fibroproliferative lesions, with thick fibrous caps [43].

Recently, attention has focused on the role of macrophage-derived apoE. Lesion macrophages express apoE, and macrophage apoE synthesis and secretion is up-regulated *in vivo* by intracellular cholesterol accumulation [95]. Studies have indicated that apoE plays a role in cholesterol efflux, reviewed in [96] and that the synthesis of apoE by macrophages in the vessel wall may pro or anti-atherogenic effects [97-99]. ApoE$^{-/-}$ mice may also be a model for lipoprotein oxidation: oxidation specific epitopes have been observed in their atherosclerotic lesions and their plasma contains high titres of autoantibodies to oxidized LDL [100,101].

1.2.5 ApoE*3 Leiden transgenic mouse

ApoE*3 Leiden is a human dysfunctional apoE variant, which is characterised by a tandem duplication of codons 120 through 126 in the apoE gene [102]. Consequently, the protein has an extra seven amino acids. The additional amino acids present in apoE*3 Leiden are responsible for an alteration in LDL receptor binding *in vitro* [103], and leads to impaired clearance of VLDL and chylomicrons from the blood by the liver. Individuals with this mutation develop type III hyperlipoproteinaemia, which is characterised by an increase in plasma cholesterol and triglyceride, due to the accumulation of chylomicron and VLDL remnants. The presence of a single apoE*3 Leiden allele is associated with a dominantly inherited form of FD [104,105]. This may be due to the high affinity of the dysfunctional apoE*3 Leiden protein for triglyceride-rich lipoproteins which results in delayed clearance of these particles from the circulation [106].

Transgenic mice with an apoE*3 Leiden – apolipoprotein CI gene construct develop hyperlipidaemia, comparable to the human condition, which can be greatly enhanced by maintaining these animals on a HFC or HFC/C diet (Table 1-6) [44,106]. Consequently, these animals develop premature atherosclerosis in the aortic root and in the thoracic and abdominal aortae, which is proportional to cholesterol levels in VLDL and LDL-sized lipoproteins [44]. The progression through the different stages of atherogenesis in this model is similar to that seen in apoE$^{-/-}$ mice. Groot *et al* [44] observed a 5 to 10-fold increase in lesion area when these mice were fed an atherogenic diet compared to their non-transgenic littermates on the same regime. Complex lesions, with an extracellular lipid core, covered by a fibrous cap are found after three months exposure to this diet [44].

The apoE*3 Leiden mouse model of atherosclerosis has been used in all studies contained in this thesis. As with any animal model, there are a number of advantages and disadvantages, and the reasons why this transgenic murine model was chosen shall be discussed in more detail. ApoE*3 Leiden mice fed an atherogenic diet will develop early and advanced atherosclerotic lesions in similar sites of predilection as the human disease [44,80]. Fatty streak lesions develop in the intima and contain macrophage foam cells, and a variable number of T-cells [107]. Thereafter, a fibrous cap forms, while at later stages, a necrotic core, calcification and cholesterol clefts are evident [44,107]. The lesions observed in these animal are well characterised and contain adhesion molecules, oxidised epitopes, scavenger receptors and macrophage foam cells [44,80,107]. Thus, atherogenesis in apoE*3 Leiden mice seems to involve the major pathophysiological features of the human disease. Importantly, the development of atherosclerosis in apoE*3 Leiden mice is diet dependent, so that lesion formation can be controlled by the type of diet administered and the duration of the experimental period [44]. For this reason, our collaborators (GSK) have used them to test established [108] and novel hypolipidaemic compounds and anti-atherosclerotic therapies.

However, apoE*3 Leiden mice develop less severe atherosclerotic lesions than $apoE^{-/-}$ and $LDLR^{-/-}$ mice. This may be due to several reasons. For example, $apoE^{-/-}$ mice do not require an atherogenic diet to drive lesion formation. Lesions will develop gradually when these animals are fed a normal chow diet. One major drawback to atherogenesis in the $apoE^{-/-}$ model fed a chow diet is that it shows a lack of correlation between total cholesterol and lesion size. This suggests that apoE deficiency has an impact on atherosclerosis in ways not relating to serum cholesterol, which may be related to the impact of apoE deficiency on cholesterol homeostasis at the vessel wall. Furthermore, apoE*3 Leiden mice still synthesise functional endogenous apoE. As lesional macrophages can synthesise large quantities of apoE [109], local arterial production of apoE may attenuate atherosclerosis [97,98]. Thus, the presence of endogenous apoE synthesised by the liver, macrophages and other tissues makes the apoE*3 Leiden mouse a useful model of atherosclerosis, as they allow the investigation of atherosclerosis while macrophage function is undisturbed. Thus, apoE*3 Leiden mice provide a useful model of hyperlipidaemia-induced atherogenesis.

The main disadvantage of the apoE*3 Leiden mouse model is the HFC/C diet required to drive lesion formation. Other semi-synthetic diets such as the HFC diet have been tested in the apoE*3 Leiden mice. However, lesion development is slowed

down considerably and the length of study required to achieve a fibrous cap with cholesterol core is approximately 30 weeks, whereas these lesions are seen after 12 weeks on a HFC/C diet [44]. Although formulated according to Nishina *et al* [4,88], this diet can induce hepatic inflammatory responses [110,111]. As controls, therefore, C57BL/6J mice (non-transgenic littermates) consuming the same diet were used. These animals will develop small fatty streak lesions after approximately 12 weeks consumption of this diet. Thus, the use of these two strains of mice allowed investigation of whether putative 'markers' of disease progression and/or inflammation could discriminate between groups of animals experiencing an identical dietary regime but possessing differing degrees of hypercholesterolaemia and rates of atherogenesis.

Model	Atherogenic Stimulus	Cholesterol level (diet)	Lesion Type
C57BL/6J	VLDL, IDL (β-VLDL)	200 to 300 mg/dl (HFC/C diet)	Fatty Streak (aortic sinus)
LDL Receptor $^{-/-}$	IDL, LDL (β-VLDL)	1500 mg/dl (HFC/C diet)	Fatty streak, progressing to necrotic core but without fibrous plaque. Lesions develop throughout the aortic tree
ApoE $^{-/-}$	Chylomicron and VLDL remnants (β-VLDL)	400 to 600 mg/dl (LFC) 1500 to 2000 mg/dl (Western type diet)	Fatty streak, progressing to fibrous, throughout the aortic tree especially at branch points of major vessels. Same pattern as for low-cholesterol, low-fat diet, but with larger lesions and faster progression.
ApoE*3Leiden	Chylomicron and VLDL remnants (β-VLDL)	1600 to 2400 mg/dl (HFC/C)	Fatty streak progressing to fibrous plaques develop throughout the aortic tree particularly at branch points

Table 1-6 Characterisation of mouse models of atherosclerosis.

Adapted from reference 68.

1.3 Mononuclear cell recruitment during atherogenesis

Endothelial activation (Section 1.1.4.1) in response to inflammatory stimuli, triggers changes in endothelial adhesiveness by the localised up-regulation of cell adhesion molecules and is a prerequisite for the selective and focal recruitment of circulating monocytes and T-lymphocytes [56,112-115]. It has been estimated that 80% of cells in early lesions are monocyte/macrophages, whereas 10-20% are T-lymphocytes [116]. Initially, circulating mononuclear cells roll along the endothelium via transient interactions with members of the selectin family (Section 1.4.1). Selectins considerably slow down the speed of the cell and allow it to sense the presence of locally secreted chemokine gradient (Section 1.6). Binding of chemokines to a receptor on monocytes triggers integrin conformational changes and increases the strength of integrin binding to members of the Immunoglobulin gene SuperFamily (IgSF) [117]. Figure 1-9 depicts the process of monocyte recruitment during atherosclerosis.

1.4 Adhesion molecules

The attachment of leukocytes and their subsequent transmigration into the subendothelial space is mediated by specific adhesion molecules expressed on the endothelial cell membrane [118-120]. Endothelial adhesion molecules belong mainly to two protein families, namely the IgSF and the selectins. Each family has a distinct function and provides 'traffic signals' for leukocytes. Their expression is up-regulated in response to pro-inflammatory cytokines such as interleukin-1β (IL-1β), interleukin-4 (IL-4) and tumour necrosis factor-α (TNF-α) [121,122]. Expression of adhesion molecules on unactivated endothelium is either absent, or at basal levels. Immunohistochemical studies of both experimental and human atherosclerotic lesions have demonstrated increased expression of adhesion molecules Vascular Cell Adhesion Molecule-1 (VCAM-1) [123,124], InterCellular Adhesion Molecule-1 (ICAM-1) [125,126], and E and P-selectin [125,127].

1.4.1 Selectins

Leukocyte adhesion to the activated endothelium starts with the capture of cells from the bloodstream. The selectins mediate the initial attachment to the vessel wall through transient adhesions, which causes leukocytes to roll slowly in the direction of blood flow. Selectins have a characteristic extracellular domain composed of an amino-terminal lectin domain that binds carbohydrate ligands, an epidermal growth factor domain, and two to nine short consensus repeat (SCR) units homologous to domains found in complement proteins [129]. Members of this family include P-, E- and L-selectin.

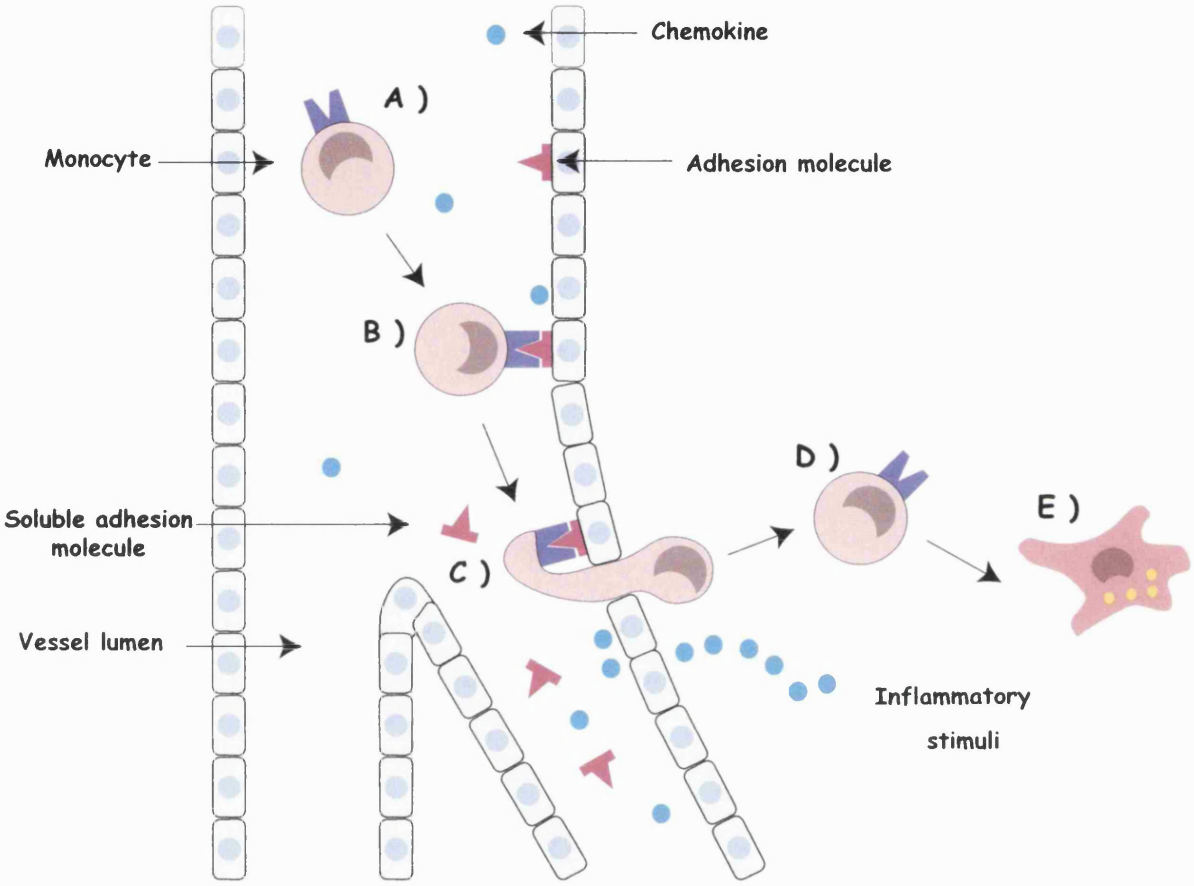

Figure 1-9 Process of monocyte recruitment

Monocytes are attracted to sites of inflammation by the presence of a chemotactic gradient (A). Initially, they roll along the endothelium, a process mediated by members of the selectin family of adhesion molecules (not shown). Chemokines present on the artery wall engage specific G-protein receptors (chemokine receptors) expressed on the monocyte (not shown). This initiates conformational changes in the integrin molecules expressed on the surface of the monocyte, and mediates firm adhesion to their endothelial counter-receptor, VCAM-1 or ICAM-1 (B). This causes the monocyte to come to a halt and to migrate via the aid of platelet-endothelial cell adhesion molecule-1 (PECAM-1) into the subendothelial space (C + D). Once within the intima, the monocyte differentiates into a tissue macrophage (E). During the inflammatory process, the endothelium can release truncated, but functional adhesion molecules into the blood. Chemokines are also secreted directly into the circulation or presented by proteoglycans on the artery wall to attract further mononuclear cells to the inflammatory site. Adapted from reference 128.

1.4.1.1 P-selectin

P-selectin (CD62P), previously named Platelet Activation Dependent Granule External Membrane protein (PADGEM), has nine SCR domains and acts as a receptor for neutrophils and monocytes. It is found in a pre-formed state co-localised with von Willebrand factor in Weibel-Palade bodies of endothelial cells and alpha granules of platelets [129], and can be rapidly translocated to the membrane within minutes of cell activation. P-selectin interacts with P-selectin glycoprotein ligand-1 (PSGL-1) its major co-receptor which is expressed on monocytes.

1.4.1.2 E-selectin

E-selectin (CD62E), previously known as Endothelial Leukocyte Adhesion Molecule-1 (ELAM-1), has six SCR domains [129] and binds to leukocytes expressing sialyated Lewis antigens, including neutrophils, monocytes and T-cells. E-selectin is rapidly induced on activated endothelium and mediates a stronger interaction than P-selectin with carbohydrate ligands such as sialyl Lewis X or PSGL-1 on monocytes [130].

1.4.1.3 L-selectin

L-selectin (CD62L) has two SCR domains and was originally described as a lymphocyte 'homing receptor' involved in the initial attachment of lymphocytes to endothelial cells in lymph nodes [129]. However, L-selectin is widely distributed on leukocytes, and contributes to both lymphocyte and neutrophil entry into inflammatory sites [129]. Cell activation by chemokines, or phorbol esters, down regulates L-selectin expression on cells, by shedding the soluble form of this molecule into the plasma [131].

1.4.2 Immunoglobulin gene superfamily

Selectin-mediated adhesion does not lead to firm adhesion and transmigration of leukocytes unless members of the IgSF are involved. Following integrin activation, leukocytes adhere strongly to members of this superfamily and then flatten before extravasation can take place. IgSF members are characterised by the presence of multiple immunoglobulin-like domains. Members of this family include VCAM-1, ICAM-1 and PECAM-1. Leukocyte co-receptors for this family are the integrins, heterodimeric proteins consisting of non-covalently-linked alpha and beta units.

1.4.2.1 VCAM-1

VCAM-1 (CD106) exists predominantly as a seven-domain transmembrane glycoprotein (Figure 1-10) [132,133]. Domains 1-3 are homologous to domains 4-6 indicating an intergenic duplication event in the evolutionary history of the gene.

Alternative splicing can lead to the addition, or deletion of domains, generating minor isoforms [132]. In humans, an alternatively spliced six-domain form exists, the fourth domain being absent [134]. An identical six residue sequence found on domains one and four, is critical for VLA-4 binding [135]. In rabbits, an eight domain variant form has been reported [133]; and in mice an additional and unique truncated three-domain form with glycophosphatidylinositol (GPI) linkage has been described [136]. VCAM-1 expression is absent on resting cells, but is induced by endothelial activation (Section 1.1.4.1) and is involved in the transmigration and localisation of monocytes and lymphocytes, but not neutrophils, at sites of inflammation. Leukocyte recruitment is mediated by the interaction between VCAM-1 and its counter receptor, the β-1 integrin, very late antigen-4 (VLA-4, CD49d/CD29, $\alpha 4\beta 1$) which is found on lymphocytes, monocytes, eosinophils and basophils [137].

1.4.2.2 ICAM-1

ICAM-1 (CD54) exists as a five domain transmembrane glycoprotein (Figure 1-10) [138]. It promotes adhesion of monocytes, neutrophils and lymphocytes via the interaction with the β_2 integrins, leukocyte function associated molecule-1 (LFA-1, CD11a/CD18, $\alpha_L\beta_2$) which binds to extracellular domain 1 [138], and Mac-1 (CD11b/CD18, $\alpha_M\beta_2$), which binds to the third extracellular domain [139]. ICAM-1 is expressed weakly under resting conditions *in vivo*, but is induced upon endothelial activation (Section 1.1.4.1).

1.4.2.3 PECAM-1

PECAM-1 (CD31) is expressed in large amounts on endothelial cells at intercellular junctions, on T-Cell subsets, platelets, monocytes and neutrophils. PECAM-1 is required for transendothelial migration of leukocytes through intercellular junctions of vascular endothelial cells by inducing PECAM-1-PECAM-1 (homotypic) adhesion. It may also induce integrin activation, and is itself phosphorylated in the cytoplasmic domain following activation [118].

1.5 Adhesion molecules and atherosclerosis

Levels of certain adhesion molecules, in particular VCAM-1, ICAM-1, E- and P-selectin are elevated in human or experimental atherosclerotic lesions [124-127,140]. In particular, VCAM-1 is thought to contribute to early lesion development in animal models, because its expression has been detected focally on endothelial cells, where monocytes first accumulate. For example, VCAM-1 was observed in rabbits after just

one week on an atherogenic diet and appeared to be an early indicator of initiation of atherogenesis [56]. ApoE$^{-/-}$ mice, prone to the development of hyperlipidaemia and atherosclerosis, express VCAM-1 and ICAM-1 at aortic sites predisposed to lesion formation [112,141]. Recently, Zibara *et al* [142] found that endothelial VCAM-1 was highly expressed over fatty streak lesions and was decreased on fibro-fatty and complex lesions in apoE$^{-/-}$ mice.

Interestingly, VCAM-1 expression is largely restricted to lesion and lesion prone sites, whereas ICAM-1 appears to be constitutively expressed in all regions of the aorta including lesion-protected areas [143]. This would suggest different roles for VCAM-1 and ICAM-1 during atheroma development. Mice deficient in VCAM-1 have major developmental abnormalities, which have hindered attempts to study the role of this protein in atherogenesis [144-146]. However, blocking VLA-4 (VCAM-1 co-receptor) by the continuous administration of an anti-VLA-4 peptide decreases leukocyte entry and fatty streak lesion formation in mice consuming HFC/C diet [147]. Recently, Cybulsky *et al* [71], generated a homozygous VCAM-1 domain 4 knockout mouse on an LDL receptor$^{-/-}$ background (VCAM-1$^{D4D/D4D}$/LDL receptor$^{-/-}$). Domains 1 and 4 contain VLA-4 binding sites; these mice therefore, have only one ligand-binding site (Section 1.4.2.1). Interestingly, these animals express markedly reduced levels of VCAM-1 mRNA and protein (less than 10% of wild-type) and as a consequence have reduced foam cell formation throughout the aorta. Similar results have been obtained when the apoE$^{-/-}$ model was used as the background strain [148].

ICAM-1, P-selectin and E-selectin deficient mice have been generated on an apoE$^{-/-}$ background [70,149]. These animals also develop smaller atherosclerotic lesions than controls indicating a possible role for these adhesion molecules in atherogenesis. However, it must be noted that some investigators have reported that ICAM-1 deficiency did not affect the development of atherosclerosis. For example, Cybulsky *et al* [71] found that ICAM-1 deficiency on an LDL receptor$^{-/-}$ background did not influence foam cell formation either alone or when combined with VCAM-1$^{D4D/D4D}$.

Analysis of human atherosclerotic lesions has revealed that, as the disease develops, a number of cell types present within the lesion express adhesion molecules. These include endothelial cells, vascular smooth muscle cells and macrophages [150]. In advanced lesions, expression of E-selectin, ICAM-1 and VCAM-1 were more prevalent in the deeper portions of the plaque, in areas of neovascularisation, rather than on arterial lumenal endothelium. O'Brien *et al* [150] observed a strong correlation between

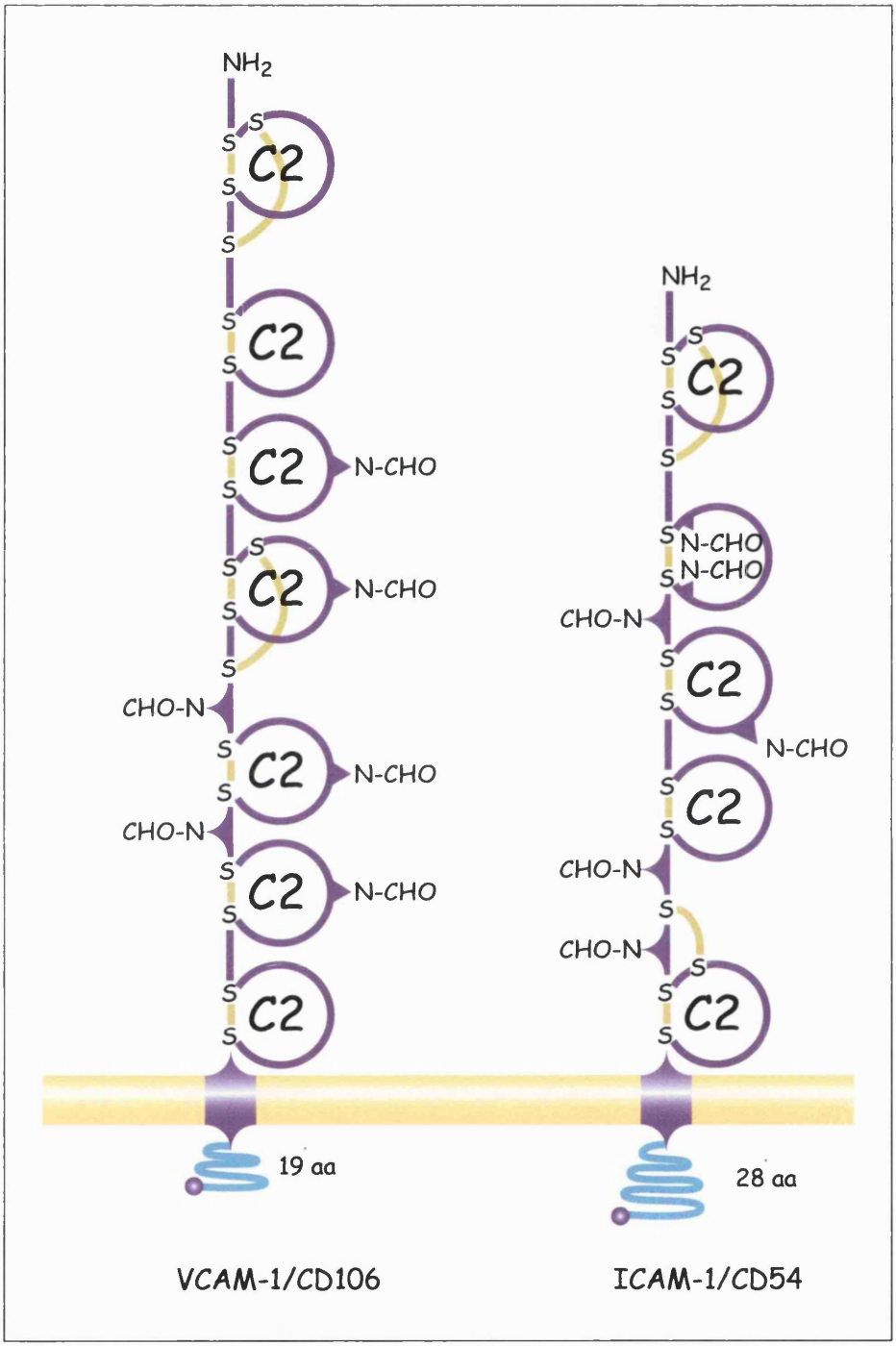

Figure 1-10 Structures of VCAM-1 and ICAM-1

VCAM-1 and ICAM-1 are members of IgSF characterised by repeated domains similar to those found in immunoglobulins (Ig), in the extracellular, amino terminal portion of the molecule. Each Ig-like domain is usually encoded by a discrete exon and consists of a primary sequence of 70-110 amino acid residues arranged in a β-barrel stabilized with a disulphide bridge to form an 'Ig fold'. The extracellular portion is N-glycosylated. Both ICAM-1 and VCAM-1 have a transmembrane region and a short cytoplasmic tail. Adapted from www.rndsystems.com

macrophage accumulation and VCAM-1 expression on neovasculature and on non-endothelial cells in established atherosclerotic plaques [150]. Therefore, this suggests that VCAM-1 may mediate the recruitment of monocytes to sites located deep within the lesion via neovessels. Furthermore, after endothelial penetration, monocytes must be retained in the intima to exert their pathological role in atherogenesis. This may involve adherence to activated smooth muscle cells expressing VCAM-1 [151], which may encourage a more permanent residence of monocytes in the lesion [152]. E-selectin and P-selectin were also detected in areas of neovascularisation, but no association was found between expression of these molecules and the accumulation of macrophages [150]. However, a significant correlation was observed between the degree of macrophage infiltration and the prevalence of E-selectin and ICAM-1 on the arterial surface. This observation was not true of VCAM-1 [150]. Thus, adhesion molecules appear to be involved in the recruitment of mononuclear cells via the intima and regions of neovascularisation.

1.6 Chemokines

Chemokines are an important group of secreted proteins that exhibit selective chemoattractant properties for target leukocytes, thereby ensuring the correct leukocyte is recruited, or activated, into sites of inflammation [153]. At least four subfamilies have been described based on the arrangement of the first two of four-conserved cysteine residues [153]. In the CXC or alpha (α) subfamily, these two cysteines are separated by a single amino acid, whereas in the CC or beta (β) subfamily they are adjacent (Figure 1-11) [153]. Members within each subfamily exhibit 25 - 70% sequence identity, while the amino acid identity between members of the both subfamilies range from 20 - 40% [154]. In general, the first cysteine residue forms a disulphide bond with the third cysteine, and the second with the fourth, resulting in a similar tertiary structure for many chemokines [154]. However, the quaternary structures of members of these subfamilies are completely different [154]. A diagram illustrating the tertiary structures of the prototypical members of the each family, MCP-1 and Interleukin-8 (IL-8) respectively is shown in Figure 1-12. Two chemokines that do not fit into either the CC or the CXC subfamiles have been described: lymphotactin (C), with only two rather than four cysteine residues, and fractalkine (CXXXC), a membrane bound glycoprotein in which the first two cysteine residues are separated by three amino acids. Lymphotactin and fractalkine could be representatives of two additional chemokine subfamilies [155].

CC chemokines predominantly act as chemoattractants for monocytes and T-cells, but not neutrophils [153,156,157], whereas, CXC chemokines primarily induce the migration of neutrophils and not monocytes [153,156,157].

1.6.1 CC chemokines

The CC subfamily of chemokines, in general, do not attract neutrophils, but act with variable selectivity on monocytes, eosinophils, basophils and lymphocytes (Table 1-7) [156]. The amino acids preceding the first cysteine residue of the CC chemokines are of critical importance to their biological activity and leukocyte selectivity. The function of MCP-1 can be altered dramatically, by adding or deleting one amino acid near the N-terminus [158,159]. For example, the addition of an amino acid residue, significantly reduces the ability of MCP-1 to chemoattract monocytes [158], while the deletion of an amino acid residue changes MCP-1 from an activator of basophils to an attractant of eosinophils [159].

1.6.2 CXC chemokines

The CXC subfamily of chemokines can be further sub-divided into those that contain the sequence glutamate-leucine-arginine (ELR), immediately preceding the first cysteine residue, near the amino (N) terminus, and those that do not (Table 1-8). The presence of this structural motif determines the ability of CXC chemokines to attract and activate neutrophils, and promote angiogenesis. Chemokines lacking the ELR sequence attract lymphocytes and inhibit angiogenesis [155,157,160].

1.6.3 Chemokine receptors

The biological activities of chemokines on target cells are mediated by members of a superfamily of 7-transmembrane spanning G-protein coupled receptors (Figure 1-13) [160,161]. G-protein coupled receptors are the largest known family of cell surface receptors and mediate transmission of stimuli as diverse as hormones, neurotransmitters, inflammatory mediators, taste and smell molecules [161]. To date, 18 human chemokine receptors have been identified and their nomenclature has been assigned according to which chemokine subfamily they bind to [161]. Receptors that bind to CXC chemokines are designated CXCR, and those that bind CC chemokines, CCR. One exception, the Duffy antigen receptor complex (DARC), expressed on red blood cells and endothelial cells, binds both CXC and CC chemokines. DARC does not appear to be coupled to a G-protein and therefore the precise physiological role of this receptor has yet to be elucidated [161]. However, it may function as a 'sink' for clearing excess chemokines from the circulation, thereby maintaining a positive concentration

gradient from tissues to blood [162]. Chemokines far outnumber their receptors, and for this reason chemokine-receptor interactions may either be exclusive or promiscuous [117,160,163].

1.6.4 Intracellular signalling by chemokine receptors

Intracellular signalling by chemokine receptors depends upon coupling to heterotrimeric G-proteins composed of $\alpha\beta\gamma$ subunits (Figure 1-13) [161]. G-proteins are inactive when guanosine diphosphate (GDP) is bound to the G-protein subunit, but they become active after exchange of GDP for guanosine triphosphate (GTP) [161]. For example, IL-8 induced activation of the CXCR-1 or CXCR-2 facilitates the exchange of GDP for GTP on the G-protein. This subsequently allows the dissociation of $G\alpha$ from $G\beta\gamma$ subunits. The latter activates the membrane associated enzyme phospholipase C which in turn cleaves phosphatidylinositol 4,5-bisphosphate to form phosphatidylinositol 1, 4, 5-triphosphate (IP_3) and diacyl-glycerol (DAG). DAG and IP_3 are second messengers, which activate protein kinase C (PKC) and elicit the release of intracellular calcium (Ca^{2+}) respectively.

After activation, chemokine receptors have altered sensitivity to repeated stimulation with the same agonist(s) and become desensitised [164]. This may involve phosphorylation of the serine and threonine residues in the C-terminus of the receptor by G-protein coupled receptor kinases and the subsequent binding of arrestin molecules. Receptors are also sequestered by internalisation resulting in down regulation of the receptor at the cell surface. Desensitisation and down-regulation may be of critical importance in the ability of the cell to sense the presence of a chemoattractant gradient [161].

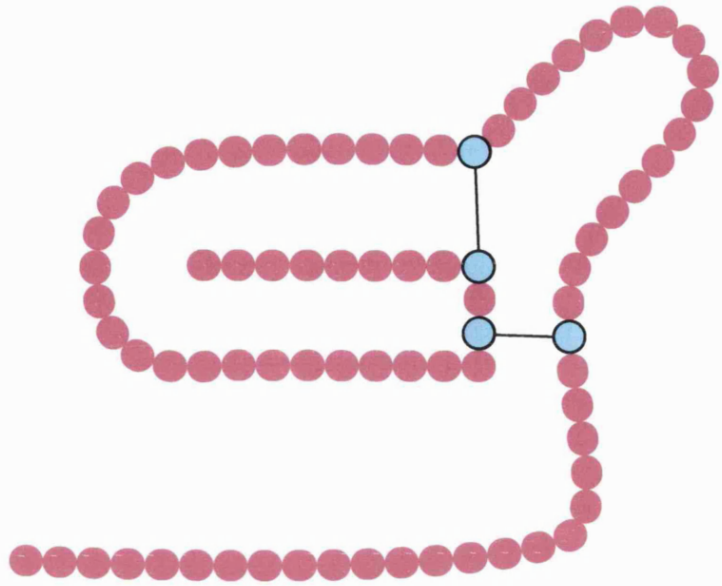

CXC chemokine

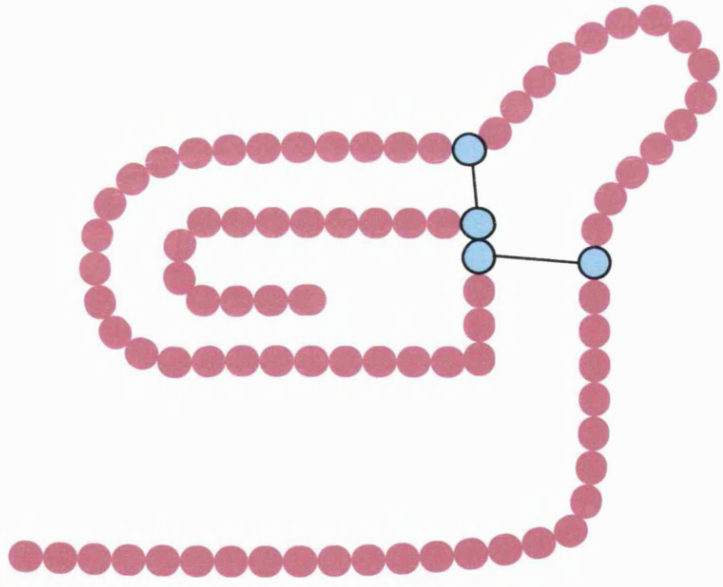

CC chemokine

Figure 1-11 A diagram showing the arrangement of the conserved cysteine residues in CC and CXC chemokines.

Chemokines can be separated into two major subfamilies based on whether the first two of four cysteine residues are separated by an amino acid (CXC) or are adjacent (CC). Adapted from [157].

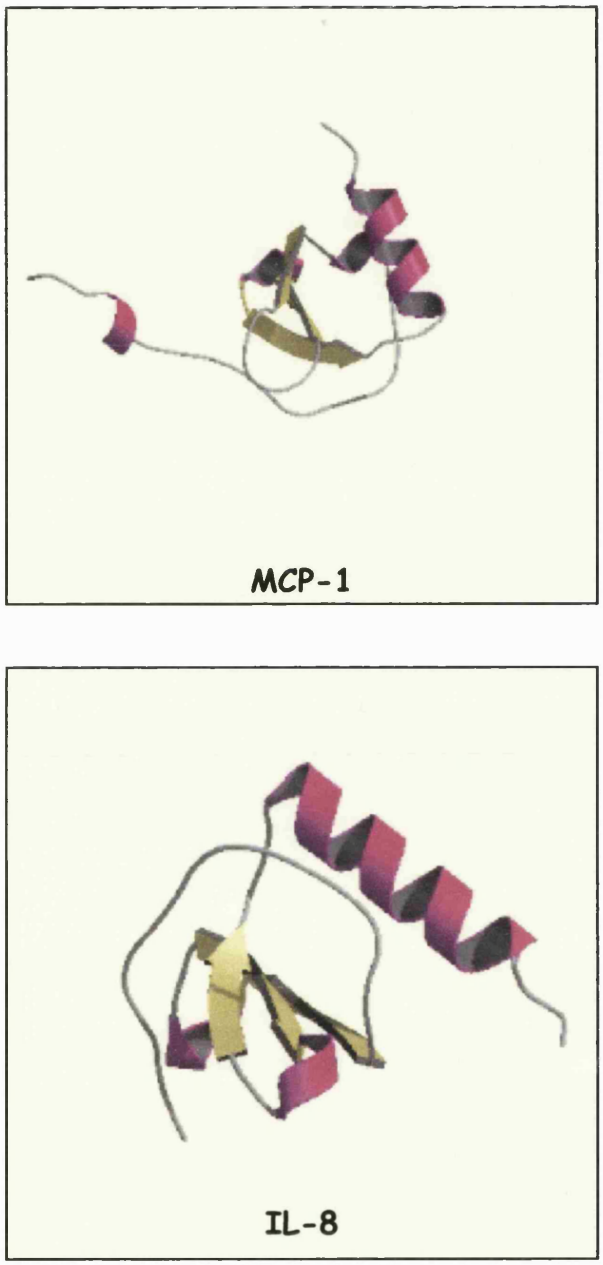

Figure 1-12 Tertiary structures of MCP-1 and IL-8

Images representing the tertiary structures of two canonical chemokines (MCP-1 and IL-8), taken from CATH website at www.biochem.ucl.ac.uk/bsm/cath_news.

C-C β-Chemokines	
Chemokine and target cell	**Biological activity *in vitro***
Monocyte chemotactic protein-1 (MCP-1), Mouse JE Monocytes T-cells Mast cells Basophils Stem cells	 Chemotaxis, adhesion, superoxide release, arachidonic acid activity, phagocytosis, killing Chemotaxis Chemotaxis, histamine release Chemotaxis, histamine release leukotriene synthesis Inhibited colony formation (CFU GM)
Monocyte chemotactic protein-2 (MCP-2) Monocytes T-cells Mast cells Eosinophils	 Chemotaxis Chemotaxis Chemotaxis, histamine release Chemotaxis
Monocyte chemotactic protein-3 (MCP-3) Monocytes T-cells Mast cells Eosinophils Dendritic cells	 Chemotaxis, arachidonate activity Chemotaxis Chemotaxis, histamine release Chemotaxis Chemotaxis
Monocyte chemotactic protein-4 (MCP-4) Monocytes T-cells Eosinophils	 Chemotaxis Chemotaxis Chemotaxis
Monocyte chemotactic protein-5 (MCP-5) mouse only Monocytes T-cells Eosinophils	 Chemotaxis Chemotaxis Chemotaxis
Eotaxin Eosinophils	 Chemotaxis
Macrophage inflammatory protein-1α (MIP-1α) Monocytes T-cells B-cells Natural killer cells Mast cells Eosinophils Basophils Dendritic cells Stem cells	 Chemotaxis, respiratory burst Chemotaxis, adhesion, collagenase release, tumour cytotoxicity Chemotaxis Chemotaxis, adhesion, tumour cytotoxicity Chemotaxis, histamine release Chemotaxis, cationic protein release Chemotaxis, histamine release Chemotaxis Inhibited colony formation (CFU-S)
Macrophage inflammatory protein-1β (MIP-1β) Monocytes T-cells Stem cells	 Chemotaxis Chemotaxis, adhesion Antagonises anti-proliferative effects of MIP-1α
Regulated on activation normal T-cell expressed and secreted (RANTES) Monocytes T-cells Natural killer cells Eosinophils Basophils Dendritic cells	 Chemotaxis Chemotaxis, adhesion Chemotaxis Chemotaxis, cationic protein release Chemotaxis, histamine release Chemotaxis
I-309 Monocytes	 Chemotaxis

Table 1-7 CC chemokines, their target cells and biological activity

Adapted from reference 157.

C-X-C α-Chemokines	
ELR containing chemokines and target cells	**Biological activity *in vitro***
Interleukin-8 (IL-8), Neutrophils T-cells Natural killer cells Keratinocytes Basophils Endothelial Cells	 Chemotaxis, adhesion, superoxide release, granule release, killing. Chemotaxis Chemotaxis Mitogenesis Chemotaxis, histamine release Angiogenesis
Growth related oncogene-α (GRO-α)/ Mouse KC **Growth related oncogene-β (GRO-β)/ Mouse MIP-2α** **Growth related oncogene-γ (GRO-γ)/ Mouse MIP-2β** Neutrophils Endothelial cells	 Chemotaxis, adhesion, activation Angiogenesis
Mouse macrophage inflammatory protein-2 (MIP-2) Neutrophils	 Chemotaxis, adhesion, activation
Epithelial cell derived neutrophil activating peptide-78 (ENA-78) Neutrophils	 Chemotaxis, activation
Granulocyte chemotactic protein-2 (GCP-2) Neutrophils	 Chemotaxis
Platelet basic protein (PBP) **Connective tissue activating peptide 111 (CTAP 111)** **β-Thromboglobulin (β-TG)** **Neutrophil activating peptide-2 (NAP-2)** Fibroblasts Neutrophils	 Chemotaxis Chemotaxis
Non-ELR chemokines and target cells	**Biological activity *in vitro***
Interferon-inducible protein of 10kd (IP-10) T-cells Natural killer cells Endothelial cells	 Chemotaxis, adhesion Chemotaxis, cytolytic activity Inhibits angiogenesis
Monokine induced by interferon-γ (MIG) Monocytes Activated T-cells Natural killer cells	 Chemotaxis Chemotaxis Chemotaxis
Platelet factor-4 (PF-4) Monocytes Neutrophils Endothelial Cells	 Chemotaxis Chemotaxis Inhibits angiogenesis
Stromal cell-derived factor-1 (SDF-1) Lymphocytes Monocytes	 Chemotaxis Chemotaxis

Table 1-8 CXC Chemokines, their target cells and biological activity.

Adapted from reference 157.

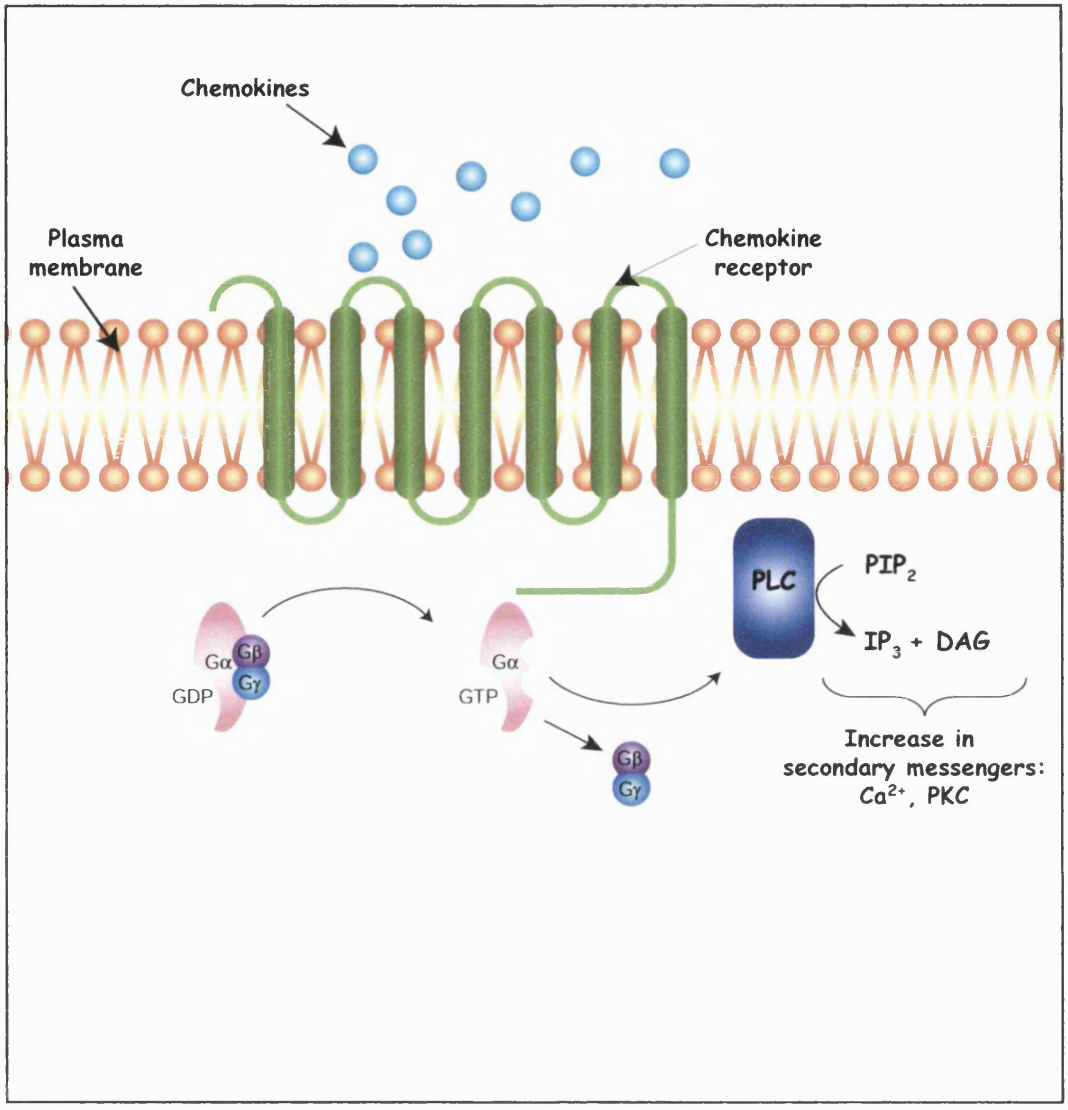

Figure 1-13 Chemokine receptor activation

G proteins contain α, β and γ subunits and exist in either an inactive GDP-bound or an active GTP-bound state. When a chemokine binds to its receptor, the GDP on the α subunit is exchanged for GTP. This causes the Gα-GTP complex to dissociate from the βγ subunit and activate the appropriate enzyme such as phospholipase C. This in turn can hydrolyze phosphatidyl inositol 4,5 bisphosphate (PIP_2), a phospholipid in the plasma membrane into the second messengers inositol 1,4,5-triphosphate (IP_3) and diacylglycerol (DAG). IP_3 causes the rapid release of Ca^{2+} from intracellular stores, whereas DAG activates protein kinase C. The system is controlled by an inherent GTPase activity which causes the bound GTP to slowly hydrolyze back to GDP, such that the α, β and γ subunits reunite in the inactive GDP bound form (not shown). The cascade nature of the pathway ensures that each bound chemokine can result in many Gα-GTPs to generate an amplified response. Adapted from reference 117.

1.7 Chemokines and atherosclerosis

Recently, the role of chemokines in atherogenesis have become the focus of intense interest and discussion. This is primarily due to their ability to attract different subsets of leukocytes, which has led to the proposition that they are key components in the pathogenesis of diseases with characteristic leukocyte infiltrates [156]. In atherosclerosis, monocyte-macrophages and T-cells are the chief inflammatory cells detected at all stages of the disease [15]. Macrophages are the precursors of lipid-laden foam cells and as a source of growth factors and inflammatory mediators are central to atherogenesis [55]. Thus, chemokines implicated in recruiting monocytes to artery wall are thought to be key initiators of atherogenesis and, therefore, targets for drug therapy.

1.7.1 Monocyte chemoattractant protein-1

As members of the CC chemokine subfamily predominantly chemoattract monocytes and lymphocytes they are intrinsically linked to the mononuclear infiltrate that characterises atherogenesis. Extensive experimental evidence supports the role of the prototypical CC chemokine, MCP-1, in the recruitment of monocytes to atherosclerotic lesions. Expression of MCP-1 is up-regulated in human atherosclerotic lesions [165-167] and is found in the arteries of rabbits [167] primates [168] and transgenic mice [73-75,169] consuming hypercholesterolaemic diets. Furthermore, monocyte transmigration into the intima, has been found to correlate with MCP-1 expression, and is inhibited by neutralising antibodies against MCP-1. Over-expression of the murine JE/MCP-1 transgene by leukocytes accelerates lesion formation in apoE$^{-/-}$ mice [169]. Equally, absence of the murine homologue, JE/MCP-1 markedly reduces atherosclerosis in LDL receptor$^{-/-}$ mice consuming a high fat/high cholesterol diet [75]. MCP-1 deficiency also reduces susceptibility to atherosclerosis in mice that over-express human apoB-100 [73]. Similarly, absence of CCR-2, the major monocyte receptor for JE/MCP-1, reduces monocyte migration [170] and markedly inhibits lesion formation in apoE$^{-/-}$ mice [74,171]. However, while the absence of MCP-1 and/or CCR-2 can delay and diminish atherosclerosis, it does not completely arrest the progression of this complex disease process [74,75,171].

1.7.2 Interleukin-8

Interleukin-8 is the prototypical member of the CXC chemokine subfamily. As this chemokine is a potent chemoattractant of neutrophils it was not envisaged that IL-8 would play a role in atherosclerosis. However, recent data implicates members of the CXC chemokine subfamily in atherogenesis. *In vitro* studies have suggested that IL-8

production and secretion by arterial cells is enhanced following incubation under pro-atherogenic stimuli, including; cholesterol loading [172], oxidised LDL [173], oxysterols [174] and inflammatory cytokines [175]. Furthermore, macrophages isolated from human atheromatous plaques show increased capacity to produce IL-8 [176] and immunoreactive IL-8, GRO-α and murine KC have been detected in macrophage-rich areas of lesions [177]. However, despite the presence of IL-8 and the adhesion molecules required for neutrophil recruitment (E-selectin, ICAM-1), few if any, neutrophils are found in atherosclerotic lesions [116]. A possible explanation for this paradox is that under certain conditions, IL-8 can inhibit neutrophil adhesion to cytokine activated endothelium. Indeed, mice overexpressing human IL-8 have been shown to have impaired neutrophil migration to inflammatory sites [178]. Furthermore, it has been shown that the intravenous injection of IL-8 inhibits inflammation [179]. This is maybe due to the loss of the chemokine gradient needed for the attraction and transmigration of leukocytes to sites of inflammation [178]. Alternatively, chronic high circulating concentrations may induce receptor desensitisation and down regulation in leukocytes (Section 1.6.4).

However, under certain conditions neutrophils are recruited to the vessel wall and involved in arterial injury. Evidence suggests a role for neutrophils during restenosis after percutaneous intervention [180-182] and in experimental induced arteriopathies [183-185]. For example, neutrophils accumulate in the tunica media following the first few hours after balloon injury following percutaneous transluminal coronary angioplasty (PTCA) [183] and after myocardial injury as a result of an acute myocardial infarction [186,187]. Recently, transient but significant rises in serum concentrations of IL-8 were observed during the very early phase of acute myocardial infarction [186]. Thus, IL-8 may be an important mediator in the development of myocardial injury during acute myocardial infarction.

The contribution of IL-8 to atherogenesis is not yet fully elucidated. Studies *in vitro* have established the ability of IL-8 to chemoattract lymphocytes and promote neovascularisation of the cornea [188,189]. These properties may be relevant for lymphocyte recruitment into plaques, and neovascularisation of the intima. Recently, however, an IL-8 receptor, CXCR-2, was discovered in macrophage-rich areas of human atherosclerotic plaques [177]. Furthermore, the murine homologue of CXCR2, murine IL-8 receptor homologue (mIL-8RH), was also detected in macrophage-rich areas of aortic lesions in LDL receptor$^{-/-}$ mice, consuming an atherogenic diet for sixteen weeks. Significantly, the absence of this receptor (mIL-8RH$^{-/-}$) in bone marrow

derived peripheral blood leukocytes was associated with reduced lesion area, and markedly reduced recruitment of mIL-8RH positive and MOMA-2 (monocyte-macrophage marker) positive cells [177]. This implicates the CXCR2 chemokine receptor in the recruitment of monocytes into atherosclerotic lesions. However, the effects of receiving mIL-8RH$^{-/-}$ bone marrow were more pronounced at later stages of lesion development *in vivo*, suggesting that this receptor may play a role in retention and expansion of intimal macrophages, rather than in the initial process of monocyte recruitment [177,190]. Other CXC chemokines that bind to CXCR-2, such as growth related oncogene-α (GRO-α), may also be involved in atherogenesis; indeed endothelial cell-bound GRO-α has been shown to promote monocyte adhesion [191] and both IL-8 and GRO-α are capable of inducing monocyte adhesion *in vitro*, particularly under flow conditions [192]

1.7.2.1 Murine KC and MIP-2

Mice lack an IL-8 homologue [193], but have two GRO chemokines, KC and macrophage inflammatory protein-2 (MIP-2), that interact with the murine equivalent of the CXCR2, namely the mIL-8RH. The expression of KC, which shares 65% mRNA sequence identity with human GRO-α, is regulated in a similar manner to human IL-8. Thus, KC is up-regulated by pro-inflammatory cytokines, such as IL-1α, IL-1β and TNF-α as well as bacterial lipopolysaccharide (LPS), and by oxidised LDL (oxLDL) [162,194]. Furthermore, KC is a potent chemoattractant and activator of neutrophils [162,194], causing the up-regulated expression of the β_1 integrin, Mac-1, on the surface of neutrophils [162,193,195] and eliciting a respiratory burst in these cells [162]. KC has been detected within atherosclerotic lesions in LDL receptor$^{-/-}$ mice consuming an atherogenic diet [177]. MIP-2, which shares 60% mRNA sequence identity to human GRO-β and GRO-γ, is also a potent neutrophil chemoattractant and activator.

Interestingly, local expression of both KC and MIP-2 are elevated during hepatic ischaemia-reperfusion injury [196,197]. Antibody neutralisation of these chemokines significantly reduced hepatic neutrophil accumulation, oedema and tissue damage [196,197]. It is tempting to speculate that neutralisation of these chemokines or their human equivalents could reduce tissue damage during myocardial infarction.

1.8 Transcriptional regulation of adhesion molecules and chemokines

1.8.1 Nuclear factor-kappa B

A possible link between risk factors for atherosclerosis and enhanced adhesion molecule and chemokine expression is the nuclear factor-kappa B (NF-κB) transcription factor pathway. Although adhesion molecules and chemokines are structurally and functionally distinct, the genes for these molecules are induced at the transcriptional level by this system [198].

NF-κB consists of dimeric complexes of members of the Rel protein family of which the heterodimer p50/p65 is the best characterised. In quiescent cells, NF-κB is sequestered in the cytoplasm by the binding of an inhibitor from the inhibitor kappa B family (IκB), to the p65 subunit of NF-κB. Upon activation of the cell, NF-κB inducing kinase (NIK) phosphorylates the IκB kinase complex which in turn phosphorylates IκB to signal its ubiquination and degradation (Figure 1-14). Degradation of IκB exposes a nuclear localisation sequence on the p65 subunit of NFκB, which is then able to translocate to the nucleus and bind to a specific promotional DNA sequence, thereby influencing the transcription of NF-κB-dependent genes (Figure 1-14).

NF-κB and its inhibitor, IκB act in an autoregulatory mechanism. After removal of the inflammatory stimulus, the IκB pool is replenished because NF-κB induces expression of the gene for IκB. IκB translocates to the nucleus and displaces the transactivating form of NF-κB. The inactive NF-κB/IκB complex is transported back to the cytoplasm, therefore reducing gene expression and returning the activated cell to the resting state [198]. In atherosclerosis, dysfunction of this control mechanism may contribute to prolonged NF-κB activation and thus contribute to the changes in gene expression during the disease [198].

The NF-κB system is activated by a variety of diverse pro-atherogenic stimuli such as cytokines, bacterial LPS, oxidative stress, advanced glycosylation end products and physical forces [198]. Conversely, antioxidants and other anti-inflammatory agents are potent inhibitors of this system [198]. Atherosclerotic lesions contain many molecules that can activate NF-κB, thereby enhancing the expression of genes for monocyte recruitment. Indeed, there is increased expression of a variety of genes regulated by NF-κB at sites of lesion formation including VCAM-1, ICAM-1, MCP-1 and IL-8 [198]. Recently, it was demonstrated that blocking NF-κB activity in endothelial cells, using anti-sense oligonucleotides, inhibited ICAM-1 and MCP-1 expression [199].

Activated NF-κB has been identified *in-situ* in smooth muscle cells, macrophages and endothelial cells of atherosclerotic lesions [200]; activated NF-κB was not evident in vessels obtained from healthy controls [200]. Interestingly, a correlation exists between pro-atherogenic agents and NF-κB activation, and anti-atherogenic factors and stabilisation of the system, again suggesting that NF-κB may play a key role in switching on genes involved in atherogenesis [198].

1.9 Oxidative stress and atherosclerosis

Oxidative stress can be regarded as an increase in free radical generation and/or decrease in antioxidant defences. As such, it is thought to play an important contributory role in the pathogenesis of many diseases including atherosclerosis. The oxidation hypothesis of atherosclerosis proposes that LDL oxidation plays a key causative role in early atherogenesis (Figure 1-15) [201,202]. Oxidised LDL has been identified in atherosclerotic lesions [203-206] and autoantibodies that recognise products of LDL oxidation have been found in the serum of patients with carotid atherosclerosis [207]. Importantly, these autoantibodies have been shown to have some predictive value in assessing the severity of atherosclerosis [207].

The process of LDL oxidation is believed to begin in the subendothelial space in which all major cells, including endothelial cells, smooth muscle cells and monocyte/macrophages are capable of oxidising LDL [7]. Trapped LDL (Section 1.1.2.1.4) can undergo oxidative modification to become mildly oxidised. Mildly oxidised LDL or minimally modified LDL (mmLDL) is a particle in which lipid peroxidation and lipid hydroperoxide decomposition are in the early stages and the apoB-100 molecule is still intact [7]. Further oxidation leads to chemical alterations in the apoB-100 component of the LDL molecule (oxLDL) such that the particle is now recognised and internalised by macrophages via scavenger receptors [7]. Biological properties of mmLDL and oxLDL differ considerably [208]. For example, mmLDL does not cause macrophage lipid accumulation, whereas oxLDL can be taken up by scavenger receptors leading to eventual foam cell formation [19,209]. Highly oxLDL is also cytotoxic to cells leading to further endothelial damage and increased endothelial permeability, which favours the entry of LDL, circulating monocytes and hence a continuation of the disease process [19,210].

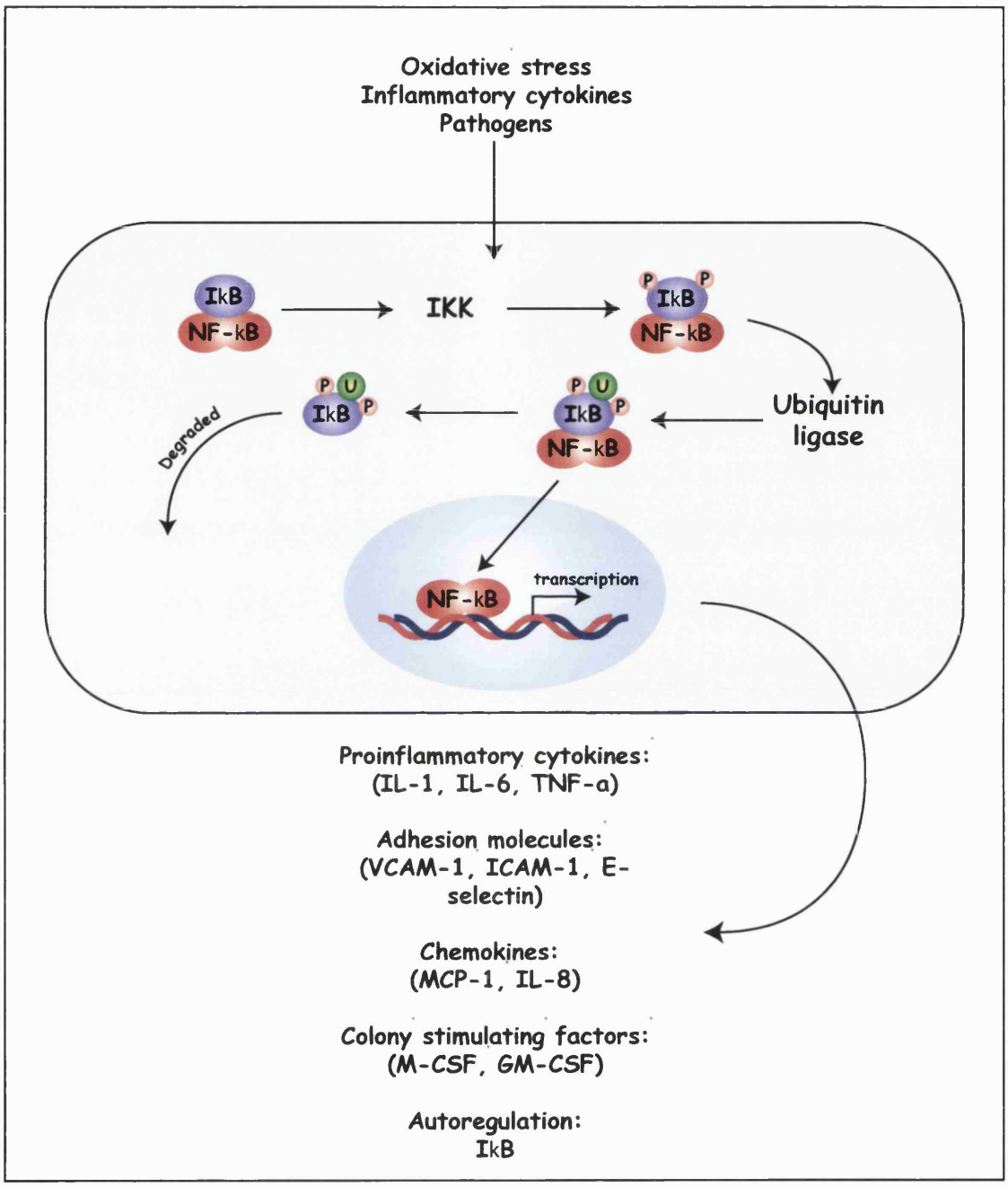

Figure 1-14 Activation of NF-κB.

NF-κB inducing kinase (NIK) activity (not shown) is induced following stimulation of the cell with various agents including inflammatory cytokines, oxidative stress and pathogens. This in turn phosphorylates IκB kinase (IKK) (not shown), which is responsible for the phosphorylation of two critical serine residues on IκB. The phosphorylated IκB is then ubiquinated by IκB ligase and subsequently degraded by the 26S proteasome (not shown). NF-κB is then free to enter the nucleus and initiate transcription. Adapted from reference 198 and 211.

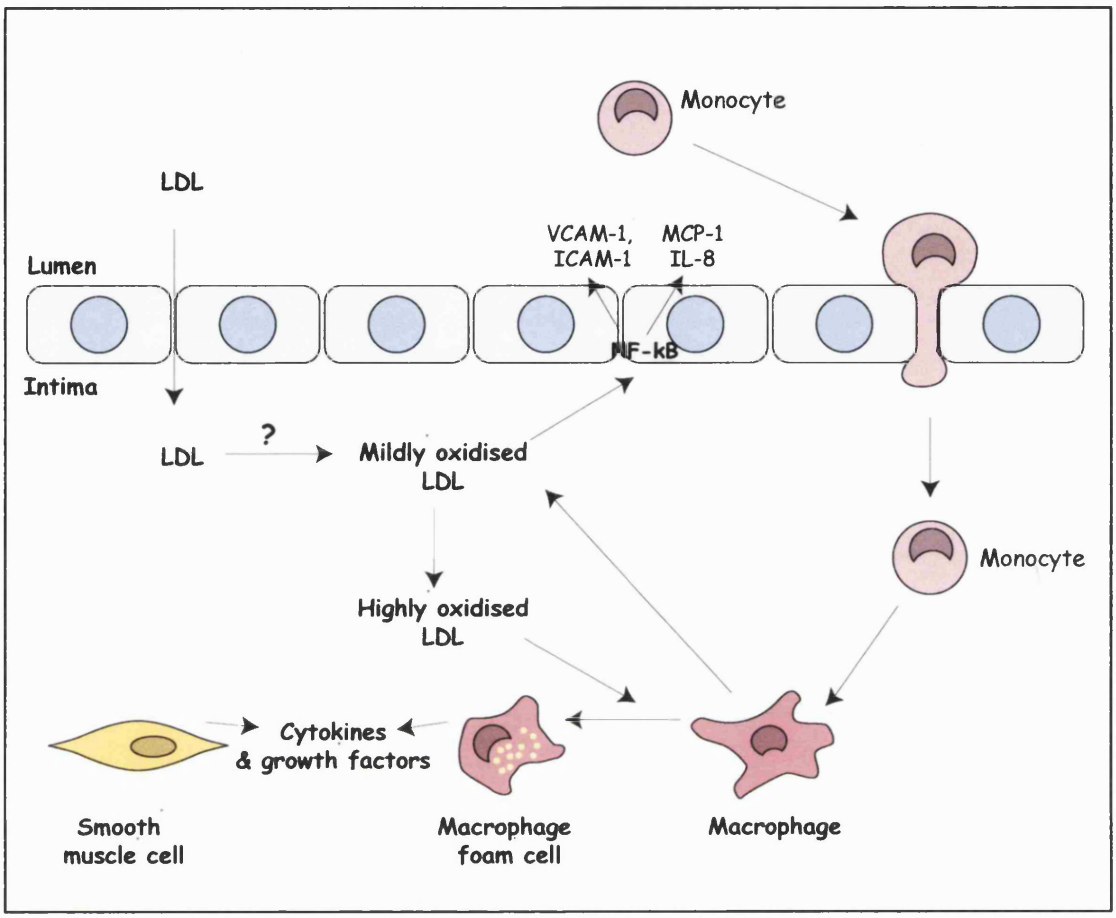

Figure 1-15 Current 'oxidation' hypothesis

Low-density lipoprotein once in the subendothelial space can become minimally modified by mechanisms, which have yet to be fully elucidated. Minimally modified LDL can stimulate cells in the arterial wall to produce adhesion molecules and chemokines via the activation of NF-κB. As a consequence, monocytes infiltrate the intima and differentiate into tissue macrophages. Further oxidation of mmLDL initiates changes in the apoB-100 moiety. Extensive lipid peroxidation generates aldelydic fatty oxidation products and results in the modification of lysine residues in apoB-100. The LDL particle is now highly oxidised and is recognised by the macrophage scavenger receptor. Lipid uptake via this route is unregulated, and the macrophage engulfs vast amounts of lipoprotein associated cholesteryl ester and becomes a lipid-laden macrophage foam cell.

Minimally modified LDL contains biologically active phospholipid oxidation products which include 1-palmitoyl-2-(5-oxovaleryl)-*sn*-glycero-3 phosphocholine (POVPC), 1 palmitoyl-2-glutaryl-*sn*-glycero-3-phosphocholine (PGPC) and 1-palmitoyl-2(5,6-epoxyisoprostane E_2)-*sn*-glycero-3-phosphorylcholine (PEIPC) [212]. These oxidised phospholipids can bring about their effects by binding to a receptor similar to the platelet-activating factor (PAF) receptor expressed on monocytes, endothelial and smooth muscle cells [213]. Indeed, all three of these oxidised phospholipids enhance monocyte binding to endothelial cells [214,215]. PGPC can induce the expression of VCAM-1 and E-selectin, and it was shown that PGPC but not POVPC induce neutrophil binding to endothelial cells [214]. However, POVPC in the presence of PGPC inhibit neutrophil binding and E-selectin expression in endothelial cells [214]. Navab *et al* [212], hypothesised that the ratio of POVPC and PGPC may determine whether an acute (neutrophilic) or chronic (monocytic) inflammation would result in any given tissue. The presence of these oxidised phospholipids have been demonstrated in rabbit atherosclerotic lesions [215] and autoantibodies, which recognise these oxidised phospholipid products are present in apoE$^{-/-}$ mice [216].

1.9.1 Mechanisms of LDL oxidation

For a number of years the association between elevated plasma LDL concentrations and accelerated atherogenesis was poorly understood. Incubation with native LDL does not generate foam cells, due to the highly regulated nature of the LDLR (Section 1.1.2.1.4) and therefore it was proposed that LDL is modified by oxidation within the vessel wall. However, the actual mechanism(s) by which LDL becomes oxidised *in vivo* has yet to be elucidated. Lipoxygenase enzymes are cytosolic enzymes that insert molecular oxygen into polyunsaturated fatty acids yielding products such as hydroperoxyeicosatetraenoic acid (HPETE) [7] which could 'seed' LDL and increase susceptibility to oxidation. Mice deficient in 12/15-lipoxygenase, on an apoE knockout background, have markedly reduced lesion area compared with control animals [217]. In contrast, the over-expression of 15-lipoxygenase in LDL receptor$^{-/-}$ mice was associated with enhanced atherogenesis and LDL isolated from these mice was more susceptible to *ex vivo* oxidation than LDL isolated from control animals [218]. Moreover, 12/15-lipoxygenase mRNA and protein are highly expressed in lesions and are associated with regions stained for the presence of oxLDL [219]. Other candidate oxidising species, which may be produced by cells in the vessel wall, include peroxynitrite and myeloperoxidase [1,220]. Peroxynitrite is formed by the reaction of superoxide with nitric oxide and can promote LDL oxidation [220]. Peroxynitrite reacts with tyrosine to yield a stable end product known as 3-nitrotyrosine.

This has been detected in human atherosclerotic tissue [221], suggesting that reactive nitrogen species may be involved in the oxidation of LDL [220]. Myeloperoxidase can generate highly reactive species such as hypochlorous acid and tyrosyl radicals, which may promote the oxidation of LDL *in vivo*. Indeed, this enzyme [222] and its oxidation products [223] have also been identified in atherosclerotic lesions. Once oxidised, LDL increases its suitability as a substrate for sphingomyelinase, an enzyme that is know to aggregate LDL and thereby enhance its uptake by macrophages [25]. Thus, it is likely that as the lesion develops, multiple oxidising species may promote the oxidation of LDL. The extent of oxidised LDL produced is likely to be determined by the balance between pro- and anti-oxidant elements within the vessel wall.

1.9.2 OxLDL and generation of macrophage foam cells

One of the most important ways in which oxLDL is pro-atherogenic is that it causes the deposition of large amounts of lipoprotein derived cholesterol within macrophages. Indeed, the hallmark of atherosclerotic lesions is the macrophage foam cell. Oxidised LDL is no longer recognised by the LDL receptor and is instead recognised by macrophage scavenger receptors [224]. Uptake via this route is unregulated, leading to internalisation and degradation of oxLDL in lysosomes. Thus, cholesteryl ester is rapidly hydrolysed by lysosomal acid lipase and free cholesterol is released into the cytosol where it is re-esterified via the action of ACAT. As scavenger receptor expression is not down-regulated by cellular cholesterol content, the macrophage take up excessive amounts of oxLDL to become a lipid-laden foam cell. A number of scavenger receptors have been identified and include Scavenger Receptor (SR)-AI/II, SR-B1, CD36, CD68 and macrosialin [19,224]. The effect of these receptors on atherosclerosis has been examined in knockout murine models. For example, Febbraio *et al* [225] demonstrated that the absence of CD36 decreases the severity of atherosclerosis by 70% in apoE$^{-/-}$ mice. Furthermore, Suzuki *et al* [226] have shown that knocking out SRA in apoE$^{-/-}$ mice reduces lesion area but the effect was less striking when compared with the CD36 x apoE$^{-/-}$ knockout mouse. Paradoxically, SR-AI/II deficiency in apoE*3 Leiden mice did not affect, or slightly increased, development of atherosclerotic lesions [227].

1.9.3 LOX-1, an endothelial receptor for oxLDL

Vascular endothelial cells internalize and degrade oxLDL through a receptor-mediated pathway that does not involve the classic macrophage scavenger receptor [228]. The endothelial receptor for oxLDL is known as LOX-1. It is a membrane protein that belongs structurally to the C-type selectin family and is expressed *in vivo* in

vascular endothelium [229]. LOX-1 does not share any structural homology with other known molecules that can acts as a receptor for oxLDL [229]. LOX-1, like scavenger receptors, does not internalise native LDL [228]. Recently, it was demonstrated that TNF-α stimulation [230] and fluid shear stress [231] markedly upregulate LOX-1 gene expression in endothelial cells. Indeed, oxLDL itself upregulates the expression of its own endothelial receptor, in a concentration dependent manner [228]. This characteristic may be the basis of the increased uptake of oxLDL and endothelial activation and dysfunction as plasma LDL concentrations rise. Furthermore, oxLDL induces apoptosis of human coronary artery endothelial cells via the action of LOX-1 [228]. This process can be blocked by the addition of chemical inhibitors to LOX-1 or highly specific antisense probes to LOX-1 mRNA [228]. This receptor is highly expressed in the blood vessels of animals and humans with hypertension [232], diabetes mellitus [233] and atherosclerosis [234,235]. Expression of this receptor may also be relevant in intra-arterial thrombogenesis and myocardial ischemia- reperfusion injury [236]. Thus, LOX-1 may initiate endothelial injury in the presence of oxLDL.

1.9.4 Antioxidants

Antioxidants are a generic term used to describe both enzymatic and non-enzymatic molecules, which scavenge free radicals and related reactive species and thus guard against oxidative processes [237]. Free radicals are atoms or molecules containing an unpaired electron and include the hydroxyl radical ($HO^{\cdot}$), the peroxyl radical ($ROO^{\cdot}$) and the superoxide radical ($O_2^{\cdot-}$) [237]. Reactive non-radical species include hydrogen peroxide (H_2O_2), peroxynitrite ($ONOO^-$) and singlet oxygen ($^1O_2$) [237]. Free radicals can cause damage to proteins, lipids and DNA either directly, or via the generation of reactive non-radical compounds [237].

Oxidative stress refers to an imbalance between the damaging effects of free radicals and the protective action of antioxidants. The most prominent dietary antioxidants are vitamin C (ascorbate), vitamin E (or α-tocopherol, the most biologically active form of vitamin E) and β-carotene (Figure 1-16). Vitamin E is lipophilic and acts as a chain breaking antioxidant: it inhibits lipid peroxidation and scavenges lipid peroxyl radicals (Figure 1-17) [237]. In doing so, vitamin E becomes a radical itself, the α-tocopheroxyl radical, however, this species is much less reactive than the peroxyl radical. Dietary sources of vitamin E include whole grains, nuts and seeds, vegetable oils and animal fats. Studies have shown that vitamin E supplementation can reduce LDL oxidation *ex vivo* [238], and that vitamin E may have other athero-protective qualities

including the ability to decrease platelet aggregation [239] and the suppression of adhesion molecule and chemokine production from endothelial cells and monocytes [240]. This may in part be due to the ability of vitamin E to inhibit the activation of NF-κB transcription factor pathway [241]. Similarly, α-tocopherol decreases stimuli-induced expression of β_1 and β_2 integrins on leukocytes and the adhesion of these cells to cultured endothelial cells [242]. Importantly, vitamin E supplementation has been shown to decrease oxidative stress as measured by the formation of F_2 isoprostanes in $apoE^{-/-}$ mice consuming an atherogenic diet [243]

Vitamin C is a water-soluble antioxidant and an effective scavenger of the $O_2^{\cdot}$, H_2O_2, $HO^{\cdot}$, $ROO^{\cdot}$ and $^1O_2$. It also regenerates vitamin E from the vitamin E radical, and dietary sources include fruit, especially citrus and green leafy vegetables. Studies on the effects of vitamin C supplementation on *ex-vivo* LDL oxidation are sparse, primarily because vitamin C is removed from LDL during its isolation from plasma [244]. However, *in-vitro* studies have demonstrated that physiological concentrations of vitamin C strongly inhibit LDL oxidation by vascular cells and neutrophils [245,246]. Vitamin C may prevent oxidative modifications of LDL by scavenging free radicals in the aqueous environment thereby preventing them from interacting with and oxidising LDL [247]. Also, vitamin C can prevent the pro-oxidant activity of α-tocopherol by reducing α-tocopheroxyl radical to α-tocopherol. Recently, the role of vitamin C in inhibiting cell adhesion has been examined in smokers [248]. These individuals have decreased plasma concentrations of vitamin C and monocytes isolated from smokers showed increased adhesion to cultured endothelial cells compared with monocytes isolated from non-smokers [248,249]. This suggests that plasma vitamin C inhibits the upregulation of ligands on monocytes possibly by inhibiting the activation of the NF-kB transcription factor pathway.

β-Carotene is a natural lipophilic antioxidant, which is also present in lipoproteins. Reactive oxygen species scavenged by this antioxidant are $^1O_2$ and $ROO^{\cdot}$. β-Carotene is the major dietary source of vitamin A and is found in fruit, carrots and green leafy vegetables. Some studies have shown that of consumption of β-carotene increases the resistance of LDL to *ex-vivo* oxidation [250], although conflicting reports exist [251,252].

1.9.4.1 Antioxidants and atherosclerosis

Since LDL oxidation in the artery wall is thought to be a key event in early atherogenesis, agents that can prevent LDL oxidation, such as antioxidants, should, in

theory, retard the development of atherosclerosis. Thus, dietary antioxidants such as ascorbate, α-tocopherol and β-carotene can protect against the development and progression of atherosclerosis in experimental animals [243,253,254]. Numerous observational studies have suggested that people with a higher intake of antioxidants either from their diet or from supplements, have a lower incidence of coronary vascular disease (CVD). Most trials have used vitamin E, the major lipid soluble antioxidant in human plasma and lipoproteins. In a trial conducted in male healthcare professionals, free from overt CHD, diabetes and hypercholesterolaemia, assessment of dietary vitamin content revealed a lower risk of subsequent CHD among men with higher vitamin E and β-carotene intakes [255]. Similar effects of vitamin E and β-carotene in protecting against CHD were observed in the Nurses' Health Study [256]. Data provided by the Massachusetts Elderly Cohort Study indicated the benefits of β-carotene on the incidence CVD mortality [257]. Finally, the First National Health and Nutrition Examination Survey (NHANES) showed a negative correlation between vitamin C intake and CV death [258]. Furthermore, a reduction in CAD events were observed in the elderly taking vitamin E compared with those not consuming additional vitamin E [259].

These promising earlier studies were followed up by large randomised clinical trials, in order to confirm the benefits of consuming dietary antioxidants, like vitamin E, vitamin C and β-carotene on CVD morbidity and mortality. However, the outcome of these trials are often disappointing and conflicting. In the Alpha-Tocopherol, Beta-Carotene Cancer Prevention Study (ATBC) which was designed to determine whether supplements of vitamin E and β-carotene had any effects on cancer rates, a follow-up study demonstrated no effects on CVD [260]. The negative results of this study were thought to be attributable to the dose of vitamin E employed, which was well below those used in the observational studies [261]. The Beta-Carotene and Retinol Efficacy Trial, represents another study with a primary end point on the incidence of cancer. However, this trial was terminated before schedule as there was a 28% increase in lung cancer in the supplemented group, and a non-significant 26% increase in CVD mortality [262]. The Heart Outcomes Prevention Evaluation (HOPE) study, investigated men and women over the age of 55 who were at high risk of a cardiovascular event because they had CVD or diabetes, plus one or more risk factors [263]. It found that no significant difference in death or morbidity from cardiovascular causes between patients receiving placebo or vitamin E. However, the study has been criticised for not measuring plasma vitamin E levels to confirm supplementation and for using natural vitamin E, which contains tocopherols and tocotrienols [264]. Alpha tocopherol is the

most potent member of the vitamin E family and therefore this may have bearings on the results of this study. Similarly, some investigators in the Gruppo Italiano per lo Studio della Sopravvivenza nell'Infarto Miocardico (GISSI) trial have reported negative results [265]. Endpoints of this study included death, non-fatal myocardial infarction and stroke. However, others have questioned the data analysis of this study and instead have reported a significant reduction (20%) in cardiovascular death in the vitamin E supplemented group compared with the control group [264].

Some trials have reported positive results using dietary antioxidants. In the Cambridge Heart Antioxidant Study (CHAOS), a strikingly positive effect of vitamin E supplementation in patients with documented CHD was observed [266]. It was found that those receiving vitamin E experienced a significant reduction in CAD deaths and non-fatal myocardial infarction. Furthermore, a significant inverse correlation of vitamin E with mortality from CHD was observed in a vitamin sub-study of the MONItoring trends and determinants of CArdiovascular disease (MONICA) trial [264]. Finally, the Secondary Prevention with Antioxidants of Cardiovascular Disease in Endstage Renal Disease (SPACE) trial demonstrated an impressive 50% reduction in cardiac events in renal patients with established disease receiving vitamin E [267]. However, the trial was small and of limited duration.

In summary then, there seems to be no clear consensus that antioxidant supplementation in humans ameliorates the effects of atherosclerosis. The reasons for this are as yet unclear, although several explanations have been proposed. One possibility relates to the dose response between antioxidants and effects on CVD. It could be that in a well nourished population, most individuals are receiving the maximum benefits of antioxidant vitamins from a healthy diet. Another common criticism is that antioxidant vitamins may be more effective in primary prevention rather than secondary intervention. However, the only large-scale studies with positive results used individuals with established disease [266,267].

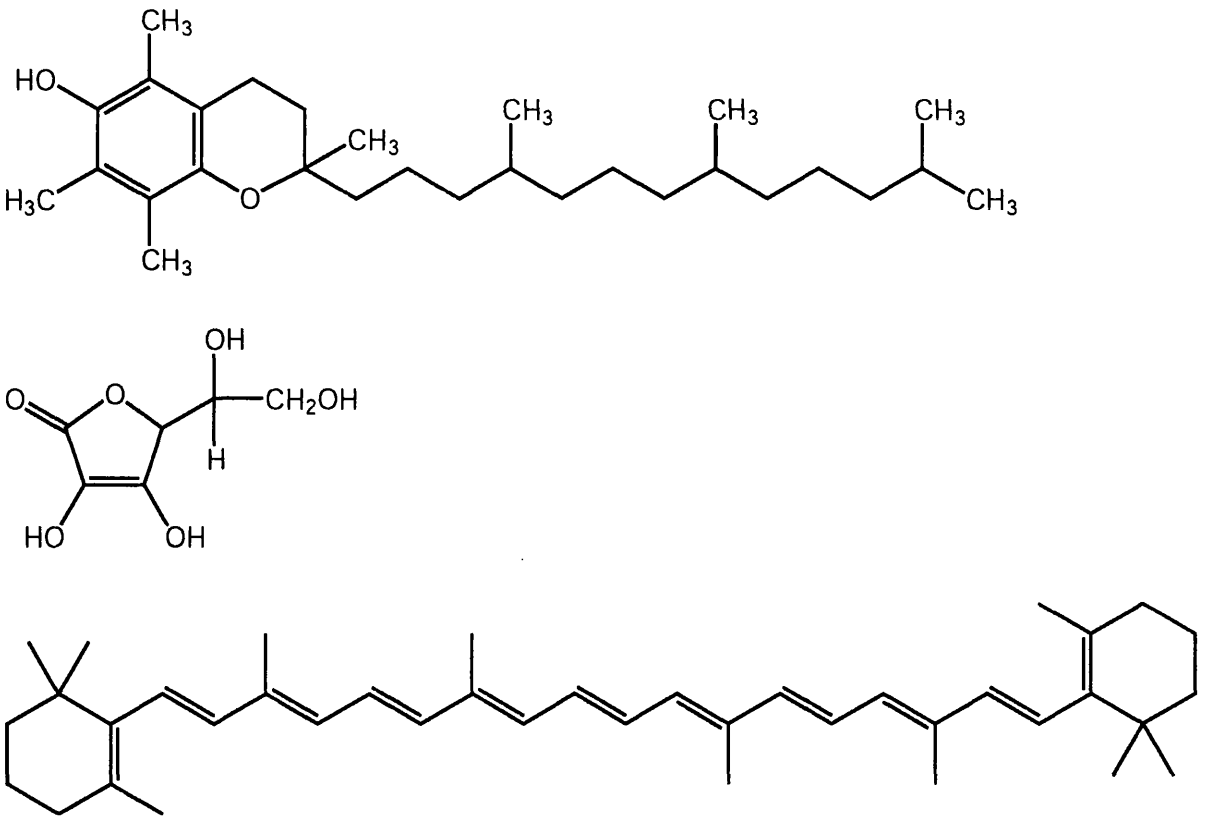

Figure 1-16 Structures of α-tocopherol, ascorbic acid and β-carotene

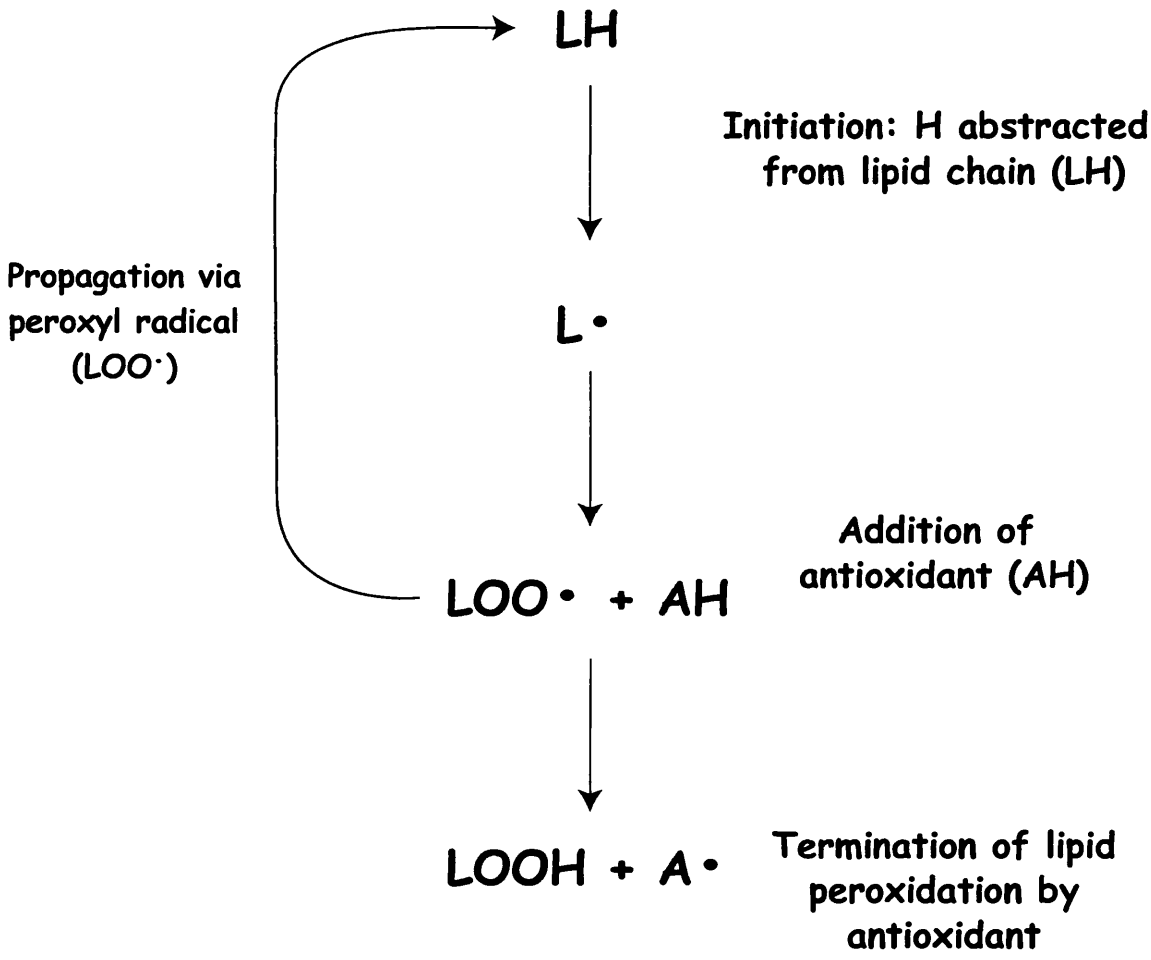

Figure 1-17 Mechanism of action of a 'chain-breaking' antioxidant

In this lipid peroxidation reaction, a hydrogen (H) is removed from the fatty acid (LH) to give a carbon centred radical (L·) which reacts to give peroxyl radical (LOO·). The peroxyl radical can attack another lipid molecule, thereby propagating lipid peroxidation. However, if an antioxidant (AH) is present, hydrogen is donated to the peroxyl radical generating a lipid peroxide which can be removed by glutathione peroxidase. The resultant antioxidant is much less reactive than the peroxyl radical.

1.9.5 Paraoxonase, LDL oxidation and atherosclerosis

Paraoxonase (PON1) is an esterase associated with HDL, thought to confer protection against LDL oxidation *in vivo* [268]. This activity may, in part, explain the anti-atherogenic properties of this lipoprotein [268]. PON1 can destroy biologically active phospholipids and lipid peroxides (Section 1.9) [269]. In doing so, PON1 may protect against the induction of inflammatory genes in arterial cells by destroying the biologically active lipids in mildly oxidised LDL [268].

PON1 is a member of a multigene family with 2 other PON like genes designated PON2 and PON3 [270]. However, PON1 is the only allozyme that has been found in human plasma to date [268]. The gene product of PON2 has yet to be identified in biological tissues whereas PON3 has been found on rabbit HDL, reviewed in reference 269. Recent data suggests that PON3 has similar anti-atherogenic properties as PON1 [271]. Major polymorphisms of PON1 include the replacement of glutamine (Q) by arginine (R) at position 192, and of leucine (L) by methionine (M) at position 55 [268]. PON1 variants possess different activities towards different substrates. HDL isolated from individuals with the PON1 55 MM/PON1 192 QQ possessed the greatest ability to protect against LDL oxidation *ex vivo*, reviewed in reference 269. However, there is currently a great deal of controversy over whether certain polymorphisms of the PON1 gene are associated with altered coronary heart disease risk. Some studies suggest a positive association [272,273] while others show no relationship [274,275].

Shih *et al* [276] examined the association between paraoxonase activity and atherosclerosis in inbred strains of mice differing in their susceptibility to atherosclerosis. C57BL/6J mice are susceptible to diet-induced fatty streak lesions (Section 1.2.2) whereas C3H/HeJ mice are resistant to atherosclerosis. When both strains were fed a non-atherogenic diet, the HDL from both strains protected against LDL oxidation *in vitro* [276]. However, when fed an atherogenic diet, HDL isolated from C57BL/6J mice was unable to inhibit LDL oxidation whereas HDL isolated from C3H/HeJ retained this property. The ability of HDL to prevent LDL oxidation was correlated with levels of paraoxonase. The expression of paraoxonase was decreased in C57BL/6J mice fed an atherogenic diet but maintained in the C3H/HeJ mice [276]. Further, in mice derived from crossing C57BL/6J with C3H/HeJ, paraoxonase expression co-segregated with the extent of atherosclerosis [276]. Notably, HDL isolated from PON1 knockout (PON1$^{-/-}$/C57BL/6J) mice failed to protect LDL against oxidation and these animals were more susceptible to diet induced atherosclerosis [277]. Recently,

a PON1$^{-/-}$/apoE$^{-/-}$ double knockout mouse has been generated [278]. These mice have increased lipoprotein oxidation, higher levels of POVPC, PGPC and PEIPC in their IDL and LDL fractions and markedly increased lesion development compared with apoE$^{-/-}$ controls [278]. Decreased levels of paraoxonase were also noted in apoE$^{-/-}$ and LDL receptor$^{-/-}$ mice after consumption of an atherogenic diet [276]. Furthermore, serum activity and hepatic expression of PON1 mRNA are dramatically decreased during the acute phase response (APR, Section 1.10.5) by exposure to LPS, TNF-α or IL-1 [279].

Immunohistochemical analysis of atheromatous tissue removed from individuals undergoing coronary artery bypass has shown PON1 accumulation to be enhanced compared with arteries obtained from healthy controls [280]. Low serum PON1 concentrations and activity are associated with several patient groups at increased risk of atherosclerosis, such as individuals with hypercholesterolaemia, diabetes, patients with vascular disease and those recovering from myocardial infarction [268]. Indeed, Navab *et al* [281] have suggested that apoJ/PON1 ratio to be a better marker of atherogenic risk than the total cholesterol/HDL cholesterol ratio.

1.10 Serum markers of atherogenesis

1.10.1 Soluble adhesion molecules

Soluble forms of E-selectin, ICAM-1 and VCAM-1 were first discovered in the supernatant of cytokine-activated cultured endothelial cells [282], initiating a plethora of studies looking at soluble adhesion molecules in relation to disease. The precise mechanism by which adhesion molecules are released into the circulation is unclear. Available evidence suggests that soluble P-selectin may be the product of alternative splicing and not cleavage of a longer cell associated form [128]. In contrast, soluble forms of VCAM-1, ICAM-1 and E-selectin appear to be generated by proteolytic cleavage, at a site close to the transmembrane domain, releasing a virtually intact extracellular domain which retains ligand binding activity. Recent data suggests the enzyme responsible for VCAM-1 release may be a zinc dependent metalloprotease activated by PKC [283]. L-selectin, an adhesion molecule present on leukocytes can be cleaved by the metalloproteinase L-selectin sheddase [284]. In mice, the truncated minor isoform of VCAM-1, which is attached to the membrane via GPI linkage, is released by phospholipase C [136].

Shedding of soluble adhesion molecules may provide a rapid means of de-adhesion, down-regulating the inflammatory response and subsequent leukocyte recruitment. Alternatively, soluble adhesion molecules may compete with their

membrane bound forms by acting as competitive inhibitors of cell-cell interactions [128]. In support of this, recombinant sVCAM-1, at the concentrations seen in patients with hypertriglyceridaemia, was shown to significantly reduce monocyte adhesion to IL-1 stimulated cultured endothelial cells under flow conditions [285].

1.10.2 Soluble adhesion molecules and atherosclerosis

Elevated levels of soluble adhesion molecules are associated with a number of disease states, including rheumatoid arthritis [286], cancer [287] and tuberculosis [288]. Measurement of these molecules may also provide insights into the pathogenesis of atherosclerosis.

In support of this, raised levels of soluble (s) P-selectin have been detected in patients with acute myocardial infarction [289], unstable angina [290], stroke [291] and peripheral arterial vascular disease [292]. Increased levels of sE-selectin are found in patients with familial hypercholesterolemia [293], non-rheumatic aortic stenosis [294], unstable angina [295] and during restenosis following angioplasty [296]. Patients with ischaemic heart disease [297], peripheral vascular disease [297] and unstable angina have raised levels of sICAM-1 [295]. Furthermore, sICAM-1 concentrations have been found to be elevated among apparently healthy men at risk of future myocardial infarction [298].

Finally, elevations in circulating sVCAM-1 levels have been found in patients with aortic atherosclerosis [299], non-rheumatic aortic stenosis [294] and unstable angina [295]. Importantly, a strong correlation exists between VCAM-1 mRNA expression within the atheromatous lesion and soluble VCAM-1 [300]. Recent evidence suggests that sVCAM-1 is a better predictor of the extent and severity of the disease than other cell adhesion molecules or plasma markers of inflammation tested to date, with its concentration correlating strongly with intimal thickness [301].

1.10.3 Soluble adhesion molecules and dyslipidaemia

Severe dyslipidaemia is associated with elevated levels of soluble cell adhesion molecules (CAM). Increased levels of sICAM-1, sE-selectin and sP-selectin have been found in patients with hypercholesterolaemia [302,303] whereas increased levels of sVCAM-1 and sICAM-1 have been noted in individuals with hypertriglyceridaemia [285]. In patients with familial hypercholesterolaemia, LDL apheresis resulted not only in a massive reduction in serum cholesterol, but also a marked decrease in both sE-selectin and sICAM-1 levels [302]. However, aggressive lipid lowering, by drug therapy, appears to exert only limited effects on soluble levels of CAMs [293]. Thus, it is not clear

whether dyslipidaemia causes endothelial dysfunction, resulting in an increased expression of CAMs and their subsequent release into the circulation, or whether the increased levels of circulating CAMs are a reflection of the underlying atheroma in these individuals.

1.10.4 Circulating levels of chemokines and atherogenesis

Circulating levels of chemokines have been identified in a variety of acute and chronic inflammatory and immune-related conditions [63,304], suggesting that their levels may reflect enhanced tissue expression and secretion of these molecules during disease. Little is known about circulating chemokines during atherogenesis but elevated levels of CC [305-307] and/or CXC chemokines [306,308,309] have been reported in patients with congestive heart failure [305,308], ischaemia-reperfusion injury [309,310], aortic aneurysms [306] and after percutaneous transluminal coronary angioplasty [307]. Recently, circulating concentrations of MCP-1 was identified as a powerful independent predictor of restenosis following coronary angioplasty [307]. However, it is not known whether elevated serum concentrations of CC or CXC chemokines can directly modulate leukocyte recruitment. As described earlier (Section 1.7.2), over-expression of chemokines can destroy chemokine gradients, and prevent leukocyte infiltration to sites of inflammation [178]. Prolonged exposure to circulating chemokines could result in desensitisation and down regulation of chemokine receptors on circulating leukocytes (Section 1.6.4). Alternatively, physiological levels of chemokines may be able to activate leukocytes, increasing their migratory or inflammatory responses, achieving the opposite result.

1.10.5 Circulating levels of acute phase proteins

Acute phase proteins (APP) are produced during the APR and are synthesised predominantly by the liver during acute infection or trauma [311]. A local inflammatory stimulus can give rise to a series of changes that result in the generation of heat, swelling and pain. However, localised inflammation can develop into a systemic response characterised by changes in hormones and electrolyte levels, fever and changes in a wide range of serum proteins. This is known as the APR, the purpose of which is to provide optimal conditions for counteracting an inflammatory stimulus and for the restoration of homeostasis [311]. The magnitude of changes in the concentration of individual APP can vary considerably. Plasma levels of major APP, increase dramatically during the APR, and include C-reactive protein (CRP), serum amyloid A (SAA) and serum amyloid P (SAP) [311]. Other APP include complement and coagulation proteins, proteinase inhibitors and metal-binding proteins [311]. So-called

'negative' APP are decreased in the plasma during the APR, presumably to allow the liver to synthesise the induced APP. These include plasma proteins such as albumin and apolipoproteins such as apoA-I and II. In general, the APR lasts only a few days; however, in cases of chronic or recurring inflammation, continuation of some aspects of the APR may contribute to the underlying tissue damage that accompanies disease [311]. This may explain the link between episodes of infection and risk of CHD [311].

In general, in a given mammalian species, there is usually only one major acute phase protein. For example, in man, CRP can increase by 1000-fold during the inflammatory response, whereas SAP has an approximate serum concentration of 30 μg/ml, which remains constant during inflammation [311]. By contrast, mice only produce trace amounts of CRP [311]. Major murine APPs are SAA and SAP circulating levels of, which can increase by up to 50-fold and 100-fold respectively [311]. Haptoglobin (Hp) is one of the few APP in which increased synthesis during inflammation is conserved in all vertebrate species [311].

1.10.5.1 Acute phase proteins and atherosclerosis

Recently, attention has focused on APP, in particular CRP, as potential indicators of underlying atherosclerotic disease and predictors of future clinical events. Indeed, there is evidence to suggest that CRP levels may be a useful indicator of future risk of myocardial infarction, stroke and death in middle-aged men and women free of clinical coronary disease and independent of other established risk factors [312-314]. However, it remains to be demonstrated whether APP are causally involved in atherosclerosis, or simply reflect the underlying disease process. It is therefore pertinent to discuss some of the APP in relation to atherosclerosis.

1.10.5.1.1.1 Serum amyloid A

The serum amyloid A family of polymorphic proteins (SAA 1-5) are encoded by multiple genes in a number of mammalian species [315]. They are multi-functional small apolipoproteins that mediate immune responses to infection, trauma or stress [311]. During the APR, they rapidly associate with HDL_3 and become the predominant apolipoprotein on this fraction, displacing apoA-I in quantity [311]. This can diminish the ability of HDL to mediate reverse cholesterol transport. In addition, levels of HDL are depressed during the APR reflecting its status as a negative acute phase protein. Van Lenten *et al* [316] reported that HDL loses its PON1, PAF-AH and LCAT activities during the APR and as a consequence, HDL is transformed from an anti-inflammatory molecule to pro-inflammatory particle. In contrast anti-inflammatory HDL, the pro-

inflammatory particle is unable to protect LDL against oxidation and can enhance LDL-induced monocyte chemotaxis [316]. Furthermore, SAA when unassociated with HDL can induce the recruitment of monocytes, neutrophils and T-cells and the expression of adhesion molecules [317]. Therefore, individuals with chronic or recurrent infection may have a persistence of pro-inflammatory HDL, which may increase their risk of atherosclerosis [212].

Although the liver is the primary site of synthesis of SAA, extrahepatic production has been reported for most family members [315]. Hepatic production of SAAs can increase up 1000-fold during the acute phase, reflecting the status of this molecule as a major acute phase protein [315]. Serum amyloid A mRNA has also been detected in human atherosclerotic lesions [318], and induction of acute phase SAA mRNA by pro-atherogenic oxLDL [319] suggests that SAA may also play a role in vascular injury and atherogenesis. Elevated levels of these plasma proteins are associated with atherosclerosis [320], and spontaneous and transplant cardiac coronary artery disease [321].

1.10.5.1.1.2 Haptoglobin

Haptoglobin is a highly conserved dimeric plasma glycoprotein ($\alpha_2\beta_2$) that binds haemoglobin with high avidity, forming stable complexes that are responsible for the rapid clearance of free haemoglobin from the plasma during haemolysis, thereby preventing tissue damage by haemoglobin-driven lipid peroxidation [322]. Haem iron can catalyze the oxidation of LDL, which can then be taken up by macrophage scavenger receptor. Therefore, Hp may protect against LDL oxidation by binding to free haemoglobin. Indeed, LDL oxidation can be enhanced by haemoglobin loading of macrophages [323] but can be protected by the haemoglobin binding capacity of haptoglobin [324]. Hepatic production of Hp is induced 3-fold during the APR, categorising this molecule as a minor positive APP [311]. In man, two common alleles (Hp1 and Hp2) code for three main phenotypes: Hp 1-1, 2-1 and 2-2. The Hp 2-2 phenotype is associated with elevated serum cholesterol levels [322], essential arterial hypertension [325] and susceptibility to CAD [326]. The Hp β chain has been found within early fatty streak lesions in human aortae [327], and changes in the measured concentration of Hp in serum are found in a number of inflammatory disorders, including atherosclerosis [328]

1.11 Aims of this thesis

The aim of this studentship was to investigate the utility of circulating levels of serum chemokines, and soluble adhesion molecules, as 'markers' of atheroma development in apoE*3 Leiden and C57BL mice, fed a diet high in fat and cholesterol and containing sodium cholate.

Using this murine model of atherosclerosis, my objectives were:

(i) To define the temporal relationships between circulating CC (JE) and CXC (KC and MIP-2) chemokines and changes in serum lipids (cholesterol and triglyceride) and lipoproteins, and to compare hepatic chemokine expression and lipid accumulation with chemokine expression, macrophage content and lesion development in the aortic root

(ii) To compare circulating concentrations of chemokines with serum levels of (a) acute phase proteins, serum amyloid A and haptoglobin, and (b) paraoxonase activity.

(iii) To establish the effects of dietary antioxidants (vitamin E, vitamin C and β-carotene) on circulating concentrations of chemokines (JE, KC) and soluble adhesion molecules (sICAM-1, sVCAM-1), compared with changes in serum lipids, and with the development of atheroma in the aortic arch.

Chapter 2

General Methods

2 General Methods

2.1 Materials

All reagents/chemicals were obtained from either Sigma Chemical Company or BDH Laboratory Supplies, except where stated in the text. Names and addresses of suppliers are given in the Appendix 9.1.

2.2 Mice

Transgenic mice expressing both human apoE*3 Leiden and apoC1 transgenes were generated as previously described [44,106]. Subsequent generations were produced by mating male transgene carriers with C57BL/6J females. Non-transgenic littermates (C57BL/6J) were used as controls. Mice had free access to food and water, and were maintained in specific pathogen-free conditions throughout the study. Mice were bred by members of the Department of Laboratory Animal Safety (GSK). All studies were subjected to internal ethical review and were covered by UK Home Office regulations. In addition, all studies were subjected to COSHH regulations.

ApoE*3 Leiden mice were developed to include the human apoCI gene because it is close to a DNA element mediating liver expression [106]. High-level expression of apoCI in transgenic mice increased plasma cholesterol and triglyceride levels [329], suggesting that hyperlipidaemia in apoE*3 Leiden mice is caused by apoCI. However, mice that express both human apoE and apoCI did not show hyperlipidaemia and had no evidence of abnormal lipid profiles [329]. ApoE*3 Leiden mice were developed using a similar construct as this model and therefore, it is likely that apoE*3 Leiden is the major cause of hyperlipidaemia [106].

2.2.1 Analysis of murine phenotype : human apoE ELISA

Mice expressing human apoE*3 Leiden were identified using a sandwich enzyme-linked immunoabsorbent assay (ELISA) for human apoE. This ELISA was originally established by Mr John Yates and Dr Nigel Pearce (Dept. Vascular Biology, GSK), in accordance with published methods [330].

Purified goat anti-human apoE polyclonal antibody (Incstar, ATAB Atlantic) was diluted in phosphate buffered saline (PBS) (26.8 mM KCl, 14.7 mM KH_2PO_4, 56.4 mM Na_2HPO_4 and 1.5 mM NaN_3, pH 7.5) and 100 µl of diluted antibody (final concentration 2.5 µg/ml) added to each well of a 96-well plate (Maxisorp ELISA plates, NUNC). After an overnight incubation (4°C), the contents of each well were removed by aspiration

and non-specific binding sites blocked by the addition of 250 μl/well of blocking buffer: 50 mM Tris-HCl, 150 mM NaCl, 1 mM $MgCl_2$ pH 7.4, containing bovine serum albumin (BSA) (1%, w/v). The plate was incubated for 1 h at 37°C, before the contents of each well were aspirated, and washed (4x) with 300 μl/well of washing buffer (10 mM Tris, 150 mM NaCl pH 7.4, containing Tween-20 (0.05%, v/v)) using an automated plate washer (Wallac). Mouse serum samples were diluted (1:100) with assay buffer (50 mM Tris, 150 mM NaCl, pH 7.4 containing BSA (0.5%, w/v), gamma-globulins (0.05%, w/v), Tween-20 (0.01%, v/v)). Human serum containing a known concentration of apoE was used as a standard in the assay and diluted in assay buffer to a final concentration of 160 ng/ml. Assay buffer was used as a negative control. Biotinylated rabbit anti-human apoE polyclonal antibody (generated in-house at GSK) was diluted to a final concentration of 2 μg/ml in assay buffer supplemented with normal goat serum (1%, v/v), and 50 μl added to each well, followed by the addition of the diluted (1:100) samples and standards (50 μl). The plate was placed on an orbital plate shaker (Johnson & Johnson) and incubated at room temperature (RT) for 3 h. The contents of each well were then aspirated and washed (5x) as before. Streptavidin-horseradish peroxidase (Amersham) was diluted in assay buffer (1:2000) and 100 μl added to each well (30 min). The wells were again aspirated and the plate washed (4x) as previously. Immunoreactive human apoE was detected by incubating (30 min, RT) with 100 μl of 3, 3', 5, 5'-tetramethyl benzidine (TMB) substrate (Pierce) containing 0.01% hydrogen peroxide (H_2O_2). The reaction was stopped by the addition of 100 μl 2M sulphuric acid (H_2SO_4), and the absorbance of each well was determined at 450 nm (Molecular Devices, Thermomax). Animals were positively identified as transgenic for human apoE*3 Leiden, if they had high readings close to that of the positive control.

2.2.2 Diets

Normal mouse chow was purchased from Special Diet Services, UK (Diet RM1, Appendix 9.2). The high-fat/high-cholesterol/cholate diet (Diet HFC/C) was from Hope Farm, The Netherlands and contained, by weight, cocoa butter (15%), sodium cholate (0.5%), cholesterol (1%), sucrose (40.5%), cornstarch (10%), corn oil (1%), cellulose (4.7%), casein (20%), 50% w/v choline chloride (2%), methionine (0.2%) and vitamin/mineral mixture (5.1%). This highly atherogenic diet was formulated according to Nishina *et al* [3,4] in order to minimize liver damage. Animals were fed by the Department of Laboratory Animal Safety (GSK).

2.3 Collection and analyses of blood and serum samples

All blood sampling was carried out by the Department of Laboratory Animal Safety (GSK). Serum was isolated by Nuala Murphy.

2.3.1 Blood sample collection

In-life blood samples were taken from the tail vein (200 μl), and collected into capillary tubes (Sarstedt, Microvette). Terminal blood samples (~600 μl) were taken from the aorta post mortem, and collected into 1 ml microfuge tubes. All blood samples were taken at least 4 h into the light phase when food consumption is expected to be minimal.

2.3.2 Preparation of serum samples

Serum was prepared by allowing blood samples to clot on melting ice. After 4 h, the samples were centrifuged (4°C, 3000 x *g*, 15 min) and the supernatants collected. Samples were then either stored at -80°C for analysis by ELISA and/or enzyme assays at 4°C for lipoprotein determination.

2.3.3 Separation of serum lipoproteins

Lipoprotein profiles were analysed by size-exclusion chromatography using a SMART™ micro-fast performance liquid chromatography (FPLC) system (Pharmacia, Sweden) and a method similar to that described by Hennes *et al* [331]. Briefly, equal volumes of serum from all mice within each group were pooled, and filtered (0.2 μm filter, Anotop 10, Whatman, UK) before being applied (30 μl) to a Superose 6 column. The column was eluted at a constant flow rate of 65 μl/min, using an FPLC pump system, and a solution containing NaCl (150 mM), ethylenediaminetetraacetic acid (EDTA) (1 mM), and sodium azide (7.7 mM), pH 8.0. The first 920 μl of column eluate represented the void volume. The lipoproteins were contained in the next 42 fractions of 20 μl each, which were deposited in the wells of a 96-well plate (Costar). Each fraction was assessed for cholesterol or triglyceride content as described in Section 2.3.4 and 2.3.5.

2.3.4 Measurement of serum or lipoprotein cholesterol content

Cholesterol concentrations were determined using the SIGMA Diagnostic cholesterol kit, which is based on a method by Allain [332]. Cholesterol esters are first hydrolysed by cholesterol esterase to free cholesterol and fatty acid. The cholesterol is then converted to cholest-4-en-3-one and H_2O_2 by cholesterol oxidase. The H_2O_2

produced is then coupled with the chromogen, 4-aminoantipyrine and *p*-hydroxybenzenesulfonate, in the presence of peroxidase to yield a quinoeimine dye which has an absorbance maximum of 500 nm.

In brief, standards and diluted (neat - 1:10) samples (5 μl) were added to appropriate wells of a 96-well plate, followed by the addition of cholesterol reagent (95 μl). The plate was then gently tapped to aid mixing and incubated for 10 min at 37°C. The absorbance of each well was measured at 550 nm and the cholesterol concentration determined by reference to the standard curve, which was linear from 0-400 mg/dl.

2.3.5 Measurement of serum or lipoprotein triglyceride content

Triglyceride concentrations were determined using the SIGMA Diagnostic triglyceride kit which is based on a method by Wako Pure Chemical Industries Ltd., with modifications by Fossati *et al* [333] and McGowan *et al* [334]. Triglyceride is first hydrolysed by triacylglycerol lipase to free fatty acids and glycerol. The glycerol is then phosphorylated by glycerol kinase, using adenosine triphosphate, to yield glycerol-3-phosphate and adenosine diphosphate. The glycerol-3-phosphate is then oxidised to dihydroxyacetone phosphate by glycerol-3-phosphate oxidase producing hydrogen peroxide. The hydrogen peroxide produced is then coupled with the chromogen, 4-aminoantipyrine and 3,5 dichloro-2-hydroxybenzene sulfonate in the presence of peroxidase to yield a quinoeimine dye which has an absorbance maximum of 500 nm. Assays were carried out exactly as described for cholesterol (Section 2.3.4) except the samples were diluted 1:1. The triglyceride concentration was determined by reference to the standard curve, which was linear from 0 - 250 mg/dl.

2.3.6 Measurement of serum ICAM-1 concentrations

Murine soluble ICAM-1 was detected using a commercially available two-site capture ELISA kit (Endogen). Serum samples were diluted 1:100 with the diluent provided, and assayed in duplicate. Briefly, plate reagent (50 μl) was added to each well, followed by the addition of samples and standards (50 μl). The plate was incubated at RT for 2 h. The contents of each well were then aspirated, and the plate washed (5x) by adding 200 μl of the wash buffer supplied to each well. Anti-mouse sICAM-1 conjugate reagent (100 μl) was then added to each well and incubated for 1 h at RT. The contents of each well were then aspirated and the plate washed, as before. Premixed 3,3', 5,5'-tetramethylbenzidine (TMB) substrate was added (100 μl) and the

plate incubated at RT, in the dark, for 30 minutes. The reaction was halted by the addition of 100 µl of the stop solution provided in the kit. The absorbance of each well was determined at 450 nm. Sample concentrations of sICAM-1 were calculated with reference to the standard curve, which was linear from 0 - 1000 ng/ml.

2.3.7 Measurement of serum JE/MCP-1 concentrations

Murine soluble MCP-1 (JE) was determined by a two-site capture ELISA kit (R&D Systems). Briefly, assay diluent (50 µl), supplied with the kit, was added to each well, followed by the addition of diluted samples (1:1 - 1:4), standards or kit control (50 µl). The 96-well plate was incubated for 2 h at RT after which time it was thoroughly washed (5x) with the supplied wash buffer; anti-mouse JE conjugate (100 µl) was then added to each well and incubated for 1 h at RT. The wells were aspirated and washed as previously (5x), before the addition of 100 µl of the substrate (TMB) solution supplied; the plate was then developed in the dark for 30 min. The reaction was halted by the addition of 50 µl stop solution provided in the kit, and the absorbances of each well at 450 nm determined as described previously. Sample concentrations of JE were calculated with reference to the recombinant JE standard curve, which was linear from 0 – 1000 pg/ml.

2.3.8 Measurement of serum KC concentrations

Murine soluble KC was detected by a two-site capture ELISA kit (R&D Systems). This kit employs exactly the same method as described in Section 2.3.7. Sample concentrations of KC were calculated with reference to the recombinant KC standard curve, which was linear from 0 – 1000 pg/ml.

2.3.9 Measurement of serum MIP-2 concentrations

Murine soluble MIP-2 was detected by a two-site capture ELISA kit (R&D Systems). This kit employs the same method as described in Section 2.3.7. Sample concentrations of MIP-2 were calculated with reference to the recombinant MIP-2 standard curve, which was linear from 0 – 500 pg/ml.

2.3.9.1 Characterisation of murine chemokine ELISA's

Hyperlipidaemic serum samples were 'spiked' with a known concentration of recombinant chemokine protein to ensure that the lipaemia evident in these samples was not adversely affecting the ELISA. Recovery of the recombinant protein was between 98 - 100% (data not shown) and therefore these commercially available

ELISAs are suitable for measuring chemokine concentration in hyperlipidaemic serum samples.

2.4 Collection and preparation of tissue sections

Hearts, livers, kidneys, spleens and lungs were removed immediately post mortem, snap-frozen in liquid nitrogen and fresh frozen sections cut as described in Section 2.4.1.2 and 2.4.1.3. Perfuse-fixed hearts were either stored in formalin until sectioning (Section 2.4.1.1) or were bisected immediately after perfusion, equilibrated in OCT compound (Bayer Diagnostics) and frozen that day as described in Section 2.4.1.1.

2.4.1 Cryostat sectioning of tissues

2.4.1.1 Perfuse-fixed hearts

The heart was perfused fixed *in-situ* as outlined in Section 3.2.1.6. Sections were cut as previously described [44,335]. Briefly, the hearts were bisected below the level of the atrium and the apex discarded. The superior aspect of the heart plus the aortic root were taken for analysis and equilibrated overnight in OCT compound. The heart was then immersed in OCT compound and orientated on a cryostat chuck (Bright Instrument Company Ltd, UK) so that the aorta was facing the chuck. The tissue was then frozen within the cryostat on the quick-freeze stage (-70°C) and then sectioned (-20°C) perpendicular to the axis of the aorta, starting within the heart and proceeding in the direction of the aorta. Alternate sections (10 μm) were taken, from the site where the three valve leaflets were first identified and mounted onto gelatinised slides. Sections were air dried for 1 h before being stained with Oil-Red-O (ORO) and Coles haematoxylin (Section 2.5).

2.4.1.2 Fresh frozen hearts

The hearts were removed immediately post mortem and bisected as described in Section 2.4.1.1 leaving approximately 2 mm of aorta still attached. The superior aspect of the heart plus aortic root were gently rinsed in saline and excess fluid removed by placing the heart on absorbent paper. The heart was then orientated cut-side down onto labelled cork discs and surrounded in OCT compound. The tissue was snap frozen in liquid nitrogen, wrapped in cling film and stored at -80°C until sections could be cut. Hearts were sectioned, starting at the aorta and proceeding in the direction of the heart. After the aortic root had been identified by the appearance of the three valve leaflets, sections (6 μm) were taken and thaw mounted onto Superfrost

Plus Gold slides, refrozen immediately and stored at -80°C awaiting analysis. Sections were taken for lesion analysis, immunohistochemistry (IHC) or *in-situ* hybridisation as described in Chapters 3 to 5.

2.4.1.3 Fresh frozen spleen and liver sections

The spleen and a lobe of liver were removed immediately post mortem, placed onto labelled cork discs and immersed in OCT compound. The tissues were then frozen in liquid nitrogen, wrapped in cling film and stored at -80°C awaiting analysis. The cork disc was attached to the chuck as described previously (Section 2.4.1.2) and sections (6 μm), thaw mounted onto Superfrost Plus Gold slides, refrozen immediately and stored at -80°C.

2.5 Histochemical analysis of aortic tissue sections

2.5.1 Oil-Red-O Staining

Oil-Red-O staining solution was prepared by mixing three parts of a saturated ORO stock solution (ORO, 10% w/v in propan-2-ol) with two parts dextrin (1% w/v in distilled water). The resulting solution was allowed to stand for 1 h and then filtered through a piece of Whatman filter paper (grade 1). Transverse sections of aortae were thaw mounted onto gelatinised slides or Superfrost Plus Gold slides as described in Sections 2.4.1.1 and 2.4.1.2. Sections were allowed to air dry for 1 h before being dipped briefly in isopropyl alcohol (60%) and then immersed in the ORO staining solution. After 15 min, the slides were dipped in isopropyl alcohol (60%), and then rinsed in running tap water (2 min). The sections were then counterstained in Cole's haematoxylin (15 s), washed in running tap water (5 min) and then coverslipped using glycerol/gelatine as a mountant. Once the mountant had set the slides were cleaned and the coverslip sealed with clear nail varnish.

2.5.2 Analysis of lesion area

Cross sectional lesion area was determined by morphometric evaluation of ten sections of aortic root, commencing where the three valve leaflets first appeared [44], as described in Chapters 3 to 5. Images were analysed using an Olympus BH-2 microscope and video-imaging systems, exactly as described previously [44]. All images were captured under identical lighting, microscope, camera and computer conditions. Atherosclerotic lesion areas were quantified by drawing around the lesions using Optimas software (version 6.1, Optimas Corp., USA). Colour thresholds were set that quantified the areas stained red within the lesion. Absolute values for the cross-sectional area of the lesion, and the regions stained red, were obtained by calibrating

the software using a stored image of a micrometer slide taken at the same magnification

2.6 Recombinant DNA methodologies

The techniques described in this section were used in the isolation of plasmid DNA for use in the production of riboprobes. Subsequent methods employed in the synthesis of riboprobes and their use during *in-situ* hybridisation are found in Section 4.2.4.

2.6.1 Transformation of JM109 competent cells

For each transformation, 100 µl aliquots of JM109 bacterial cells (Promega) were thawed on ice (5 min). The cells were gently mixed, DNA (10 ng) (Section 4.2.4.2.5) added, and mixed well before being placed on ice (15 min). The cells were heat shocked (45 s, 42°C) and placed back on ice (2 min) to induce a transient state of competence, during which time the bacteria took up the plasmid DNA. Luria-Bertani (LB) medium (Appendix 9.4.1) was added (900 µl) and the transformation reaction incubated for 60 min (37°C, 225 rpm). LB agar plates (Appendix 9.4.2) containing 50 µg/ml ampicillin (LB_{AMP}, Section 4.2.4.2.2) were coated with 20 µl of 5-bromo-4-chloro-3-indolyl-B-D-galactopyranoside (X-gal) (50 µg/ml) and 100 µl of isopropyl-thiogalactoside (IPTG) (100 mM) and incubated for 30 min (37°C). The transformation mix (100 µl) was plated out onto the LB_{AMP} agar plates and incubated overnight (37°C). The inserted DNA will disrupt the *lacZ* gene contained in the plasmid, which encodes for the enzyme, β-galactosidase (which normally cleaves lactose into galactose and glucose). This enzyme also metabolises X-gal in the presence of IPTG which ensures that *lacZ* expression is not repressed. X-gal is broken down by the enzyme into a deep blue product (4-chloro-3-bromo-indigo). Therefore, bacterial colonies containing non-recombinant vectors are blue, whereas those harbouring recombinant vectors are white.

2.6.2 Identification of recombinant clones

Eight white colonies were selected (Section 2.6.1), and cultured in LB_{AMP} medium overnight (37°C, 225 rpm). Plasmid DNA was isolated (Section 2.6.3) and recombinant clones verified by restriction digest using the enzymes *Not* I and *Bam*H I and 1x REACT buffer 3 (Life Technologies, Appendix 9.3) to release the KC insert and analysed using electrophoresis. A correct clone was identified and the bacterial culture

was scaled up as outlined in Section 2.6.4 so that there was enough plasmid DNA for the transcription of the riboprobes.

2.6.3 Isolation of plasmid DNA – mini preparation

The QIAprep Mini Kit (Qiagen) was used to isolate and purify up to 20 μg of plasmid DNA. The QIAprep miniprep procedure uses the modified alkaline lysis method [336,337]. The bacterial suspension (1.5 ml) was centrifuged (1 min, 7000 x *g*) in a sterile microfuge tube (2 ml) and the supernatant discarded to leave a bacterial pellet. The pellet was resuspended in buffer P1 (250 μl) and the bacteria lysed with buffer P2 (250 μl). After 5 min, buffer N3 was added (350 μl) and the solution gently inverted several times and centrifuged (10 min, 13,000 x *g*). The supernatant was removed and loaded onto a QIAprep spin column and centrifuged (30 s, 13,000 x *g*). The eluate was discarded and the column washed with buffer PE (750 μl) and centrifuged again (30 s, 13,000 x *g*). Residual buffer remaining in the column was removed by centrifugation (1 min, 13,000 x *g*). The QIAprep column was placed in a clean microfuge tube (1.5 ml) and the DNA eluted by adding 30 μl of sterile distilled water, incubating for 1 min and then centrifugation (1 min, 13,000 x *g*). The DNA was stored at -20°C until required.

The purity and concentration of the plasmid preparation was measured by UV spectrophotometry of diluted samples (typically 1/70 dilution) and determined using the equation below. At 260 nm, an optical density (A_{260}) of 1 corresponds to approximately 50 μg/ml of double stranded DNA.

Plasmid DNA concentration (μg/ml) = A_{260}nm x dilution factor x 50 μg/ml

The purity was estimated by the ratio between readings at 260 nm and 280 nm (A_{260}:A_{280}). Protein and phenol contaminants have an absorbance at 280 nm. A ratio of 1.8-1.9 indicated a pure solution of DNA, whereas samples with values less than these were considered contaminated with phenol or protein and discarded.

2.6.4 Isolation of plasmid DNA - midi preparation

The Qiagen Plasmid Midi Kit and protocol were used to isolate and purify plasmid DNA at a 20 – 100 μg level. The starter culture produced from one of the recombinant clones was diluted 1/1000 into LB^{AMP} medium (25 ml) and incubated overnight (300 rpm, 37°C). The bacterial cells were harvested by centrifugation (6000 x *g*, 15 min, 4°C), and the bacterial pellet resuspended in buffer P1 (4 ml). Next, buffer

P2 was added mixed gently by inversion (4-6x) and incubated at RT for 5 min. This was followed by the addition of chilled buffer P3, inversion to mix (4 - 6 x) and incubation on ice (15 min). The solution was centrifuged (20,000 x *g*, 30 min, 4°C), the supernatant removed to a fresh tube and centrifuged again (20,000 x g, 15 min, 4°C) to avoid particulate matter clogging the QIAGEN-tip 100. A QIAGEN-tip 100 was equilibrated with 4 ml of QBT buffer, and the column emptied by gravity flow. The supernatant was loaded onto the QIAGEN-tip promptly and allowed to enter the resin by gravity flow. The QIAGEN-tip was washed with 2 x 10 ml of buffer QC and the DNA eluted with buffer QF (5 ml) into a tube. The DNA was precipitated by adding isopropanol (3.5 ml) and centrifuged (15,000 x *g*, 30 min, 4°C). The supernatant was carefully decanted and the DNA pellet washed with 2 ml of ethanol (70 %). The pellet was air-dried (10 min, RT) and then redissolved in sterile distilled water. The DNA was quantified as previously described (Section 2.6.3)

2.6.5 Separation of DNA fragments by agarose gel electrophoresis

The percentage of agarose used to isolate DNA fragments varied depending on size; typically, 1% was used. The mini gel apparatus (Flowgen, UK) was set up as per manufacturers instructions. Briefly, 1 x Tris/acetate buffer (TAE; 40 mM Tris acetate, 10 mM EDTA, Life Technologies) (50 ml) was added to the agarose (0.5 g), and the mixture heated in a microwave oven with mixing at regular intervals until the agarose had just dissolved. The solution was cooled to 50 - 60°C, ethidium bromide (0.5 μg/ml, Life Technologies) added, and the gel poured into the cast. Ethidium bromide intercalates with nucleic acids and allows visualisation within the gel matrix. The gel was allowed to set (30 min, RT), the comb and blocks removed and enough 1 x TAE buffer added to the tank so that the gel was completely covered. The restriction digest was mixed with loading buffer (1:6) and loaded (10 - 30 μl) into the wells. A 100 bp DNA ladder (Life Technologies) (1 μl of ladder per mm of lane) was also run to ensure the correct size product had been released from the plasmid. The gel was run at a constant voltage of 80 V for ~ 45 min or until the dye front had migrated 2 cm from the bottom of the gel. After electrophoresis, the gel was visualised and photographed under UV light (Eagle Eye II, Stratagene).

2.6.6 Extraction and purification of DNA from agarose gel

The cDNA of interest was extracted from the agarose gel using the QIAquick Gel Extraction Kit (Qiagen) and protocol. This kit is designed for the extraction of 70 bp to 10 kb DNA fragments from standard or low-melt agarose gels in TAE or TBE

buffers. The digested DNA was run on an agarose gel (1%) (Section 2.6.5) and the KC cDNA band was identified (under U.V illumination) and excised from the gel using a sterile scalpel blade. The slice was weighed and added to a microfuge tube (1.5 ml). Three volumes of buffer QG was added to 1 volume of gel (100 mg ≡ 100 µl) and incubated at 50°C for 10 min with vortexing every 2 min. A QIAquick spin column was placed in the provided collection tube (2 ml). One gel volume of isopropanol was added to the sample, mixed and then applied to the spin column. The column was centrifuged (1 min, 13,000 x *g*) and the eluate discarded. The column was then washed with buffer PE (750 µl), allowed to stand for 5 min and centrifuged (1 min, 13,000 x *g*). The flow through was discarded and the column centrifuged (13,000 x *g*) for an additional 1 min. The column was then placed in a microfuge tube (1.5 ml) and the DNA eluted by adding sterile distilled water (30 µl) to the centre of the column. The column was allowed to stand for 1 min and then centrifuged (13,000 x *g*) for 1 min. The DNA was quantified (Section 2.6.3), the KC insert excised (Section 4.2.4.2.3), 'polished' (Section 4.2.4.2.4) and then ligated into pPCR-Script Amp SK (+) cloning vector (Section 4.2.4.2.5) before being transformed into JM109 bacterial cells (Section 2.6.1).

2.6.7 Wizard DNA Clean-up Kit

Linearised plasmid DNA (Section 4.2.4.2.7) was purified using a Wizard DNA Clean-Up Kit and protocol (Promega). Wizard DNA Clean-Up Resin (1 ml) was added to a microfuge tube (1.5 ml) and the DNA sample made up to 50 µl with sterile distilled water. The sample was added to the resin and inverted several times to mix before being loaded into a syringe barrel. The sample was gently pushed into the Minicolumn, which was then washed twice with 2 ml of isopropanol (80%). The Minicolumn was transferred to a microfuge tube (1.5 ml) and centrifuged (2 min, 10,000 x *g*) to dry. The DNA was eluted by addition of 30 µl of sterile distilled water (70°C) to the Minicolumn (1 min) and then centrifuging for 20 s at 10,000 x *g*. The purified DNA was stored at -20°C until use.

Chapter 3

*Hypercholesterolaemia and circulating levels of CXC chemokines in apoE*3 Leiden mice*

3 Hypercholesterolaemia and circulating levels of CXC chemokines in apoE*3 Leiden mice

3.1 Introduction

Chemokines are an important group of secreted proteins that exhibit selective chemoattractant properties for target leukocytes, thereby ensuring the correct leukocyte is activated and recruited to sites of inflammation [153]. This has led to the proposition that they are key players in the pathogenesis of diseases with characteristic leukocyte infiltrates [156]. Chemokines can be separated into two major subfamilies based on whether the first two of four cysteine residues is separated by one amino acid residue (CXC) or are adjacent (CC) (Section 1.6).

Members of the CC chemokine subfamily predominantly induce the migration of monocytes and T-lymphocytes and are, therefore intrinsically linked with the monocytic infiltrate that characterises atherosclerosis (Section 1.6.1). In contrast, CXC chemokines are classically thought of as neutrophil chemoattractants and activators (Section 1.6.2). Few neutrophils are found in atherosclerotic lesions [116], and it was not envisaged that CXC chemokines would play a central role in lesion development. However, recent data suggests that CXC chemokines may play a hitherto unrecognised role in monocyte recruitment during atherogenesis (Section 1.7.2 and 1.7.2.1). For example, GRO-α [191] and IL-8 [192] may trigger the adhesion of monocytes under flow conditions to a model of vascular endothelium. Macrophages in human and murine atherosclerotic lesions express CXCR-2 and mIL-8RH respectively [177]. Importantly, studies using bone marrow transplantation have demonstrated that the absence of leukocyte mIL-8RH resulted in diminished monocyte recruitment and reduced lesion size in the LDL receptor$^{-/-}$ model of atherosclerosis [177]. Thus, CXC chemokines may play an important role in the recruitment of monocytes to atherosclerotic lesions and we hypothesised that measurement of these molecules could provide useful information on events occurring at the vessel wall during atherogenesis.

The aim of this initial investigation was to examine whether circulating CXC chemokines were elevated in response to an atherogenic diet in apoE*3 Leiden mice and their non-transgenic littermates. ApoE*3 Leiden mice have impaired hepatic clearance of chylomicrons and VLDL remnants from the blood and, when fed an atherogenic diet, develop marked hyperlipidaemia and accelerated atherogenesis compared with their non-transgenic littermates (Section 1.2.5) [6,44,106]. Importantly,

lesion development in apoE*3 Leiden mice is correlated to the duration of exposure to elevated levels of serum lipoproteins; this means that atherogenesis can be regulated in these animals, according to composition and duration of diet treatment. Indeed, small type I and II fatty streak lesions are visible in apoE*3 Leiden mice after 4 weeks consumption of the HFC/C diet, allowing the hypothesis to be tested in a short preliminary study. Accordingly, serum concentrations of CXC chemokines during the early stages of 'fatty streak' development in apoE*3 Leiden and C57BL/6J mice consuming the high fat/high cholesterol/sodium cholate (HFC/C) diet (Table 1-5) were measured.

3.2 Methods

3.2.1 Study protocol

3.2.1.1 Mice

Mice were generated and phenotyped as described in Section 2.2. Twenty-two female apoE*3 Leiden mice and 20 female non-transgenic mice, aged 8-10 weeks, were allocated randomly to experimental groups on the basis of age and litter.

3.2.1.2 Diets

Before the study, animals were maintained on RM1 diet, a standard mouse diet. During the experimental period, groups of mice were fed either the high-fat/high-cholesterol/cholate (HFC/C) diet or continued to receive RM1 diet (Section 2.2.2). Fourteen apoE*3 Leiden mice, and 20 of their non-transgenic littermates were fed the HFC/C diet and 8 apoE*3 Leiden mice were fed RM1 diet. Body weights were measured prior to the start of the study and after 1 and 3 weeks of diet feeding. Half the mice from each group were culled after two weeks, and the remainder after four weeks. Body weights were measured by the Department of Laboratory Animal Safety (GSK).

3.2.1.3 Collection of blood samples

In-life blood samples (Section 2.3.1) were taken prior to the start of the study and then after 2 weeks of diet treatment. Terminal blood samples were taken from each mouse by cardiac puncture under halothane anaesthesia after 2 and 4 weeks. Serum was prepared and stored as described in Section 2.3.2.

3.2.1.4 Lipid and lipoprotein analysis

Cholesterol and triglyceride concentrations were measured enzymatically using commercially available kits (Section 2.3.4 and 2.3.5). These assays were performed

by the Clinical Chemistry Department (GSK). Serum lipoproteins were separated by agarose gel electrophoresis, using Lipo+Lp(a) gels (Sebia, UK) and stained for lipid using Sudan Black. Briefly, samples (5 μl) were loaded onto the agarose gel and allowed to diffuse. The gel was run at 50 V for 90 min using the Tris-Barbital buffer (pH 9.2) supplied in the kit and then dried at 80°C for 20 min. The migrated samples were visualised by immersing the gel in Sudan Black staining solution (160 ml ethanol, 2 ml Sudan Black staining solution and 140 ml distilled water; 15 min), followed by destaining (45 % ethanol in distilled water; 5 min). The gel was then washed in distilled water and dried as before.

3.2.1.5 Chemokine analysis

Serum concentrations of KC and MIP-2 were determined in diluted serum samples (1:1 - 1:4), using commercially available ELISA kits as described in Section 2.3.8 and 2.3.9.

3.2.1.6 Tissue preparation and sectioning of aortic root

Mice were killed by cervical dislocation, and their hearts perfuse-fixed *in-situ* using oxygenated Krebs-Henseleit buffer (89.2 mM NaCl, 44 mM $NaHCO_3$, 5 mM KCl, 1 mM $Na_2HPO_4.12H_2O$, 0.5 mM $MgSO_4.7H_2O$, 0.04 mM $Na_2.EDTA.2H_2O$, 3.6 mM fumaric acid, 5 mM L-glutamic acid, 10.1 mM D-glucose, 5 mM sodium pyruvate and 2.3 mM $CaCl_2$) at 37°C under a pressure of approximately 110 cm of water via a cannula inserted in the left ventricle and an outlet created by cutting the right atrium. After 30 min, the buffer was replaced by neutral-buffered formalin and the perfusion continued for a further 30 min. Hearts were dissected out, stored in neutral buffered formalin and subsequently embedded in OCT compound, as described previously (Section 2.4.1.1).

3.2.1.6.1 Assessment of atherosclerosis in sections of aortic root

Lesion cross-sectional areas were measured in alternate sections (10 μm) of the aortic root as described in Section 2.5.2. Sections were photographed at x40 magnification, using a Zeiss photomic III photomicroscope and Fujichrome 50 Velvia film.

3.2.2 Statistics

Statistical analysis was carried out by Phil Overend (Department of Statistical Science, GSK). All the parameters except for body weight were log transformed in order to normalise the variances and in these cases geometric means with 95%

confidence intervals are quoted. The variance in body weight decreased with increasing body weight. Prior to analysis it was, therefore, normalised by power transforming the data using the fourth power. The treatment data for serum cholesterol, triglyceride and body weights were analysed using a 2 way analysis of variance (ANOVA) because the data were from mice culled after either 2 or 4 weeks. MIP-2 and KC were analysed using a repeated measures ANOVA because these parameters were measured on the same sub-set of mice throughout the 4 week study. Comparisons were made between the apoE*3 Leiden mice fed the HFC/C diet and either the apoE*3 Leiden mice fed normal diet or the non-transgenic mice using a Dunnetts multiple comparison post-test. Differences between the apoE*3 Leiden mice fed normal diet and the non-transgenic mice were analysed post-hoc using a Bonferroni test. Pre-treatment data were transformed using the same method as the treatment data and were then analysed using a 1-way ANOVA. Comparisons were made as described above. Differences from initial values were analysed by separate repeated measures ANOVAs for weeks 0 to 2 and 0 to 4 (weeks 0 to 1 and 0 to 3 for body weights). Differences were considered to be statistically significant if $p<0.05$.

3.3 Results

3.3.1 Body weights

ApoE*3 Leiden mice fed RM1 diet gained weight during the study by 9% and 12% at weeks 1 and 3 respectively whereas the weights of the mice in the other groups did not change significantly (Figure 3-1). As a consequence, the apoE*3 Leiden mice fed normal diet were 14% and 11% heavier than the apoE*3 Leiden mice fed the HFC/C diet at weeks 1 and 3 respectively.

3.3.2 Serum cholesterol and triglyceride

The effects of feeding HFC/C diet on serum cholesterol and triglyceride in female apoE*3 Leiden mice, or their non-transgenic littermates are shown in Figure 3-2. Serum cholesterol levels were 28% and 42% lower ($p<0.05$) at the start of the study in the non-transgenic mice than in the apoE*3 Leiden mice that were subsequently fed either normal or HFC/C diet respectively. Serum cholesterol concentrations decreased significantly from initial values ($p=0.025$) by week 4 of the study in apoE*3 Leiden mice consuming normal diet. In contrast, serum cholesterol increased dramatically ($p=0.0001$) by approximately 12 and 4 fold respectively in apoE*3 Leiden mice and their non-transgenic littermates after two weeks consumption of the HFC/C diet. Serum cholesterol was over 4-fold higher in the apoE*3 Leiden mice fed HFC/C diet compared with their non-transgenic littermates ($p<0.0001$) (Figure

3-2). No further changes in serum cholesterol were observed at week four in either group fed the atherogenic diet.

Serum triglycerides were significantly lower (p=0.0001) than initial values throughout the experiment in the apoE*3 Leiden and C57BL/6J mice fed HFC/C diet. In apoE3* Leiden mice fed normal diet the reduction was only significant (p=0.01) after 4 weeks. Triglyceride levels were higher in both groups of apoE*3 Leiden mice, compared with their non-transgenic littermates (Figure 3-2 B) throughout the feeding period (p<0.05). At both 2 and 4 weeks, serum triglyceride levels in the non-transgenic animals were approximately 30% of the levels seen in the apoE*3 Leiden mice consuming the same HFC/C diet. However, serum triglyceride levels did not differ significantly between the two groups of apoE*3 Leiden mice.

Agarose electrophoresis of the serum lipoproteins (Figure 3-3) showed that preβ migrating VLDL was the predominant lipoprotein fraction in serum isolated from apoE*3 Leiden mice consuming normal RM1 diet, or from the non-transgenic mice fed HFC/C diet. Consumption of the HFC/C diet was associated with an apparent decline in HDL, as judged by Sudan black staining and, in apoE*3 Leiden mice, the generation of a slower, β-migrating VLDL fraction.

3.3.3 Effects of HFC/C diet on serum CXC chemokines

The effects of feeding the HFC/C diet on serum KC and MIP-2 concentrations (Figure 3-4) were analysed using terminal and in-life samples from subsets of mice, derived from each of the 3 groups culled at four weeks. Analysis of the serum cholesterol and triglyceride concentrations for each subset indicated that they did not differ from the data presented for all the mice in each group (Figure 3-2 A and B). No significant differences in serum KC or MIP-2 concentrations were evident at the start of the study, and no significant changes in either chemokine were noted in apoE*3 Leiden mice consuming the normal diet throughout the study.

Consumption of HFC/C diet, for 2 or 4 weeks, caused significant increases in both KC and MIP-2 in both apoE*3 Leiden (p<0.0005) and C57BL/6J (p<0.05) mice, compared with apoE*3 Leiden mice consuming normal RM1 diet (Figure 3-4). Serum concentrations of KC in apoE*3 Leiden mice consuming HFC/C diet, were higher than those found in their non-transgenic littermates (+ 109%, p<0.018) after 4 weeks (Figure 3-4). Although the geometric means for the serum concentrations of MIP-2 also

tended to be higher in apoE*3 Leiden mice consuming the HFC/C diet for 2 or 4 weeks, compared with their non-transgenic littermates, the differences were not significant.

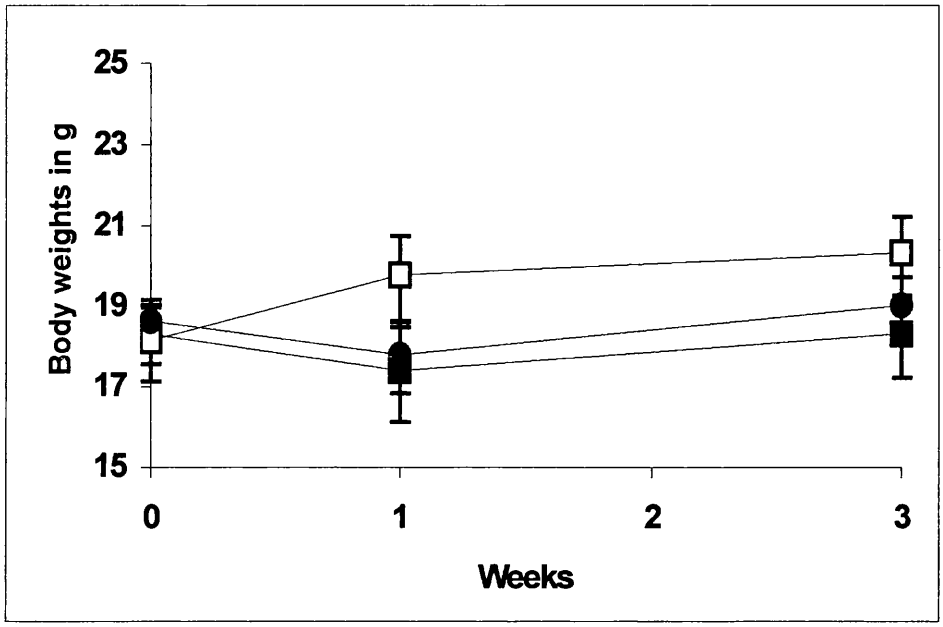

Figure 3-1 Effects of diet on body weights

Black squares: apoE*3 Leiden mice consuming HFC/C diet; black circles, non-transgenic controls consuming HFC/C diet; open squares, apoE*3 Leiden mice consuming RM1 diet. Values shown are geometric means ± 95% confidence intervals.

3.3.4 Effects of HFC/C diet on lesion development in the aortic sinus

Consumption of the HFC/C diet for 2 or 4 weeks led to the formation of early, Type I lesions in the apoE*3 Leiden mice (Figure 3-5 A). These stained intensely with Oil-Red-O and were predominantly restricted to the aortic valve leaflet. No lesions were evident in the non-transgenic mice (Figure 3-5 B) or in the apoE*3 Leiden mice consuming the RM1 diet (Figure 3-5 C) at any time-point.

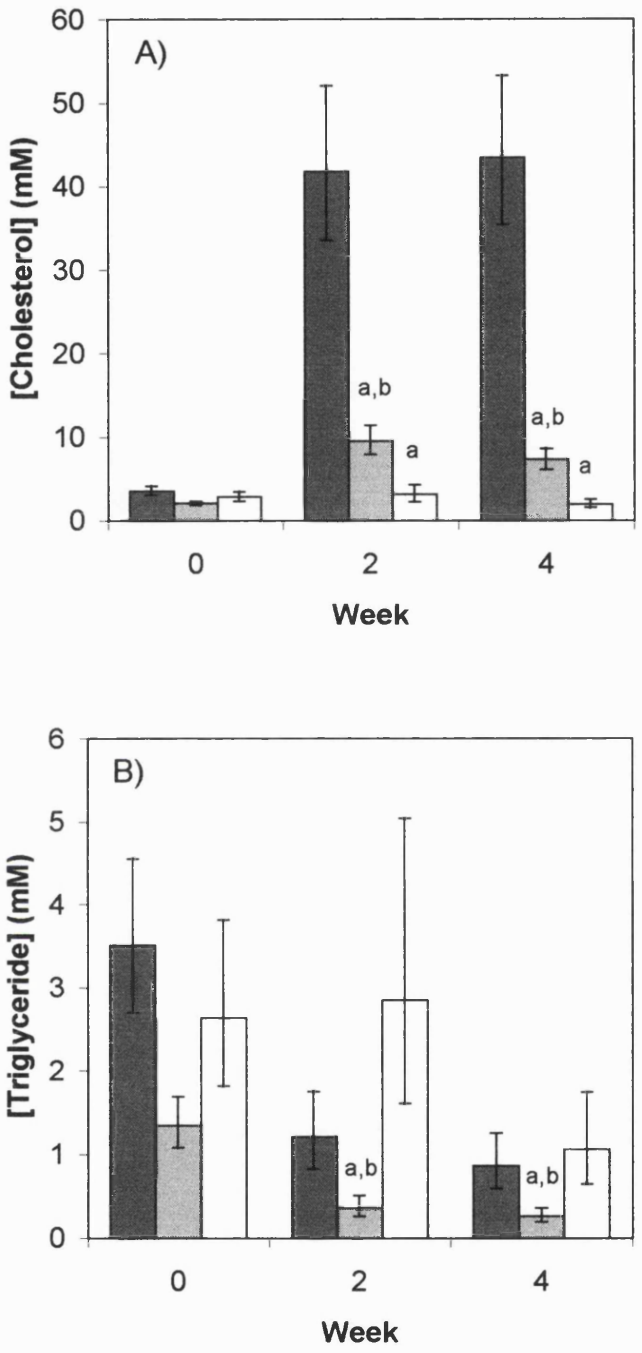

Figure 3-2 Effects of diet and strain of mouse on serum lipids

Effects of diet and strain of mouse on serum cholesterol (A) and triglyceride (B) concentrations (dark grey bar, apoE*3 Leiden mice consuming HFC/C diet; light grey bar, non-transgenic controls consuming HFC/C diet; open bar, apoE*3 Leiden mice consuming RM1 diet). Values shown are geometric means ± 95% confidence intervals (a = significantly different ($p<0.001$) to apoE*3 Leiden mice consuming HFC/C diet, b = significantly different ($p\leq0.05$) to apoE*3 Leiden mice consuming RM1 diet).

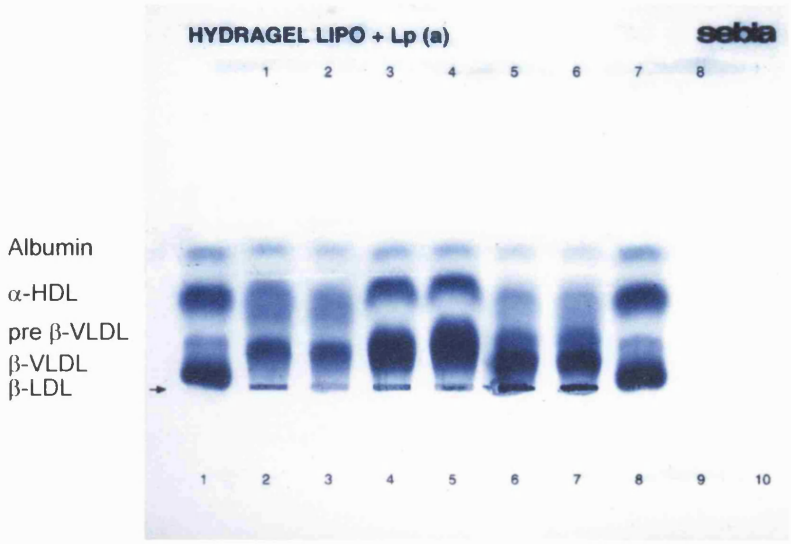

Figure 3-3 Lipoprotein analysis using gel electrophoresis.

Lane 1 & 8 human serum, lanes 2 & 3 apoE*3 Leiden mouse consuming the normal RM1 diet, lanes 4 & 5 non-transgenic littermate consuming the HFC/C diet, and lanes 6 & 7 apoE* 3 Leiden mouse consuming the HFC/C diet. Sudan black staining (Section 3.2.1.4).

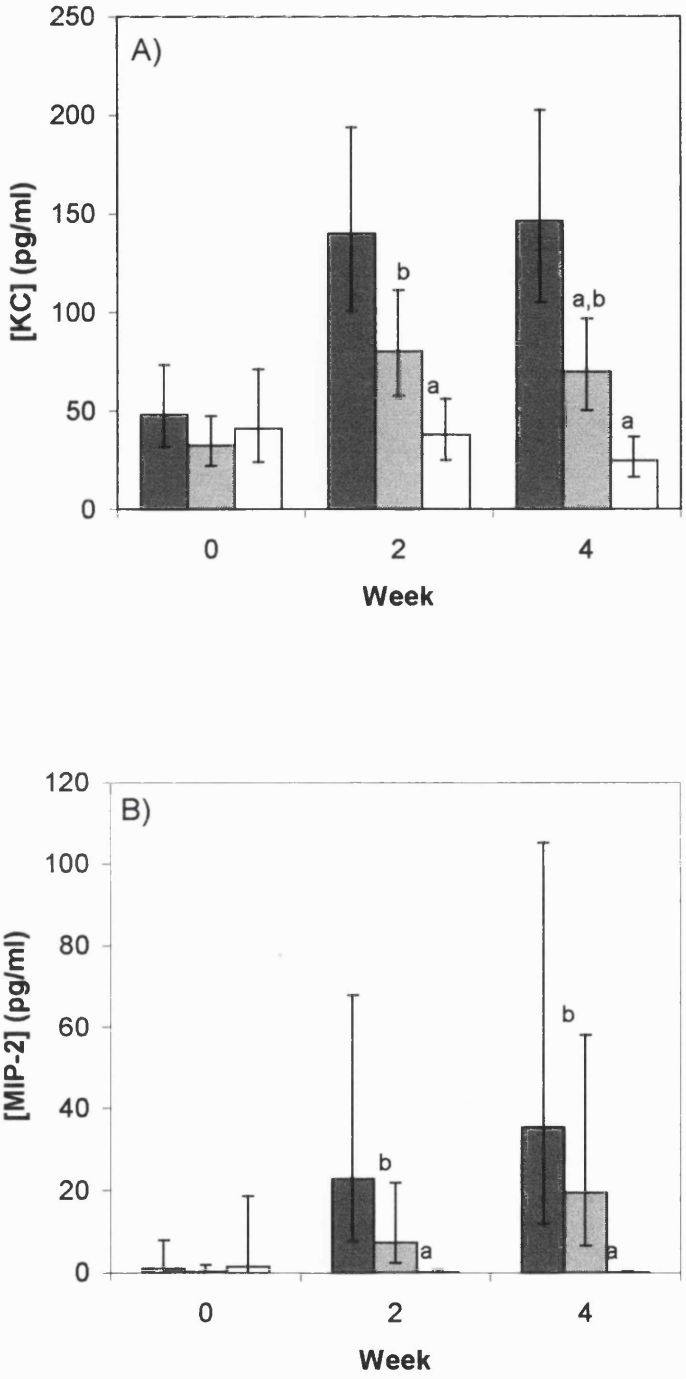

Figure 3-4 Effects of diet and strain of mouse on serum CXC chemokines

Effect of diet and strain of mouse on serum KC (A) and MIP-2 (B) concentrations (dark grey bar, apoE*3 Leiden mice consuming HFC/C diet (n=6); light grey bar, non-transgenic controls consuming HFC/C diet (n=6); open bar, apoE*3 Leiden mice consuming RM1 diet (n=4)). Values shown are geometric means ± 95% confidence intervals (a = significantly different ($p \leq 0.02$) to apoE*3 Leiden mice consuming HFC/C diet, b = significantly different ($p \leq 0.05$) to apoE*3 Leiden mice consuming RM1 diet).

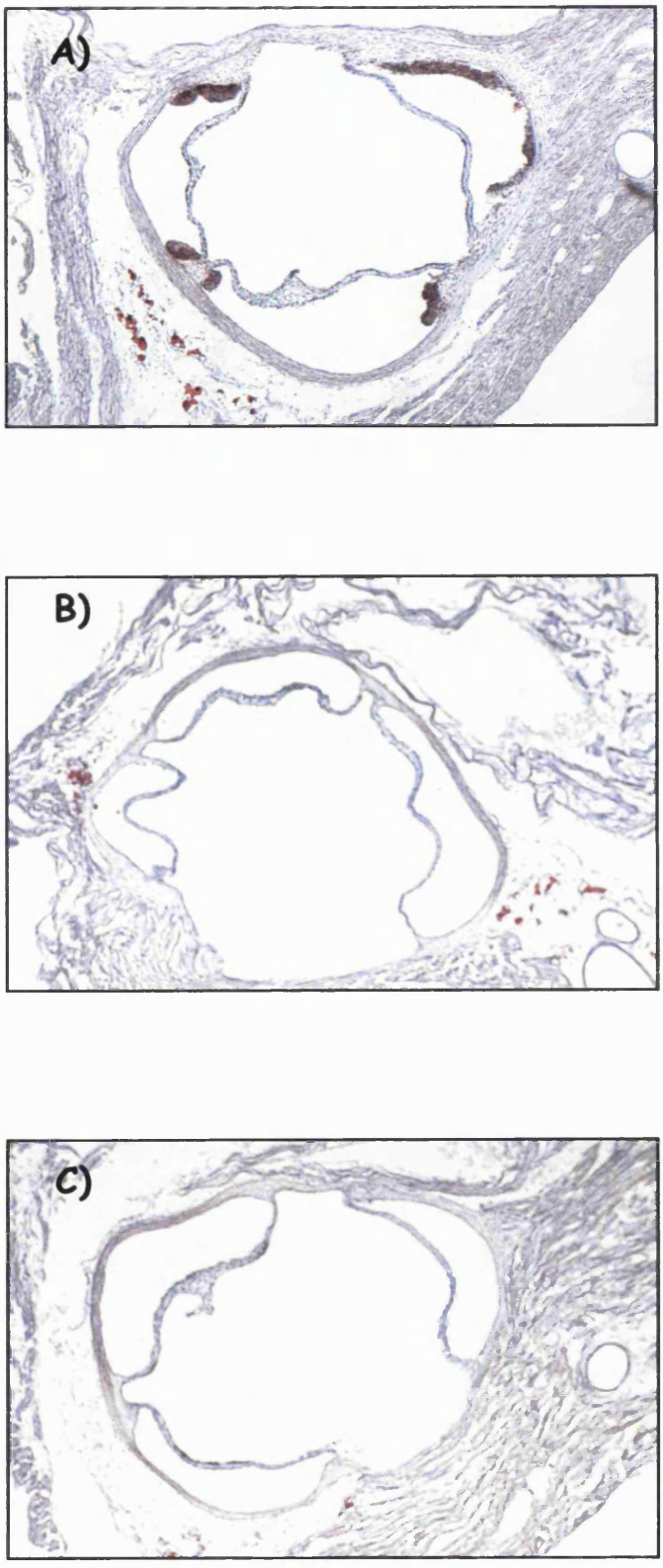

Figure 3-5 Photomicrographs of aortic root sections

Typical histological sections of aortic root (original magnification x40) taken from (A) apoE*3 Leiden mice and (B) non-transgenic littermate, following consumption of the atherogenic diet HFC/C diet for four weeks. (C) ApoE*3 Leiden mice consuming the normal RM1 diet. Oil-Red-O staining.

3.4 Discussion

This study examined whether CXC chemokines were elevated during the development of diet-induced hypercholesterolaemia in apoE*3 Leiden mice and their non-transgenic littermates. Elevated serum levels of murine IL-8RH ligands, KC and MIP-2 were seen in both apoE*3 Leiden mice and their non-transgenic littermates consuming an atherogenic diet. Furthermore, KC was found to be significantly elevated in apoE*3 Leiden mice compared with the non-transgenic animals, and was associated with the grossly elevated serum cholesterol levels and fatty streak lesions observed in this group. This raised the possibility that circulating levels of CXC chemokines could reflect enhanced expression of these molecules during atherogenesis and prove useful as serum markers of lesion development.

However, this study provided no information on the site(s) of production of these elevated CXC chemokines. They may evolve from a number of different cells or tissues. It is possible that the developing atherosclerotic lesions seen in apoE*3 Leiden mice consuming the HFC/C diet could contribute directly to the levels of circulating KC and MIP-2. *In vitro* studies have suggested that IL-8 production and secretion by arterial cells is enhanced following incubation under pro-atherogenic stimuli, including; cholesterol loading [172], oxidised LDL [173], oxysterols [174] and inflammatory cytokines [175]. Furthermore, macrophages isolated from human atheromatous plaques show increased capacity to produce IL-8 [172,174,176] and immunoreactive IL-8, GRO-α and murine KC have been detected in macrophage-rich areas of lesions [177,338].

Alternatively, blood leukocytes may be an important source of serum chemokines. Hypercholesterolaemia is a well-known risk factor for atherosclerosis (Section 1.1.2). Recently, it was shown that monocytes isolated from hypercholesterolaemic patients had enhanced IL-8 expression and secretion compared to normocholesterolaemic individuals [339]. Furthermore, plasma concentrations of IL-8 correlated with IL-8 expression by blood mononuclear cells [340]. Thus, activated blood leukocytes may be an important contributing source of serum chemokines.

Elevated levels of circulating chemokines may also be derived from hepatic cells. Consumption of an atherogenic diet by C57Bl/6J mice is reported to induce oxidative stress, inflammation and lipid accumulation in both aortic and hepatic tissues [110,111]. Moreover, atherogenic diets generate similar responses to injection of minimally modified LDL, namely activation of NF-κB and induction of genes for macrophage-

colony stimulating factor, JE, KC, haem oxygenase and serum amyloid A in the liver [20,110,111]. Importantly, susceptibility to hepatic oxidative stress and inflammation appear to co-segregate with aortic atherosclerotic lesion formation [111].

Finally, serum CXC chemokine concentrations could be affected by the rate of clearance of these molecules from the bloodstream. The mechanisms involved may include binding to the IL-8RH [341,342], proteoglycans [343] on cells or tissues, the Duffy antigen receptor complex on red blood cells [344], or to high affinity antibodies generated during inflammation [345]. Therefore, differences in both production and clearance of chemokines may influence circulating levels of KC and MIP-2.

In summary, this study shows that circulating levels of murine KC and MIP-2 are associated with the marked hypercholesterolaemia and accelerated atherosclerosis seen in apoE*3 Leiden mice consuming an atherogenic diet. Serum chemokines may not solely be derived from arterial cells, but from other sites including activated blood leukocytes or hepatocytes. Therefore, although the site(s) of production, and functional significance of these molecules have yet to be elucidated, circulating concentrations of CXC chemokines could prove useful markers of the enhanced immune activation and chronic inflammation that characterises atherogenesis.

This preliminary study raises a number of important issues, addressed by the work in the remainder of this thesis. The temporal relationships between serum chemokine concentrations, development of hypercholesterolaemia, and progression of lesion development from early 'fatty streak' to more complex fibrous lesions are not known. The site(s) of production of CXC chemokines contributing to elevated serum levels of these proteins are also unclear; these molecules could be derived predominantly from the artery wall, or from other sites such as the liver. Circulating levels of CXC chemokines, KC and MIP-2, should be compared with serum concentrations of the prototypic CC chemokine, JE/MCP-1, which plays an established role in monocyte recruitment during atherogenesis. Further, although increases in soluble adhesion molecules have been observed in individuals with the clinical complications associated with overt atherosclerosis, the temporal relationships between circulating levels of sVCAM-1 and sICAM-1 and the early stages of lesion development have not yet been investigated. Equally, systemic 'markers' of inflammation, such as Hp, SAA and PON1 activity, have been associated with increased risk of CAD. Serum levels of these proteins should be compared with putative 'markers' of monocyte recruitment, chemokines and soluble adhesion molecules, in order to establish which, if any, of

these molecules are predictive of atheroma development in apoE*3 Leiden, or C57BL/6J, mice consuming an atherogenic (HFC/C) diet.

Chapter 4

*Temporal relationships between circulating levels of chemokines, adhesion molecules, systemic inflammatory 'markers' and developing atheroma in apoE*3 Leiden mice*

4 Temporal relationships between circulating levels of chemokines, adhesion molecules, systemic inflammatory 'markers' and developing atheroma in apoE*3 Leiden mice

4.1 Introduction

Atherosclerosis is a chronic inflammatory disease, characterised by silent progression during the third, fourth and fifth decades of life, until the clinical symptoms of angina and/or myocardial infarction become evident [1]. A systemic 'marker' of atherogenesis, reflecting inflammatory events within the artery wall, with proven predictive value, would therefore be a valuable diagnostic tool. Many studies have demonstrated that a number of proteins are altered in the serum or plasma of patients at risk of future CAD, or those with established atherosclerotic disease. These include serum chemokines (Section 1.10.4), soluble adhesion molecules (Section 1.10.2), positive acute phase proteins (Section 1.10.5.1) and paraoxonase (Section 1.9.5). However, the temporal relationship between systemic concentrations of such 'marker' proteins and the initiation and progression of early fatty streak lesions to more complex fibrous plaques is not known.

Circulating levels of CXC and CC chemokines may prove useful serum 'markers' of pathogenic changes occurring during lesion development. Specifically, this study sought to repeat and extend the findings from the first preliminary investigation i.e. that serum CXC chemokines were elevated during development of diet-induced hypercholesterolaemia and were associated with accelerated lesion development in apoE*3 Leiden mice (Chapter 3). The lesions developed by these mice alter in composition and complexity over extended periods of high fat/high cholesterol feeding (Section 1.2.5) [44] and this study was therefore extended to 18 weeks in order to investigate the temporal relationship between circulating CXC chemokines and lesion development.

Members of the CC chemokine subfamily (Section 1.6.1) predominantly chemoattract monocytes and T-lymphocytes, but not neutrophils, and extensive experimental evidence supports a role for the prototypical CC chemokine, MCP-1, and its receptor CCR2, in the monocytic infiltration that characterises atherogenesis [73-75,169,171]. Therefore, in addition to the measurement of CXC chemokines, serum concentrations of JE, the murine homolgue of MCP-1, were also examined.

Further, in order to identify the possible site(s) of production of CC and CXC chemokines, aortic, hepatic and spleen tissues were taken for immunohistochemical and *in-situ* hybridisation analyses. These were supposed to allow investigation of whether serum chemokine concentrations reflected expression at the vessel wall during the development of the disease.

Cell adhesion molecules of the immunoglobulin gene superfamily (Section 1.4.2), such as ICAM-1 are involved in the firm adhesion of monocytes to the endothelium during atherogenesis [346]. Soluble adhesion molecules are found in the circulation, following 'shedding' of these molecules from cells by proteolytic cleavage at a site close to the transmembrane domain (Section 1.10.1). Therefore, in this study circulating levels of sICAM-1 during the early development of atheroma in apoE*3 Leiden mice was measured.

As chemokines and adhesion molecules are intimately involved in the recruitment of mononuclear cells to sites of aortic inflammation, they seemed an obvious choice to follow during the development of atherosclerosis. Recently, APPs originating from the liver have been proposed to have some utility in predicting clinical events associated with underlying atheroma. However, as these proteins are predominantly expressed by the liver, it is unclear whether these proteins are simply 'messengers of risk', or whether they are pathologically involved in atherogenesis. One possible link between the expression of APPs and the development of atherosclerosis is provided by pro-inflammatory cytokines, including interleukin (IL)-6, IL-1α/β and TNF-α. These cytokines may derive from the atherosclerotic lesion and modulate the expression of APPs via nuclear factors (NF), such as NF-κB, NF-IL-6/CAAT enhancer binding proteins β or δ (C/EBPβ or δ), AP-1 or acute phase response factors (APRF). These nuclear factors interact with *cis*-acting elements in the promoter regions of their genes [311]. Positive acute phase proteins include CRP, Hp and SAA. Serum PON-1 activity and hepatic expression of PON1 mRNA are dramatically decreased during the acute phase response (Section 1.10.5) by exposure to LPS, TNF-α or IL-1 [279]. Thus, the potential predictive power of paraoxonase was also investigated, in addition to the afore-mentioned APPs

In order to investigate whether these proteins, singly or in combination, can provide a 'signature' for differing stages of lesion development, systemic levels of KC, MIP-2, JE/MCP-1, sICAM-1, Hp, SAA and PON during the development of atheroma in

apoE*3 Leiden mice and their non-transgenic littermates fed a HFC/C diet were measured.

4.2 Methods

4.2.1 Study protocol

4.2.1.1 Mice

Mice were generated and phenotyped as previously described (Section 2.2). Sixty female apoE*3 Leiden mice and 40 female non-transgenic mice, aged 8-10 weeks, were allocated randomly to experimental groups on the basis of age and litter, and housed in groups of up to 8.

4.2.1.2 Diet

Animals were maintained on the normal mouse diet (RM1), before the experimental period. During the study, mice were fed either RM1 or the atherogenic HFC/C diet (Section 2.2.2). Mice were weaned onto the HFC/C diet over 4 days. In total, 40 apoE*3 Leiden mice, and 40 of their non-transgenic littermates were fed the HFC/C diet; 20 apoE*3 Leiden mice were fed RM1.

4.2.1.3 Collection of blood samples

After 2, 4, 8, 12 and 18 weeks of diet treatment, subgroups of 8 apoE*3 Leiden mice (HFC/C), 8 non-transgenic mice (HFC/C) and 4 apoE*3 Leiden mice (RM1) were culled and also terminal blood samples collected (Section 2.3.1). In-life blood samples were also taken from mice remaining in the study at each time-point (Section 2.3.1). Serum was prepared as previously described (Section 2.3.2)

4.2.1.4 Serum analysis

4.2.1.4.1 Lipid and lipoprotein analysis

Total cholesterol and triglyceride concentrations were measured enzymatically using commercially available kits. Serum lipoproteins were separated by FPLC as previously described in Section 2.3.3, and cholesterol and triglyceride concentrations determined in each fraction of column eluate (Section 2.3.4 and 2.3.5).

4.2.1.4.2 Chemokine analysis

JE, KC and MIP-2 concentrations were determined in diluted serum samples (1:1 - 1:4) using commercially available ELISA kits as previously described in Sections 2.3.7, 2.3.8 and 2.3.9.

4.2.1.4.3 Paraoxonase activity assay

Serum PON activities were assessed by determining the hydrolysis of phenylacetate as previously described [41]. Briefly, the arylesterase activity of the enzyme was measured by the hydrolysis of phenylacetate in 50 mM Tris acetate buffer (pH 7.8) containing $CaCl_2$ (20 mM). The reaction was initiated by the addition of serum (1:10, 10 μl) in a final volume of 1 ml. Increases in absorbances (270 nm) were recorded every 30 s during 10 min incubation at RT. Values are expressed as units (U) (1 μmol hydrolyzed per min) per ml of serum.

4.2.1.4.4 Haptoglobin assay

Levels of Hp were assessed indirectly by measuring peroxidase activity associated with this protein, using a kit provided by Tridelta Development Ltd. The assay works on the principle that free haemoglobin exhibits peroxidase activity, which is inhibited at low pH; Hp present in the sample combines with haemoglobin and at low pH preserves the peroxidase activity of the bound haemoglobin. Preservation of the peroxidase activity of haemoglobin is directly proportional to the amount of Hp in the sample. Serum samples were diluted with the provided calibrator diluent (1:1) and assayed in duplicate. Diluted samples or standards (7.5 μl) were added to the wells of a 96-well plate, followed by the addition of premixed haemoglobin (100 μl). Pre-mixed chromogen/substrate (140 μl) was then added to the wells and the plate incubated for 15 min at RT. The plate was read immediately at 630 nm. Sample concentrations of Hp activity were calculated with reference to the Hp standards, at concentrations ranging from 0.06 – 2 mg/ml.

4.2.1.4.5 Serum amyloid A

Murine SAA concentrations were determined using a commercially available kit (BioSource International). Serum samples were diluted 1:100 with the provided diluent, and assayed in duplicate. Briefly, the wells were washed with kit wash buffer (2x 300 μl) and aspirated after each wash. Anti-mouse SAA (50 μl) was added to the wells followed by the samples and standards (50 μl). The 96-well plate was incubated for 2 h after which time it was thoroughly washed (3x 300 μl) with wash buffer. The

substrate solution was prepared by adding two disodium p-nitrophenyl phosphate (PNPP) tablets to PNPP substrate buffer (10 ml). Substrate was added (100 μl) to the wells and the plate covered and incubated at 37°C for 1 h. The reaction was halted by the addition of the provided stop solution (50 μl) and the absorbance of each well determined at 405 nm. Sample concentrations of SAA were calculated with reference to the recombinant SAA standards, at concentrations ranging from 0.23 – 3.80 μg/ml.

4.2.2 Tissue preparation

After 2, 4, 8, 12 or 18 weeks of the study, mice were culled by CO_2 inhalation, and the heart, liver, kidneys, spleen and lungs dissected out immediately and prepared as described in Section 2.4.1.2 and 2.4.1.3.

4.2.3 Tissue analysis

4.2.3.1 Lesion analysis

Cross-sectional lesion area was determined by morphometric evaluation of every third section of the aortic root, commencing from the appearance of the three valve leaflets (Section 2.4.1.2). Ten sections in total were analysed as previously described in Section 2.5.2.

4.2.3.2 Macrophage immunostaining

Serial sections (6 μm) of the aortic root, commencing from the appearance of the valve leaflets were used to assess macrophage content. Briefly, sections were air-dried (30 min) and fixed in acetone (-20°C, 5 min). All subsequent incubations were carried out at RT with the exception of the primary antibody step (4°C). Endogenous peroxidase activity was quenched by incubating sections with H_2O_2 (0.3%, v/v) in methanol. Sections were washed (3x) with Tris-buffered saline/Tween (TBST; DAKO), and non-specific binding to endogenous biotin blocked using an avidin/biotin blocking kit (Vector Labs). Sections were washed (3x) with TBST and then incubated overnight at 4°C with either MOMA-2 (10 μg/ml) (Serotech) or the equivalent concentration of the isotype control, rat $IgG2_B$ (Serotech). After washing (3x) with TBST, sections were incubated with mouse preabsorbed goat anti-rat immunoglobulins (Biogenex), washed (3x) with TBST and then incubated with streptavidin conjugated peroxidase (Biogenex). Slides were washed again (3x) with TBST, and immunoreactive staining visualised by the addition of diaminobenzidine tetrahydrochloride (DAB) substrate (Vector Labs). Sections were counterstained with Mayer's haematoxylin, dehydrated through a graded series of alcohols, cleared in xylene and mounted with DPX (Raymond A Lamb).

4.2.3.3 Chemokine immunostaining

4.2.3.3.1 Culture of murine b.End5 cells

The murine endothelioma cell line, b.End.5 (European Collection of Cell Cultures), was used to establish an immunostaining protocol for the detection of chemokine proteins. Cells were grown in 75cm^2 flasks containing Dulbecco's Modified Eagle Medium (DMEM) supplemented with 10% v/v foetal bovine serum, 100 IU/ml penicillin, 100 μg/ml streptomycin, 2 mM L-glutamine and 1% v/v non-essential amino acids. Flasks (Triple Red) were incubated in a humidified atmosphere at 37°C with 5% CO_2.

4.2.3.3.2 Immunocytochemical analysis of murine b.End5 cells

Murine b.End 5 cells were seeded at a density of 250,000 cells per well on to Tech well slides (NUNC), and incubated overnight at 37°C. Cells were treated for 4 h (37°C) in DMEM medium (Section 4.2.3.3.1) +/- LPS (10 μg/ml). After this time, the medium was removed and assayed for the presence of KC and JE (Section 2.3.7 and 2.3.8). The chamber boundaries were carefully removed from the slide, the cells washed with Hanks Balanced Salt Solution (HBSS), and chamber sections defined using a paraffin pen (DAKO). The cells fixed for 15 min with paraformaldehyde (4%, w/v)/HBSS, and then probed for KC expression using a goat anti-mouse polyclonal antibody (R&D Systems). Briefly, endogenous peroxidase activity was quenched by incubating the slide in H_2O_2 (0.5%, v/v)/HBSS. After washing with HBSS, the primary antibody (10 μg/ml) was applied for 45 min. Bound primary antibody was detected by incubation with biotinylated rabbit anti-goat immunoglobulins (DAKO) diluted to 1:600 in neat rabbit serum; secondary antibody was detected by the addition of StreptABComplex/horseradish peroxidase (1:600, DAKO). Immunoreactive staining was visualised by the addition of DAB, followed by counterstaining with haematoxylin and mounting with glycerol/PBS. Negative controls were provided by omission of the primary antibody, or incubation with non-immune goat IgG (R&D Systems).

4.2.3.4 Analysis of hepatic iipid content

4.2.3.4.1 Bligh and Dyer extraction

Hepatic lipids were extracted using a modified version of the Bligh and Dyer (1959) extraction method. Liver samples were removed from storage (-70°C), defrosted, weighed and placed in 5 ml Tris/HCl buffer (50 mM Tris, 150 mM NaCl, pH 7.4) on ice. The samples were homogenised and further diluted (1:1) with Tris/HCl buffer.

The extraction efficiency was determined by incorporating radiolabelled [^{3}H] cholesterol, cholesterol [^{3}H] oleate, [^{3}H] phosphatidyl choline and [^{14}C] triolein into the extraction buffer. Briefly, working stock solutions of each radiolabeled lipid containing 10^6 dpm/ml were prepared in extraction buffer (chloroform/methanol; 1:2 v/v). From each working stock solution, 26.7 μl was added to 10 ml of extraction buffer to yield a radioactive count of 2.6 x10^4 dpm/ml for each lipid. The radioactivity (dpm) associated with each solution was checked by liquid scintillation counting (Beckman Coulter, model LS5000CE). It must be noted that the concentration of each radiolabel added to the extraction buffer was negligible (<1 μM).

The diluted liver homogenate samples (1 ml) were added to 3.75 ml of labelled extraction buffer, and left to stand with intermittent shaking for 1 h. Chloroform (1.25 ml) and potassium chloride (1.25 ml) were added to give a final extraction ratio of chloroform: methanol: potassium chloride of 10:10:9 by volume. The samples were centrifuged (10 min, 300 x *g*) to assist phase separation and the lower organic phase containing the lipids (2 ml) removed to a clean glass tube and dried under a steady stream of nitrogen. The walls of the glass tube were rinsed with chloroform (1 ml) and re-dried down under nitrogen to ensure the entire lipid extract was concentrated at the base of the tube. An additional 100 μl of bottom phase was removed for liquid scintillation counting in order to facilitate calculation of extraction efficiencies.

4.2.3.4.2 Separation of hepatic lipids by thin layer chromatography

Lipids were re-dissolved in chloroform (200 μl) and mixed thoroughly before being placed on ice. Samples (50 μl) were applied to a thin layer chromatography (t.l.c) plate (Linear-K preadsorbent silica t.l.c plate, Whatman) and allowed to dry. Standards of cholesterol, cholesteryl ester, triglyceride and phospholipid (2.5 mg/ml) were also applied (25 μl) to aid identification of bands of interest. The t.l.c plate was then placed in a solvent tank containing petroleum ether: diethyl ether: glacial acetic acid (90:30:1 by volume) for approximately 45 min or until the solvent front had migrated 2 inches from the top of the plate. The plate was allowed to dry and the bands visualised with iodine vapour.

4.2.3.4.3 Re-extraction of lipids using hexane and propan-2-ol

The triglyceride, phospholipid, free and esterified cholesterol bands were scraped from the t.l.c plate and transferred to labelled glass tubes. The lipid was extracted with hexane:propan-2-ol (3:2 v/v) and vortexed to aid the elution of lipid from the silica. The eluate was transferred to a clean glass tube and evaporated to dryness under nitrogen, as before.

4.2.3.4.4 Lipid assays

Each dried hepatic lipid extract was re-dissolved in 50 µl of propan-2-ol and 20 µl removed for liquid scintillation counting to check the efficiency of the elution process. Further aliquots (5 µl) were removed to assess hepatic triglyceride, and free and esterified cholesterol as described previously (Section 2.3.4 and 2.3.5). Phospholipid content was quantitatively determined by an enzymatic colourimetric method using the Phospholipids B kit (WAKO). Phospholipids are first hydrolysed by phospholipase D to release choline. The free choline is subsequently oxidised to betaine with the simultaneous production of H_2O_2. The hydrogen peroxide oxidatively couples 4-aminoantipyrine and phenol to yield a chromogen with an absorbance maximum of 505 nm. Briefly, standards and samples were added in duplicate to appropriate wells of a 96-well plate, followed by the addition of colour reagent (95 µl). The plate was incubated at 37°C for 10 min and the absorbance of each well was read at 550 nm. The phospholipid concentration was determined with reference to the standard curve (0 – 300 mg/dl).

Equation for working out the recovery:

$$\text{hepatic lipid content (mg/g wet weight)} = \frac{\left(\text{measured lipid (mg/ml)}\right) \times \left(\frac{\text{total dpm in extraction solvent (3.75 ml)}}{\text{total dpm in eluate (50 µl)}}\right) \times 10}{\text{g liver (wet weight)}}$$

4.2.4 Localisation of KC and JE mRNA expression in tissue sections by *in-situ* hybridisation

4.2.4.1 Probes

JE/MCP-1 and KC cDNAs were purchased from American Tissue Type Collection (Rockville, MD, USA). The JE insert was contained within the plasmid pGEM-1 (Figure 4-1). This plasmid was suitable for generating sense and anti-sense riboprobes as the insert was flanked by T7 and Sp6 promotor sites. However, the KC

insert was contained within plasmid pSP64 (Figure 4-1), which contained only an Sp6 promotor site and was therefore unsuitable for generating sense and anti-sense riboprobes. Therefore, the KC cDNA was excised with restriction enzymes and cloned into pPCR Script Amp SK (+) cloning vector (pPCR-Script™ Cloning Kit, Stratagene) which had T3 and T7 promotor sites. This is described in detail below and in Section 2.6.

4.2.4.2 Subcloning of KC insert

4.2.4.2.1 Microbiology

Freeze-dried bacteria were innoculated into 5 ml of sterile LB medium (Appendix 9.4.1) containing ampicillin (Section 4.2.4.2.2) (LB_{AMP} medium) and cultured overnight in a gyratory shaker-incubator (37°C, 225 rpm). LB agar plates containing ampicillin (LB_{AMP} agar; Appendix 9.4.2) were prepared and streaked with the bacterial culture and incubated overnight (37°C). From this, a single colony was picked and used to innoculate LB_{AMP} medium (5 ml) to produce a starter culture (16 h, 37°C, 225 rpm).

4.2.4.2.2 Ampicillin selection

The antibiotic ampicillin interferes with a number of enzymes involved in bacterial wall synthesis. Both the plasmid vectors used in this study contained an ampicillin resistance gene and therefore ampicillin was used as a selectable marker at a concentration of 50 μg/ml.

4.2.4.2.3 Restriction digest

Plasmid DNA was isolated as described previously (Section 2.6.3). The KC cDNA was excised from the pSP64 vector using the restriction enzyme *Pst* I (Life Technologies). Briefly, the plasmid (1 μg) was incubated (1 h, 37°C) with 1 unit of *Pst* I and 1x REACT buffer 2 (Appendix 0). The restriction digest was analysed using gel electrophoresis (Section 2.6.5) and the KC cDNA extracted from the agarose gel (Section 2.6.6). To confirm the concentration and the size of the KC cDNA, an aliquot (~200 ng) was run on an agarose gel (1%) against a DNA Mass ladder (Life Technologies; 4 μl) and a 100 bp DNA ladder (Life Technologies).

4.2.4.2.4 'Polishing' of KC insert

The KC cDNA was 'polished' to remove sticky ends. This was achieved by adding the purified insert (10 µl) (Section 4.2.4.2.3), deoxynucleotide triphosphate (dNTP) mix (1 µl, 10 mM), 10x polishing buffer (1.3 µl) and cloned *Pfu* DNA polymerase (1 µl, 0.5 U) in order to a microfuge tube (0.5 ml) (pPCR-Script™ Cloning Kit, Stratagene). The polishing reaction was mixed, and overlaid with a drop of mineral oil. The reaction was then incubated for 30 min at 72°C. The KC cDNA was stored at 4°C until use.

4.2.4.2.5 Ligation of KC insert into the cloning vector

The KC insert was ligated into pPCR-Script Amp SK (+) cloning vector (pPCR-Script™ Cloning Kit, Stratagene). The following components were added, in the stated order, to a microfuge tube (0.5 ml): pPCR-Script Amp SK (+) cloning vector (1 µl, 10 ng/µl), PCR-Script 10x reaction buffer (1 µl), rATP (0.5 µl, 10 mM), blunted ended (polished) KC insert (4 µl), *Srf* I restriction enzyme (1 µl, 5U/µl), T4 DNA ligase (1µl) and sterile distilled water (1.5 µl). The ligation reaction was gently mixed, centrifuged briefly and incubated for 1 h at RT. The reaction was incubated at 65°C for 10 minutes and stored on ice until transformation (Section 2.6.1). A correct clone was identified (Section 2.6.2) and the bacterial culture was scaled up as outlined in Section 2.6.4 so that there was enough plasmid DNA for the transcription of the riboprobes.

4.2.4.2.6 Automated DNA sequencing

The pPCR-Script Amp SK (+) cloning vector containing the KC cDNA was sequenced to determine the orientation of the insert so that sense and anti-sense riboprobes could be synthesised. The vector was sequenced on an ABI377 automated sequencer (PE Applied Biosystems) by Gene Expression Sciences at GSK using T7 and T3 primers.

4.2.4.2.7 Linearisation of plasmid DNA to produce sense and antisense templates

The plasmids were linearised at an appropriate restriction site prior to transcription so that sense and antisense transcripts were obtained virtually free of vector sequence (Figure 4-2). Plasmid DNA containing the KC insert (10 µg) was linearised with *Not* I (Life Technologies) to produce the KC sense template or *BamH* I (Life Technologies) to produce the KC anti-sense template. Plasmid DNA containing the JE insert (10 µg) was linearised with *Pvu* II to produce the JE sense template or *BamH* I to produce the JE anti-sense template. The plasmids were incubated for 2 h at

37°C with the appropriate restriction enzymes and buffer to ensure the restriction digest ran to completion. This is important because a small amount of undigested plasmid DNA can give rise to very long transcripts, which may incorporate a substantial fraction of the radiolabeled rUTP. Linearised plasmids were purified using a commercially available kit (Wizard DNA Clean-Up Kit, Promega). To ensure the plasmids had been linearised, 0.5 μg was run on an agarose gel (1%) along side some uncut plasmid (0.5 μg). As the uncut plasmid is more compact, it will migrate faster on the gel than the linearised plasmid. The DNA was purified using the Wizard DNA Clean-up Kit (Section 2.6.7).

4.2.4.3 Transcription of riboprobes

As mRNA is extremely sensitive to RNase degradation, care was taken to prevent contamination at every stage of the protocol (including cryostat section cutting; Appendix 9.5). Gloves were worn for all manipulations and, where possible disposable RNase-free plasticware or baked (120°C) RNase free glassware were used. Pipettes and work surfaces were sprayed with 'Rnase-away'. In general, all solutions were prepared with diethyl pyrocarbonate (DEPC; 0.1%) treated sterile distilled water and autoclaved where possible.

Sense and anti-sense RNA probes were transcribed from the linear templates and labelled with ^{35}S UTP (Amersham Pharmacia Biotech) using Sp6 or T7 polymerase (Promega) and a riboprobe transcription kit (Promega). An RNA century marker (Ambion) was also prepared to check that full-length riboprobes had been transcribed successfully. Briefly, reaction mixes were set up in sterile microfuge tubes as outlined in Table 4-1 and incubated at 37°C. After 40 min, another 1 μl of appropriate RNA polymerase was added to the reaction mix and incubated for a further 40 min. RNase-free DNase (1 μl) was added to degrade the DNA template, followed by RNasin (Promega, 1 μl) and incubated for 15 min at 37°C. Unincorporated nucleotides were removed using G-50 Sephadex columns as outlined in section 4.2.3.3.1

4.2.4.3.1 Purification of riboprobes

The radiolabelled RNA probes were purified to remove unincorporated nucleotides using Quick Spin columns (Boehringer Mannheim) as per manufacturers instructions. Briefly, the storage buffer was removed (1100 x *g*, 2 min, 4°C) and discarded and the sample applied carefully to the centre of the column bed. The

column was placed in a collection tube, centrifuged (1100 x *g*, 2 min, 4°C) and the purified sample collected in a sterile tube. Prior to ethanol precipitation of the probe, 1μl of each reaction was run on a QuickPoint gel (Novex) to check for full-length transcripts (Figure 4-3). The appearance of the transcript bands in the autoradiograph (Figure 4-3) are faint, this is an unavoidable effect in reproduction.

4.2.4.3.2 QuickPoint rapid nucleic acid separation system

Full-length transcripts were identified using the QuickPoint gel electrophoresis system (Novex). A pre-cast gel (polyacrylamide/urea) was loaded into the QuickPoint cell as per manufacturers instructions. QP running buffer (Novex) was diluted to give 1x and 5x strength, and the lower buffer chamber of the cell filled with 1x QP running buffer (55°C, 750 ml). The upper buffer chamber was filled with 5x QP running buffer (65 ml) ensuring that the gel wells were completely covered. The gel was pre-run for 5 minutes at a constant voltage of 1200 V. Samples were diluted (1:1) with sample loading buffer (Ambion) and 1 μl loaded into each well. Empty wells were loaded with sample loading buffer (0.5 μl) to ensure a straight banding pattern and the gel run at a constant voltage of 1200 V for 10 min. The gel cassette was opened leaving the gel on the shorter notched glass plate. The gel was wrapped in Saran wrap, placed in a film cassette with photographic film, exposed (-70°C) for 30 min and then developed (Figure 4-3).

4.2.4.3.3 Ethanol precipitation of riboprobes

The riboprobes were ethanol precipitated by adding 20 μl of sodium acetate (3M, pH 7.5), 10 μl tRNA and 250 μl of ice-cold ethanol (100%). The riboprobes were incubated at -70°C for 30 min.

4.2.4.4 In-situ hybridisation of aortic root and liver sections

4.2.4.4.1 Preparation of sections for in-situ *hybridisation*

Cryostat sections of aortic root and liver (6 μm) were thaw-mounted onto Superfrost plus gold microscope slides as described in sections 2.4.1.2 and 2.4.1.3 and stored at -70°C until use. Sections were fixed in fresh paraformaldehyde (4%, w/v) in DEPC treated PBS, pH 7.4, acetylated in acetic anhydride (0.25% v/v)/triethanolamine (0.1 M)/NaCl (0.1 M) and dehydrated and delipidated through a graded series of alcohols and chloroforms (Appendix 9.5). Sections were air-dried.

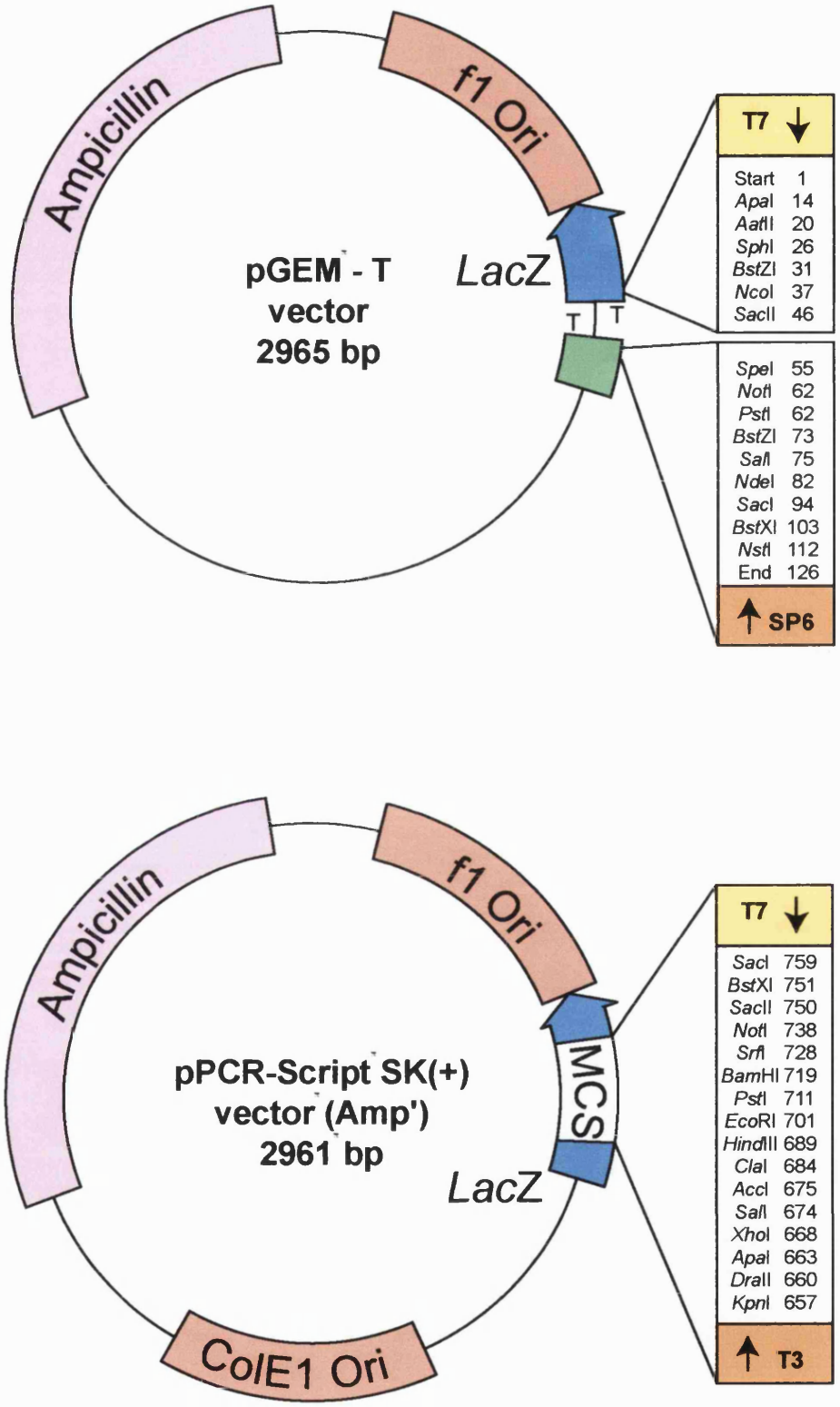

Figure 4-1 Vector maps of pGEM-1 and pPCR Script

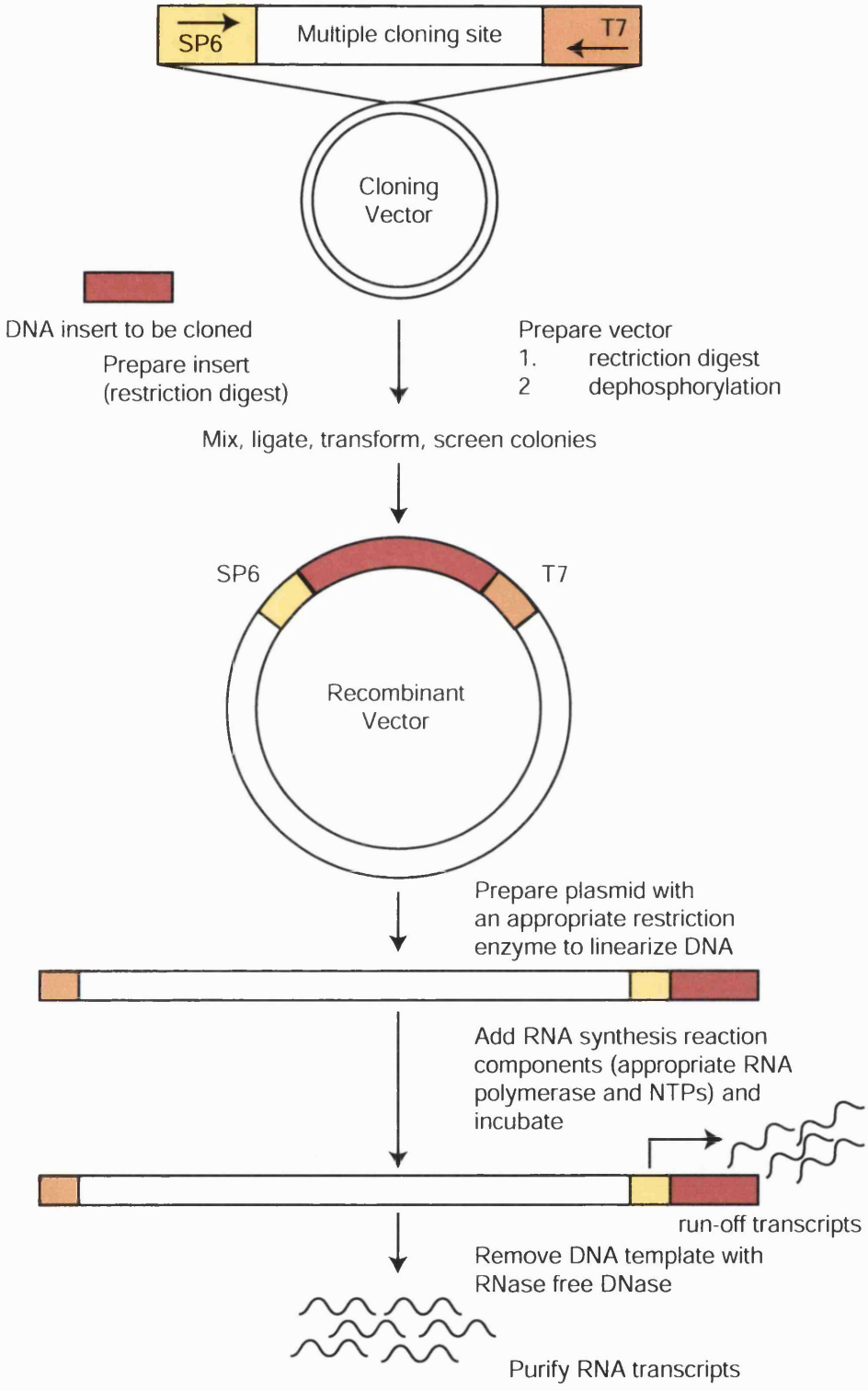

Figure 4-2 Riboprobe *in vitro* transcription

Adapted from www.promega.com

	JE sense	JE anti-sense	KC Sense	KC anti-sense	Century marker
Transcription buffer	5 μl	5 μl	5 μl	5 μl	4 μl
DTT	2 μl	2 μl	2 μl	2 μl	2 μl
rATP (10 mM)	1 μl	1 μl	1 μl	1 μl	1 μl
rCTP (10 mM)	1 μl	1 μl	1 μl	1 μl	1 μl
rGTP (10 mM)	1 μl	1 μl	1 μl	1 μl	1 μl
rUTP (0.5 mM)	1 μl	1 μl	1 μl	1 μl	1 μl
Rnasin	0.5 μl	0.5 μl	0.5 μl	0.5 μl	0.5 μl
Template	3.5 μl	3.5 μl	3.5 μl	3.5 μl	1 μl
^{35}S-UTP	6 μl	6 μl	6 μl	6 μl	6 μl
DEPC dH_2O	3 μl	3 μl	3 μl	3 μl	4 μl
T3 RNA polymerase	-	-	-	1 μl	-
T7 RNA polymerase	-	1 μl	1 μl	-	2 μl
Sp6 RNA polymerase	1 μl	-	-	-	-

Table 4-1 **Reaction mixes for the generation of sense and antisense riboprobes**

Figure 4-3 Autoradiograph of successfully transcribed anti-sense (AS) and sense (S) KC riboprobes

4.2.4.4.2 In-situ hybridisation

The riboprobes were removed from the -70°C freezer and centrifuged (10 mins, 13,000 x *g*, 4°C). The supernatant was discarded and the pellet washed with ice-cold ethanol (75%, 250 μl) and centrifuged (5 min, 13,000 x *g*, 4°C). The supernatant was discarded and the pellet air-dried for 5 min at RT before being resuspended in dithiothreitol (DTT, 10 mM, 100 μl). To 10 ml of scintillation fluid, 2 μl of sample was added to measure emission of β-radiation.

Sense and anti-sense riboprobes were resuspended at 25,000 cpm/μl in hybridisation buffer (deionised formamide (50%), DTT (20 mM), Denhardts (1x) containing sodium chloride (0.6M), sodium citrate (0.06M) polyadenylate (100 μg/ml), denatured salmon sperm DNA (100 μg/ml), yeast tRNA (100 μg/ml), 4 x sodium chloride (0.6 M)/sodium citrate (0.06 M) (4 x SSC)). Probes were applied to the relevant labelled slide (80 μl) and a coverslip gently placed over the section. Slides were incubated overnight in a sealed humid chamber at 55°C.

4.2.4.4.3 Stringency washes

After hybridisation, the sections were washed with sodium chloride (0.15M)/sodium citrate (0.015 M) (1 x SSC) (RT, 30 min), treated with RNase A (20μg/ml) in buffer and then with buffer alone (NaCl (500 mM), Tris (10 mM), pH 8.0, EDTA (1 mM), 30 min each at 37°C), washed with 1 x SSC (RT, 30 min), followed by a high-stringency wash (0.5 x SSC at 65°C for 30 min) and 0.5 x SSC at room temperature for 2 x 10 min. Slides were dehydrated through a series of alcohols, air-dried and dipped in photographic emulsion (Amersham Pharmacia Biotech).

4.2.4.4.4 Slide development

Slides were exposed for 8 weeks at 4°C and developed using Kodak D19 (1:1 water), counterstained in toluidine blue, dehydrated through a graded series of alcohols and coverslipped for microscope analysis.

4.2.5 Statistics

Statistical analysis was carried out by Phil Overend (Department of Statistical Science, GSK). All the parameters described, except those indicated, were log-transformed in order to normalise the variances, and geometric means with 95% confidence intervals are quoted. Data for serum cholesterol, triglyceride, and chemokines were analysed using a 2 way analysis of variance (ANOVA) because the data were from mice culled after either 2, 4, 8, 12 or 18 weeks. Comparisons were made between apoE*3 Leiden mice fed HFC/C or normal diets, or the transgenic mice fed HFC/C diet, at each time-point using a Dunnetts test. Differences between the apoE*3 Leiden mice fed normal diet and the non-transgenic mice were analysed *post-hoc* using a Bonferroni method. Pre-treatment data were transformed using the same method as the treatment data and then analysed using a 1-way ANOVA. Comparisons were made as described above. For each time-point in the study, the data for the available animals at that time was compared back to its baseline data using a repeated measures analysis of variance. From this analysis, the within-animal variability was used to estimate the change from baseline/initial values for each group, along with a 95% confidence interval. Where the data was log-transformed, the change from baseline on the log scale was back-transformed to provide a ratio to baseline with confidence interval. The data for total lesion area were log-transformed and all sections analysed simultaneously using a split plot ANOVA. Comparisons of groups were made on the data from each week at the middle aortic section using the Bonferroni method. Differences were considered to be statistically significant if $p<0.05$

4.3 Results

4.3.1 Serum cholesterol and triglyceride

The effects of feeding HFC/C diet on serum cholesterol and triglyceride concentrations in apoE*3 Leiden mice, or their non-transgenic littermates, are shown in Figure 4-4. In confirmation of previous results [44], significant ($p<0.05$) differences in serum cholesterol concentration were evident between all of the groups of animals, throughout the study (Figure 4-4 A). Consumption of diet HFC/C for up to 18 weeks resulted in serum cholesterol levels that were 4 - 8 fold higher in the apoE*3 Leiden mice compared with their non-transgenic littermates ($p<0.00001$), and 10-18 fold higher than those in the transgenic animals fed normal RM1 diet.

Serum triglyceride concentrations were higher in both groups of apoE*3 Leiden mice, compared with their non-transgenic littermates (Figure 4-4 B) throughout the study. Triglyceride concentrations in apoE*3 Leiden mice fed normal diet increased with time, reaching a plateau after 4 weeks. At all time points, serum triglyceride levels in the non-transgenic animals were between 20-38% of the levels seen in the apoE*3 Leiden mice consuming the same HFC/C diet. However, serum triglyceride levels in the two groups of apoE*3 Leiden mice only differed significantly ($p<0.05$) at week 4 of the study, when the group consuming HFC/C diet had serum triglyceride levels that were 44% of those seen in the mice fed normal RM1 diet.

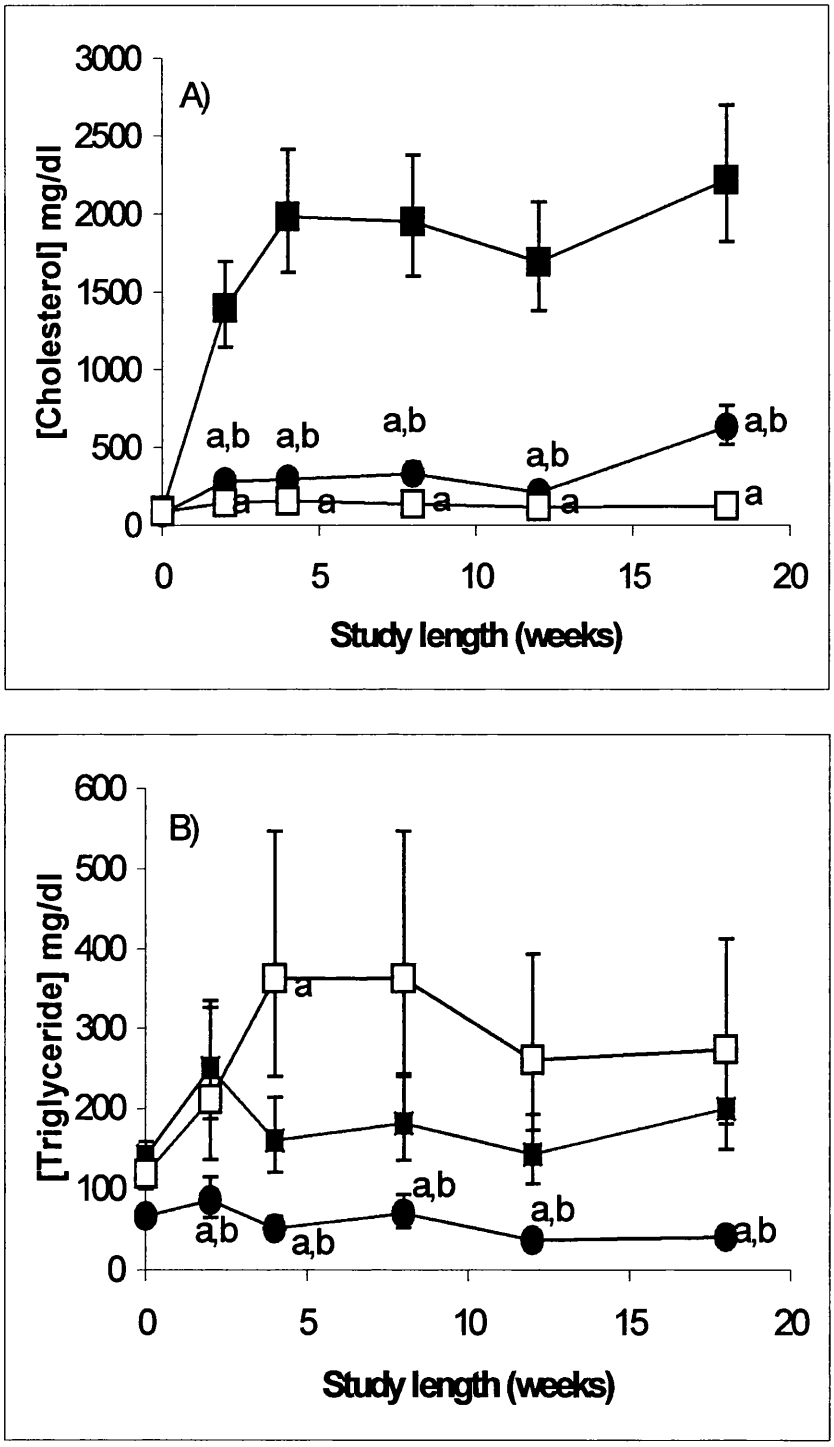

Figure 4-4 Effects of diet and strain of mouse on serum lipids

Serum cholesterol (A) and triglyceride (B) from apoE*3 Leiden mice consuming the HFC/C diet (■), their non-transgenic littermates on the same diet (●) and apoE*3 Leiden mice consuming the RM1 diet (□). Values are geometric means ± 95% confidence intervals (a = significantly different ($p<0.05$) to apoE*3 Leiden mice consuming HFC/C diet, b = significantly different ($p\leq0.05$) to apoE*3 Leiden mice consuming RM1 diet). Cholesterol 1 mM = 38.67 mg/dl, Triglyceride 1 mM = 87.94 mg/dl.

4.3.2 Lipoprotein profiles

The distribution of cholesterol between differing lipoprotein fractions was analysed by Superose 6B column chromatography, using pooled serum samples from animals within the same experimental group. Lipoprotein profiles were determined at 2, 4, 8, 12 and 18 weeks; after 4 weeks consumption of the HFC/C diet, the lipoprotein profile for each group of animals did not alter substantially and so representative data from this timepoint is shown in Figure 4-5. As expected [44], consumption of diet HFC/C increased the proportion of cholesterol within the VLDL/LDL-sized fraction in the non-transgenic animals, but more dramatic increases in the VLDL/LDL-sized fraction were seen in the apoE*3 Leiden mice.

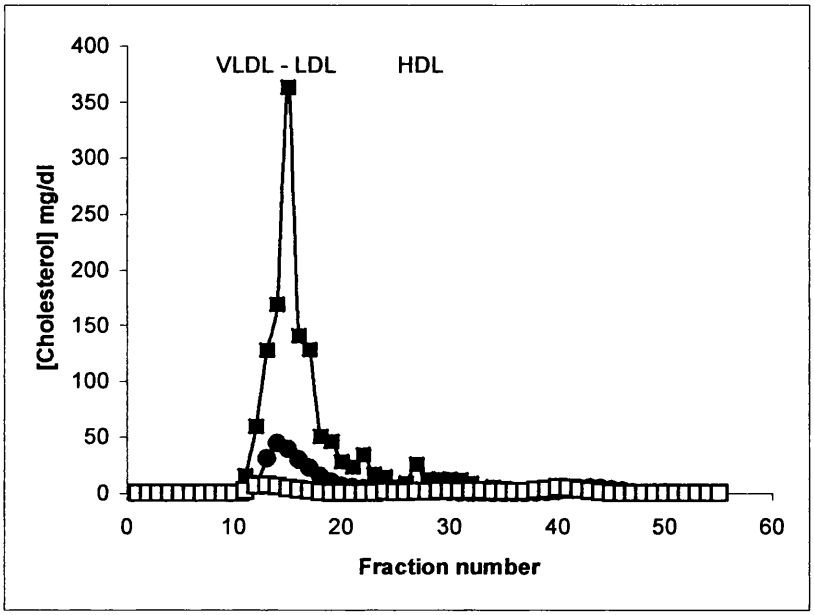

Figure 4-5 Lipoprotein analysis by FPLC

Lipoprotein profiles from apoE*3 Leiden mice consuming the HFC/C diet (■), their non-transgenic littermates on the same diet (●) and apoE*3 Leiden mice consuming the chow diet (□).

4.3.3 Hepatic lipids

The livers of mice consuming the HFC/C diet contained more total cholesterol compared with those from apoE*3 Leiden mice consuming the RM1 diet (Table 4-2). However, the triglyceride content of livers from both groups of mice consuming HFC/C diet were 3 and 4 fold lower ($p<0.05$) than in apoE*3 Leiden mice consuming a normal

diet. No significant differences in phospholipid or free cholesterol content were evident in the three groups of animals.

	Cholesterol				
	Free	**Esterified**	**Esterified/ Free**	**Triglyceride**	**Phospholipid**
Group	***mg/g wet weight***			***mg/g wet weight***	
E*3 Leiden (diet HFC/C)	7.9±1.1	88.5±4.9[a]	11.7±1.5[a]	14.0±1.6[a]	15.8±1.6
C57BL/6J (diet HFC/C)	6.6±0.8	92.5±14.1[a]	13.9±0.7[a]	18.1±2.3[a]	13.3±0.8
E*3 Leiden (chow diet)	9.5±1.9	7.4±0.7	0.9±0.3	48.0±11.1	16.3±4.5

Table 4-2 Hepatic cholesterol, triglyceride and phospholipid content

Values represent the mean ± S.E. of at least three animals per group, fed either the HFC/C diet, or the standard RM1 for 18 weeks. The data was not log-transformed prior to statistical analyses as described in section 4.2.5. [a]significantly different to apoE*3 Leiden mice consuming the RM1 diet.

4.3.4 Development of atherosclerosis in the aortic root

The atherosclerotic lesions observed in mice consuming the HFC/C diet were quantified in cross sections of the aortic root using video image analysis (Figure 4-6). Previously, it has been established that analysis of ten alternate sections, after the appearance of the three valve leaflets, accurately reflects lesion development over this region of the aorta [44,335]. Lesion size was assessed by total area involved (Figure 4-6) and area of Oil-Red-O staining (not shown). No lesions were detected in apoE*3 Leiden mice consuming the RM1 diet. As expected [44], atherosclerotic lesions in apoE*3 Leiden mice were almost two orders of magnitude larger ($p<0.05$) than those seen in the non-transgenic controls. The latter developed small 'fatty streak' lesions within the aortic arch after 12 to 18 weeks consumption of the atherogenic HFC/C diet (Figure 4-7); at earlier time points (Figure 4-7), minimal Oil-Red-O staining was present. By contrast, small intimal 'fatty streak' lesions were evident in the aortic sinus of apoE*3 Leiden mice after 4 weeks consumption of HFC/C diet (Figure 4-7). After 8 weeks, larger intimal lesions had developed in apoE*3 Leiden mice, particularly in the

aortic root (Figure 4-7) which progressed rapidly towards more complex fibrous plaques at week 12 and 18 (Figure 4-7). After 18 weeks consumption of the HFC/C diet some of the lesions observed in the transgenic mice had evidence of calcification (data not shown).

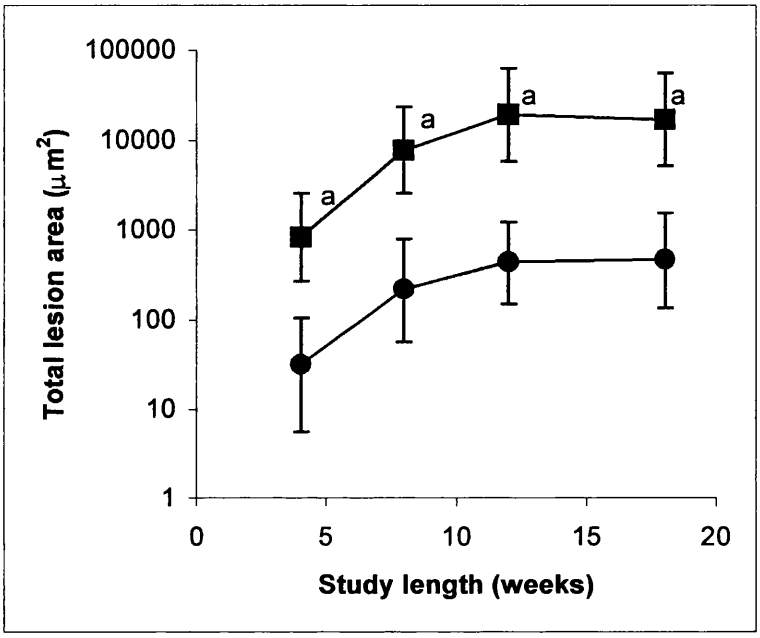

Figure 4-6 Effects of feeding HFC/C diet on cross-sectional area of atherosclerotic lesions in the aortic roots of apoE*3 Leiden mice and their non-transgenic controls

Total lesion area graph for apoE*3 Leiden mice (■, n=8) and non-transgenic littermates (●, n=8) consuming the HFC/C diet. Values shown are geometric means ± 95% confidence intervals, [a]significantly different ($p \leq 0.05$) from non-transgenic mice consuming HFC/C diet.

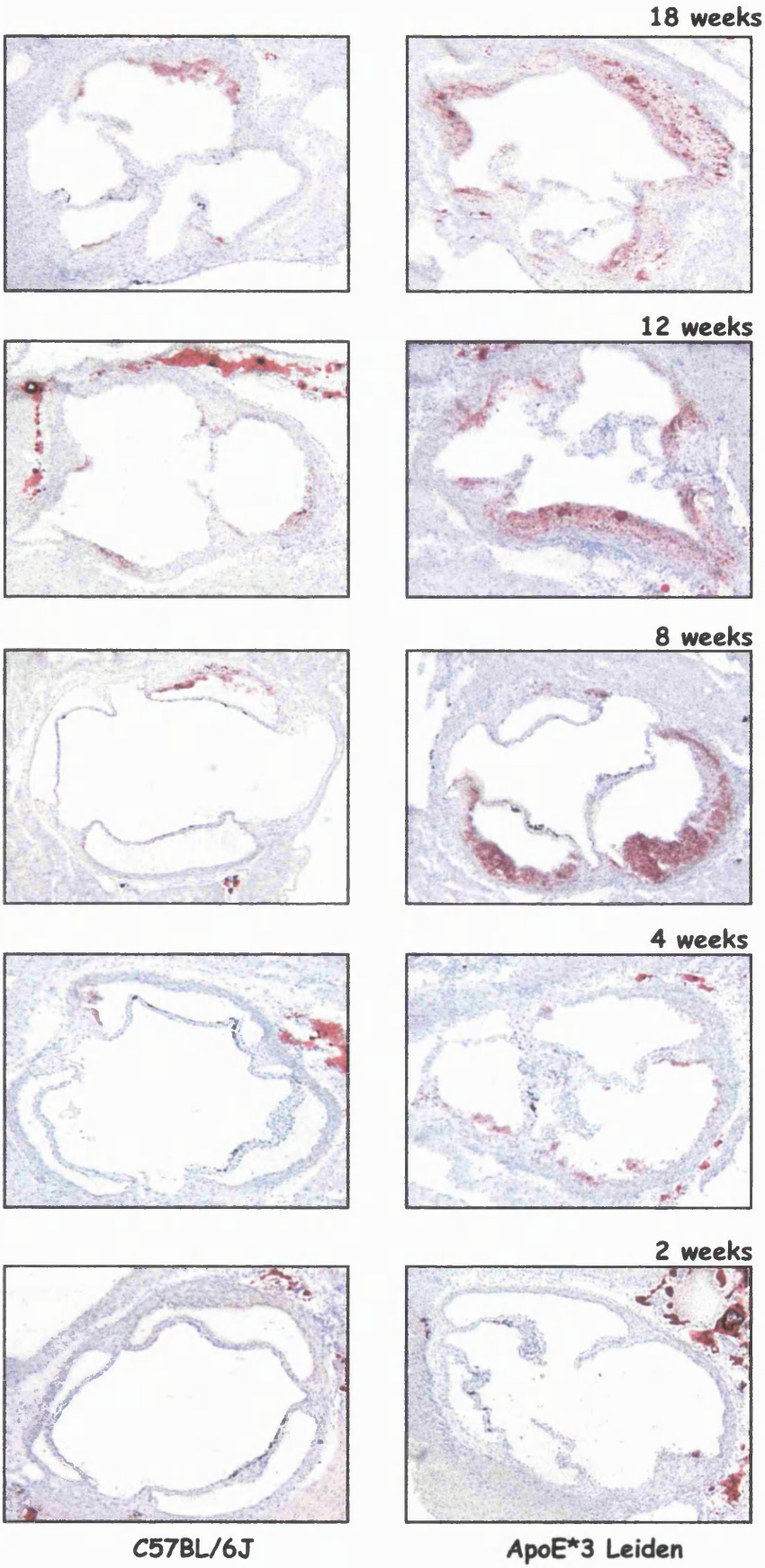

Figure 4-7 Lesion development in apoE*3 Leiden mice and C57BL/6J

Photomicrographs of sections of aortic root sections from apoE*3 Leiden mice (n=8 at each time-point) and their non-transgenic littermates (n=8 at each time-point) consuming the HFC/C for 2, 4, 8, 12 and 18 weeks. Sections were stained with ORO and haematoxylin as described in Section 2.5.1; original magnification x 40.

4.3.5 Macrophage staining

Aortic sections from half the mice in each group (4 apoE*3 Leiden: HFC/C, 4 non-transgenic: HFC/C and 2 apoE*3 Leiden: RM1) were stained using the macrophage specific monoclonal antibody, MOMA-2. Positive staining is shown in brown. No staining was detected in any of the experimental groups after 2 weeks of diet treatment (Figure 4-8 A and Figure 4-9 A) or at any time in the apoE*3 Leiden mice fed the chow diet (Figure 4-9 G). However, after 4 weeks consumption of the atherogenic diet, early intimal lesions and MOMA-2 positive staining were evident in the aortae from all (4/4) of the apoE*3 Leiden mice (Figure 4-9 C + D). Evidence of MOMA-2 staining was visible in only one of the non-transgenic mice at week 4 (Figure 4-8 C). After 12 and 18 weeks consumption of the atherogenic HFC/C diet, more advanced lesions were seen in sections isolated from the apoE*3 Leiden mice, accompanied by extensive positive staining for macrophages within the core of the lesion (Figure 4-9 F + I). The lesions observed in the non-transgenic littermates at weeks 12 and 18 (Figure 4-8 E + F) appeared to stain similarly to those seen in the apoE*3 Leiden mice on the same diet for 4 weeks (Figure 4-9 D).

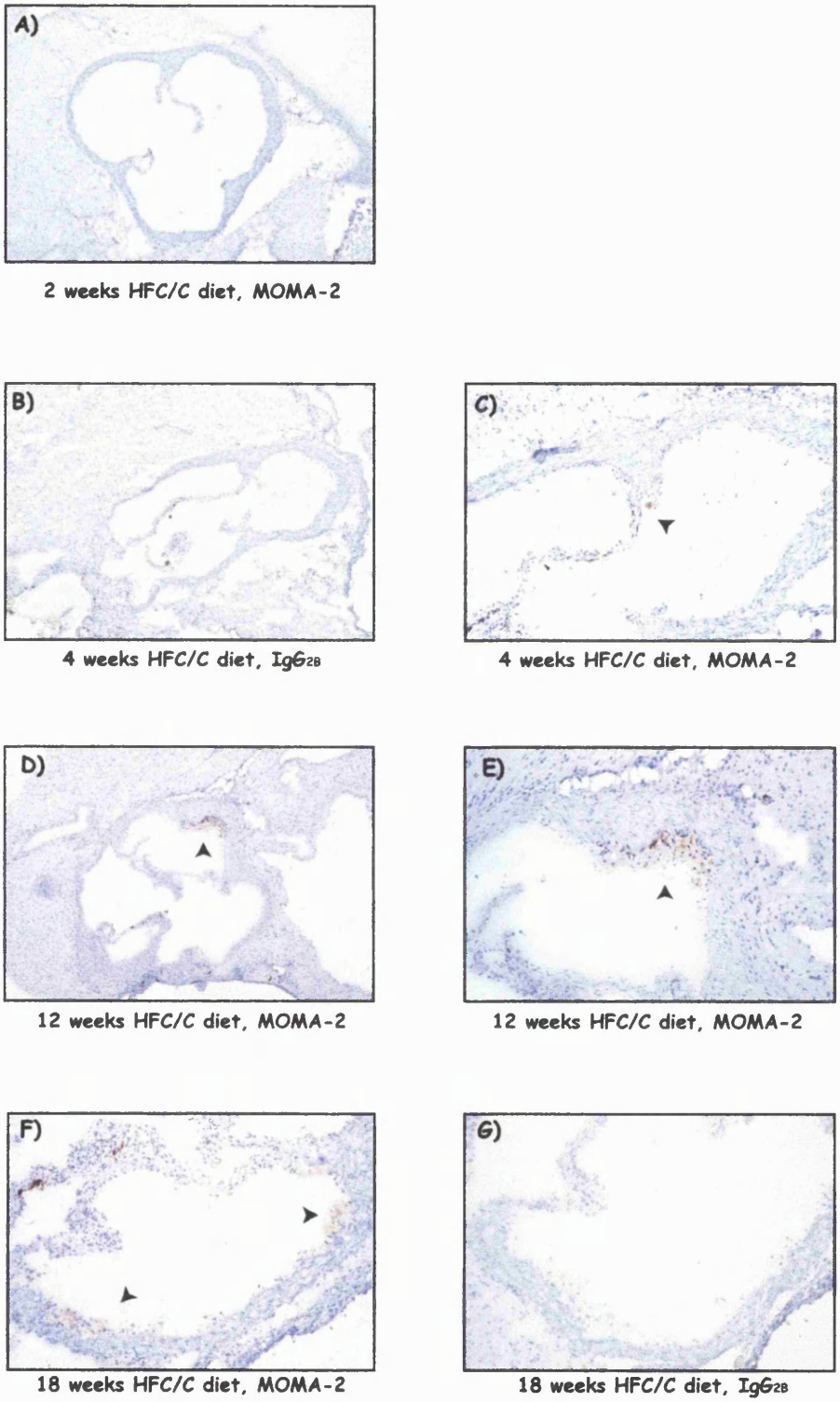

Figure 4-8 Aortic root sections from non-transgenic mice, stained for the presence of macrophages with MOMA-2 antibody.

Panel ***A***): typical section of aortic root taken from a non-transgenic mouse consuming HFC/C diet for 2 weeks. Panels ***B + C***): sections from non-transgenic mice consuming the HFC/C diet for 4 weeks (alternate sections from the same animal). Arrowheads indicate positive macrophage immunostaining. Panels ***D - G***): aortic sinus sections from non-transgenic mice consuming HFC/C diet for 12 (***D + E***) and 18 (***F + G***) weeks. When sections ***B + G***) were incubated with the isotype-matched control, no specific staining was observed. Panels ***A, B + D):*** original magnification x 40. Panels ***C, E, F + G***): original magnification x 100.

Figure 4-9 Aortic root sections taken from apoE*3 Leiden mice, stained for the presence of macrophages with MOMA-2 antibody.

Panel ***A***): typical section of aortic root taken from apoE*3 Leiden mouse consuming HFC/C diet for 2 weeks. Panels ***B - D***): sections from an apoE*3 Leiden consuming the HFC/C diet for 4 weeks. Panel ***D*** is a higher magnification image of panel **C**. Arrowheads indicate positive macrophage immunostaining. Panels ***E - F***): apoE*3 Leiden mice consuming the HFC/C diet for 12 weeks. Panels ***G - J)*** typical sections from apoE*3 Leiden mouse consuming the normal RM1 (***G***) or HFC/C (***H - J***) diet for 18 weeks. Panels ***I + J*** are higher magnification images of ***H***. When sections ***B, E + J***) were incubated with the isotype-matched control, no specific staining was observed. Panels ***A – C, G + H***): original magnification x 40. Panels ***D - F, I + J***): original magnification x 100

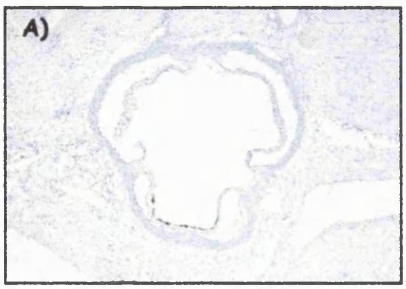

2 weeks HFC/C diet, MOMA-2

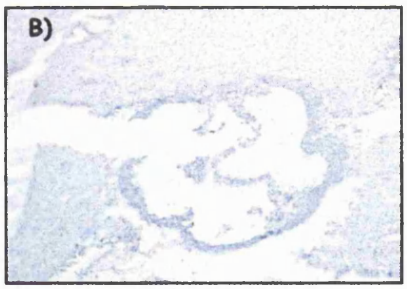

4 weeks HFC/C diet, IgG_{2B}

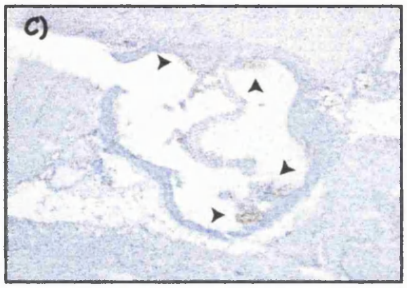

4 weeks HFC/C diet, MOMA-2

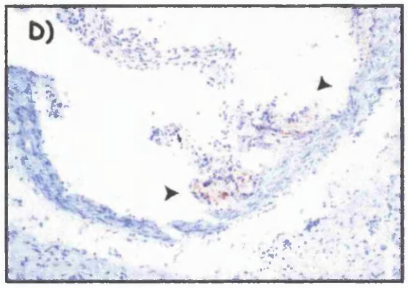

4 weeks HFC/C diet, MOMA-2

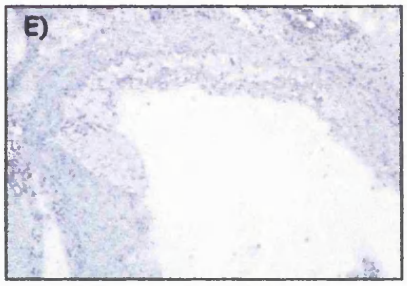

12 weeks HFC/C diet, IgG_{2B}

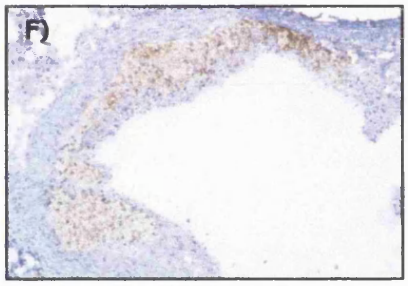

12 weeks HFC/C diet, MOMA-2

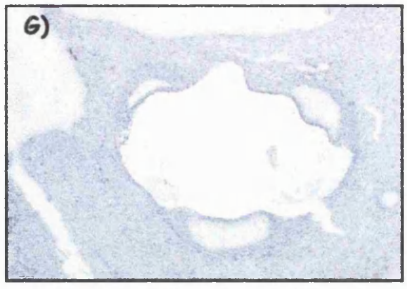

18 weeks RM1 diet, MOMA-2

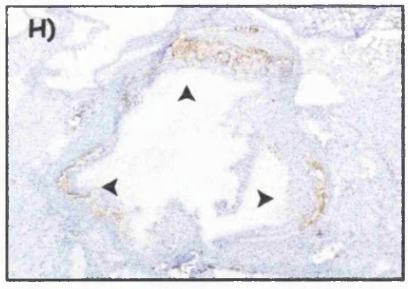

18 weeks HFC/C diet, MOMA-2

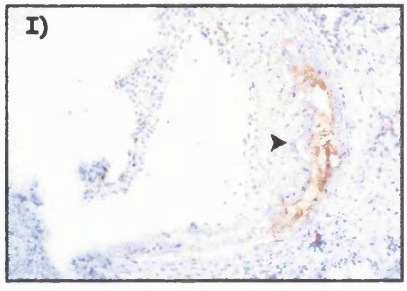

18 weeks HFC/C diet, MOMA-2

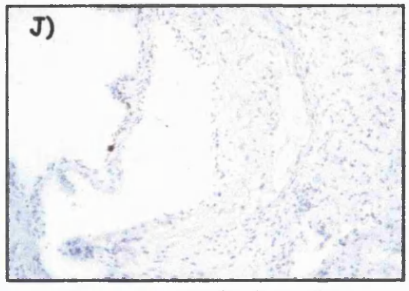

18 weeks HFC/C diet, IgG_{2B}

4.3.6 Serum chemokines

The effects of feeding HFC/C diet on serum CC (JE) and CXC (KC and MIP-2) chemokine concentrations (Figure 4-10) were analysed using terminal samples from each group of mice culled at the time points indicated. At the start of the study, serum JE concentrations were significantly higher ($p<0.05$) in the apoE*3 Leiden mice that would subsequently be fed either normal RM1 chow or HFC/C diet than in the non-transgenic mice (Figure 4-10 A). No significant differences were noted between the groups of apoE*3 Leiden mice assigned to different dietary regimes at the start of the study. Consumption of HFC/C diet caused rapid and approximately equivalent, increases from baseline in serum JE in both apoE*3 Leiden mice and their non-transgenic littermates. Serum JE concentrations were significantly (3-5 fold, $p<0.05$) higher at 4, 8 and 18 weeks in the group of apoE*3 Leiden mice and 3-4 fold higher at 4, 12 and 18 weeks in the non-transgenic mice consuming diet HFC/C, compared with the transgenic animals fed normal diet.

Serum levels of the CXC chemokine, KC, were also higher ($p<0.05$) at the start of the study in the apoE*3 Leiden mice than in the non-transgenic animals (Figure 4-10 B), but there was no difference between the groups of apoE*3 Leiden mice assigned to the different dietary groups. Consumption of HFC/C diet, for up to 18 weeks, caused significant ($p<0.05$) increases from initial values in serum KC concentrations in apoE*3 Leiden mice and their non-transgenic littermates. However, serum KC levels increased much more rapidly in apoE*3 Leiden mice, than in their non-transgenic littermates (Figure 4-10 B). At 2 and 4 weeks, serum levels of KC were significantly ($p<0.05$) higher (3.4 and 2.9 fold respectively) in the apoE*3 Leiden mice than in the non-transgenic controls consuming the same diet. By week 12, serum KC levels were approximately equivalent in the two groups of animals fed the atherogenic diet and remained so at the end of the study (week 18). Serum KC levels were also significantly higher ($p<0.05$) at weeks 4, 8 and 18 in apoE*3 Leiden mice and at weeks 4 and 18 in non-transgenic mice fed diet HFC/C, than in apoE*3 Leiden mice consuming normal RM1.

Concentrations of the other mIL-8RH ligand, MIP-2, exhibited a more complex, almost biphasic profile, and did not remain elevated throughout the study (Figure 4-10 C). At the start of the study, serum MIP-2 levels were higher ($p<0.05$) in the non-transgenic animals compared with the groups of apoE*3 Leiden mice. Increases ($p<0.05$) in serum MIP-2 concentrations were observed at weeks 2, 4, 8 and 12 in apoE*3 Leiden mice fed HFC/C diet, but these increases were not sustained and by

week 18 fell below initial values values. By contrast, serum MIP-2 levels were only significantly elevated at week 2 in the non-transgenic controls. At weeks 2, 4 and 18, levels of MIP-2 in apoE*3 Leiden and non-transgenic mice consuming HFC/C diet were significantly higher ($p<0.05$) than those in the group of apoE*3 Leiden mice consuming a normal chow diet. However, at no time point were serum levels of MIP-2 higher in the apoE*3 Leiden mice compared with their non-transgenic littermates consuming the same diet.

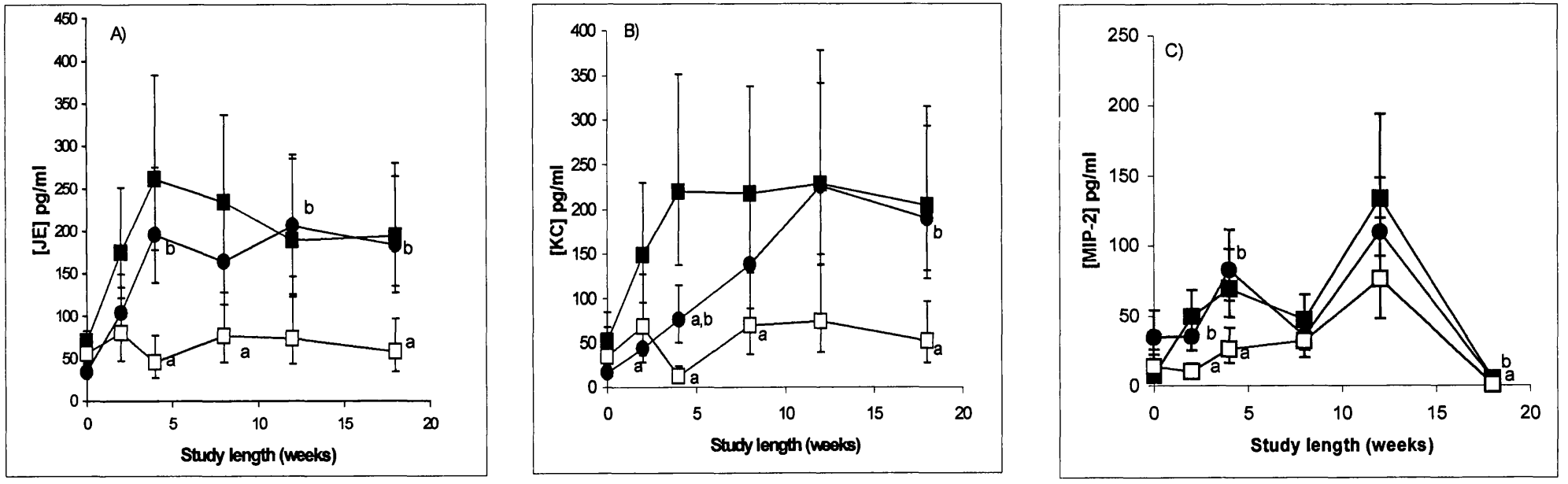

Figure 4-10 Effects of diet and strain of mouse on serum chemokines

Serum JE (A), KC (B) and MIP-2 (C) concentrations in apoE*3 Leiden mice fed the HFC/C diet (■), their non-transgenic littermates consuming the same diet (●) and apoE*3 Leiden mice fed the normal RM1 diet (□). Values shown are geometric means±95% confidence intervals (a = significantly different ($p<0.05$) to apoE*3 Leiden mice consuming HFC/C diet, b = significantly different ($p\leq0.05$) to apoE*3 Leiden mice consuming RM1 diet)

4.3.7 Chemokine expression on murine b.End.5 cells

In order to establish a protocol for the detection of chemokine proteins in aortic valve leaflet sections, the murine endothelioma cell line, b.End.5 was used. These cells showed enhanced KC and JE secretion into the cell culture media when stimulated with LPS (Figure 4-11). Our successful immunostaining protocol detected positive cellular expression of KC (Figure 4-12 A); no staining was observed with the relevant isotype control (Figure 4-12 B). Stimulated murine b.End.5 cells were to be used as a positive control to accompany staining experiments with aortic valve leaflet sections. However, positive aortic chemokine staining could not be detected using the same technique despite extensive attempts.

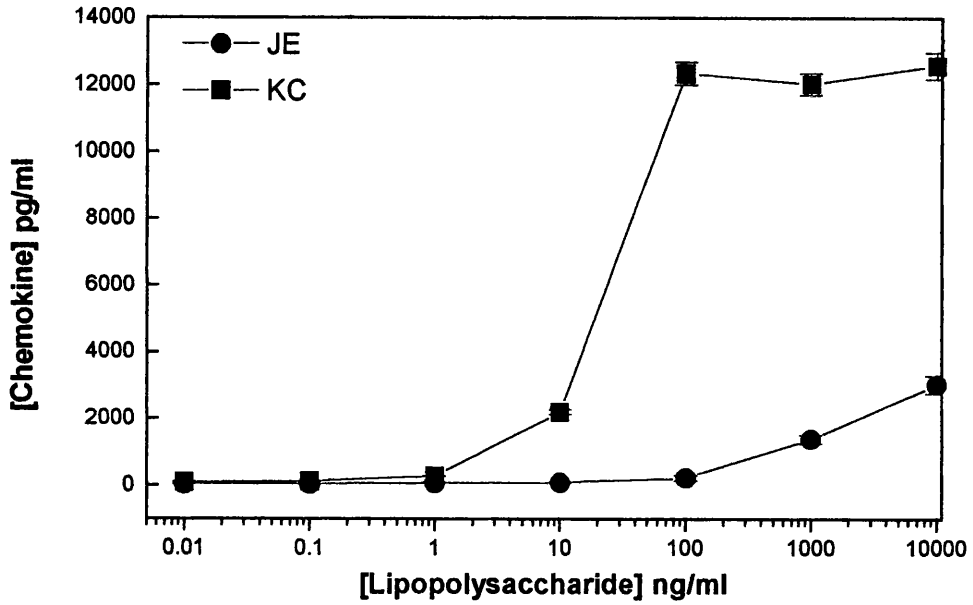

Figure 4-11 Secretion of KC and JE by b.End.5 cells stimulated with LPS

Murine b.End5 cells were stimulated for 4 h with lipopolysaccharide (0 - 10μg/ml). The 'conditioned' medium was removed and assayed for KC (■) and JE (●) by ELISA, as described in sections 2.3.7 and 2.3.8. Values shown are means ± SEM.

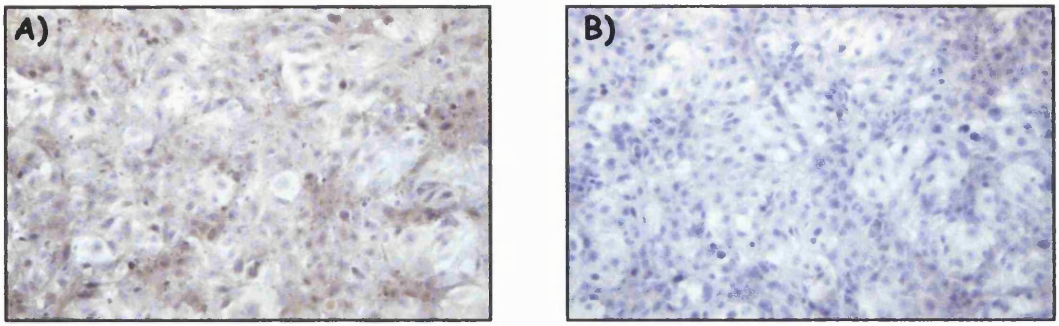

Figure 4-12 KC expression on murine b.End.5 cells stimulated with LPS

LPS stimulated murine b.End.5 cells (***A*** **+** ***B***), probed with an anti-mouse KC polyclonal antibody (***A***) or non-immune goat IgG (***B***). Cells were counterstained with haematoxylin. Immunoreactive staining is shown in brown. Original magnification x100.

4.3.8 In-situ hybridisation of aortic and hepatic sections

4.3.8.1 Aortic root mRNA expression

As chemokine proteins could not be identified using immunohistochemistry (Section 4.3.7), *in-situ* hybridisation was used in order to identify chemokine mRNA expression within arterial sections. Using this technique, we were able to detect JE mRNA expression in aortic tissue from this study. Aortic sections from half the animals in each group (4 apoE*3 Leiden: HFC/C, 4 non-transgenic: HFC/C and 2 apoE*3 Leiden: RM1) were probed for JE or KC expression using specific anti-sense RNA probes. Control sections were incubated with non-specific sense RNA probe. After 4 weeks consumption of the atherogenic diet, early intimal lesions were evident in the aortae from all (4/4) of the apoE*3 Leiden mice probed. However, no expression of KC mRNA was found, and expression of JE mRNA was detected in aortic sections from only one of four mice (1/4) in the apoE*3 Leiden group (data not shown). After 8 weeks consumption of this diet, larger intimal lesions had developed in apoE*3 Leiden mice, particularly in the aortic root and this coincided with the sites of JE mRNA expression (3/4 animals) (Figure 4-14 A - D). After 12 and 18 weeks consumption of the HFC/C diet, more advanced lesions were observed and JE mRNA expression was more prominent and appeared focally around single cells, possibly macrophages in the lesion and in the adventitia (4/4 animals). Again, more extensive expression of JE mRNA (Figure 4-14 G, J + K) but not KC mRNA, accompanied lesion development. Early fatty streak lesions had developed in the non-transgenic littermates by week 18 and JE mRNA expression was observed in 1/4 animal at this time-point (Figure 4-13 C + D). Only minimal evidence of KC mRNA expression was detected by *in-situ* hybridisation in this study (1 animal). JE (Figure 4-14 H) or KC mRNA expression was not detected in apoE*3 Leiden mice consuming the RM1 diet at any time. Equally, no

signal was detected when aortic sections were incubated with non-specific sense RNA probes (Figure 4-14 L).

4.3.8.2 Hepatic chemokine expression

Hepatic sections from half the animals in each group were collected for chemokine expression using *in-situ* hybridisation. The earliest time-point at which JE and/or KC mRNA could be detected in both apoE*3 Leiden mice and their non-transgenic littermates consuming the HFC/C diet was week 2 (Figure 4-15 A + B and Figure 4-16 A + B). More extensive expression of both chemokines were evident in mice consuming the atherogenic HFC/C diet for 4 weeks (data not shown). However, no difference in either KC or JE expression was detected between these two groups at any time probed. Indeed, after 4, 8, 12 and 18 weeks no obvious temporal differences were observed within each group of mice and therefore only representative sections from week 18 are shown (Figure 4-15 C + D and Figure 4-16 C + D). Expression of JE or KC (Figure 4-16 E) was not detected in hepatic sections from apoE*3 Leiden mice consuming the RM1 diet at any time. Equally, no expression was observed when hepatic sections were incubated with sense RNA probes. The diffuse expression of chemokine mRNA in the liver would suggest that the cells responsible for its production are most likely to be infiltrating inflammatory cells.

4.3.8.3 Spleen expression

Spleen sections from half the animal in each group were analysed for chemokine expression by *in-situ* hybridisation. No signal was observed at any time-point with specific anti-sense probes for KC or JE (data not shown).

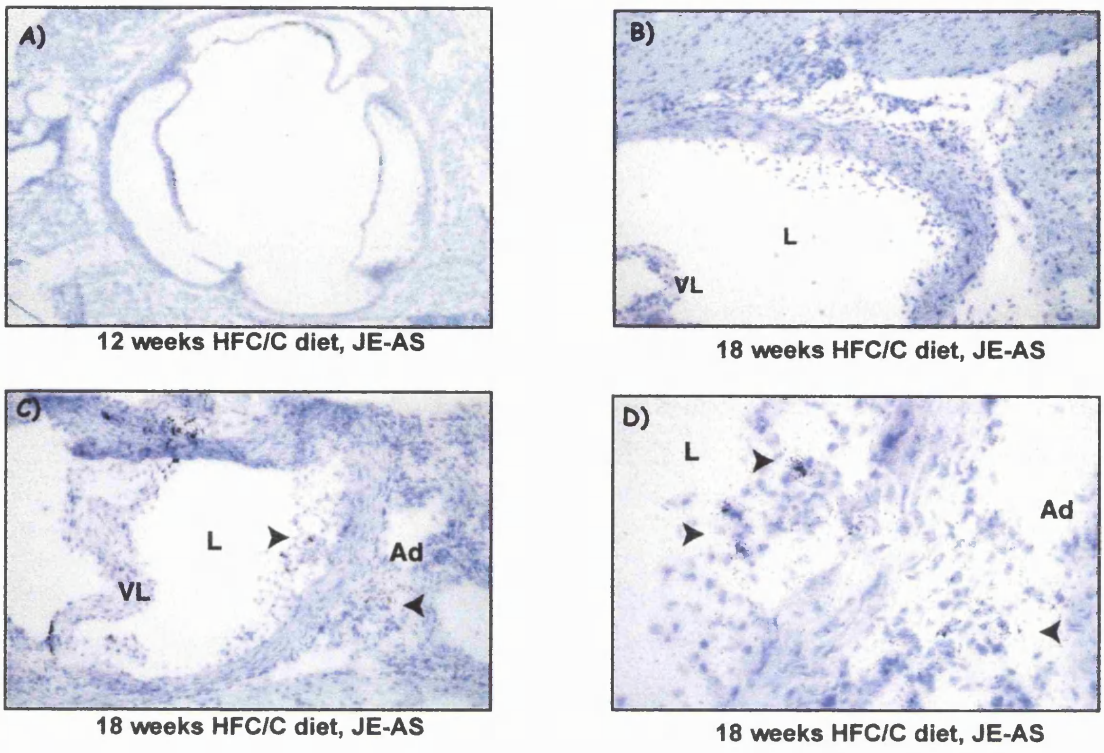

Figure 4-13 Aortic chemokine expression in non-transgenic mice

Photomicrographs of cross sections of aortic root from non-transgenic animals. Panel ***A***): section of aortic root from a mouse consuming HFC/C diet for 12 weeks, incubated with JE anti-sense probe (**AS**), no signal was detected. Panels ***B - D***): sections of aortic root from a non-transgenic animals consuming the HFC/C diet for 18 weeks, incubated with JE anti-sense probes. Panel ***D*** is a higher magnification image of panel ***C***. Panel ***B*** no specific signal detected in this animal at week 18, whereas panel ***C***, positive clusters of JE found in the lesion and in the adventita. Arrowheads indicate positive expression of JE mRNA. Ad = adventitia, L = lumen, VL = valve leaflet. Panel ***A***): original magnification x 40. Panel ***B + C***): original magnification x 100. Panel ***D***): original magnification x 250.

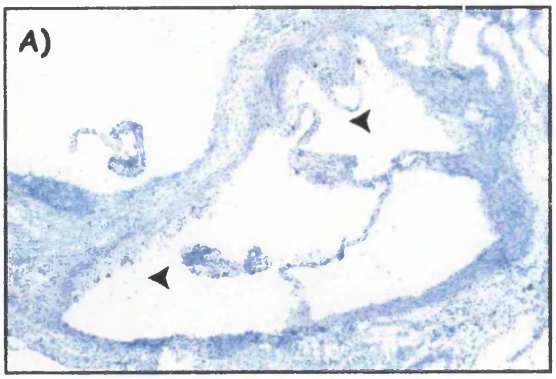

8 weeks HFC/C diet, JE-AS

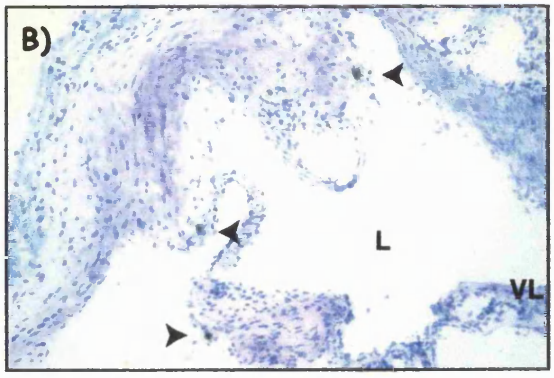

8 weeks HFC/C diet, JE-AS

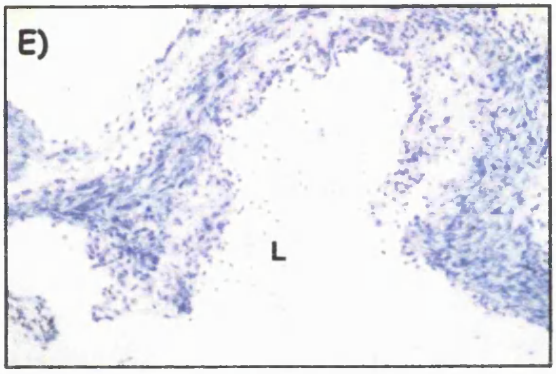

8 weeks HFC/C diet, KC-AS

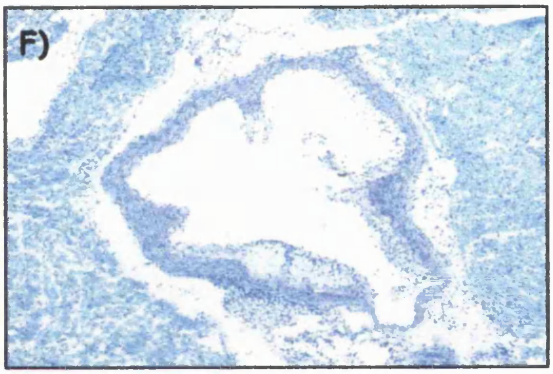

12 weeks HFC/C diet, JE-AS

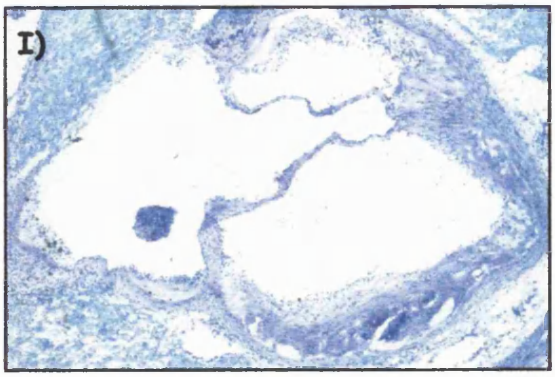

18 weeks HFC/C diet, JE-AS

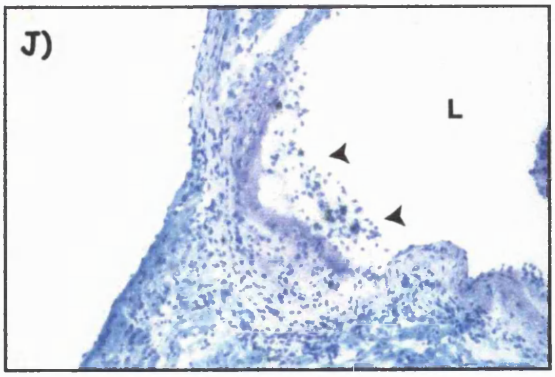

18 weeks HFC/C diet, JE-AS

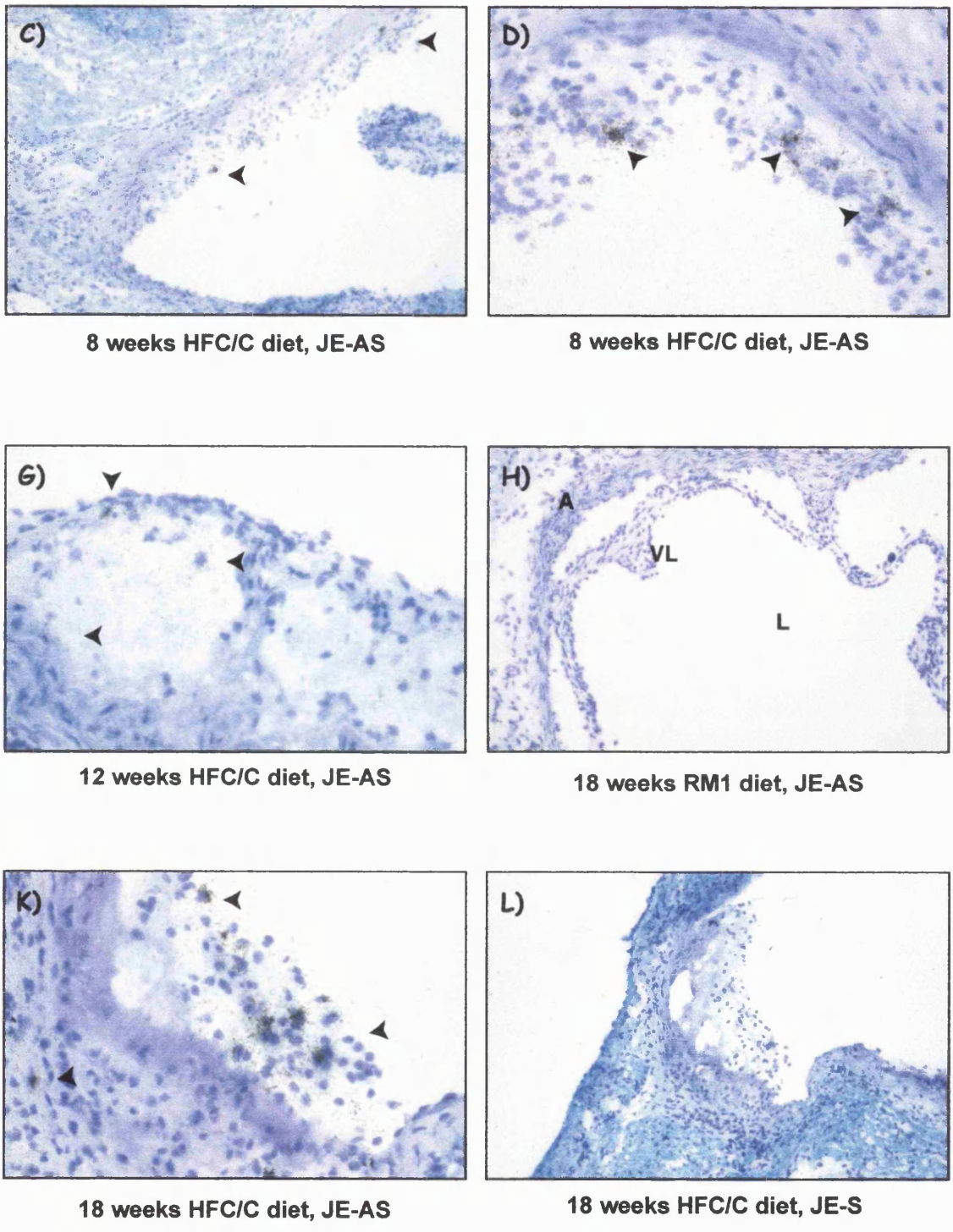

Figure 4-14 Aortic chemokine expression in apoE*3 Leiden mice

Photomicrographs of cross sections of the aortic root from apoE*3 Leiden mice. Panels ***A*** - ***E***): sections of aortic root from apoE*3 Leiden mice consuming HFC/C diet for 8 weeks, incubated with specific JE (***A-D***) or KC (***E***) anti-sense probes (**AS**) Panel ***F + G***) section of aortic root from an apoE*3 Leiden mouse consuming the HFC/C diet for 12 weeks, incubated with specific JE anti-sense probe. Panel ***G*** is a higher magnification image of panel ***F***. Panels ***H - L***): sections of aortic root from apoE*3 Leiden mice consuming RM1 (***H***) and HFC/C diet (***I - L***) for 18 weeks; incubated with JE anti-sense (***H - K***) or sense (**S**) (***L***) probes. Arrowheads indicate positive expression of JE mRNA; L = lumen, VL = valve leaflet. Panels ***A, F + I***) original magnification x 40. Panels ***B, C, E, H, J + L)*** original magnification x 100. Panel ***D, G + K)*** original magnification x 250.

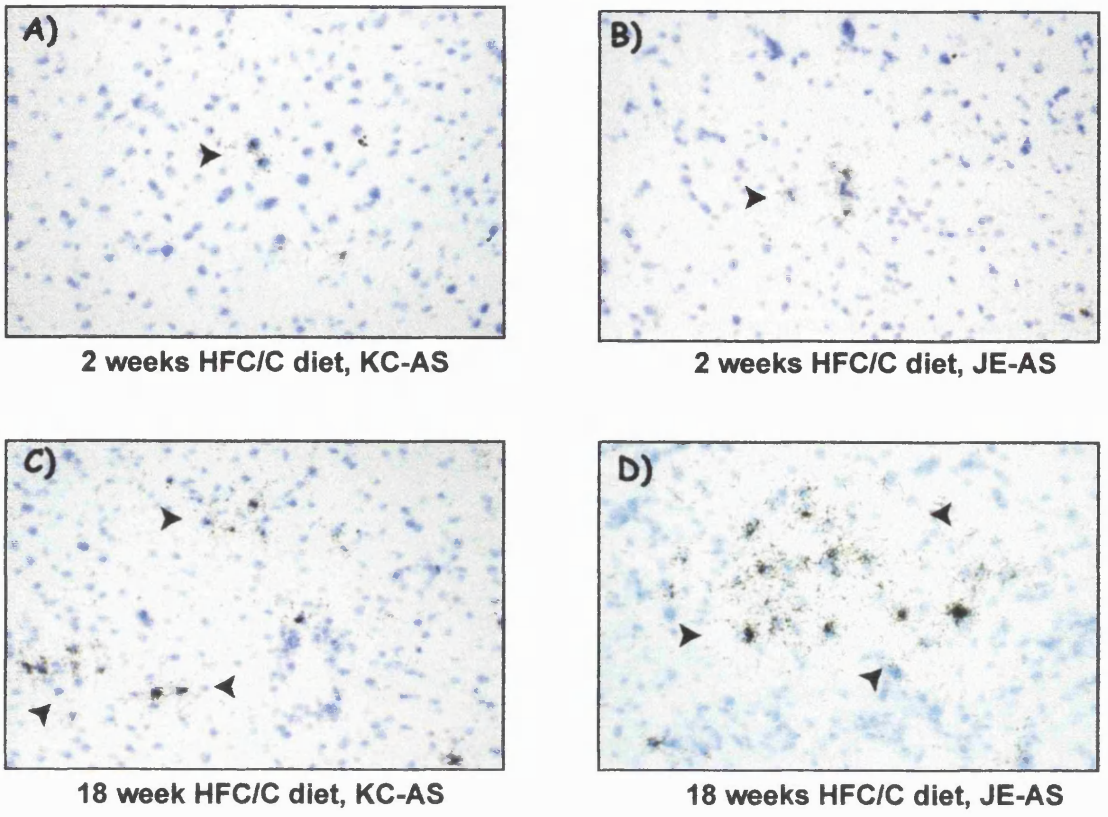

Figure 4-15 Hepatic chemokine expression in non-transgenic mice

Photomicrographs of hepatic sections incubated with specific anti-sense (**AS**) probes to either KC or JE (original magnification x 250). Panels ***A- D)***: sections of liver from non-transgenic animals consuming **HFC/C** diet for 2 (***A, C***) or 18 (***B, D***) weeks, incubated with either KC (***A, B***) or JE (***C, D***) anti-sense probes. Arrowheads indicate positive clusters of chemokine expression.

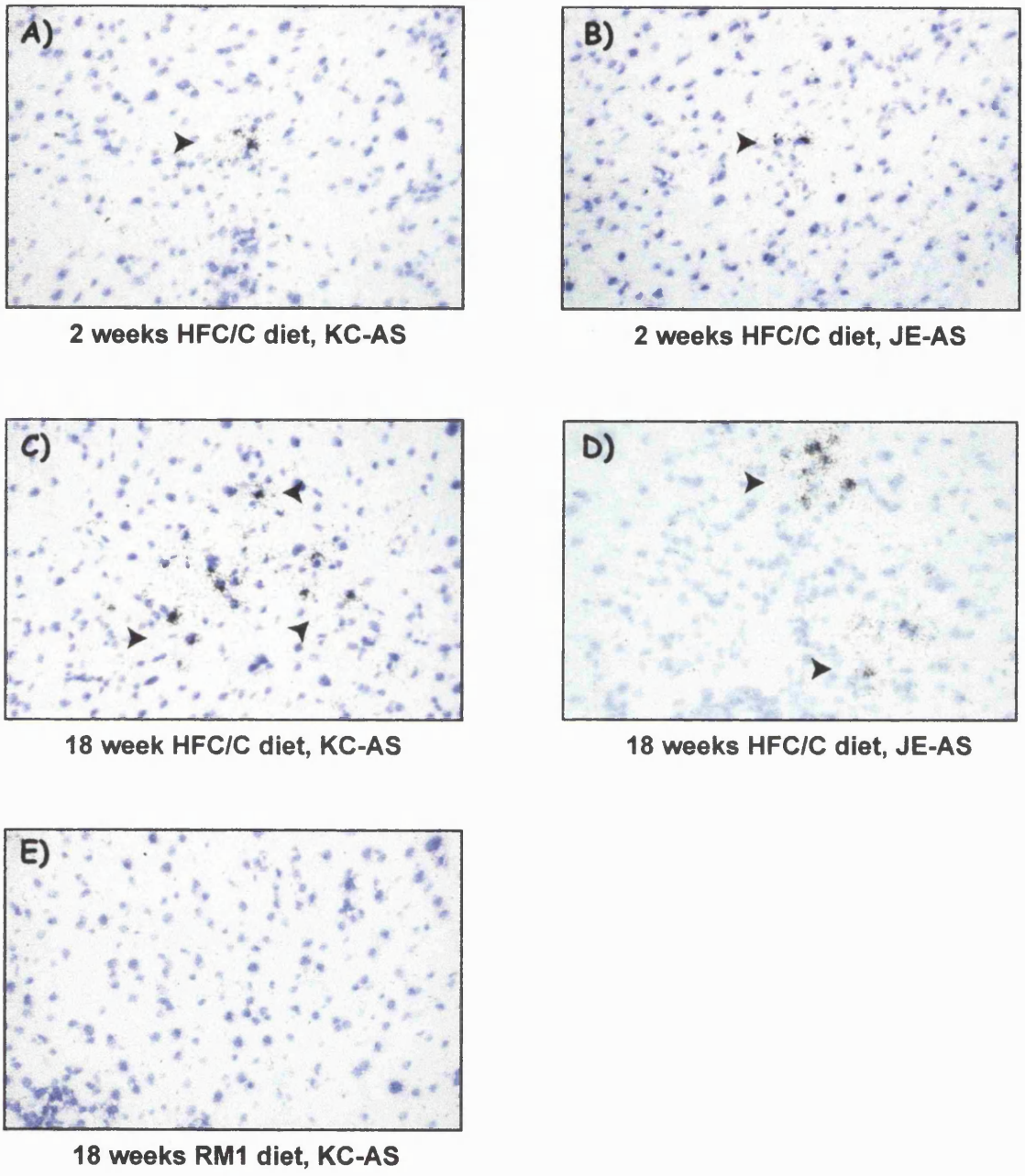

Figure 4-16 Hepatic chemokine expression in apoE*3 Leiden mice

Photomicrographs of hepatic sections incubated with specific anti-sense (**AS**) probes to either KC or JE (original magnification x 250). Panels ***A- D)***: sections of liver from apoE*3 Leiden mice consuming HFC/C diet for 2 (***A, C***) or 18 (***B, D***) weeks, incubated with either KC (***A, B***) or JE (***C, D***) anti-sense probes, Arrowheads indicate positive clusters of chemokine expression. Panel ***E)*** typical section from an apoE*3 Leiden mouse consuming the normal RM1 diet for 18 weeks, section incubated with specific KC anti-sense probe

4.3.9 Serum ICAM-1

Soluble ICAM-1 (sICAM-1) concentrations in the serum of apoE*3 Leiden mice and their non-transgenic littermates are shown in Figure 4-17. Serum levels of sICAM-1 were significantly lower (25 - 27%; $p<0.05$) in the non-transgenic animals than in the apoE*3 Leiden mice at the start of the study. Consumption of the atherogenic HFC/C diet induced significant increases in circulating sICAM-1 levels in the apoE*3 Leiden mice (1.7 - 1.9 fold; $p<0.05$) and their non-transgenic littermates (1.7 - 2.5-fold; $p<0.05$). Systemic levels of sICAM-1 were significantly higher (1.6 – 1.9 fold; $p<0.05$) in apoE*3 Leiden mice fed HFC/C diet, compared with apoE*3 Leiden fed RM1, at all time points tested. However, no statistically significant differences were detected between the apoE*3 Leiden mice and the non-transgenic animals fed the same atherogenic diet.

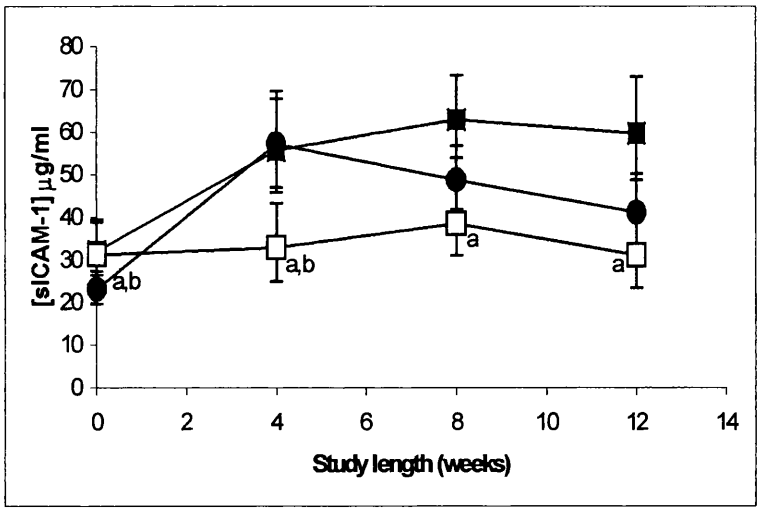

Figure 4-17 Effects of diet and strain of mouse on sICAM-1

Effects of diet and strain of mouse on sICAM-1 in apoE*3 Leiden mice consuming the HFC/C diet (■), their non-transgenic littermates on the same diet (●) and apoE*3 Leiden mice consuming the RM1 diet (□). Values shown are geometric means ± 95% confidence intervals (a = significantly different ($p<0.05$) to apoE*3 Leiden mice consuming the HFC/C diet, b = significantly different ($p\leq0.05$) to apoE*3 Leiden consuming RM1 diet).

4.3.10 Systemic inflammatory 'markers'

4.3.10.1 Paraoxonase activity

Serum PON activity was significantly higher (20-30%; $p<0.05$) in the non-transgenic C57BL mice, than in either group of apoE*3 Leiden mice, at the start of this

study (Figure 4-18). Consumption of the atherogenic HFC/C diet did not seem to induce marked changes in serum PON activity in either the non-transgenic animals or apoE*3 Leiden mice. However, by week 12 serum PON activity was significantly lower in the apoE*3 Leiden mice consuming HFC/C, compared with either the non-transgenic controls (25%; $p<0.05$) or the apoE*3 Leiden mice consuming normal chow (36%; $p<0.005$). In this last group, levels of PON activity were increased (70 - 88%; $p<0.05$) from initial values throughout the study (Figure 4-18).

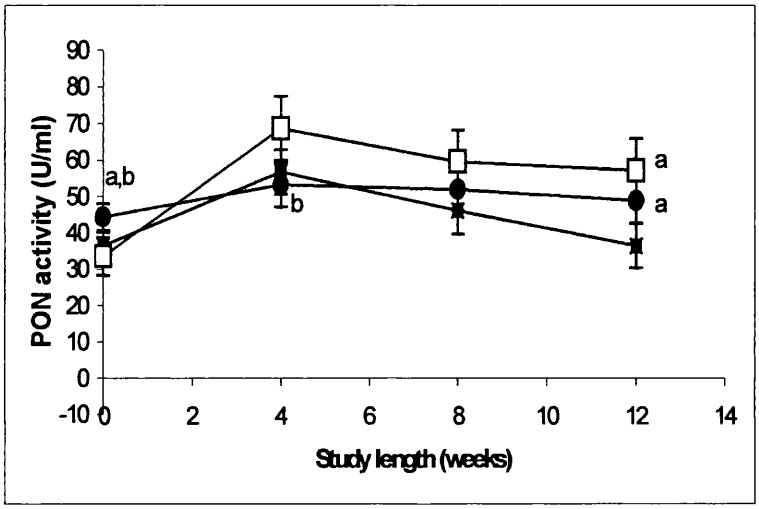

Figure 4-18 Effects of diet and strain of mouse on serum PON activities

Effects of diet and strain of mouse on serum paraoxonase activities in apoE*3 Leiden mice consuming the HFC/C diet (■), their non-transgenic littermates consuming the same diet (●) and apoE*3 Leiden mice fed the chow diet (□). Values shown are geometric means ± 95% confidence intervals (a = significantly different ($p<0.05$) to apoE*3 Leiden mice consuming the HFC/C diet, b = significantly different ($p\leq0.05$) to apoE*3 Leiden consuming RM1 diet).

4.3.10.2 Haptoglobin

The effects of feeding HFC/C diet on serum haptoglobin concentrations in apoE*3 Leiden mice and their non-transgenic littermates are shown in Figure 4-19. All groups had equivalent circulating haptoglobin levels at the start of the study, and no changes were observed in the apoE*3 Leiden mice fed the RM1 diet during the study period. Consumption of HFC/C diet induced dramatic increases ($p<0.05$) from initial values in serum haptoglobin levels in both apoE*3 Leiden mice and their non-transgenic littermates. Serum Hp concentrations were significantly higher (98%

p<0.05) in apoE*3 Leiden mice consuming the atherogenic diet for 8 weeks, compared with their non-transgenic controls. However, after 12 weeks, approximately equivalent serum haptoglobin levels were seen in both groups consuming diet HFC/C.

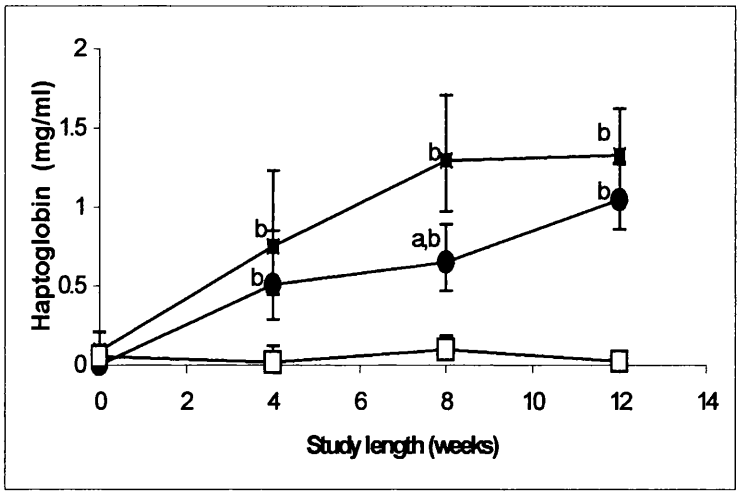

Figure 4-19 Effects of diet and strain of mouse on serum haptoglobin levels

Effects of diet and strain of mouse on serum haptoglobin concentration in apoE*3 Leiden mice consuming the HFC/C diet (■), their non-transgenic littermates consuming the same diet (●) and apoE*3 Leiden mice fed the RM1 diet (□). Values are geometric means ± 95% confidence intervals (a = significantly different (p<0.05) to apoE*3 Leiden mice consuming the HFC/C diet, b = significantly different ($p \leq 0.05$) to apoE*3 Leiden consuming RM1 diet)

4.3.10.3 Serum amyloid A

Serum amyloid A measurements were made on in-life samples at weeks 0, 4 and 8 (Figure 4-20). At the start of the study no significant differences in SAA concentrations were noted between the 3 groups of mice used in this study. By week 8, serum amyloid A were significantly higher (46%; p<0.05) in apoE*3 Leiden mice consuming HFC/C diet, compared with the non-transgenic controls, but did not differ significantly from the apoE*3 Leiden mice consuming normal RM1 diet.

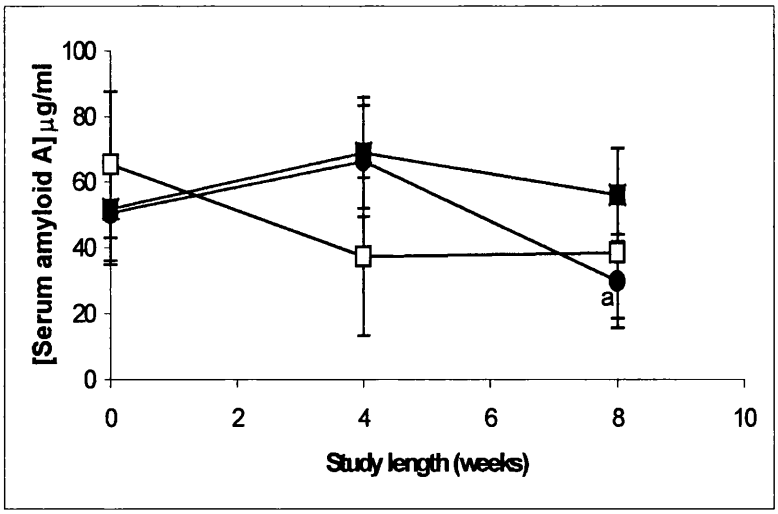

Figure 4-20 Effects of diet and strain of mouse on serum amyloid A

SAA concentrations in apoE*3 Leiden mice consuming the HFC/C diet (■), their non-transgenic littermates on the same diet (●) and apoE*3 Leiden mice consuming the chow diet (□). Values shown are geometric means ± 95% confidence intervals (a = significantly different ($p<0.05$) to apoE*3 Leiden mice consuming the HFC/C diet, b = significantly different ($p\leq0.05$) to apoE*3 Leiden consuming RM1 diet).

4.4 Discussion

In this study, apoE*3 Leiden mice and their non-transgenic (C57BL/6J) littermates consuming either an atherogenic (HFC/C) or normal RM1 diet were used. Consumption of this diet induces gross hypercholesterolaemia and markedly accelerated atherogenesis in apoE*3 Leiden mice compared with the non-transgenic controls. Thus, the use of these two strains of mice allowed investigation of whether putative 'markers' of disease progression and/or inflammation could discriminate between groups of animal experiencing an identical dietary regime but possessing differing rates of atherogenesis. In particular, the potential utility of systemic CC and CXC chemokines as 'markers' of atherogenesis could be determined, as prototypic members of each of these chemokine subfamilies have been implicated in the recruitment and/or retention of monocyte-macrophages during atherogenesis. It was found that consumption of an atherogenic diet induced sustained increases in systemic levels of CC and CXC chemokines, JE and KC, in both apoE*3 Leiden mice and their non-transgenic littermates. Serum levels of JE increased, and remained approximately equivalent, in both groups of animals but serum KC levels increased much more rapidly in the apoE*3 Leiden mice compared with their non-transgenic littermates. Indeed, the achievement of maximal levels of serum KC appeared to coincide with the

onset of fatty streak development in both groups of mice (Figure 4-6 and Figure 4-10 B). Therefore, the temporal relationship(s) between circulating chemokine concentrations, hepatic and aortic chemokine expression, and lipid accumulation in the liver and serum and the development of atherosclerotic lesions in these animals was investigated.

ApoE*3 Leiden mice, and their non-transgenic littermates, consuming a diet high in fat and cholesterol, developed atherosclerosis at markedly different rates [44,106]; indeed, lesion development in apoE*3 Leiden mice seemed directly related to the duration of hypercholesterolaemia induced in these animals [44]. Maximal increases in serum cholesterol concentrations were detected in both models after four weeks consumption of the atherogenic diet (Figure 4-4 A), although serum cholesterol levels in the C57BL/6J mice did not approach the gross hypercholesterolaemia seen in apoE*3 Leiden mice. However, despite the very differing rates of atherogenesis (Figure 4-6 and Figure 4-7), and degree of hypercholesterolaemia, induced by consumption of the HFC/C atherogenic diet, apoE*3 Leiden mice and their non-transgenic littermates exhibited very similar hepatic accumulation of lipid, particularly cholesteryl ester, after 18 weeks (Table 4-2).

4.4.1 Circulating concentrations of chemokines and adhesion molecules

Temporal increases in serum JE reflected the onset of hypercholesterolaemia in both groups of animals consuming the atherogenic diet; however, the extent of the rise was similar in both groups, suggesting that the absolute concentration of serum lipids was not a key determinant of serum JE levels. This contrasts with the reported effect of hypercholesterolaemia on the expression of the JE/MCP-1 receptor, CCR-2, by circulating monocytes [347]. Rather, serum levels of JE may be more closely associated with hepatic inflammation, possibly due to lipid accumulation (Table 4-2). Indeed, hepatic expression of JE mRNA was detected in apoE*3 Leiden mice, and their non-transgenic littermates, after 2 weeks consumption of the atherogenic HFC/C diet (Figure 4-15 and Figure 4-16). This leads to speculation that the liver may be a primary source of serum JE in this study. Indeed, consumption of an atherogenic diet by C57BL/6J mice has previously been shown to be associated with enhanced hepatic oxidative stress, activation of NFκB, and increased expression of JE, KC, serum amyloid A and haem oxygenase mRNA [110,111].

The contribution of JE from developing aortic lesions to serum JE concentrations does not appear to be substantial, as serum JE levels in apoE*3 Leiden mice did not

exceed those in the non-transgenic controls. Aortic expression of JE mRNA was also not seen until much later (8 weeks) in apoE*3 Leiden mice consuming the HFC/C diet (Figure 4-9 A - D). Interestingly, positive macrophage staining could be detected within early lesions in both apoE*3 Leiden (4 weeks) and non-transgenic (4 weeks) mice (Figure 4-8 C and Figure 4-9 C + D), before detection of JE mRNA by *in situ* hybridisation. Thus, apoE*3 Leiden mice seem to differ from apoE- and LDL receptor-deficient models of atherogenesis, in which JE/MCP-1 expression appears to coincide directly with monocyte infiltration [348-350]. This could be explained by the relative sensitivities of the techniques and/or probes used; alternatively, another chemokine may be involved in the very early stages of monocyte recruitment to the vessel wall in this murine model.

Systemic levels of ligands for the mIL-8RH, KC and MIP-2, exhibited markedly different profiles. The almost biphasic profile of serum MIP-2, seen in each of the groups of animals under investigation, is intriguing but the reasons underlying this finding is not clear. However, since serum MIP-2 levels clearly could not provide a reliable estimate of inflammatory status, they were not investigated further. By contrast, circulating levels of KC seemed to be associated with the very differing rates of early atherogenesis seen in the three groups of animals in this study. Maximal levels of serum KC were detected by 4 weeks in apoE*3 Leiden mice consuming HFC/C diet, by 12 weeks in the non-transgenic controls, and did not increase significantly in the apoE*3 Leiden mice consuming the normal RM1 diet. Again, hepatic expression of KC mRNA was detected by week 2 of the study, but a scoring assessment did not reveal differences between the two groups of animals consuming the atherogenic diet at any of the time points examined. Rather, maximal serum KC levels appeared to coincide with the development of early 'fatty streak' lesions in both apoE*3 Leiden mice, and their non-transgenic littermates. Previous reports of aortic CXC chemokine expression [172,176,177,190,192,341,342,351] suggested intra-lesional expression of KC could be a factor contributing to the enhanced serum KC levels seem in the apoE*3 Leiden mice. However, the apparent absence of KC mRNA within developing lesions in this study as judged by *in-situ* hybridisation, does not support this explanation: it seems more likely that the observed increases in serum KC are due to enhanced production of KC from other sites. Increased serum cholesterol concentrations may be sufficient to elicit leukocyte activation and chemokine expression [339]. Recent studies have shown that plasma concentrations of IL-8 correlate directly with IL-8 expression by blood mononuclear cells [340,352] and that exposure to IL-8 enhances the expression of IL-8 by monocytes probably via the CXCR1 receptor [353].

Monocytes isolated from patients with hypercholesterolaemia [339] or congestive heart failure [308] also exhibit enhanced IL-8 expression.

In addition to *in-situ* hybridisation, aortic valve leaflet sections were probed for chemokine protein expression by immunohistochemistry. As aortic valve leaflet sections from this study were very limited, we initially established a successful immunostaining protocol using murine b.End5 cells (Figure 4-12). However, no staining was observed using this method on tissue sections and there may be several reasons for this. For example, KC and JE may be present at low concentrations, or in a diffuse pattern, which may be below the sensitivity of the polyclonal antisera used. Alternatively, chemokines attached to the surface of the endothelium via proteoglycans, may become detached during the IHC procedure. Further, chemokine staining reported in the literature [177,350] has been shown in different mouse models of the disease, with larger lesions than those seen in this study. Finally, it has been suggested that lipid accumulation may mask cytokine epitopes in atheromatous tissue [354] and this may be another potential reason for the lack of signal in aortic and, indeed, hepatic (Table 4-2) sections in this study.

Like chemokines, adhesion molecules are intimately involved in the recruitment of mononuclear cells to atherosclerotic lesions (Section 1.3). Soluble adhesion molecules are found in the circulation, following 'shedding' of these molecules from cells by proteolytic cleavage at sites close to the transmembrane domain (Section 1.10.1) [128]. In this study, the predictive value of sICAM-1, during the early development of atheroma in apoE*3 Leiden mice and their non-transgenic littermates was assessed. It was found that consumption of an atherogenic diet markedly increased sICAM-1 concentrations in both apoE*3 Leiden and the non-transgenic mice (Figure 4-17). It is possible that this initial increase in sICAM-1 may reflect the onset of hypercholesterolaemia, which reached maximal levels at week 4 in both groups of animals (Figure 4-4). Absolute concentrations of sICAM-1 did not distinguish the very differing rates of atherogenesis observed in both groups of animals consuming the HFC/C diet. However, at week 8 and 12, apoE*3 Leiden mice tended to have higher sICAM-1 than their non-transgenic littermates. Unfortunately, it was not possible to map the temporal aortic expression of ICAM-1 due to the limitation in the number of tissue sections available for analysis. Circulating levels of sICAM-1, seen in murine serum were substantially higher than levels found in human serum [298,355-357]. Soluble adhesion molecules bind to their respective integrin receptors on circulating leukocytes and can negatively regulate monocyte adhesion [285]. Thus, it is possible to speculate

that the high circulating levels of sICAM-1 found in mice may contribute to the relative resistance of these animals to atherogenesis.

4.4.2 Systemic inflammatory 'markers'

In addition to serum chemokines and adhesion molecules, we measured systemic 'markers' of inflammation. Previously, it has been shown that feeding a diet high in fat and cholesterol induces oxidative stress, inflammation and lipid accumulation in both aortic and hepatic tissues of C57CL/6J mice [110,111]. Although formulated to minimise liver damage [3,4], atherogenic diets of the type used in this study generate similar responses to injection of mmLDL [20,110,111], namely the activation of the Rel family of transcription factors, NF-κB, and induction of genes for chemokines, colony-stimulating factors, haem oxygenase and SAA in the liver [20,110,111]. Importantly, susceptibility to hepatic oxidative stress and inflammation appears to co-segregate with aortic lesion formation [111]. Altered hepatic expression of systemic inflammatory markers, such as SAA, Hp and indeed, PON1 activity, in individuals with CHD, are proposed to be due to the release of inflammatory cytokines, such as IL-6 and IL-1 [328], from the developing arterial lesion. Therefore, SAA, Hp and PON during the early development of the atherosclerosis in apoE*3 Leiden and non-transgenic mice was measured.

Circulating levels of serum amyloid A (SAA), were not markedly increased following consumption of HFC/C diet in apoE*3 Leiden mice and their (C57BL) non-transgenic littermates, or in apoE*3 Leiden mice consuming normal chow (Figure 4-20). Earlier reports from Liao *et al* [20,110,111] showed that inflammation induced by feeding atherogenic diets, or injection of mildly oxidized LDL, markedly increased levels of SAA protein in atherosclerosis-susceptible (C57BL) but not atherosclerosis-resistant (C3H) mice. The difference between C57BL and C3H mice was attributed to the accumulation of oxidized lipids, and greater responsiveness to these species, in tissues of C57BL mice [110,111]. In this study all mice were of the same (C57BL) background, obviating these strain-specific differences in hepatic inflammatory responses to dietary fat and cholesterol. Under these conditions, SAA does not seem to be associated with either the gross hyperlipidaemia or accelerated atherogenesis seen in C57BL mice expressing the human apoE*3 Leiden transgene. It should be noted, however, that the different SAA isotypes were not distinguished in this study. Evidence suggests that members of the serum amyloid A family are differentially induced by a high-fat high-cholesterol diet, or by injection of mildly oxidized LDL [20]; isotypes SAA1-3 are markedly increased, whereas SAA5 is unaffected by this diet [319].

Reduced levels of HDL and, in particular, serum PON1, in C57BL mice may explain their increased susceptibility to oxidative damage, inflammation and atherosclerosis compared with C3H mice [276]. In particular, in recombinant in-bred strains, derived from C57BL and C3H parental strains, low PON1 expression and activity co-segregated with aortic lesion development [276]. Low levels of serum/HDL PON1 activity are also seen in apoE$^{-/-}$ and LDL receptor$^{-/-}$ models of atherogenesis [276], and mice lacking serum PON1 activity are more susceptible to atherosclerosis compared with their wild type littermates [277]. However, in apoE*3 Leiden mice, and their non-transgenic littermates, consuming HFC/C diet (Figure 4-18), only limited changes in PON activity were observed. By week 12 of the study, consumption of this atherogenic diet induced a significant decrease in serum PON activity in apoE*3 Leiden mice, compared with their non-transgenic littermates or apoE*3 Leiden mice fed a normal RM1 diet. However, it was evident that measurement of serum PON levels could not distinguish the markedly accelerated atherogenesis in these groups of animals (Figure 4-6 and Figure 4-7). Instead, our recent work using 2-D gel electrophoresis and mass spectrometry demonstrated that plasma levels of Hp were increased in apoE*3 Leiden mice consuming an atherogenic diet, compared with their non-transgenic littermates [358]. Quantitative measurement of serum Hp levels (Figure 4-19) confirmed the trend to higher levels of serum haptoglobin in apoE*3 Leiden mice, compared with the non-transgenic animals, with significant differences between the groups detected at week 8 of the study. Further, striking changes in serum Hp levels were seen in response to the atherogenic HFC/C diet, compared with the other systemic inflammatory 'markers' investigated in this study.

A specific role of Hp in atherogenesis has yet to be confirmed. However, baseline levels of serum Hp were found to be elevated in patients with peripheral arterial disease [328] and recent data suggest that the human Hp polymorphism may play a role in regulating lipoprotein metabolism and contribute to the risk of coronary heart disease [322]. Haptoglobin null (Hp$^{-/-}$) mice are much more susceptible to the deleterious effects associated with induced haemolysis, and suffer greater tissue oxidative damage, compared with wild type controls [359]. Thus, the antioxidant properties associated with haptoglobin, found within the artery wall [327], may help protect against the arterial oxidative stress considered a hallmark of developing atherosclerotic lesions.

4.4.3 Conclusion

In summary, circulating levels of chemokines may prove to be useful, albeit non-specific, markers in chronic inflammatory diseases, including atherosclerosis.

Serum concentrations of these molecules may reflect their output from one, or more, sites of inflammation, assuming that clearance of these molecules from the circulation remains a constant factor. Here, consumption of an atherogenic diet appears to trigger hepatic inflammation [110,111], indicating that the liver may be an important source of the observed increases in systemic CC and CXC chemokine levels. Furthermore, while serum concentrations of the CXC chemokine, KC, did not directly reflect lesional expression of this chemokine, systemic KC did appear to be a useful marker for inflammatory events accompanying early atherogenesis. Finally, although temporal variations in circulating levels of sICAM-1, PON1 and SAA were observed, no obvious association with onset of atheroma emerged. However, systemic levels of serum Hp are acutely sensitive to the inflammatory effects of an atherogenic diet, and appear to be associated with the accelerated atheroma seen in apoE*3 Leiden mice.

Chapter 5

*Supplementary data relating to chemokine and chemokine receptor mRNA expression in aortic and hepatic tissues from apoE*3 Leiden mice and their non-transgenic littermates consuming an atherogenic diet*

5 Supplementary data relating to chemokine and chemokine receptor mRNA expression in aortic and hepatic tissues from apoE*3 Leiden mice and their non-transgenic littermates consuming an atherogenic diet

5.1 Introduction

This small study was designed to probe hepatic and aortic chemokine and chemokine receptor mRNA expression using quantitative polymerase chain reaction (PCR), namely the TaqMan assay. Our previous investigation using *in-situ* hybridisation (Section 4.3.8) failed to detect aortic expression of KC mRNA. Furthermore, this technique also failed to detect JE mRNA before 8 weeks, despite the presence of macrophages within aortic root sections. Assessing chemokine expression by *in-situ* hybridisation remains essentially subjective and is limited by the sensitivity of this technique. In contrast, the TaqMan assay provides a highly sensitive way of quantifying mRNA expression in tissues of interest. Therefore, in this study we compared the relative amounts of mRNA in groups of apoE*3 Leiden mice and their non-transgenic littermates consuming either HFC/C or RM1 diet for 4 weeks. Specifically, we analysed aortic and hepatic mRNA expression of KC, JE and their respective receptors CXCR2 and CCR2 in these animals. In addition, the expression of house keeper gene 36B4, encoding acidic ribosomal phosphoprotein P_0 was also quantified and used to normalise the expression data.

5.2 Methods

5.2.1 Study protocol

5.2.1.1 Mice

Mice were bred and phenotyped as described in Section 2.2. Seven female apoE*3 Leiden mice and 10 female non-transgenic animals aged 8 - 10 weeks, were allocated randomly to experimental groups on the basis of age and litter, and housed in groups of up to 5.

5.2.1.2 Diets

Animals were maintained on the standard mouse RM1 diet before the experimental period. During the study, mice were fed either RM1 or the atherogenic HFC/C diet (Section 2.2.2). Mice were weaned onto the HFC/C diet over 4 days. In total, 4 apoE*3 Leiden mice, and 5 of their non-transgenic littermates were fed the HFC/C diet, and 3 apoE*3 Leiden mice and 5 non-transgenic mice continued to receive RM1 diet.

5.2.1.3 Tissue preparation

Mice were culled after 4 weeks and their aortae and livers removed and immediately snap frozen in liquid nitrogen. Samples were stored at -80°C until the RNA could be isolated.

5.2.2 Principles of the TaqMan assay

PCR involves the amplification of target nucleic acid sequences using two specific oligonucleotide primers and DNA polymerase. Traditionally, detection of PCR products takes place after the amplification process is complete, usually by agarose gel electrophoresis. Comparison of band intensities between samples allows only semi-quantitative assessment of the templates amplified in different tissues or cells. The TaqMan assay utilises the 5'→3' exonuclease activity of *Thermus aquaticus* (Taq) polymerase to cleave a dual-labelled probe annealed to a target sequence during amplification. Primers are designed to amplify up a short region of cDNA from the gene of interest. A probe is designed to a region of cDNA within the DNA amplicon, but not overlapping with the primers. The probe is labelled at its 5' end with a fluorescent reporter dye, 6-carboxyl-fluorescein (FAM), and at the 3' end with a quencher, 6-carboxyl-tetramethyl-rhodamine (TAMRA). When the quencher is in close proximity to the reporter, the release of fluorescence is inhibited. During the annealing phase of the PCR reaction, the primers and probe hybridise to the template strands. As the primers are extended the probe is displaced from the template and is cleaved by the polymerase. This distances the reporter from the quencher, resulting in an increase in fluoresence of the reporter which is proportional to the amount of product accumulated. This can be measured in 'real time', where the increase in emission intensity is followed on a per-cycle basis using the ABI PRISM 7700 sequence detector (Perkin-Elmer Applied Biosystems). Thus, this allows the real time quantification of PCR products as the amplification reaction proceeds. Fluorescence is measured every 7 s, and the cycle number at which fluorescence becomes detectable is recorded, and is defined as the threshold cycle C_t. The C_t value is inversely related to the amount of cDNA of the gene of interest. Using a standard curve of C_t values from a known amount of cDNA, values can be determined for the unknowns. The main steps of the reaction are shown in Figure 5-1. A typical amplification plot and standard curve are shown in Figure 5-2.

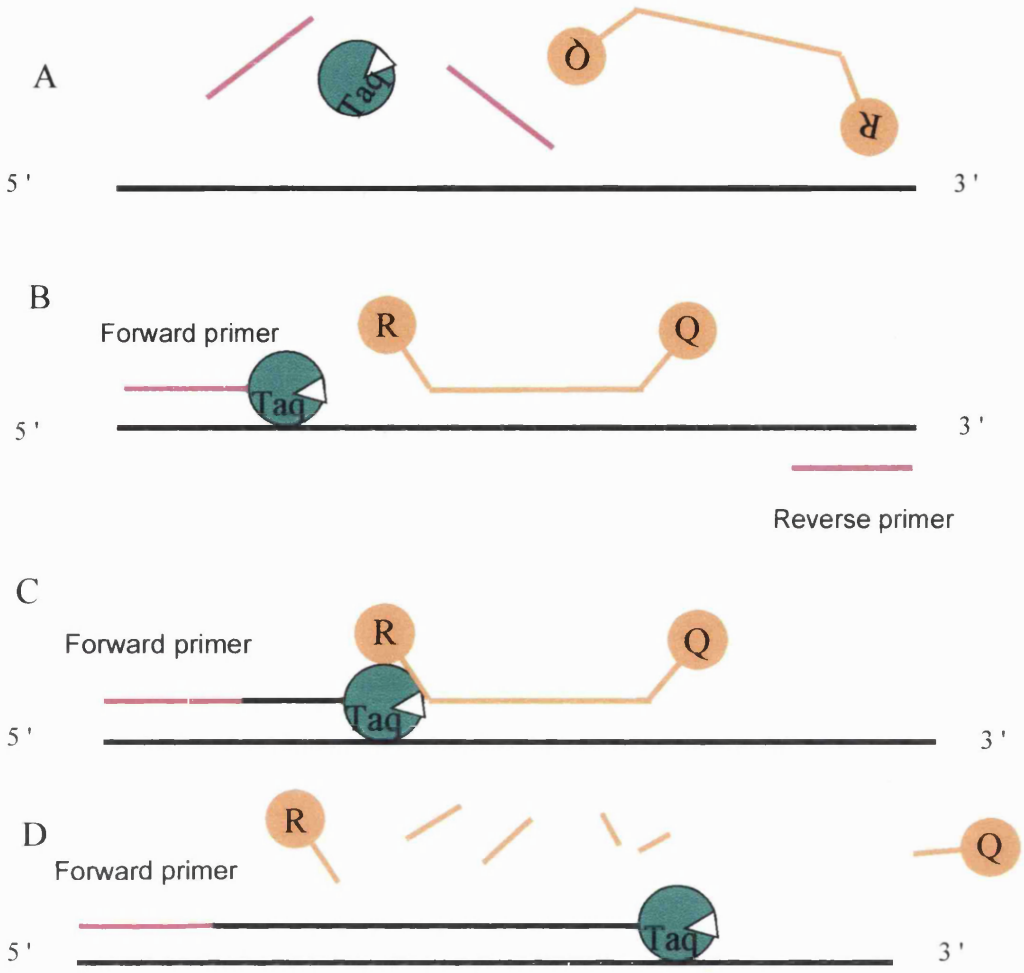

Figure 5-1 Principles of the TaqMan assay

After the reverse transcription step (not shown), successful quantification requires the annealing of three oligonucleotides to the cDNA template. Two specific primers (shown in pink) define the endpoints of the amplicon and provide the first level of specificity. A third oligonucleotide probe (shown in orange) that hybridises to the amplicon during the annealing/extension phase of PCR provides additional specificity. The probe contains a fluorescent reporter dye (R) at its 5' end, the emission spectrum of which is quenched by a second fluorescent dye (Q) at its 3' end. Initially A): the reaction is heated to 95°C so that all secondary structures and dimers are denatured, B): cooling to 60°C allows the primers, probe and Taq polymerase to anneal, C): the polymerase displaces and hydrolyses the labelled probe, D): and the fluorescent reporter dye (R) becomes spatially separated from the quencher dye (Q) and the fluorescence detected. Increases in fluorescence (R) over time is measured and allows quantification of specific cDNA

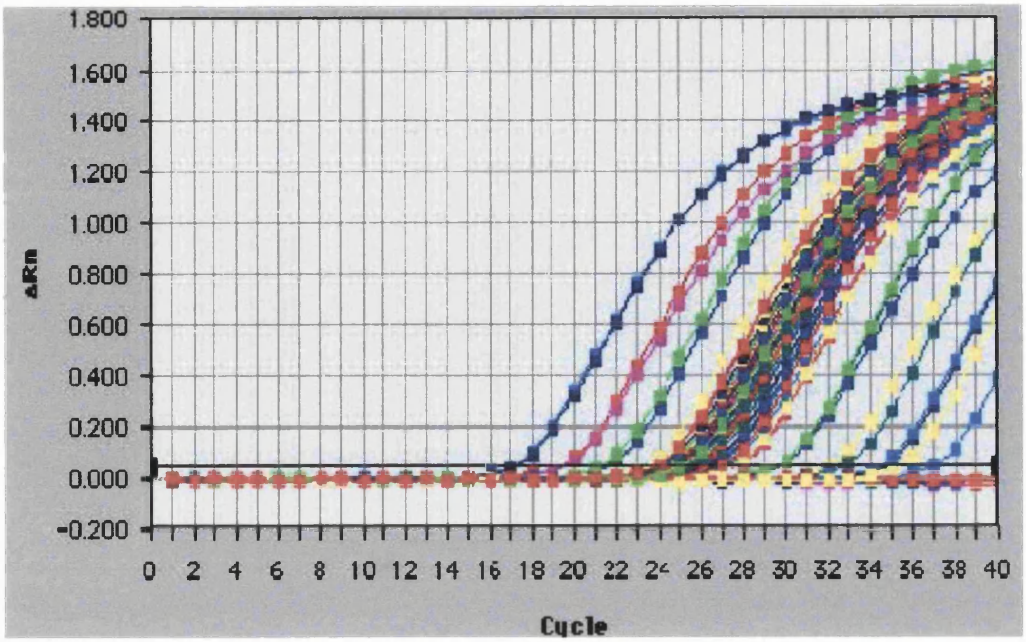

A)

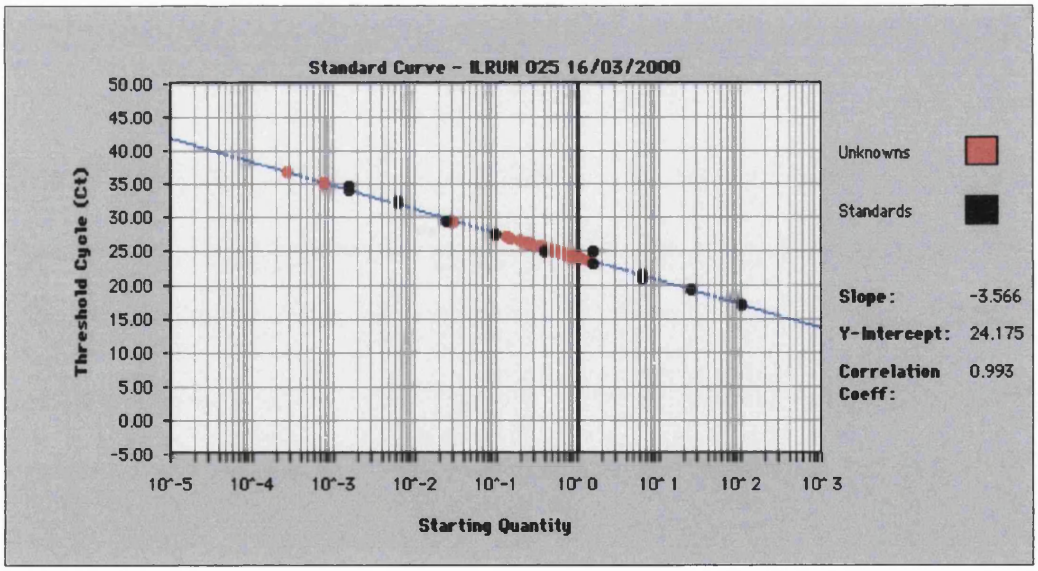

B)

Figure 5-2 TaqMan amplification plot and standard curve

A typical TaqMan amplification plot (A) and standard curve (B)

5.2.2.1 Isolation of RNA from mouse aortae and liver

RNA was extracted from mouse aortae and liver using TRIZOL™ (Life Technologies) following manufacturers instructions, and using modification of the method of Chomczynski and Sacchi [360]. All equipment was treated as described previously to eliminate RNase contamination (Section 4.2.4.3) and where possible nuclease free plasticware was used. Mouse aortae and liver were homogenised in TRIZOL™ reagent. Samples were maintained on ice for 5 min and then centrifuged (4°C, 10 min, 12,000 x *g*) to pellet insoluble material such as extracellular membranes, polysaccharides and high molecular weight DNA. The supernatant was collected and chloroform (1 ml) added to isolate RNA. Samples were shaken vigorously (15 s), incubated at RT (10 min), centrifuged (4°C, 20 min, 12,000 x *g*) and the aqueous phase containing the RNA transferred to fresh tubes. The RNA was precipitated by the addition of isopropanol (2.5 ml). Samples were mixed and incubated at -20°C (1 h), then centrifuged (4°C, 20 min, 12,000 x *g*) to pellet the RNA. The supernatant was discarded and the pellet washed with ethanol (5ml, 75%). The pellet was resuspended by mixing and was centrifuged (4°C, 20 min, 12,000 x *g*). The wash procedure was repeated with ethanol (1 ml, 75%), the supernatant removed and the pellet air dried before being resuspended in DEPC-treated water (300 µl). The RNA concentration was determined by UV spectrometry (see equation below). An optical density of 1 at 260 nm (A_{260}) corresponds to approximately 40 µg/ml for single stranded RNA.

$$[\text{RNA}]\ \mu g/\mu l = A_{260} \times \text{dilution factor} \times 40\ \mu g/ml\ /1000$$

5.2.2.2 DNase treatment of RNA samples

Prior to RT-PCR, samples were treated with deoxyribonuclease (RQ1 DNase I; Life Technologies) to digest contaminating genomic DNA. The following were added to nuclease-free microfuge tubes on ice: RNA (2 µg), DNase I reaction buffer (10x, 20 mM Tris-HCl, 2 mM $MgCl_2$, 50 mM KCl), DEPC treated distilled water and DNase I, Amplification Grade (2 U). The reaction was incubated for 15 min at RT after which time the DNase was inactivated by the addition of EDTA (2 µl, 25 mM) followed by heating (10 min, 65°C).

5.2.2.3 Reverse transcription of RNA samples

RNA samples (1 µg) were reverse transcribed (RT+) to cDNA. Negative control reactions, omitting the reverse transcriptase enzyme (RT-) were performed for each RNA sample (1 µg). The RT+ and RT- reaction mixes were set up in nuclease-free

microfuge tubes as outlined in Table 5-1. In brief, RNA (1 μg) was combined with random 9-mers (500 ng, Stratagene) and denatured at 70°C for 10 min, followed by 10 min on ice. The RNA was reverse transcribed under standard conditions, using SuperScript II (200 U, Life Technologies). cDNA was stored at -20°C until use in the TaqMan assay.

RT+	RT-
10 μl RNA (1 μg)	10 μl RNA (1 μg)
1μl Random 9mers (500 ng/μl)	1 μl Random 9mers (500 ng/μl)
9 μl DEPC-treated sterile water	9 μl DEPC-treated sterile water
Tubes were incubated (70°C, 10 mins) and then placed on ice (10 mins) and the following added:	
4 μl First strand buffer (5x)	4 μl First strand buffer (5x)
2 μl DTT (0.1 M)	2 μl DTT (0.1 M)
0.5 μl RNasein (40 U/μl)	0.5 μl RNasein (40 U/μl)
0.5 μl dNTPs (20 mM)	0.5 μl dNTPs (20 mM)
1 μl DEPC-treated water	1 μl DEPC-treated water
1 μl SuperScript II (200 U/μl)	1 μl DEPC-treated water
Tubes were incubated at 25°C for 15 min, 42°C for 50 min and 70°C for 15 min	

Table 5-1 Reverse transcription of RNA samples

5.2.2.4 Primer design

Sequences for murine KC, JE/MCP-1 and their receptors CXCR2 and CCR2 were obtained from the GenEMBL database. Primers and probes were designed using the Primer Express programme (PE Applied Biosystems), which selects probes and primers specifically for the TaqMan assay. Several criteria must be met when choosing a probe and primer set: (i) the primers and probe must have at least 50% G + C content, (ii) the primers and probe must not be complementary to each other, nor capable of forming secondary structures, nor must there be more than 4 consecutive identical residues, (iii) the probe and primers must not overlap, but should be in close proximity to each other, (iv) the melting temperature (T_M) of both primers should be identical, and the T_M of the probe should be greater than 10°C, (v) the amplicon should be 70 - 100 bp long, (vi) the probe must have more C residues than G residues and should be 20 -30 bp long, (vii) there must not be a G residue at the 5' end of the probe. Primers and probes were made by PE Applied Biosystems UK.

Gene	Forward primer	Reverse primer	Probe
Mouse CCR2	CAG-GAA-TCC-TTG-GGA-ATG-AGT-AAC	TCC-AAG-AGT-CTC-TGT-CAC-CTG-C	TGT-GAT-TGA-CAA-GCA-CTT-AGA-CCA-GGC-CA
Mouse CXCR2	TGA-GAA-CCA-AGC-TGA-TCA-AGG-A	GAA-TCT-CCG-TAG-CAT-TCA-AGG-C	AGC-GCC-GCG-ATG-ACA-TTG-ACA-A
KC	AGA-GCT-TGA-AGG-TGT-TGC-CCT	CGC-GAC-CAT-TCT-TGA-GTG-TG	CCC-ACT-GCA-CCC-AAA-CCG-AAG-TCA-T
JE	TCT-GGG-CCT-GCT-GTT-CAC-A	GAG-TAG-CAG-CAG-GTG-AGT-GGG	TGT-TGG-CTC-AGC-CAG-ATG-CAG-TTA-ACG
Mouse 36B4	GCT-TCA-TTG-TGG-GAG-CAG-ACA	TGC-GCA-TCA-TGG-TGT-TCT-TG	TCC-AAG-CAG-ATG-CAG-CAG-ATC-CGC

Table 5-2 TaqMan primers and probes

5.2.2.5 Quantitative PCR

cDNA equivalent to 50 ng of RNA was incubated for 40 cycles (95°C, 15 s and 60°C, 1 min, preceded by 2 min at 50°C and 10 min at 95°C) with TaqMan Universal mix containing AmpliTaq Gold DNA polymerase (Perkin Elmer), 200 nM probe, 300 nM forward primer and 300 nM reverse primer, made up to 25 μl with sterile distilled water. The TaqMan analysis was performed using the ABI PRISM 7700 Sequence Detection System for thermal cycling and real-time fluorescence measurements (PE Applied Biosystems). A 3-fold serial dilution of transgenic murine spleen total cDNA, equivalent to 0.0025 to 150 ng total RNA, was assayed for each transcript and used to construct a standard curve.

5.2.2.5.1 Calculation of results

For each gene of interest, C_t values from unknown samples were compared to a standard curve of C_t values generated from 3-fold dilutions of known concentrations of cDNA. From this, values for the unknown cDNAs could be calculated. To control for inter-animal variations, results were expressed relative to the housekeeping gene 36B4 which encodes for acidic ribosomal phosphoprotein P_0. Values were expressed on a relative scale rather than absolute values.

5.2.3 Statistics

Levels of chemokine and chemokine receptor mRNA in aortic and hepatic tissues were compared by 1-way ANOVA and using the following post-tests. Comparisons were made between the apoE*3 Leiden mice fed the HFC/C diet and the apoE*3 Leiden fed normal diet or the non-transgenic mice using the Dunnetts test. Differences

between the apoE*3 Leiden mice fed normal diet and the non-transgenic mice were analysed post-hoc using the Bonferroni method. Differences were considered to be statistically significant if $p<0.05$

5.3 Results

5.3.1 Effects of feeding HFC/C diet on KC and JE mRNA expression in aortic and hepatic tissue

Expression of KC and JE mRNA was detected in both aortic and hepatic tissues in apoE*3 Leiden mice and their non-transgenic littermates (Figure 5-3 and Figure 5-4). Consumption of diet HFC/C for 4 weeks induced a trend towards increased KC mRNA expression in the aortae from both apoE*3 Leiden and the non-transgenic controls (Figure 5-3 A). However, a significant degree of variation in this data was observed, possibly due to variability in the amount of atheroma associated with different regions of the aorta. Interestingly, no significant differences in JE mRNA expression were observed in aortae from mice consuming either HFC/C or RM1 diet (Figure 5-4 A). Levels of expression of both KC and JE in aortic samples were much lower (20 to 30 fold) than those seen in hepatic tissues (Figure 5-3 B and Figure 5-4 B). As expected from previous reports [110,111], both groups of mice fed the atherogenic diet exhibited significant ($p<0.05$) increases in hepatic KC and JE mRNA expression, compared with either apoE*3 Leiden or non-transgenic mice fed the normal chow diet. However, no significant differences in hepatic expression of KC and JE were detected in the two groups of mice consuming the atherogenic (HFC/C) diet (Figure 5-3 B and Figure 5-4 B).

Expression of CCR2 and CXCR2 was detected in both aortic and hepatic tissues in apoE*3 Leiden mice and their non-transgenic littermates (Figure 5-5 and Figure 5-6). The expression of chemokine receptor mRNA appeared to follow a similar pattern as its ligands. For example, no significant differences in CXCR2 aortic mRNA expression was observed between the different strains of mice or diets used (Figure 5-5 A). However, hepatic expression of this receptor was significantly elevated in both groups of HFC/C fed animals (Figure 5-5 B). Aortic expression of CCR2 was not significantly different between any of the groups of mice (Figure 5-6 A). Further, the expression of hepatic CCR2 mRNA was higher in apoE*3 Leiden mice consuming the HFC/C diet compared with apoE*3 Leiden mice consuming normal RM1 diet (Figure 5-6 B). However, due to the variability in the results, animals consuming the HFC/C diet were only significantly different to apoE*3 Leiden mice consuming RM1 diet.

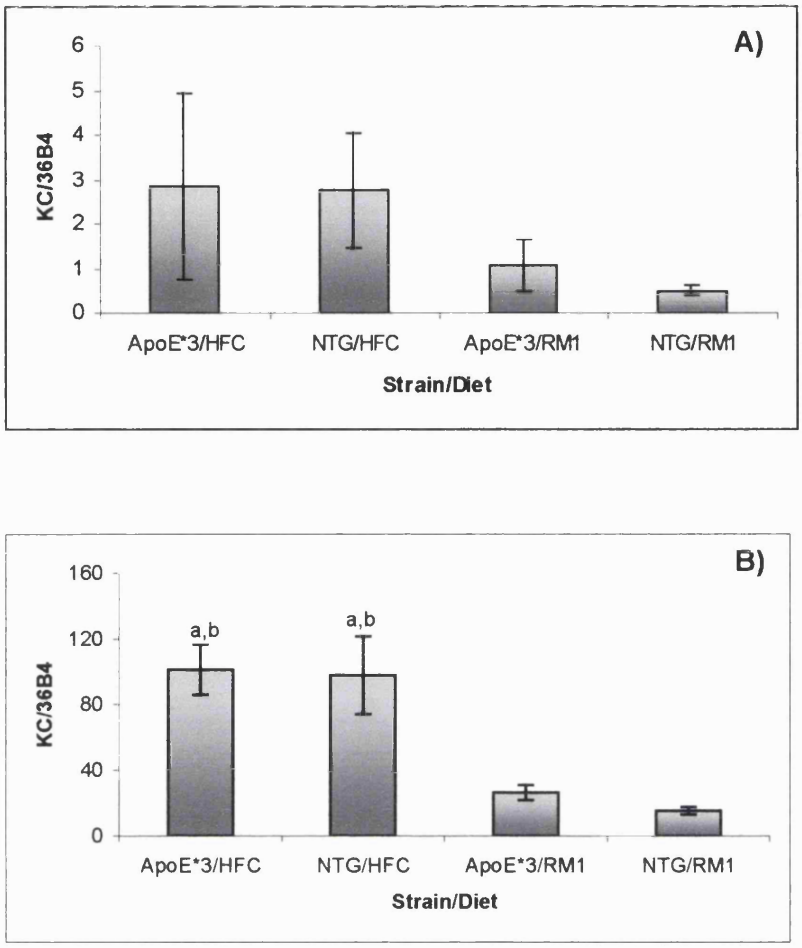

Figure 5-3 Aortic and hepatic KC mRNA expression

Effect of diet and strain of mouse on aortic (A) and hepatic (B) expression of KC mRNA, expressed relative to the housekeeper gene, 36B4. Values shown are the means ± SEM for between 3 - 5 mice in each group; data were not log transformed before statistical analyses were performed. (a = significantly different ($p<0.05$) to apoE*3 Leiden mice consuming RM1 diet; b = significantly different ($p<0.05$) to non-transgenic mice consuming RM1 diet).

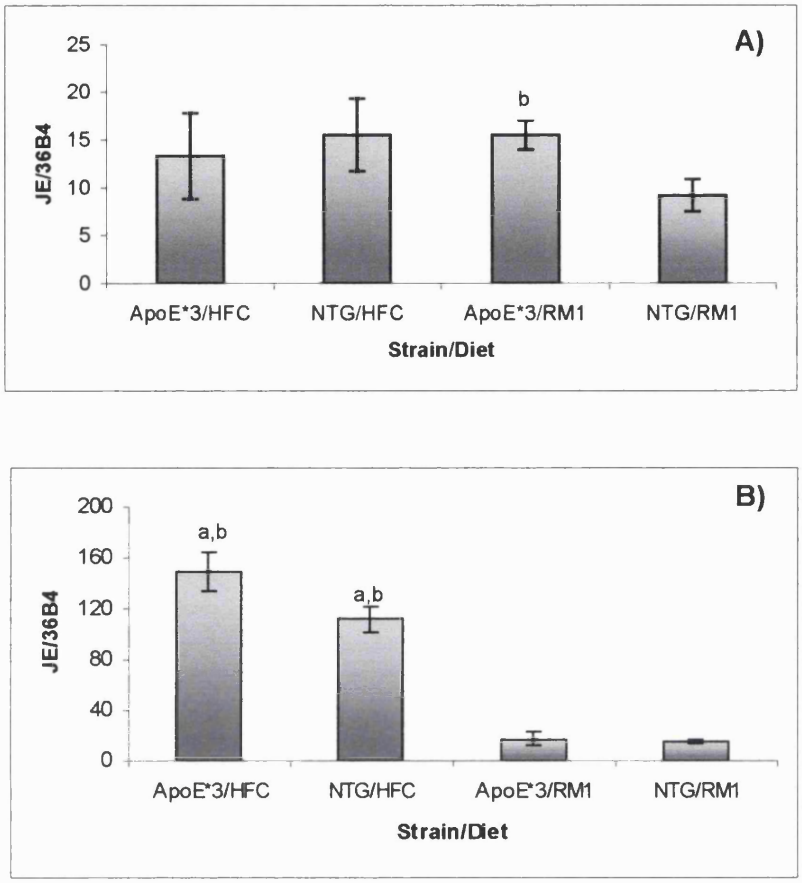

Figure 5-4 Aortic and hepatic JE mRNA expression

Effect of diet and strain of mouse on aortic (A) and hepatic (B) expression of JE mRNA, expressed relative to the housekeeper gene, 36B4. Values shown are the means ± SEM for between 3 - 5 mice in each group; data were not log transformed before statistical analyses were performed. (a = significantly different ($p<0.05$) to apoE*3 Leiden mice consuming RM1 diet; b = significantly different ($p<0.05$) to non-transgenic mice consuming RM1 diet).

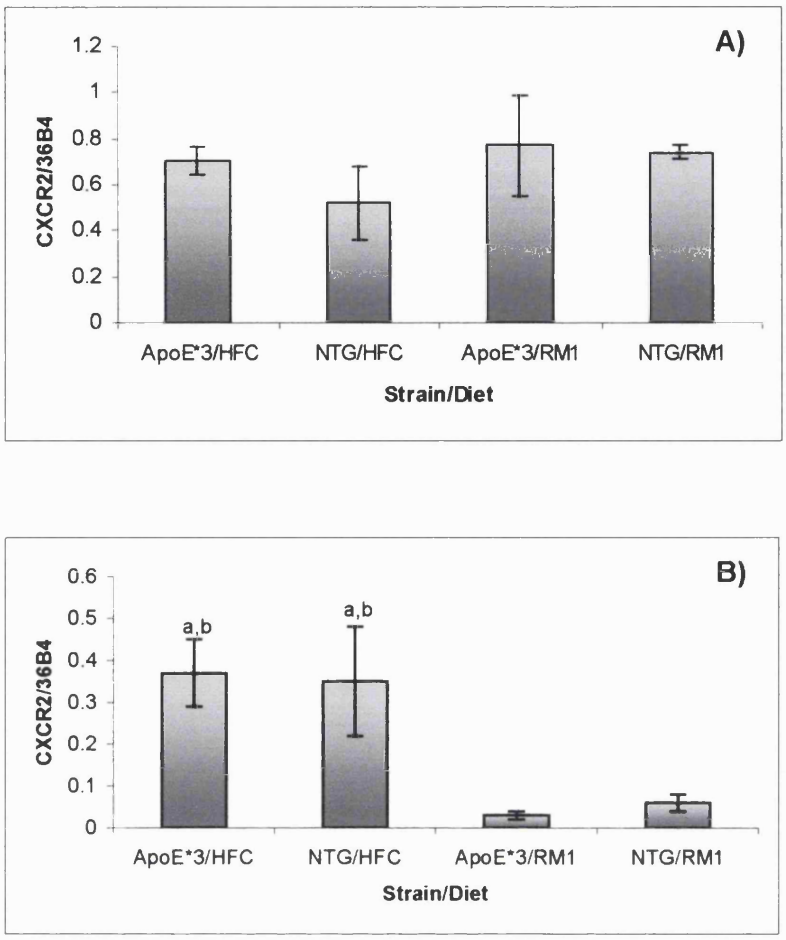

Figure 5-5 Aortic and hepatic CXCR2 mRNA expression

Effect of diet and strain of mouse on aortic (A) and hepatic (B) expression of CXCR2 mRNA, expressed relative to the housekeeper gene, 36B4. Values shown are the means ± SEM for between 3 - 5 mice in each group; data were not log transformed before statistical analyses were performed. (a = significantly different (p<0.05) to apoE*3 Leiden mice consuming RM1 diet; b = significantly different (p<0.05) to non-transgenic mice consuming RM1 diet).

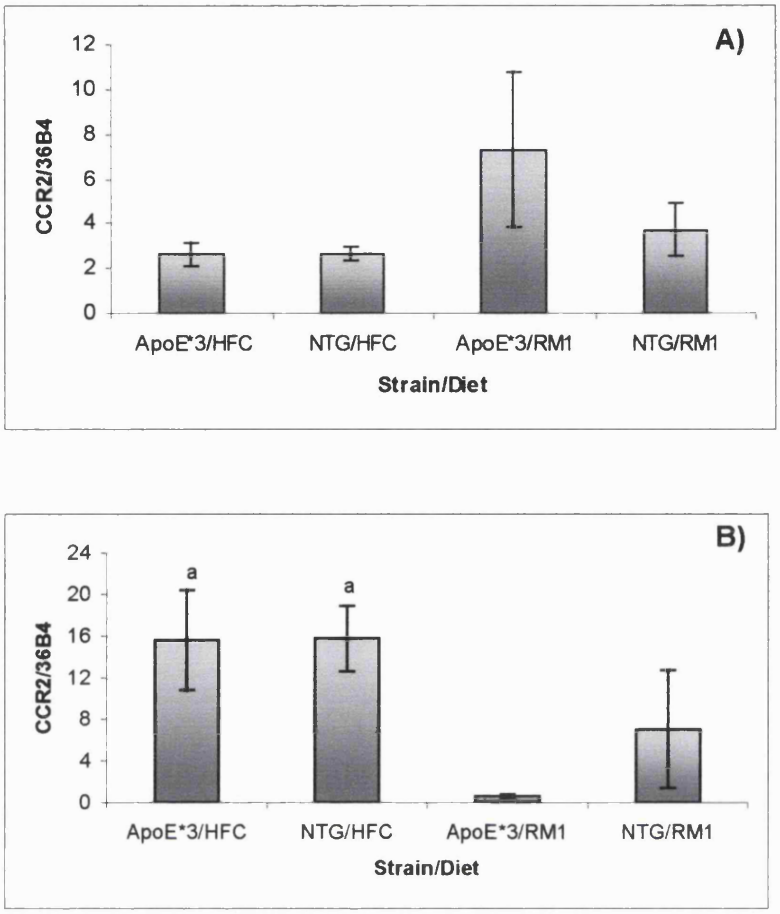

Figure 5-6 Aortic and hepatic CCR2 mRNA expression

Effect of diet and strain of mouse on aortic (A) and hepatic (B) expression of CCR2 mRNA, expressed relative to the housekeeper gene, 36B4. Values shown are the means ± SEM for between 3 - 5 mice in each group; data were not log transformed before statistical analyses were performed. (a = significantly different ($p<0.05$) to apoE*3 Leiden mice consuming RM1 diet).

5.4 Discussion

In this small study, we investigated hepatic and aortic chemokine (JE, KC) and chemokine receptor (CXCR2, CCR2) expression in apoE*3 Leiden mice, and their non-transgenic littermates, fed an atherogenic (HFC/C) or normal chow (RM1) diet. Real-time quantitative PCR was used to measure relative levels of mRNA. By using this highly sensitive technique the expression of all these genes in hepatic and aortic tissues was demonstrated.

One of the aims of this thesis was to examine potential sources of circulating chemokines. Previously, it has been demonstrated that feeding atherogenic diets to C57BL/6J mice induces oxidative stress, inflammation and lipid accumulation in both aortic and hepatic tissues [110,111]. Indeed, atherogenic diets generate similar responses to injection of mmLDL, namely activation of NF-κB and the induction of genes for JE and KC in the liver [20,111,361]. It was therefore of no surprise to detect elevated hepatic expression of KC and JE mRNA in apoE*3 Leiden mice and their non-transgenic littermates. Indeed, the relatively high expression levels of KC and JE in this tissue suggest the liver may be a major source of circulating chemokines. Interestingly, however, hepatic expression of KC mRNA was identical in both groups of animals consuming the atherogenic diet, suggesting that other sites of inflammation were contributing to the higher serum levels of KC seen in apoE*3 Leiden mice (Figure 3-4 A and Figure 4-10 B). As discussed elsewhere (Sections 1.7.2 and 1.7.2.1), it seems probable that the developing atherosclerotic lesion could contribute directly to the levels of circulating KC [172,176,177,190,192,341,342,351]. Indeed, KC mRNA was detected in isolated murine aortae; a trend, albeit not significant, towards higher aortic expression of KC mRNA was seen in apoE*3 Leiden and non-transgenic mice consuming the atherogenic diet. Aortic JE mRNA expression was also detected in mice from this study, however, no significant differences were noted between groups of mice consuming the HFC/C or RM1 diet. This may suggest as discussed previously (Section 4.4.1) that JE may not be the initial stimulus for the recruitment of monocytes to the vessel wall during the early stages of lesion development and that other chemokines may be involved. Indeed, we found that positive macrophage immunostaining preceeded JE mRNA expression (Sections 4.3.5 and 4.3.8.1). Further, a study by Rayner *et al* [348] examining the mRNA expression of JE in developing lesions of apoE$^{-/-}$ mice indicated that JE did not appear to be the initial signal for the infiltration of monocytes to the arterial intima.

Systemic chemokine concentrations may be influenced by the rate of clearance of these molecules from the bloodstream. There may be many mechanism(s) involved (Section 3.4) including binding to chemokine receptors such as CCR2 and CXCR2 or its murine equivalent mIL-8RH. Results from this study indicate markedly increased hepatic mRNA expression of CCR2 and CXCR2 in mice consuming the atherogenic HFC/C diet. Indeed, chemokine receptor expression tended to mirror that of its respective ligand. Thus, it is probable that differences in both production and clearance of chemokines may influence systemic chemokine concentrations. It is interesting to note that both aortic and hepatic CCR2 expression is approximately 10 to 40-fold higher than CXCR2 expression. Little is known about the regulation of CXCR2 or mIL-8RH expression; however it is clear that exposure to their respective ligands induces rapid desensitisation/down regulation of receptors at the cell surface. By contrast, CCR2 mRNA expression on monocytes is influenced by exposure to lipoproteins [362,363]. High concentrations of plasma LDL result in an up-regulation of CCR2 expression [362] and enhanced monocyte chemotaxis, while HDL down-regulates CCR2 expression [363].

Although CCR2 expression is thought to be central to monocyte recruitment into the intima [74,171], no difference in aortic expression of this receptor was observed between mice consuming the HFC/C or RM1 diet. This was only a short study and differences in aortic CCR2 expression may become evident at later time-points. Indeed, aortic mRNA expression of CCR2 in apoE$^{-/-}$ mice is not seen until between 4 - 12 weeks consumption of a 'Western' type diet [348]. ApoE$^{-/-}$ mice develop more advanced intimal lesions than apoE*3 Leiden mice, so it is possible that changes in CCR2 expression levels would not be detected in apoE*3 Leiden mice till 8 weeks of HFC/C feeding. Furthermore, as transcript levels in the whole of the aorta were measured, subtle changes in expression in different regions of the aorta would be over-looked. It would have been interesting to measure the temporal expression of chemokine/chemokine receptor in different regions of the aorta over longer periods of HFC/C feeding.

No obvious differences in aortic CXCR2 expression was observed between the HFC/C or RM1 fed animals. Again, this may be due to the same reasons as outlined for CCR2. Analysis of human/murine atherosclerotic lesions has revealed abundant CXCR2 or mIL-8RH expression [177]. Recently it was demonstrated that the absence of leukocyte mIL-8RH resulted in reduced lesion area and MOMA-2 positive cells in lesions from LDLR$^{-/-}$ mice [177]. However, at earlier time-points (3 weeks) lesion size was comparable between recipients of mIL-8RH$^{-/-}$ and mIL-8RH$^{+/+}$ bone marrow leukocytes

suggesting that this receptor may not play a role in the initial entry of monocytes into the arterial intima. By weeks 6 and 16, lesions were significantly smaller and less advanced in $LDLR^{-/-}$ mice who had received $mIL\text{-}8RH^{-/-}$ bone marrow leukocytes. This suggests that perhaps CXCR2 may play a role in the retention, expansion and activation of intimal macrophages [190].

In summary, hepatic expression of chemokine and chemokine receptor mRNA is associated with the marked hypercholesterolaemia seen in apoE*3 Leiden mice and their non-transgenic littermates after 4 weeks consumption of the HFC/C diet. Previous analysis of aortic root sections by *in-situ* hybridisation was unable to detect KC and JE mRNA expression. However, by using real-time quantitative PCR we were able to detect transcripts for KC, and JE, and their receptors CXCR2 and CCR2. Despite no significant differences in aortic transcript levels for any of the genes tested, KC mRNA tended to be higher in HFC/C fed mice. Thus, it is likely that circulating chemokines may originate from a number of tissues, including the liver and possibly the aorta.

Chapter 6

*Effects of antioxidants on circulating levels of chemokines, soluble adhesion molecules and atheroma in apoE*3 Leiden mice*

6 Effects of antioxidants on circulating levels of chemokines, soluble adhesion molecules and atheroma in apoE*3 Leiden mice

6.1 Introduction

Current theories of atherosclerosis (Figure 1-15) suggest that enhanced oxidative stress within the artery wall, resulting in oxidation of LDL, may be involved in several stages of atherogenesis. Multiple oxidising species (Section 1.9.1) may promote LDL oxidation; these include lipoxygenase enzymes [72], reactive nitrogen species [364] or myeloperoxidase-derived oxidants [365]. In particular, 'minimally modified' LDL (mmLDL) can mediate the activation of members of the redox-sensitive Rel family of transcription factors, namely NF-κB [366-368], thereby increasing endothelial expression of genes encoding chemokines and adhesion molecules involved in recruiting monocytes within the artery wall [366-368].

One obvious consequence of the 'oxidation hypothesis' is that dietary or synthetic antioxidants should, in theory, retard the development of atherosclerosis. Studies measuring the protection against *ex vivo* LDL oxidation provided by consumption of vitamin E [238], vitamin C [369] and β-carotene [250], either singly [238,369] or in combination [250,370], suggested that dietary modifications might prevent coronary artery disease. Indeed, antioxidants can prevent NF-κB activation [241,371,372] and suppress expression of chemokines and adhesion molecules [240,241,371,372] involved in monocyte recruitment to the artery wall. Furthermore, naturally occurring antioxidants reduce isoprostane formation *in vivo* [243] and can inhibit lesion development in primates [373], rabbits [374], and murine models of atherosclerosis [243,253]. In this study, we have examined the effect of a combination of dietary antioxidants on systemic levels of chemokines and soluble adhesion molecules in order to track inflammatory responses during the development of atheroma in apoE*3 Leiden mice. Specifically, a modified version of the HFC/C diet (Section 1.2.1), which was deficient in, or supplemented with dietary antioxidants, vitamin E (α-tocopherol;0.1% w/v), vitamin C (0.05% w/v) and β-carotene (0.5% w/v) was used. ApoE*3 Leiden mice or their non-transgenic littermates were fed these experimental diets for a period of 12 weeks, in order to influence the induction of redox-sensitive inflammatory genes and/or subsequent development of atheroma. Circulating levels of adhesion molecules, sVCAM-1, sICAM-1 and chemokines JE/MCP-1 and KC, ligand for the mIL-8RH, were measured.

6.2 Methods

6.2.1 Study protocol

6.2.1.1 Mice

Thirty female apoE*3 Leiden mice and 30 female non-transgenic mice, aged 10 - 12 weeks, were allocated randomly to experimental groups based on weight and litter.

6.2.1.2 Diet

Animals were maintained on a normal RM1 diet before the experimental period. During the study (0 - 12 weeks), mice were fed a high fat/high cholesterol/cholate (HFC) containing diet, supplied by Hope Farm (Section 2.2.2). The diet was modified so that it was either deficient in β-carotene and vitamin C, and contained a reduced content of vitamin E (<30 IU of vitamin E/kg of diet) (HFC/LAO), or supplemented with vitamin E (0.1% w/v), β-carotene (0.5% w/v) and ascorbic acid (0.05% w/v) (HFC/HAO). Mice were weaned onto their specific diet over 4 days. In total, 15 apoE*3 Leiden mice and 15 of their non-transgenic littermates were fed the HFC/LAO; the same numbers were fed HFC/HAO.

6.2.1.3 Collection of blood samples

In-life blood samples were taken prior to the start of the study and then after 4 and 8 weeks of diet treatment; terminal blood samples were taken at week 12 (Section 2.3.1). Serum was prepared as previously described (Section 2.3.2).

6.2.1.4 Serum analysis

6.2.1.4.1 Lipid analysis

Total cholesterol and triglyceride concentrations were measured enzymatically using commercially available kits as described previously in Sections 2.3.4 and 2.3.5.

6.2.1.4.2 Measurement of serum chemokine concentrations

JE and KC concentrations were determined in diluted serum samples (1:1-1:4) using commercially available ELISA kits as previously described in Sections 2.3.7 and 2.3.8.

6.2.1.4.3 Measurement of soluble adhesion molecules in serum

Soluble ICAM-1 levels were determined in diluted serum samples (1:100) as described in Section 2.3.6. Soluble VCAM-1 levels were determined in diluted samples (1:40) by establishing an ELISA protocol as described in Section 6.2.1.5.

6.2.1.5 Murine sVCAM-1 ELISA

An ELISA for the detection of murine sVCAM-1 was developed as a quantitative assay to determine sVCAM-1 concentration in mouse serum samples from this study. As with any ELISA, reagents were titrated and optimal concentrations of 'capture' and 'detection' antibodies used, to achieve reliable and reproducible results. The 'titre' of an antibody is defined as the highest dilution of that antibody which results in optimum specific signal with the least amount of background [330]. Titration curves for each antibody are shown Figure 6-1 and Figure 6-2.

The 'capture' antibody (goat anti-mouse VCAM-1 polyclonal antibody, R&D Systems), was diluted (2 μg/ml) in PBS (26.8 mM KCl, 14.7 mM KH_2PO_4, 56.4 mM Na_2HPO_4 and 1.5 mM NaN_3, pH 7.5) and 100 μl added to each well of a 96-well plate. After an overnight incubation (4°C), the contents of each well were removed by aspiration and non-specific binding sites blocked by the addition of 300 μl/well of blocking buffer: 50 mM Tris-HCl, 150 mM NaCl, 1 mM $MgCl_2$, pH 7.4, containing BSA (1% w/v). The plate was incubated for 1 h at 37°C, before the contents of each well were aspirated, and washed (5x) with 300 μl/well of washing buffer (10 mM Tris, 150 mM NaCl, pH 7.4, containing Tween-20 (0.05% v/v)). Mouse serum samples were diluted (1:40) with assay buffer (50 mM Tris, 150 mM NaCl, pH 7.4, containing Tween-20 (0.01% v/v) and BSA (0.5% v/v)). Murine recombinant VCAM-1 (R&D Systems) was diluted in assay buffer to give the following final concentrations: 6.25, 12.5, 25, 50, 100 and 200 ng/ml. Assay buffer was used as a negative control. Biotinylated MVCAM.A(429) ('detecting' antibody, Pharmingen) was diluted to a final concentration of 10 μg/ml in assay buffer supplemented with normal goat serum (1% v/v), and 50 μl added to each well, followed by the addition of the diluted (1:40) serum samples and standards (50 μl). The plate was incubated for 3 h at RT. The contents of each well were then aspirated and washed (5x) as before. StreptABComplex-Horseradish peroxidase (DAKO) was diluted in assay buffer (1:1000) and 100 μl added to each well (30 min). The wells were again aspirated and the plate washed (5x) as before. Immunoreactive murine VCAM-1 was detected by incubating (30 min, RT) with 100 μl of 3, 3', 5, 5'-tetramethyl benzidine (TMB) substrate (Sigma) containing 0.01%

hydrogen peroxide. The reaction was stopped by the addition of 100 µl 2 M sulphuric acid (H_2SO_4), and the absorbance of each well was determined at 450 nm. A typical standard curve is shown in Figure 6-3.

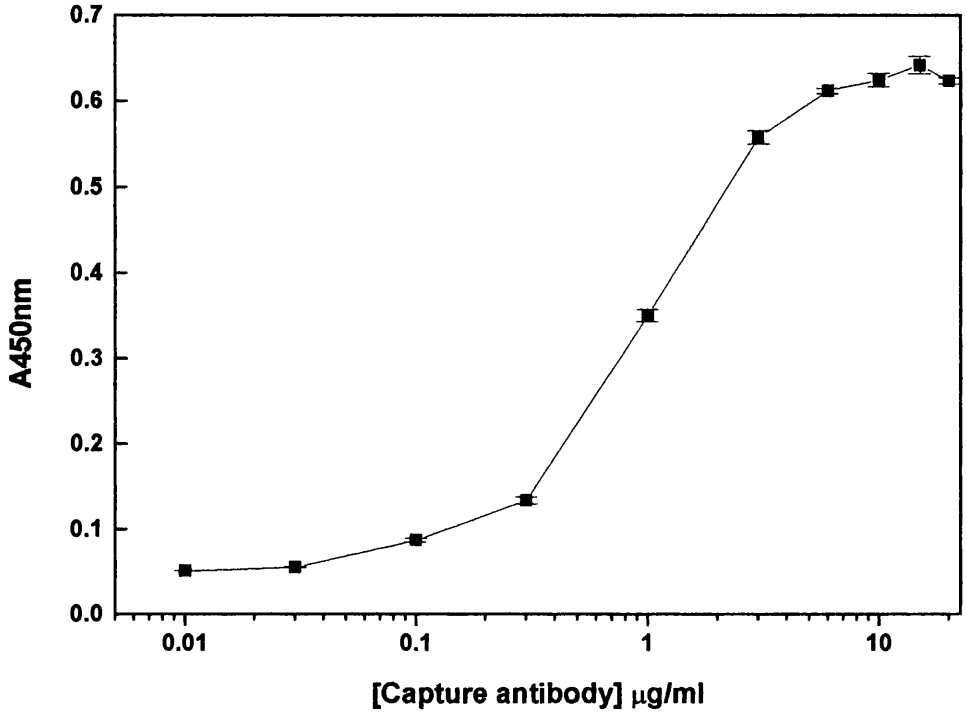

Figure 6-1 Titration of anti-mouse VCAM-1 polyclonal antibody

Goat anti-mouse VCAM-1 polyclonal antibody was titrated in the sVCAM-1 ELISA. The optimal dilution was found to be 2 µg/ml. To titrate the 'capture' antibody, the 'detecting' antibody was used at a concentration of 10 µg/ml, recombinant murine VCAM-1 at 30 ng/ml and Streptavidin HRP at a 1:1000 dilution. Values shown are means ± S.D. for triplicate wells

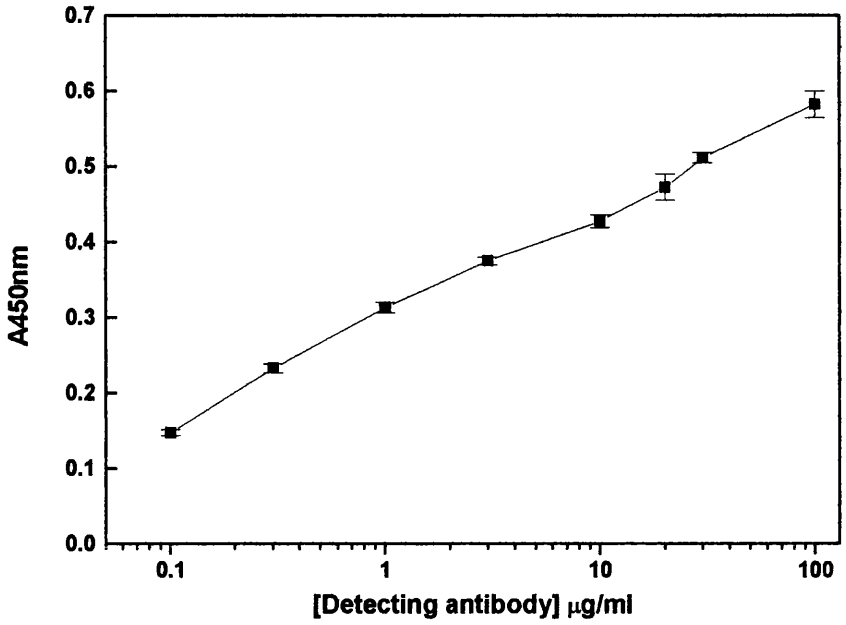

Figure 6-2 Titration of biotinylated anti-mouse VCAM-1 monoclonal

Biotinylated rat anti-mouse VCAM-1 monoclonal antibody was titrated in the sVCAM-1 ELISA. The optimal dilution was found to be 10 µg/ml. To titrate the 'detecting' antibody, the 'capture' antibody was used at a concentration of 2 µg/ml, the recombinant murine VCAM-1 was at 30 ng/ml and the Streptavidin HRP was used at a 1:1000 dilution. Values shown are means ± S.D. for triplicate wells.

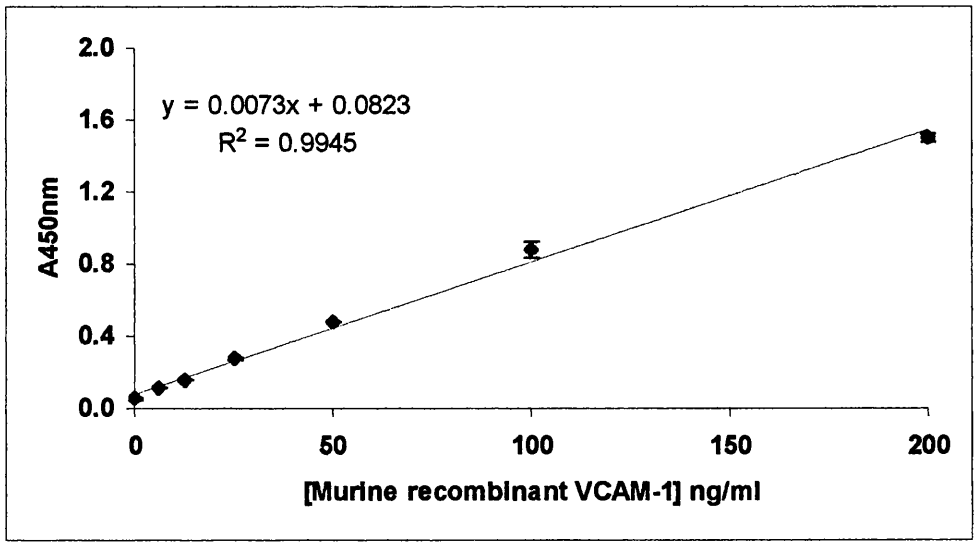

Figure 6-3 Typical standard curve for murine sVCAM-1 ELISA

The ELISA was linear from 0 - 200 ng/ml. Values shown are means ± S.D. for triplicate wells.

6.2.1.6 Statistical analysis

All the parameters described, except lesion areas, were log-transformed in order to normalise the variances, and geometric means with 95% confidence intervals are quoted. Parameters describing lesion area (ORO staining and regions of interest) were transformed by taking the square root of the raw values. Pre-treatment data was analysed using 1-way ANOVA, followed by pair-wise comparisions using the Bonferroni method. Post-baseline, in-life, data were analysed by repeated measures ANOVA, again followed by pair wise comparisions of groups using the Bonferroni test. The following comparisions were made between the groups of mice used: (a) apoE*3 Leiden (HFC/HAO) versus apoE*3 Leiden mice (HFC/LAO); (b) apoE*3 Ledien (HFC/HAO) versus non-transgenic (HFC/HAO); (c) apoE*3 Leiden (HFC/LAO) versus non-transgenic (HFC/LAO); and (d) non-transgenic (HFC/HAO) versus non-transgenic (HFC/LAO). Differences were considered to be statistically significant if $p<0.05$

6.3 Results

6.3.1 Serum cholesterol and triglyceride

The effects of feeding HFC/LAO or HFC/HAO on serum cholesterol and triglyceride concentrations in apoE*3 Leiden mice or their non-transgenic littermates are shown in Figure 6-4. As previously reported [44], consumption of the HFC diet for up to 12 weeks resulted in serum cholesterol levels that were 4 - 8 fold higher ($p<0.05$) in the apoE*3 Leiden mice compared with their non-transgenic littermates (Figure 6-4 A). The presence or absence of antioxidants in the diet modulated serum cholesterol concentrations slightly in both groups of mice. ApoE*3 Leiden mice consuming diet HFC/HAO had significantly (37%; $p<0.05$) higher cholesterol levels at week 8 (Figure 6-4 A); by contrast, serum cholesterol levels decreased by 35% ($p<0.05$) at week 12 in the non-transgenic animals consuming the same diet.

Serum triglyceride concentrations were significantly ($p<0.05$) higher in both groups of apoE*3 Leiden mice throughout the study, compared with their non-transgenic littermates (Figure 6-4 B). At all time points, serum triglyceride levels in the apoE*3 Leiden mice were 3 - 8 fold higher than in the non-transgenic littermates consuming HFC/LAO or HFC/HAO diets. The presence of the antioxidants did not seem to affect serum triglyceride concentrations in the non-transgenic animals; however, at week 4, increased (82%; $p<0.05$) serum triglycerides were seen in the group of apoE*3 Leiden mice consuming diet HFC+AO, compared with diet HFC/LAO (Figure 6-4 B).

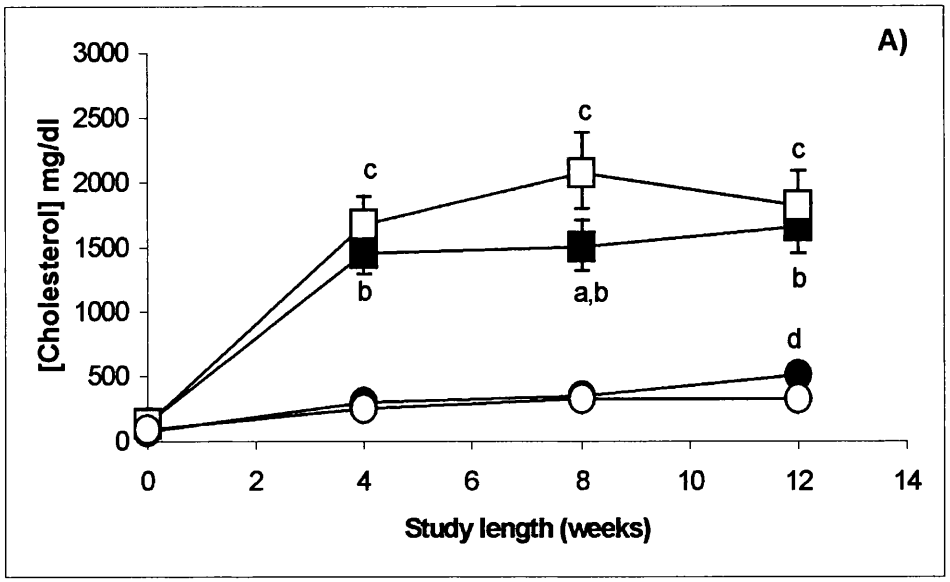

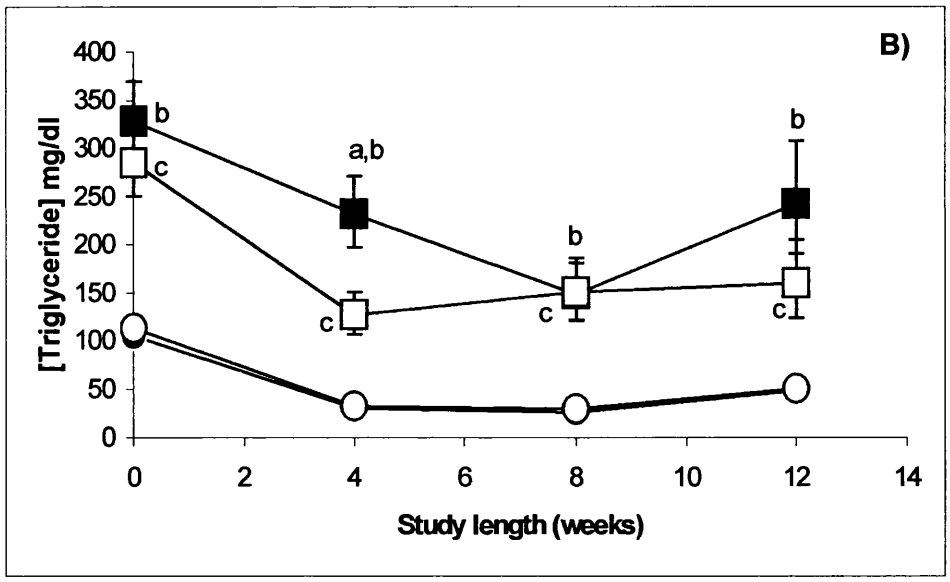

Figure 6-4 Effects of diet and strain of mouse on serum lipids

Serum cholesterol (A) and triglyceride (B) concentrations in (■,□) apoE*3 Leiden mice (n=15) or their (●,○) non-transgenic littermates (n=15) consuming either the antioxidant-replete diet, HFC/HAO (■,●), or the antioxidant-deficient diet, HFC/LAO (□,○). Values shown are geometric means ± 95% confidence intervals. a = significant difference (p<0.05) between apoE*3 Leiden mice consuming HFC/HAO and HFC/LAO; b = significant difference between (p<0.05) between apoE*3 Leiden mice consuming HFC/HAO and the non-transgenic animals consuming HFC/HAO; c = significant difference (p<0.05) between apoE*3 Leiden and the non-transgenic animals consuming either HFC/HAO or HFC/LAO and d = significant difference between non-transgenic animal consuming either HFC/HAO or HFC/LAO.

6.3.2 Atheroma data

Lesion areas were quantified in apoE*3 Leiden mice and the non-transgenic animals consuming HFC/LAO or HFC/HAO diets for 12 weeks (Figure 6-5). Large intimal lesions, staining intensely with ORO, developed in both groups of apoE*3 Leiden mice; by contrast, only early fatty streak lesions were detected in the aortic root of the non-transgenic animals. Both ORO staining and lesion areas, were 10 - 20 fold greater in the apoE*3 Leiden mice than in the non-transgenic controls (Figure 6-5). Consumption of dietary antioxidants did not affect the extent of lesion formation in either the apoE*3 Leiden mice or their non-transgenic controls, as judged by lesion area or ORO staining. However, although these values did not reach significance, both parameters were slightly lower in the animals consuming diet HFC/HAO compared with diet HFC/LAO (Figure 6-5).

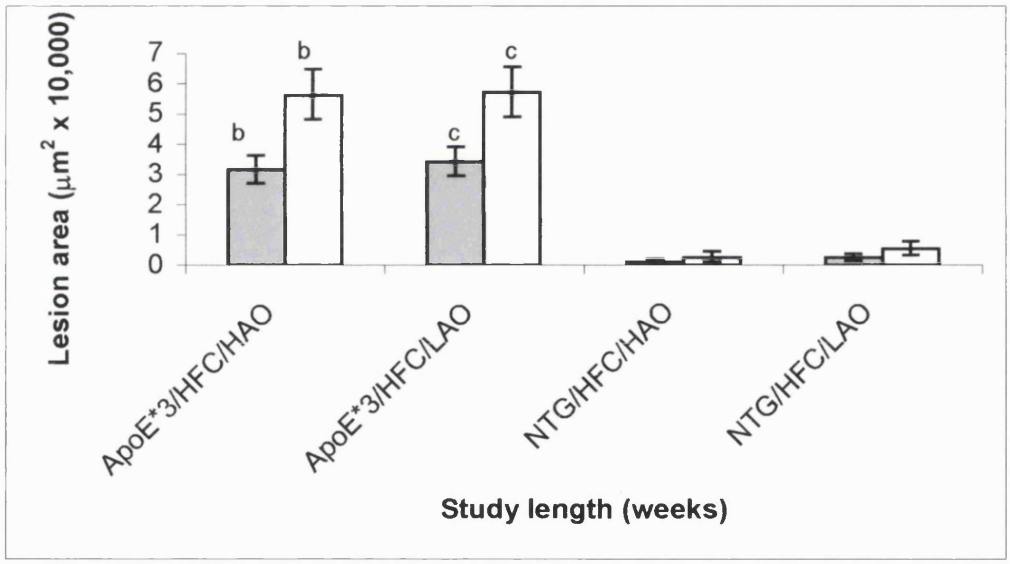

Figure 6-5 Lesion development in mice fed HFC/HAO or HFC/LAO

Effects of feeding diets HFC/HAO and HFC/LAO for 12 weeks on Oil-Red-O intensity (■) and cross-sectional area (□) of atherosclerotic lesions in the aortic roots of apoE*3 Leiden (ApoE*3; n=15) and their non-transgenic littermates (NTG; n=15). Values shown are geometric means ± 95%confidence intervals. b = significant differences (p<0.05) between apoE*3 Leiden mice and their non-transgenic animals consuming HFC/HAO; c = significant differences (p<0.05) between apoE*3 Leiden and non-transgenic mice consuming HFC/LAO.

6.3.3 Serum adhesion molecules

The effects of feeding HFC/LAO or HFC/HAO diets to apoE*3 Leiden mice, or their non-transgenic littermates, on serum concentrations of soluble VCAM-1 and soluble ICAM-1 are shown in Figure 6-6. Serum levels of sVCAM-1 were equivalent in all groups of mice at the start of the study. Rapid increases in serum concentrations of sVCAM-1 from baseline occurred in both groups of animals consuming the diet deficient in antioxidants (HFC/LAO), reaching maximal recorded levels by week 4 of the study (Figure 6-6 A). The highest sVCAM-1 levels were seen in the non-transgenic group of animals consuming HFC/LAO. Consumption of the dietary antioxidants significantly ($p<0.05$) blunted this response in both apoE*3 Leiden mice and their non-transgenic animals. Levels of sVCAM-1 were significantly ($p<0.05$) higher in the groups of apoE*3 Leiden mice fed HFC+AO and the non-transgenic animals consuming HFC-AO, compared with the non-transgenic animals fed HFC+AO, at week 8 of the study. By week 12, however, all groups of animals showed a decline in circulating levels of sVCAM-1 tending towards baseline levels.

Serum sICAM-1 concentrations were slightly higher (20 - 45%; $p<0.05$) in the two groups of apoE*3 Leiden mice compared with their non-transgenic controls at the start of the study (Figure 6-6 B). Circulating levels of sICAM-1 increased in all groups of mice (1.8 - 2.4 fold; $p<0.05$) following consumption of the atherogenic HFC/C diet. Feeding antioxidant vitamins did not affect sICAM-1 levels in apoE*3 Leiden mice. However, at weeks 8 and 12, apoE*3 Leiden mice consuming diet HFC/HAO had significantly ($p<0.05$) higher levels of sICAM-1 than the non-transgenic controls consuming the same diet. Further, at early time points (weeks 4 and 8), non-transgenic animals consuming HFC/LAO had significantly ($p<0.05$) higher levels of sICAM-1 than the group of non-transgenic animals consuming HFC/HAO (Figure 6-6 B). It is noteworthy that the levels of sICAM-1 in murine serum appear considerably higher than the concentrations of murine sVCAM-1, although the reasons for this are not clear at present.

6.3.4 Serum chemokines

The effects of feeding the HFC/LAO or HFC/HAO diets on serum CC (JE) and CXC (KC) chemokine concentrations (Figure 6-7) were analysed using in-life and terminal samples from each group of mice culled at 12 weeks. At the start of the study, serum JE concentrations did not differ significantly in any of the groups of animals. Consumption of diet HFC caused rapid increases ($p<0.05$) from initial values in serum JE in all groups of mice, that were not affected by the presence or absence of dietary

antioxidants (Figure 6-7 A). Circulating levels of JE were 2.7- and 2.4-fold ($p<0.05$) higher at week 8, in groups of apoE*3 Leiden mice consuming HFC/HAO and HFC/LAO respectively, compared with their non-transgenic controls. However, by week 12 all groups of animals had approximately equivalent serum JE concentrations.

Serum levels of the CXC chemokine, KC, were also equivalent all groups of animals at the start of the study. Consumption of the HFC/LAO or HFC/HAO diets for up to 12 weeks caused significant ($p<0.05$) 2 – 4 fold increases from baseline in serum KC concentrations in apoE*3 Leiden mice and their non-transgenic littermates. However, serum KC levels increased more rapidly in the apoE*3 Leiden mice than in the non-transgenic controls (Figure 6-7 B). Consumption of dietary antioxidants did not appear to reduce serum levels of KC in apoE*3 Leiden mice or their non-transgenic littermates. However, serum KC levels were significantly (2.2 fold; $p<0.05$) higher in the group of apoE*3 Leiden mice consuming diet HFC/HAO, compared with the non-transgenic controls consuming the same diet at week 8.

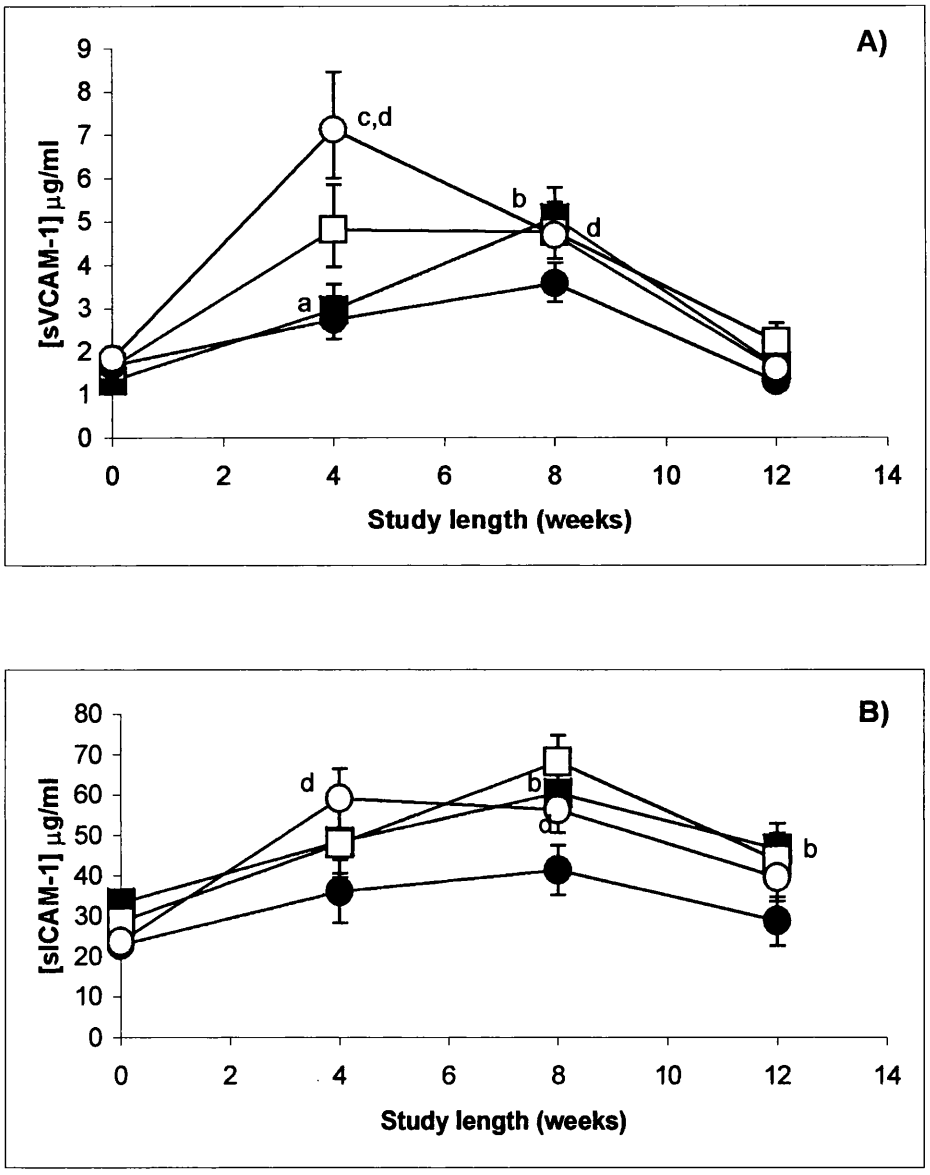

Figure 6-6 Effects of diet and strain of mouse on soluble adhesion molecules

Serum sVCAM-1 (A) and sICAM-1 (B) concentrations in (■,□) apoE*3 Leiden mice (n=15) or their (●,○) non-transgenic littermates (n=15) consuming either the antioxidant-replete diet, HFC/HAO (■,●), or the antioxidant-deficient diet, HFC/LAO (□,○). Values shown are geometric means ± 95% confidence intervals. a = significant difference ($p<0.05$) between apoE*3 Leiden mice consuming HFC/HAO and HFC/LAO; b = significant difference ($p<0.05$) between apoE*3 Leiden mice and non-transgenic animals consuming HFC/HAO; c = significant difference between ($p<0.05$) apoE*3 Leiden and non-transgenic mice consuming HFC/LAO and d = significant difference ($p<0.05$) between non-transgenic animals consuming either HFC/HAO or HFC/LAO.

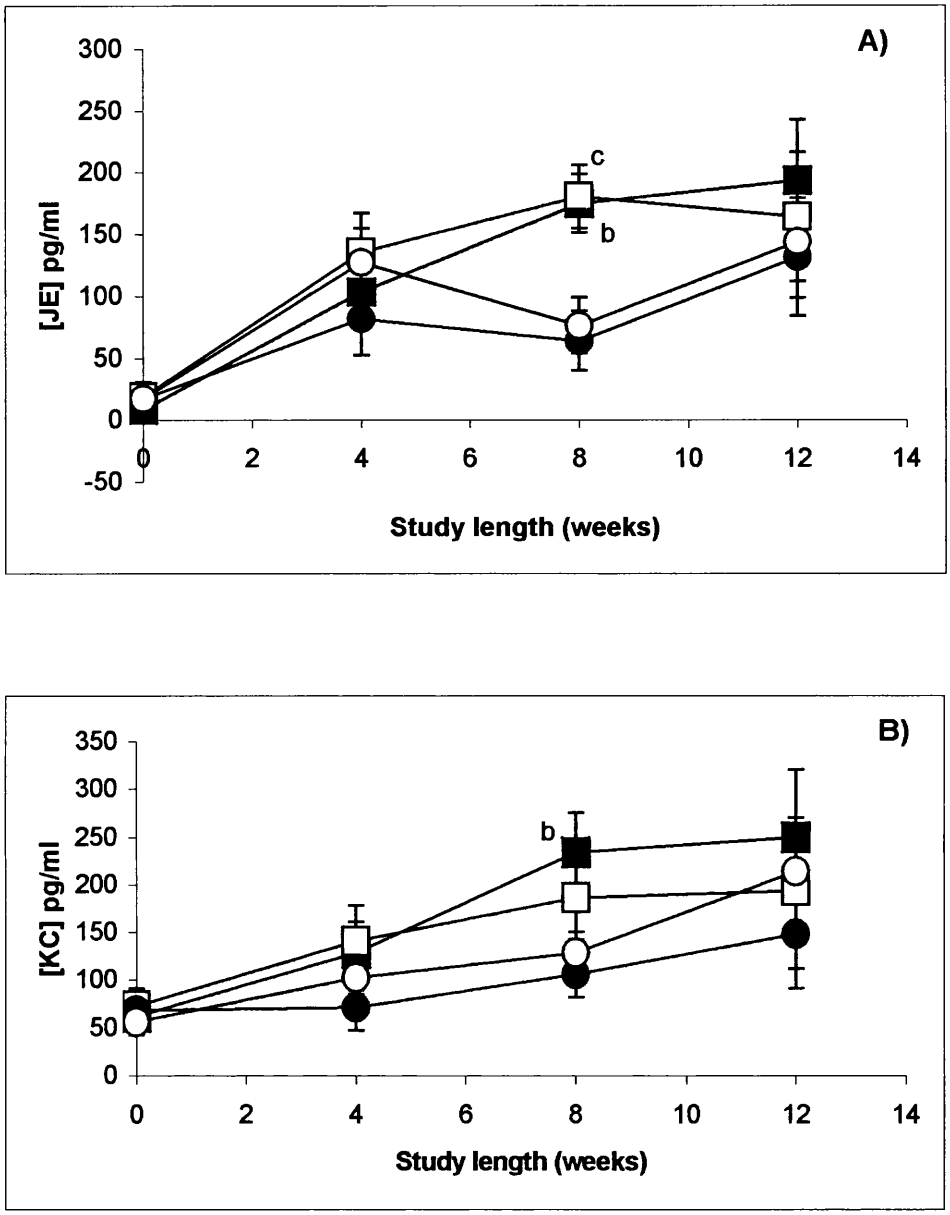

Figure 6-7 Effects of diet and strain of mouse on serum chemokines

Serum JE (A) and KC (B) concentrations in (■,□) apoE*3 Leiden mice (n=15) or their (■,□) non-transgenic littermates (n=15) consuming either the antioxidant-replete diet, HFC/HAO (■,●), or the antioxidant-deficient diet, HFC/LAO (□,○). Values shown are geometric means ± 95% confidence intervals. a = significant difference (p<0.05) between apoE*3 Leiden mice consuming HFC/HAO and HFC/LAO; b = significant difference (p<0.05) between apoE*3 Leiden mice and non-transgenic animals consuming HFC/HAO; c = significant difference between (p<0.05) apoE*3 Leiden and non-transgenic mice consuming HFC/LAO and d = significant difference (p<0.05) between non-transgenic animals consuming either HFC/HAO or HFC/LAO.

6.4 Discussion

In this study, we investigated circulating levels of chemokines (JE, KC) and soluble adhesion molecules (sVCAM-1, sICAM-1) as putative redox-sensitive 'markers' of inflammation and/or developing atheroma in apoE*3 Leiden mice, or their non-transgenic littermates, fed an atherogenic diet deficient in, or supplemented with, dietary antioxidants. The results indicate that although the absolute levels of these inflammatory markers did not differentiate the markedly different rates of atherogenesis in apoE*3 Leiden mice and their non-transgenic littermates, they provided evidence of the enhanced inflammatory status of animals consuming the HFC/C atherogenic diet. Serum chemokine levels tended to increase more rapidly in apoE*3 Leiden mice, compared with non-transgenic animals, but their levels were not obviously affected by the presence or absence of dietary antioxidants. By contrast, the highest levels of soluble adhesion molecules were observed in non-transgenic animals, and were clearly sensitive to consumption of dietary antioxidants during the early stages of this study.

Available evidence in transgenic murine models of atherosclerosis generally supports a role for oxidative stress in their disease aetiology. Oxidation-specific epitopes have been identified within macrophage-rich regions of atherosclerotic lesion in both apoE$^{-/-}$ [101] and apoE*3 Leiden [80] mice. ApoE$^{-/-}$ [101] and LDLR$^{-/-}$ [375] mice exhibit high serum titres of autoantibodies to malondialdehyde (MDA)-modified lysine, and immunisation with MDA-modified LDL reduced the progression of atherosclerosis in both models [376,377]. Indeed, circulating autoantibodies to oxidised LDL correlate with arterial accumulation and depletion of oxidised LDL in LDLR$^{-/-}$ mice [378]. Vitamin E deficiency, induced by disruption of the α-tocopherol transfer protein gene, increased the generation of isoprostanes and the severity of atherosclerotic lesions in the proximal aortae of apoE$^{-/-}$ mice [379]. Dietary antioxidants, vitamin E, vitamin C and β-carotene, have been reported to reduce both circulating autoantibodies [378,380], aortic and plasma isoprostane levels [243,380], and lesion formation [243,253,378,380] in apoE$^{-/-}$ [243,380] and LDLR$^{-/-}$ [253,378] mice. However, other studies using apoE$^{-/-}$ mice fed a normal RM1 diet supplemented with a combination of dietary β-carotene and α-tocopherol failed to demonstrate inhibition of atherogenesis [381].

Under the conditions used here, apoE*3 Leiden mice develop gross hypercholesterolaemia and markedly accelerated atherogenesis, compared with their non-transgenic littermates [44]. The presence of dietary antioxidants, vitamin E, vitamin C and β-carotene, were associated with relatively modest shifts in serum cholesterol

and triglyceride levels in either apoE*3 Leiden mice or the non-transgenic controls (Figure 6-4). Consumption of these antioxidants signally failed to reduce atheroma development in apoE*3 Leiden mice, or their non-transgenic littermates, despite the very differing rates of atherogenesis observed in these groups of animals (Figure 6-5), and the fact that similar experimental diets, and concentrations of antioxidants, were employed as previous studies [253]. While the reasons for this are not clear, it is possible that distinct mechanism(s) of lipoprotein oxidation, or underlying cause atherosclerosis, may exist in differing murine models of atherogenesis. For example, circulating lipids from C57BL/6J mice are more resistant to oxidative stress than those isolated from apoE$^{-/-}$ mice [382]. Alternatively, paradoxical effects of antioxidants, like vitamin E, have been reported in various animal models. Under certain circumstances, α-tocopherol can promote lipid peroxidation [382] and exacerbate endothelial dysfunction [383]. Certainly, the results from this study imply that dietary antioxidants are not sufficiently potent to limit arterial oxidative stress, or that oxidative processes are not of primary importance in lesion development in apoE*3 Leiden mice and their non-transgenic littermates consuming a high fat/high cholesterol diet.

In our previous studies, we demonstrated that hypercholesterolaemic apoE*3 Leiden mice exhibit elevated serum concentrations of the mIL-8RH ligands, KC and MIP-2 (Chapter 3) [61]. In particular, serum concentrations of KC were significantly higher in apoE*3 Leiden mice fed the atherogenic diet, compared with non-transgenic littermates consuming the same diet, and were associated with early lesion development in the former (Chapter 3 and Chapter 4) [61]. In this study, we used a modified form of the same diet deficient in, or supplemented with, dietary antioxidants. Levels of circulating chemokines, JE and KC, tended to increase more rapidly in apoE*3 Leiden mice compared with the non-transgenic animals (Figure 6-7), although approximately equivalent levels were reached in all groups of mice by the end of the study. Serum concentrations of JE and KC (Figure 6-7) were not reduced by the consumption of antioxidants by either apoE*3 Leiden mice, or their non-transgenic controls. Absolute concentrations of serum chemokines were clearly not predictive of lesion size under these conditions, probably because their levels reflect inflammatory responses in a number of differing cells and/or tissues including the liver. Indeed, we have found that chemokine expression in the liver is significantly elevated in mice consuming the HFC/C diet (Section 4.3.8.2 and Section 5.3.1). Expression of JE [165] and KC [172,177] within macrophage-rich regions of developing atherosclerotic lesions may indeed contribute to circulating chemokine levels.

However, elevated serum cholesterol levels may be sufficient to elicit leukocyte activation and increase chemokine expression [339]. Recent studies have shown that plasma concentrations of IL-8 correlate directly with IL-8 expression by blood mononuclear cells [340] and that monocytes isolated from hypercholesterolaemic patients exhibit enhanced IL-8 expression [339]. Further, atherosclerosis-susceptible C57BL/6J mice fed a diet high in fat and cholesterol develop oxidative stress, inflammation and lipid accumulation in both aortic and hepatic tissues [110,111]. Thus, the elevated and sustained serum chemokine levels seen in apoE*3 Leiden mice, and their non-transgenic littermates, seem to reflect a chronic inflammatory response in these animals. However, serum concentrations of JE and KC (Figure 6-7) were not reduced by the consumption of antioxidants by apoE*3 Leiden or non-transgenic mice. Again, this suggests that the inflammatory response is either not triggered by oxidative stress, or that dietary antioxidants lack the necessary potency to limit the enhanced expression of JE and KC chemokines.

Hyperlipidaemia [293,302] and existing cardiovascular disease [298,300,301,356,384-387] are associated with circulating levels of sVCAM-1 and/or sICAM-1. Equally, reductions in plasma triglyceride and cholesterol concentrations achieved either by lipid lowering therapy [293] or, more drastic, by LDL apheresis [302] are associated with decreases in circulating concentrations of sVCAM-1 and sICAM-1. As with circulating chemokines, a number of tissues could potentially contribute to serum levels of soluble adhesion molecules [128,388,389]. Interestingly, initial circulating concentrations of sICAM-1 were significantly higher in apoE*3 Leiden mice compared with their C57BL littermates (Figure 6-6 B). This was also noted in our previous investigation (Section 4.3.9). The same was not true of sVCAM-1. This finding suggests that sICAM-1 levels may be particularly sensitive to mild perturbations in lipid levels in apoE*3 Leiden mice fed a 'normal' chow diet (Figure 6-4 A + B). It was also apparent that circulating levels of sICAM-1 were much higher at baseline than levels of sVCAM-1, and did not increase to the same extent. These differences may reflect the highly inducible nature of VCAM-1 expression during inflammation, compared with the constitutive expression of ICAM-1 seen under normal conditions [388]. As observed in the last investigation, circulating levels of sICAM-1 in murine serum were substantially higher than levels found in human serum [298,356,384,385].

However, the gross hypercholesterolaemia and accelerated atherogenesis evident in apoE*3 Leiden mice did not result in higher serum levels of soluble adhesion molecules, compared with non-transgenic controls (Figure 6-6). Instead, the presence

or absence of dietary antioxidants appeared to be the major factor modulating serum levels of sVCAM-1 and sICAM-1, particularly in the non-transgenic animals. Current dogma suggests that activation of the NF-kB system of transcription factors results in a co-ordinated up-regulation of adhesion molecules and chemokines [366-368]. Our results show that levels of soluble adhesion molecules were particularly redox-sensitive, compared with serum chemokine concentrations, during the initial responses to consumption of an atherogenic diet by these animals (Figure 6-6). However, hypercholesterolaemic apoE*3 Leiden mice appeared less sensitive to dietary antioxidants than the non-transgenic controls. Combinations of dietary antioxidants have proved similarly ineffective at lowering serum concentrations of sVCAM-1 in hypercholesterolaemic smokers [390]. Production of sVCAM-1 was not sustained at high levels beyond week 8 of this study (Figure 6-6). This may suggest that at least this component of the leukocyte recruitment pathway can be down regulated in response to chronic inflammation. Alternatively, however, it is possible that either changes in the proteolytic generation of soluble adhesion molecules [128,388,389], or their clearance from the circulation, may explain the observed decrease in sICAM-1 and sVCAM-1 levels in the serum.

In summary, circulating levels of inflammatory markers associated with monocyte recruitment to the arterial wall, namely, JE, KC, VCAM-1 and ICAM-1, exhibit differential sensitivities to dietary antioxidants in apoE*3 Leiden and C57BL mice fed a diet high in fat and cholesterol. The development of atheroma in both groups of animals was unaffected by the presence of absence of vitamin E, vitamin C and β-carotene. Measurement of systemic serum chemokines and soluble adhesion molecules could provide a means of monitoring the expression of these components of the inflammatory response *in vivo* and, in particular, a way of assessing the efficacy of dietary or pharmacological interventions

Chapter 7

General discussion and future work

7 General discussion and future work

Heart disease is the biggest killer in the UK and the USA. Unfortunately, the disease remains largely silent until clinical symptoms ensue. It is therefore important to find a serum marker with real predictive value. Thus, the aim of this studentship was to identify potential serum markers, which might reflect pathological events occurring at the vessel wall during the development of the disease. As atherosclerotic lesions are characterised by a predominantly monocyte/macrophage infiltrate, we hypothesized that molecules involved in monocyte recruitment, present within the circulation, might provide a means of 'tracking' pathogenic events within the vessel wall. To test this hypothesis, the apoE*3 Leiden mouse model of atherosclerosis and their non-transgenic littermates (C57BL) were fed an atherogenic diet, high in fat and cholesterol and containing sodium cholate. It was hoped that the use of these two strains of mice would allow us to test whether putative 'markers' of disease progression and/or inflammation could discriminate between groups of animal experiencing an identical dietary regime, but possessing differing rates of atherogenesis. Specifically, the temporal relationships between circulating chemokines, adhesion molecules and the development of atheroma were examined. Also, more general systemic 'markers' of inflammation were measured to test their association with developing atheroma. Finally, the ability of antioxidant vitamins to modulate circulating levels of chemokines and soluble adhesion molecules, and the development of atheroma in apoE*3 Leiden mice and their non-transgenic controls was investigated.

We conclude that circulating levels of chemokines may prove to be useful, albeit non-specific, markers in chronic inflammatory diseases, including atherosclerosis. We proposed that serum concentrations of these molecules will reflect their output from one, or more, sites of inflammation, assuming that clearance of these molecules from the circulation remains a constant factor. In agreement with previous reports [110,111], the consumption of an atherogenic diet appears to trigger hepatic inflammation, indicating that the liver may be an important source of the observed increases in systemic CC and CXC chemokine levels. Indeed, analysis by quantitative PCR and *in-situ* hybridisation suggests that the liver may be an important site of production of serum KC and JE. Although, temporal variations in circulating levels of sICAM-1, PON1 and SAA were observed, no obvious association with onset of atheroma emerged. However, systemic levels of serum haptoglobin were acutely sensitive to the inflammatory effects of an atherogenic diet, and appeared to be associated with the accelerated atheroma seen in apoE*3 Leiden mice. Elevated systemic KC levels appeared to coincide with early onset of atherogenesis, and aortic expression of KC

was detected by RT-PCR, if not by *in situ* hybridisation. In experimental models, such as apoE$^{-/-}$ mice, that do not rely upon the consumption of an atherogenic diet for lesion development or, more importantly, in man, the developing atherosclerotic lesion may prove to be the primary site of inflammation. In such cases, systemic chemokine concentrations may prove to be useful predictors of atherosclerotic lesion development, although further work is needed to substantiate this hypothesis. Indeed, the work contained in this thesis has now formed the basis of a new PhD studentship (BBSRC/GlaxoSmithKline). This project will examine the temporal relationship between circulating CXC and CC chemokines during the development of atheroma in apoE$^{-/-}$ mice on either a C57BL or C3H genetic background. As apoE$^{-/-}$ mice develop lesions spontaneously on a normal chow diet, this will eliminate the need for an atherogenic diet and the subsequent liver inflammation associated with it. Under these conditions, the developing atherosclerotic plaque should be the primary site of inflammation. Despite posessing a more atherogenic serum lipid profile, C3H mice are resistant to the development of diet-induced atheroma, compared with C57BL mice. The use of apoE$^{-/-}$ mice on these two genetic backgrounds should enable the determination of whether elevated levels of systemic chemokines are associated with dyslipidaemia or the development of atheroma.

Circulating levels of chemokines and adhesion molecules exhibited differential sensitivities to dietary antioxidants in apoE*3 Leiden and C57BL mice fed a diet high in fat and cholesterol. It was found that the development of atheroma and systemic KC and JE levels in both groups of animals was unaffected by the presence, or absence, of vitamin E, vitamin C and β-carotene. However, systemic adhesion molecule concentrations were clearly sensitive to the presence of dietary antioxidants, with particularly high levels of sVCAM-1 and sICAM-1 noted in the non-transgenic mice consuming the antioxidant-deficient (HFC/LAO) diet during the early stages of the 12 week study. It would have been interesting to test this hypothesis using the apoE$^{-/-}$ model fed a chow diet deficient in, or supplemented with, these antioxidant vitamins. Perhaps then clear differences would be observed in systemic chemokine concentration and possibly atheroma development. These differences may be masked in apoE*3 Leiden mice due to the extreme serum cholesterol concentrations caused by consumption of the HFC/C diet. Alternatively, the atherogenic diet could be triggering changes that are not antioxidant sensitive.

Current literature on circulating chemokines and adhesion molecules lack sufficient discussion concerning their origin and consequently, we can only hypothesise on

potential sources of these molecules. Almost all cells exhibit the potential to produce substantial amounts of chemokines in response to a broad spectrum of stimuli (Figure 1-5) [155,156], for example, IL-8 is produced by macrophages, neutrophils, fibroblasts, smooth muscle, endothelial and epithelial cells [155,156]. Murine KC and MIP-2 have been identified in the lung, spleen, kidney, heart, thymus and brain [351,391]. Similary, MCP-1 and its murine homologue JE are produced by variety of cell types and associated with numerous inflammatory infiltrates [155,156]. Thus it is likely that circulating chemokines as well as adhesion molecules [128,388,389] have multiple points of synthesis from which they can appear in the circulation. Recently, studies have shown that plasma concentrations of IL-8 correlates directly with IL-8 expression by blood mononuclear cells [340] and that monocytes isolated from hypercholesterolaemic patients exhibit enhanced IL-8 expression [339]. This suggests that activated blood leukocytes may be an important contributing source of serum chemokines.

In addition, it would have been interesting to quantify chemokine mRNA expression in leukocytes isolated from mice in our studies. By measuring chemokine mRNA expression in circulating leukocytes we could have determined whether systemic chemokine concentrations reflected leukocyte expression. Preliminary data using TaqMan PCR showed that both KC and JE transcripts were detectable in blood leukocytes isolated from mice fed an atherogenic diet (data not shown). Unfortunately, there was no time to follow up this observation with an additional study. Finally, as *in-situ* hybridisation is not as sensitive a technique as TaqMan PCR, it would have been wise to complement the *in-situ* hybridisation data with the analysis of tissue transcript level by quantitative PCR.

In summary, it is clear that the systemic markers investigated in this thesis were not specific to atheroma and did not provide greater predictive value than measurement of more established 'risk factors' such as serum cholesterol, in terms of lesion progression. Therefore, multiple inflammatory sites may be involved, induced by the atherogenic diet, development of gross hyperlipidaemia, or the lesion itself. Indeed, the atherogenic diet used in our studies, may have considerably masked any subtle differences in systemic chemokine and adhesion molecule concentrations. The use of apoE$^{-/-}$ mice in future studies should eliminate the need for an atherogenic diet, and the subsequent hepatic inflammation associated with it. Under these conditions the developing atherosclerotic lesion should be the primary site of inflammation and thus a more accurate assessment of these molecules, as markers of atheromas will be made.

Bibliography

8 Bibliography

1. Lusis AJ. Atherosclerosis. *Nature* 2000;407:233-241.

2. Wood D, De Backer G, Faergeman O, Graham I, Mancia G, Pyorala K. Prevention of coronary heart disease in clinical practice: recommendations of the Second Joint Task Force of European and other Societies on Coronary Prevention. *Atherosclerosis* 1998;140:199-270.

3. Nishina PM, Verstuyft J, Paigen B. Synthetic low and high fat diets for the study of atherosclerosis in the mouse. *J Lipid Res* 1990;31:859-869.

4. Nishina PM, Lowe S, Verstuyft J, Naggert JK, Kuypers FA, Paigen B. Effects of dietary fats from animal and plant sources on diet-induced fatty streak lesions in C57BL/6J mice. *J Lipid Res* 1993;34:1413-1422.

5. Zhang SH, Reddick RL, Burkey B, Maeda N. Diet-induced atherosclerosis in mice heterozygous and homozygous for apolipoprotein E gene disruption. *J Clin Invest* 1994;94:937-945.

6. van Vlijmen BJ, van den Maagdenberg AM, Gijbels MJ, van der BH, HogenEsch H, Frants RR, Hofker MH, Havekes LM. Diet-induced hyperlipoproteinemia and atherosclerosis in apolipoprotein E3-Leiden transgenic mice. *J Clin Invest* 1994;93:1403-1410.

7. Oxidative stress, lipoproteins and cardiovascular dysfunction. C.Rice Evans and K.R.Bruckdorfer. 1995. Portland Press Research Monograph.

8. Keys A. Coronary heart disease in seven countries. *Circulation* 1970;41:1-211.

9. Gordon T, Castelli WP, Hjortland MC, Kannel WB, Dawber TR. High density lipoprotein as a protective factor against coronary heart disease. The Framingham Study. *Am J Med* 1977;62:707-714.

10. Cohn JS. Postprandial lipemia: emerging evidence for atherogenicity of remnant lipoproteins. *Can J Cardiol* 1998;14 Suppl B:18B-27B.

11. Beisiegel U. Lipoprotein metabolism. *Eur Heart J* 1998;19 Suppl A:A20-A23.

12. Havel RJ. Remnant lipoproteins as therapeutic targets. *Curr Opin Lipidol* 2000;11:615-620.

13. Mangiapane EH, Salter AM. Diet, Lipoproteins and Coronary Heart Disease. Nottingham University Press; 1999.

14. Dietschy JM, Turley SD, Spady DK. Role of liver in the maintenance of cholesterol and low density lipoprotein homeostasis in different animal species, including humans. *J Lipid Res* 1993;34:1637-1659.

15. Ross R. Atherosclerosis--an inflammatory disease. *N Engl J Med* 1999;340:115-126.

16. Berliner JA, Heinecke JW. The role of oxidized lipoproteins in atherogenesis. *Free Radic Biol Med* 1996;20:707-727.

17. Andalibi A, Liao F, Imes S, Fogelman AM, Lusis AJ. Oxidized lipoproteins influence gene expression by causing oxidative stress and activating the transcription factor NF-kappa B. *Biochem Soc Trans* 1993;21 (Pt 3):651-655.

18. Kita T, Kume N, Ishii K, Horiuchi H, Arai H, Yokode M. Oxidized LDL and expression of monocyte adhesion molecules. *Diabetes Res Clin Pract* 1999;45:123-126.

19. Steinberg D. Lewis A. Conner Memorial Lecture. Oxidative modification of LDL and atherogenesis. *Circulation* 1997;95:1062-1071.

20. Liao F, Berliner JA, Mehrabian M, Navab M, Demer LL, Lusis AJ, Fogelman AM. Minimally modified low density lipoprotein is biologically active in vivo in mice [published erratum appears in J Clin Invest 1991 Aug;88(2):721]. *J Clin Invest* 1991;87:2253-2257.

21. Griffin BA, Caslake MJ, Yip B, Tait GW, Packard CJ, Shepherd J. Rapid isolation of low density lipoprotein (LDL) subfractions from plasma by density gradient ultracentrifugation. *Atherosclerosis* 1990;83:59-67.

22. Gardner CD, Fortmann SP, Krauss RM. Association of small low-density lipoprotein particles with the incidence of coronary artery disease in men and women. *JAMA* 1996;276:875-881.

23. Friedlander Y, Kidron M, Caslake M, Lamb T, McConnell M, Bar-On H. Low density lipoprotein particle size and risk factors of insulin resistance syndrome. *Atherosclerosis* 2000;148:141-149.

24. Williams KJ, Tabas I. The response-to-retention hypothesis of early atherogenesis. *Arterioscler Thromb Vasc Biol* 1995;15:551-561.

25. Williams KJ, Tabas I. The response-to-retention hypothesis of atherogenesis reinforced. *Curr Opin Lipidol* 1998;9:471-474.

26. Boren J, Gustafsson M, Skalen K, Flood C, Innerarity TL. Role of extracellular retention of low density lipoproteins in atherosclerosis. *Curr Opin Lipidol* 2000;11:451-456.

27. Hurt-Camejo E, Camejo G, Sartipy P. Phospholipase A2 and small, dense low-density lipoprotein. *Curr Opin Lipidol* 2000;11:465-471.

28. de Graaf J, Hak-Lemmers HL, Hectors MP, Demacker PN, Hendriks JC, Stalenhoef AF. Enhanced susceptibility to in vitro oxidation of the dense low density lipoprotein subfraction in healthy subjects. *Arterioscler Thromb* 1991;11:298-306.

29. Smith EB, Cochran S. Factors influencing the accumulation in fibrous plaques of lipid derived from low density lipoprotein. II. Preferential immobilization of lipoprotein (a) (Lp(a)). *Atherosclerosis* 1990;84:173-181.

30. O'Brien KD, Reichenbach DD, Marcovina SM, Kuusisto J, Alpers CE, Otto CM. Apolipoproteins B, (a), and E accumulate in the morphologically early lesion of 'degenerative' valvular aortic stenosis. *Arterioscler Thromb Vasc Biol* 1996;16:523-532.

31. Dahlen GH, Guyton JR, Attar M, Farmer JA, Kautz JA, Gotto AM. Association of levels of lipoprotein Lp(a), plasma lipids, and other lipoproteins with coronary artery disease documented by angiography. *Circulation* 1986;74:758-765.

32. Milionis HJ, Winder AF, Mikhailidis DP. Lipoprotein (a) and stroke. *J Clin Pathol* 2000;53:487-496.

33. Nielsen LB. Atherogenecity of lipoprotein(a) and oxidized low density lipoprotein: insight from in vivo studies of arterial wall influx, degradation and efflux. *Atherosclerosis* 1999;143:229-243.

34. Callow MJ, Verstuyft J, Tangirala R, Palinski W, Rubin EM. Atherogenesis in transgenic mice with human apolipoprotein B and lipoprotein (a). *J Clin Invest* 1995;96:1639-1646.

35. Gordon DJ, Probstfield JL, Garrison RJ, Neaton JD, Castelli WP, Knoke JD, Jacobs DR, Jr., Bangdiwala S, Tyroler HA. High-density lipoprotein cholesterol and cardiovascular disease. Four prospective American studies. *Circulation* 1989;79:8-15.

36. Gordon DJ, Rifkind BM. High-density lipoprotein--the clinical implications of recent studies. *N Engl J Med* 1989;321:1311-1316.

37. Rubin EM, Krauss RM, Spangler EA, Verstuyft JG, Clift SM. Inhibition of early atherogenesis in transgenic mice by human apolipoprotein AI. *Nature* 1991;353:265-267.

38. Plump AS, Scott CJ, Breslow JL. Human apolipoprotein A-I gene expression increases high density lipoprotein and suppresses atherosclerosis in the apolipoprotein E- deficient mouse. *Proc Natl Acad Sci U S A* 1994;91:9607-9611.

39. Liu AC, Lawn RM, Verstuyft JG, Rubin EM. Human apolipoprotein A-I prevents atherosclerosis associated with apolipoprotein[a] in transgenic mice. *J Lipid Res* 1994;35:2263-2267.

40. Mackness MI, Durrington PN. HDL, its enzymes and its potential to influence lipid peroxidation. *Atherosclerosis* 1995;115:243-253.

41. Graham A, Hassall DG, Rafique S, Owen JS. Evidence for a paraoxonase-independent inhibition of low-density lipoprotein oxidation by high-density lipoprotein. *Atherosclerosis* 1997;135:193-204.

42. Cohn JS, Marcoux C, Davignon J. Detection, quantification, and characterization of potentially atherogenic triglyceride-rich remnant lipoproteins. *Arterioscler Thromb Vasc Biol* 1999;19:2474-2486.

43. Smith JD, Breslow JL. The emergence of mouse models of atherosclerosis and their relevance to clinical research. *J Intern Med* 1997;242:99-109.

44. Groot PH, van Vlijmen BJ, Benson GM, Hofker MH, Schiffelers R, Vidgeon-Hart M, Havekes LM. Quantitative assessment of aortic atherosclerosis in APOE*3 Leiden transgenic mice and its relationship to serum cholesterol exposure. *Arterioscler Thromb Vasc Biol* 1996;16:926-933.

45. Nordestgaard BG, Nielsen LB. Atherosclerosis and arterial influx of lipoproteins. *Curr Opin Lipidol* 1994;5:252-257.

46. Ji ZS, Brecht WJ, Miranda RD, Hussain MM, Innerarity TL, Mahley RW. Role of heparan sulfate proteoglycans in the binding and uptake of apolipoprotein E-enriched remnant lipoproteins by cultured cells. *J Biol Chem* 1993;268:10160-10167.

47. Evans AJ, Sawyez CG, Wolfe BM, Connelly PW, Maguire GF, Huff MW. Evidence that cholesteryl ester and triglyceride accumulation in J774 macrophages induced by very low density lipoprotein subfractions occurs by different mechanisms. *J Lipid Res* 1993;34:703-717.

48. Havel RJ. Postprandial hyperlipidemia and remnant lipoproteins. *Curr Opin Lipidol* 1994;5:102-109.

49. Willems VD, Hofker MH, Havekes LM. Dissection of the complex role of apolipoprotein e in lipoprotein metabolism and atherosclerosis using mouse models. *Curr Atheroscler Rep* 1999;1:101-107.

50. Siest G, Pillot T, Regis-Bailly A, Leininger-Muller B, Steinmetz J, Galteau MM, Visvikis S. Apolipoprotein E: an important gene and protein to follow in laboratory medicine. *Clin Chem* 1995;41:1068-1086.

51. van Bockxmeer FM, Mamotte CD, Gibbons FR, Taylor RR. Apolipoprotein epsilon 4 homozygosity–a determinant of restenosis after coronary angioplasty. *Atherosclerosis* 1994;110:195-202.

52. Weisgraber KH, Mahley RW. Human apolipoprotein E: the Alzheimer's disease connection. *FASEB J* 1996;10:1485-1494.

53. Gartner LP, Hiatt JL. Color textbook of histology. 2001.

54. Griendling KK, Alexander RW. Endothelial control of the cardiovascular system: recent advances. *FASEB J* 1996;10:283-292.

55. Ross R. The pathogenesis of atherosclerosis: a perspective for the 1990s. *Nature* 1993;362:801-809.

56. Li H, Cybulsky MI, Gimbrone MA, Jr., Libby P. An atherogenic diet rapidly induces VCAM-1, a cytokine-regulatable mononuclear leukocyte adhesion molecule, in rabbit aortic endothelium. *Arterioscler Thromb* 1993;13:197-204.

57. Doi H, Kugiyama K, Oka H, Sugiyama S, Ogata N, Koide SI, Nakamura SI, Yasue H. Remnant lipoproteins induce proatherothrombogenic molecules in endothelial cells through a redox-sensitive mechanism. *Circulation* 2000;102:670-676.

58. Schmidt AM, Hori O, Chen JX, Li JF, Crandall J, Zhang J, Cao R, Yan SD, Brett J, Stern D. Advanced glycation endproducts interacting with their endothelial receptor induce expression of vascular cell adhesion molecule-1 (VCAM- 1) in cultured human endothelial cells and in mice. A potential mechanism for the accelerated vasculopathy of diabetes. *J Clin Invest* 1995;96:1395-1403.

59. Vlassara H, Fuh H, Donnelly T, Cybulsky M. Advanced glycation endproducts promote adhesion molecule (VCAM-1, ICAM- 1) expression and atheroma formation in normal rabbits. *Mol Med* 1995;1:447-456.

60. Shen Y, Rattan V, Sultana C, Kalra VK. Cigarette smoke condensate-induced adhesion molecule expression and transendothelial migration of monocytes. *Am J Physiol* 1996;270:H1624-H1633.

61. Murphy N, Grimsditch DC, VidgeonHart M, Groot PHE, Benson GM, Graham A. Serum concentrations of CXC chemokines in APOE*3 Leiden mice: implications for atherogenesis. *Atherosclerosis* 1999;147:8.

62. Nordoy I, Muller F, Nordal KP, Rollag H, Aukrust P, Froland SS. Chemokines and soluble adhesion molecules in renal transplant recipients with cytomegalovirus infection. *Clin Exp Immunol* 2000;120:333-337.

63. Bossink AW, Paemen L, Jansen PM, Hack CE, Thijs LG, Van Damme J. Plasma levels of the chemokines monocyte chemotactic proteins-1 and -2 are elevated in human sepsis. *Blood* 1995;86:3841-3847.

64. Gerrity RG. The role of the monocyte in atherogenesis: I. Transition of blood-borne monocytes into foam cells in fatty lesions. *Am J Pathol* 1981;103:181-190.

65. Brown MS, Goldstein JL. Lipoprotein metabolism in the macrophage: implications for cholesterol deposition in atherosclerosis. *Annu Rev Biochem* 1983;52:223-261.

66. Gimbrone MA, Jr. Vascular endothelium, hemodynamic forces, and atherogenesis. *Am J Pathol* 1999;155:1-5.

67. Stary HC, Chandler AB, Dinsmore RE, Fuster V, Glagov S, Insull W, Jr., Rosenfeld ME, Schwartz CJ, Wagner WD, Wissler RW. A definition of advanced types of atherosclerotic lesions and a histological classification of atherosclerosis. A report from the Committee on Vascular Lesions of the Council on Arteriosclerosis, American Heart Association. *Circulation* 1995;92:1355-1374.

68. Breslow JL. Mouse models of atherosclerosis. *Science* 1996;272:685-688.

69. Qiao JH, Xie PZ, Fishbein MC, Kreuzer J, Drake TA, Demer LL, Lusis AJ. Pathology of atheromatous lesions in inbred and genetically engineered mice. Genetic determination of arterial calcification. *Arterioscler Thromb* 1994;14:1480-1497.

70. Bourdillon MC, Poston RN, Covacho C, Chignier E, Bricca G, McGregor JL. ICAM-1 deficiency reduces atherosclerotic lesions in double-knockout mice (ApoE(-/-)/ICAM-1(-/-)) fed a fat or a chow diet. *Arterioscler Thromb Vasc Biol* 2000;20:2630-2635.

71. Cybulsky MI, Iiyama K, Li H, Zhu S, Chen M, Iiyama M, Davis V, Gutierrez-Ramos JC, Connelly PW, Milstone DS. A major role for VCAM-1, but not ICAM-1, in early atherosclerosis. *J Clin Invest* 2001;107:1255-1262.

72. Cyrus T, Witztum JL, Rader DJ, Tangirala R, Fazio S, Linton MF, Funk CD. Disruption of the 12/15-lipoxygenase gene diminishes atherosclerosis in apo E-deficient mice [see comments]. *J Clin Invest* 1999;103:1597-1604.

73. Gosling J, Slaymaker S, Gu L, Tseng S, Zlot CH, Young SG, Rollins BJ, Charo IF. MCP-1 deficiency reduces susceptibility to atherosclerosis in mice that overexpress human apolipoprotein B. *J Clin Invest* 1999;103:773-778.

74. Boring L, Gosling J, Cleary M, Charo IF. Decreased lesion formation in CCR2-/- mice reveals a role for chemokines in the initiation of atherosclerosis. *Nature* 1998;394:894-897.

75. Gu L, Okada Y, Clinton SK, Gerard C, Sukhova GK, Libby P, Rollins BJ. Absence of monocyte chemoattractant protein-1 reduces atherosclerosis in low density lipoprotein receptor-deficient mice. *Mol Cell* 1998;2:275-281.

76. Breslow JL. Transgenic mouse models of lipoprotein metabolism and atherosclerosis. *Proc Natl Acad Sci U S A* 1993;90:8314-8318.

77. Higuchi K, Kitagawa K, Kogishi K, Takeda T. Developmental and age-related changes in apolipoprotein B mRNA editing in mice. *J Lipid Res* 1992;33:1753-1764.

78. Tangirala RK, Rubin EM, Palinski W. Quantitation of atherosclerosis in murine models: correlation between lesions in the aortic origin and in the entire aorta, and differences in the extent of lesions between sexes in LDL receptor-deficient and apolipoprotein E-deficient mice. *J Lipid Res* 1995;36:2320-2328.

79. Nakashima Y, Plump AS, Raines EW, Breslow JL, Ross R. ApoE-deficient mice develop lesions of all phases of atherosclerosis throughout the arterial tree. *Arterioscler Thromb* 1994;14:133-140.

80. Leppanen P, Luoma JS, Hofker MH, Havekes LM, Yla-Herttuala S. Characterization of atherosclerotic lesions in apo E3-leiden transgenic mice. *Atherosclerosis* 1998;136:147-152.

81. Calara F, Silvestre M, Casanada F, Yuan N, Napoli C, Palinski W. Spontaneous plaque rupture and secondary thrombosis in apolipoprotein E- deficient and LDL receptor-deficient mice. *J Pathol* 2001;195:257-263.

82. Johnson JL, Jackson CL. Atherosclerotic plaque rupture in the apolipoprotein E knockout mouse. *Atherosclerosis* 2001;154:399-406.

83. Rubin EM, Smith DJ. Atherosclerosis in mice: getting to the heart of a polygenic disorder. *Trends Genet* 1994;10:199-203.

84. Vesselinovitch D, Wissler RW. Experimental production of atherosclerosis in mice. 2. Effects of atherogenic and high-fat diets on vascular changes in chronically and acutely irradiated mice. *J Atheroscler Res* 1968;8:497-523.

85. Vesselinovitch D, Wissler RW, Doull J. Experimental production of atherosclerosis in mice. 1. Effect of various synthetic diets and radiation on survival time, food consumption and body weight in mice. *J Atheroscler Res* 1968;8:483-495.

86. Thompson JS. Atheromata in an inbred strain of mice. *J Atheroscler Res* 1969;10:113-122.

87. Paigen B, Morrow A, Brandon C, Mitchell D, Holmes P. Variation in susceptibility to atherosclerosis among inbred strains of mice. *Atherosclerosis* 1985;57:65-73.

88. Nishina PM, Wang J, Toyofuku W, Kuypers FA, Ishida BY, Paigen B. Atherosclerosis and plasma and liver lipids in nine inbred strains of mice. *Lipids* 1993;28:599-605.

89. Paigen B, Ishida BY, Verstuyft J, Winters RB, Albee D. Atherosclerosis susceptibility differences among progenitors of recombinant inbred strains of mice. *Arteriosclerosis* 1990;10:316-323.

90. Ishibashi S, Brown MS, Goldstein JL, Gerard RD, Hammer RE, Herz J. Hypercholesterolemia in low density lipoprotein receptor knockout mice and its reversal by adenovirus-mediated gene delivery. *J Clin Invest* 1993;92:883-893.

91. Dobmeyer J, Lohrmann J, Feussner G. Prevalence and association of atherosclerosis at three different arterial sites in patients with type III hyperlipoproteinemia. *Atherosclerosis* 1996;119:89-98.

92. Plump AS, Smith JD, Hayek T, Aalto-Setala K, Walsh A, Verstuyft JG, Rubin EM, Breslow JL. Severe hypercholesterolemia and atherosclerosis in apolipoprotein E- deficient mice created by homologous recombination in ES cells. *Cell* 1992;71:343-353.

93. Reddick RL, Zhang SH, Maeda N. Atherosclerosis in mice lacking apo E. Evaluation of lesional development and progression [published erratum appears in Arterioscler Thromb 1994 May;14(5):839]. *Arterioscler Thromb* 1994;14:141-147.

94. Zhang SH, Reddick RL, Piedrahita JA, Maeda N. Spontaneous hypercholesterolemia and arterial lesions in mice lacking apolipoprotein E. *Science* 1992;258:468-471.

95. Basu SK, Brown MS, Ho YK, Havel RJ, Goldstein JL. Mouse macrophages synthesize and secrete a protein resembling apolipoprotein E. *Proc Natl Acad Sci U S A* 1981;78:7545-7549.

96. Mazzone T. Apolipoprotein E secretion by macrophages: its potential physiological functions. *Curr Opin Lipidol* 1996;7:303-307.

97. Bellosta S, Mahley RW, Sanan DA, Murata J, Newland DL, Taylor JM, Pitas RE. Macrophage-specific expression of human apolipoprotein E reduces atherosclerosis in hypercholesterolemic apolipoprotein E-null mice. *J Clin Invest* 1995;96:2170-2179.

98. Shimano H, Ohsuga J, Shimada M, Namba Y, Gotoda T, Harada K, Katsuki M, Yazaki Y, Yamada N. Inhibition of diet-induced atheroma formation in transgenic mice expressing apolipoprotein E in the arterial wall. *J Clin Invest* 1995;95:469-476.

99. Fazio S, Babaev VR, Murray AB, Hasty AH, Carter KJ, Gleaves LA, Atkinson JB, Linton MF. Increased atherosclerosis in mice reconstituted with apolipoprotein E null macrophages. *Proc Natl Acad Sci U S A* 1997;94:4647-4652.

100. Hayek T, Oiknine J, Brook JG, Aviram M. Increased plasma and lipoprotein lipid peroxidation in apo E-deficient mice. *Biochem Biophys Res Commun* 1994;201:1567-1574.

101. Palinski W, Ord VA, Plump AS, Breslow JL, Steinberg D, Witztum JL. ApoE-deficient mice are a model of lipoprotein oxidation in atherogenesis. Demonstration of oxidation-specific epitopes in lesions and high titers of autoantibodies to malondialdehyde-lysine in serum. *Arterioscler Thromb* 1994;14:605-616.

102. van den Maagdenberg AM, de Knijff P, Stalenhoef AF, Gevers Leuven JA, Havekes LM, Frants RR. Apolipoprotein E*3-Leiden allele results from a partial gene duplication in exon 4. *Biochem Biophys Res Commun* 1989;165:851-857.

103. Havekes L, Schouten D, van H, V, de Wit E. Characterisation of the binding of apolipoprotein E-free high density lipoprotein to cultured human endothelial cells. *Biochem Biophys Res Commun* 1984;122:785-790.

104. Havekes L, de Wit E, Leuven JG, Klasen E, Utermann G, Weber W, Beisiegel U. Apolipoprotein E3-Leiden. A new variant of human apolipoprotein E associated with familial type III hyperlipoproteinemia. *Hum Genet* 1986;73:157-163.

105. de Knijff P, van den Maagdenberg AM, Stalenhoef AF, Leuven JA, Demacker PN, Kuyt LP, Frants RR, Havekes LM. Familial dysbetalipoproteinemia associated with apolipoprotein E3- Leiden in an extended multigeneration pedigree. *J Clin Invest* 1991;88:643-655.

106. van den Maagdenberg AM, Hofker MH, Krimpenfort PJ, de B, I, van Vlijmen B, van der BH, Havekes LM, Frants RR. Transgenic mice carrying the apolipoprotein E3-Leiden gene exhibit hyperlipoproteinemia. *J Biol Chem* 1993;268:10540-10545.

107. Gijbels MJ, van der CM, van der Laan LJ, Emeis JJ, Havekes LM, Hofker MH, Kraal G. Progression and regression of atherosclerosis in APOE3-Leiden transgenic mice: an immunohistochemical study. *Atherosclerosis* 1999;143:15-25.

108. van Vlijmen BJ, Pearce NJ, Bergo M, Staels B, Yates JW, Gribble AD, Bond BC, Hofker MH, Havekes LM, Groot PH. Apolipoprotein E*3-Leiden transgenic mice as a test model for hypolipidaemic drugs. *Arzneimittelforschung* 1998;48:396-402.

109. Rosenfeld ME, Butler S, Ord VA, Lipton BA, Dyer CA, Curtiss LK, Palinski W, Witztum JL. Abundant expression of apoprotein E by macrophages in human and rabbit atherosclerotic lesions. *Arterioscler Thromb* 1993;13:1382-1389.

110. Liao F, Andalibi A, deBeer FC, Fogelman AM, Lusis AJ. Genetic control of inflammatory gene induction and NF-kappa B-like transcription factor activation in response to an atherogenic diet in mice. *J Clin Invest* 1993;91:2572-2579.

111. Liao F, Andalibi A, Qiao JH, Allayee H, Fogelman AM, Lusis AJ. Genetic evidence for a common pathway mediating oxidative stress, inflammatory gene induction, and aortic fatty streak formation in mice. *J Clin Invest* 1994;94:877-884.

112. Nakashima Y, Raines EW, Plump AS, Breslow JL, Ross R. Upregulation of VCAM-1 and ICAM-1 at atherosclerosis-prone sites on the endothelium in the ApoE-deficient mouse. *Arterioscler Thromb Vasc Biol* 1998;18:842-851.

113. Sakai A, Kume N, Nishi E, Tanoue K, Miyasaka M, Kita T. P-selectin and vascular cell adhesion molecule-1 are focally expressed in aortas of hypercholesterolemic rabbits before intimal accumulation of macrophages and T lymphocytes. *Arterioscler Thromb Vasc Biol* 1997;17:310-316.

114. Truskey GA, Herrmann RA, Kait J, Barber KM. Focal increases in vascular cell adhesion molecule-1 and intimal macrophages at atherosclerosis-susceptible sites in the rabbit aorta after short-term cholesterol feeding. *Arterioscler Thromb Vasc Biol* 1999;19:393-401.

115. Scalia R, Appel JZ, III, Lefer AM. Leukocyte-endothelium interaction during the early stages of hypercholesterolemia in the rabbit: role of P-selectin, ICAM-1, and VCAM-1. *Arterioscler Thromb Vasc Biol* 1998;18:1093-1100.

116. Jonasson L, Holm J, Skalli O, Bondjers G, Hansson GK. Regional accumulations of T cells, macrophages, and smooth muscle cells in the human atherosclerotic plaque. *Arteriosclerosis* 1986;6:131-138.

117. Saunders J, Tarby CM. Opportunities for novel therapeutic agents acting at chemokine receptors. *Drug Discov Today* 1999;4:80-92.

118. Springer TA. Adhesion receptors of the immune system. *Nature* 1990;346:425-434.

119. Carlos TM, Harlan JM. Leukocyte-endothelial adhesion molecules. *Blood* 1994;84:2068-2101.

120. Frenette PS, Wagner DD. Adhesion molecules--Part 1. *N Engl J Med* 1996;334:1526-1529.

121. Thornhill MH, Wellicome SM, Mahiouz DL, Lanchbury JS, Kyan-Aung U, Haskard DO. Tumor necrosis factor combines with IL-4 or IFN-gamma to selectively enhance endothelial cell adhesiveness for T cells. The contribution of vascular cell adhesion molecule-1-dependent and -independent binding mechanisms. *J Immunol* 1991;146:592-598.

122. Dustin ML, Rothlein R, Bhan AK, Dinarello CA, Springer TA. Induction by IL 1 and interferon-gamma: tissue distribution, biochemistry, and function of a natural adherence molecule (ICAM-1). *J Immunol* 1986;137:245-254.

123. Cybulsky MI, Gimbrone MA, Jr. Endothelial expression of a mononuclear leukocyte adhesion molecule during atherogenesis. *Science* 1991;251:788-791.

124. O'Brien KD, Allen MD, McDonald TO, Chait A, Harlan JM, Fishbein D, McCarty J, Ferguson M, Hudkins K, Benjamin CD. Vascular cell adhesion molecule-1 is expressed in human coronary atherosclerotic plaques. Implications for the mode of progression of advanced coronary atherosclerosis [see comments]. *J Clin Invest* 1993;92:945-951.

125. Johnson-Tidey RR, McGregor JL, Taylor PR, Poston RN. Increase in the adhesion molecule P-selectin in endothelium overlying atherosclerotic plaques. Coexpression with intercellular adhesion molecule-1. *Am J Pathol* 1994;144:952-961.

126. Poston RN, Haskard DO, Coucher JR, Gall NP, Johnson-Tidey RR. Expression of intercellular adhesion molecule-1 in atherosclerotic plaques. *Am J Pathol* 1992;140:665-673.

127. van der Wal AC, Das PK, Tigges AJ, Becker AE. Adhesion molecules on the endothelium and mononuclear cells in human atherosclerotic lesions. *Am J Pathol* 1992;141:1427-1433.

128. Gearing AJ, Newman W. Circulating adhesion molecules in disease. *Immunol Today* 1993;14:506-512.

129. Tedder TF, Steeber DA, Chen A, Engel P. The selectins: vascular adhesion molecules. *FASEB J* 1995;9:866-873.

130. Imhof BA, Dunon D. Leukocyte migration and adhesion. *Adv Immunol* 1995;58:345-416.

131. Rainer TH. L-selectin in health and disease. *Resuscitation* 2002;52:127-141.

132. Cybulsky MI, Fries JW, Williams AJ, Sultan P, Davis VM, Gimbrone MA, Jr., Collins T. Alternative splicing of human VCAM-1 in activated vascular endothelium. *Am J Pathol* 1991;138:815-820.

133. Cybulsky MI, Fries JW, Williams AJ, Sultan P, Eddy R, Byers M, Shows T, Gimbrone MA, Jr., Collins T. Gene structure, chromosomal location, and basis for alternative mRNA splicing of the human VCAM1 gene. *Proc Natl Acad Sci U S A* 1991;88:7859-7863.

134. Hession C, Tizard R, Vassallo C, Schiffer SB, Goff D, Moy P, Chi-Rosso G, Luhowskyj S, Lobb R, Osborn L. Cloning of an alternate form of vascular cell adhesion molecule-1 (VCAM1). *J Biol Chem* 1991;266:6682-6685.

135. Vonderheide RH, Springer TA. Lymphocyte adhesion through very late antigen 4: evidence for a novel binding site in the alternatively spliced domain of vascular cell adhesion molecule 1 and an additional alpha 4 integrin counter-receptor on stimulated endothelium. *J Exp Med* 1992;175:1433-1442.

136. Kumar AG, Dai XY, Kozak CA, Mims MP, Gotto AM, Ballantyne CM. Murine VCAM-1. Molecular cloning, mapping, and analysis of a truncated form. *J Immunol* 1994;153:4088-4098.

137. Elices MJ, Osborn L, Takada Y, Crouse C, Luhowskyj S, Hemler ME, Lobb RR. VCAM-1 on activated endothelium interacts with the leukocyte integrin VLA-4 at a site distinct from the VLA-4/fibronectin binding site. *Cell* 1990;60:577-584.

138. Marlin SD, Springer TA. Purified intercellular adhesion molecule-1 (ICAM-1) is a ligand for lymphocyte function-associated antigen 1 (LFA-1). *Cell* 1987;51:813-819.

139. Diamond MS, Staunton DE, Marlin SD, Springer TA. Binding of the integrin Mac-1 (CD11b/CD18) to the third immunoglobulin- like domain of ICAM-1 (CD54) and its regulation by glycosylation. *Cell* 1991;65:961-971.

140. Wood KM, Cadogan MD, Ramshaw AL, Parums DV. The distribution of adhesion molecules in human atherosclerosis [see comments]. *Histopathology* 1993;22:437-444.

141. Iiyama K, Hajra L, Iiyama M, Li H, DiChiara M, Medoff BD, Cybulsky MI. Patterns of vascular cell adhesion molecule-1 and intercellular adhesion molecule-1 expression in rabbit and mouse atherosclerotic lesions and at sites predisposed to lesion formation. *Circ Res* 1999;85:199-207.

142. Zibara K, Chignier E, Covacho C, Poston R, Canard G, Hardy P, McGregor J. Modulation of expression of endothelial intercellular adhesion molecule- 1, platelet-endothelial cell

adhesion molecule-1, and vascular cell adhesion molecule-1 in aortic arch lesions of apolipoprotein E- deficient compared with wild-type mice [In Process Citation]. *Arterioscler Thromb Vasc Biol* 2000;20:2288-2296.

143. Iiyama K, Hajra L, Iiyama M, Li H, DiChiara M, Medoff BD, Cybulsky MI. Patterns of vascular cell adhesion molecule-1 and intercellular adhesion molecule-1 expression in rabbit and mouse atherosclerotic lesions and at sites predisposed to lesion formation. *Circ Res* 1999;85:199-207.

144. Gurtner GC, Davis V, Li H, McCoy MJ, Sharpe A, Cybulsky MI. Targeted disruption of the murine VCAM1 gene: essential role of VCAM-1 in chorioallantoic fusion and placentation. *Genes Dev* 1995;9:1-14.

145. Kwee L, Baldwin HS, Shen HM, Stewart CL, Buck C, Buck CA, Labow MA. Defective development of the embryonic and extraembryonic circulatory systems in vascular cell adhesion molecule (VCAM-1) deficient mice. *Development* 1995;121:489-503.

146. Yang JT, Rayburn H, Hynes RO. Cell adhesion events mediated by alpha 4 integrins are essential in placental and cardiac development. *Development* 1995;121:549-560.

147. Shih PT, Brennan ML, Vora DK, Territo MC, Strahl D, Elices MJ, Lusis AJ, Berliner JA. Blocking very late antigen-4 integrin decreases leukocyte entry and fatty streak formation in mice fed an atherogenic diet. *Circ Res* 1999;84:345-351.

148. Dansky HM, Barlow CB, Cybulsky MI, Smith JD. Decreased endothelial VCAM-1 expression reduces monocyte adherence and atherosclerosis in apolipoprotein E-deficient mice. *Circulation* 2000;102(Suppl):A13660 (Abstr).

149. Collins RG, Velji R, Guevara NV, Hicks MJ, Chan L, Beaudet AL. P-Selectin or intercellular adhesion molecule (ICAM)-1 deficiency substantially protects against atherosclerosis in apolipoprotein E- deficient mice. *J Exp Med* 2000;191:189-194.

150. O'Brien KD, McDonald TO, Chait A, Allen MD, Alpers CE. Neovascular expression of E-selectin, intercellular adhesion molecule- 1, and vascular cell adhesion molecule-1 in human atherosclerosis and their relation to intimal leukocyte content. *Circulation* 1996;93:672-682.

151. Li H, Cybulsky MI, Gimbrone MA, Jr., Libby P. Inducible expression of vascular cell adhesion molecule-1 by vascular smooth muscle cells in vitro and within rabbit atheroma. *Am J Pathol* 1993;143:1551-1559.

152. Libby P, Li H. Vascular cell adhesion molecule-1 and smooth muscle cell activation during atherogenesis [editorial; comment]. *J Clin Invest* 1993;92:538-539.

153. Baggiolini M. Chemokines and leukocyte traffic. *Nature* 1998;392:565-568.

154. Clore GM, Gronenborn AM. Three-dimensional structures of alpha and beta chemokines. *FASEB J* 1995;9:57-62.

155. Rollins BJ. Chemokines. *Blood* 1997;90:909-928.

156. Luster AD. Chemokines--chemotactic cytokines that mediate inflammation. *N Engl J Med* 1998;338:436-445.

157. Adams DH, Lloyd AR. Chemokines: leucocyte recruitment and activation cytokines. *Lancet* 1997;349:490-495.

158. Gong JH, Clark-Lewis I. Antagonists of monocyte chemoattractant protein 1 identified by modification of functionally critical NH2-terminal residues. *J Exp Med* 1995;181:631-640.

159. Weber M, Uguccioni M, Baggiolini M, Clark-Lewis I, Dahinden CA. Deletion of the NH2-terminal residue converts monocyte chemotactic protein 1 from an activator of basophil mediator release to an eosinophil chemoattractant. *J Exp Med* 1996;183:681-685.

160. Bacon KB. Chemokines and chemokine receptors: therapeutic targets in inflammation and infectious disease. Drug News & Perspectives 10[3], 133-143. 2001. Ref Type: Magazine Article

161. Murdoch C, Finn A. Chemokine receptors and their role in inflammation and infectious diseases. *Blood* 2000;95:3032-3043.

162. Furie MB, Randolph GJ. Chemokines and tissue injury. *Am J Pathol* 1995;146:1287-1301.

163. Reape TJ, Groot PH. Chemokines and atherosclerosis. *Atherosclerosis* 1999;147:213-225.

164. Keane MP, Strieter RM. Chemokine signaling in inflammation. *Crit Care Med* 2000;28:N13-N26.

165. Nelken NA, Coughlin SR, Gordon D, Wilcox JN. Monocyte chemoattractant protein-1 in human atheromatous plaques. *J Clin Invest* 1991;88:1121-1127.

166. Takeya M, Yoshimura T, Leonard EJ, Takahashi K. Detection of monocyte chemoattractant protein-1 in human atherosclerotic lesions by an anti-monocyte chemoattractant protein-1 monoclonal antibody. *Hum Pathol* 1993;24:534-539.

167. Yla-Herttuala S, Lipton BA, Rosenfeld ME, Sarkioja T, Yoshimura T, Leonard EJ, Witztum JL, Steinberg D. Expression of monocyte chemoattractant protein 1 in macrophage-rich

areas of human and rabbit atherosclerotic lesions. *Proc Natl Acad Sci U S A* 1991;88:5252-5256.

168. Yu X, Dluz S, Graves DT, Zhang L, Antoniades HN, Hollander W, Prusty S, Valente AJ, Schwartz CJ, Sonenshein GE. Elevated expression of monocyte chemoattractant protein 1 by vascular smooth muscle cells in hypercholesterolemic primates. *Proc Natl Acad Sci U S A* 1992;89:6953-6957.

169. Aiello RJ, Bourassa PA, Lindsey S, Weng W, Natoli E, Rollins BJ, Milos PM. Monocyte chemoattractant protein-1 accelerates atherosclerosis in apolipoprotein E-deficient mice. *Arterioscler Thromb Vasc Biol* 1999;19:1518-1525.

170. Boring L, Gosling J, Chensue SW, Kunkel SL, Farese RV, Broxmeyer HE, Charo IF. Impaired monocyte migration and reduced type 1 (Th1) cytokine responses in C-C chemokine receptor 2 knockout mice. *Journal of Clinical Investigation* 1997;100:2552-2561.

171. Dawson TC, Kuziel WA, Osahar TA, Maeda N. Absence of CC chemokine receptor-2 reduces atherosclerosis in apolipoprotein E-deficient mice. *Atherosclerosis* 1999;143:205-211.

172. Wang N, Tabas I, Winchester R, Ravalli S, Rabbani LE, Tall A. Interleukin 8 is induced by cholesterol loading of macrophages and expressed by macrophage foam cells in human atheroma. *J Biol Chem* 1996;271:8837-8842.

173. Claise C, Edeas M, Chalas J, Cockx A, Abella A, Capel L, Lindenbaum A. Oxidized low-density lipoprotein induces the production of interleukin- 8 by endothelial cells. *FEBS Lett* 1996;398:223-227.

174. Liu Y, Hulten LM, Wiklund O. Macrophages isolated from human atherosclerotic plaques produce IL-8, and oxysterols may have a regulatory function for IL-8 production. *Arterioscler Thromb Vasc Biol* 1997;17:317-323.

175. Hartner A, Goppelt-Struebe M, Hocke GM, Sterzel RB. Differential regulation of chemokines by leukemia inhibitory factor, interleukin-6 and oncostatin M. *Kidney Int* 1997;51:1754-1760.

176. Apostolopoulos J, Davenport P, Tipping PG. Interleukin-8 production by macrophages from atheromatous plaques. *Arterioscler Thromb Vasc Biol* 1996;16:1007-1012.

177. Boisvert WA, Santiago R, Curtiss LK, Terkeltaub RA. A leukocyte homologue of the IL-8 receptor CXCR-2 mediates the accumulation of macrophages in atherosclerotic lesions of LDL receptor- deficient mice. *J Clin Invest* 1998;101:353-363.

178. Simonet WS, Hughes TM, Nguyen HQ, Trebasky LD, Danilenko DM, Medlock ES. Long-term impaired neutrophil migration in mice overexpressing human interleukin-8. *J Clin Invest* 1994;94:1310-1319.

179. Van Zee KJ, Fischer E, Hawes AS, Hebert CA, Terrell TG, Baker JB, Lowry SF, Moldawer LL. Effects of intravenous IL-8 administration in nonhuman primates. *J Immunol* 1992;148:1746-1752.

180. Merhi Y, Guidoin R, Provost P, Leung TK, Lam JY. Increase of neutrophil adhesion and vasoconstriction with platelet deposition after deep arterial injury by angioplasty. *Am Heart J* 1995;129:445-451.

181. Neumann FJ, Ott I, Gawaz M, Puchner G, Schomig A. Neutrophil and platelet activation at balloon-injured coronary artery plaque in patients undergoing angioplasty. *J Am Coll Cardiol* 1996;27:819-824.

182. Steg PG, Pasquier C, Huu TP, Chollet-Martin S, Juliard JM, Himbert D, Pocidalo MA, Gourgon R, Hakim J. Evidence for priming and activation of neutrophils early after coronary angioplasty. *Eur J Med* 1993;2:6-10.

183. Welt FG, Edelman ER, Simon DI, Rogers C. Neutrophil, not macrophage, infiltration precedes neointimal thickening in balloon-injured arteries. *Arterioscler Thromb Vasc Biol* 2000;20:2553-2558.

184. Jorgensen L, Grothe AG, Groves HM, Kinlough-Rathbone RL, Richardson M, Mustard JF. Distribution of cellular responses in rabbit aortae following one and two injuries with a balloon catheter. *Br J Exp Pathol* 1988;69:351-365.

185. Richardson M, Hatton MW, Buchanan MR, Moore S. Wound healing in the media of the normolipemic rabbit carotid artery injured by air drying or by balloon catheter de-endothelialization. *Am J Pathol* 1990;137:1453-1465.

186. Abe Y, Kawakami M, Kuroki M, Yamamoto T, Fujii M, Kobayashi H, Yaginuma T, Kashii A, Saito M, Matsushima K. Transient rise in serum interleukin-8 concentration during acute myocardial infarction. *Br Heart J* 1993;70:132-134.

187. Tillmanns H, Neumann FJ, Tiefenbacher C, Dorigo O, Parekh N, Waas W, Zimmermann R, Steinhausen M, Kuebler W. Activation of neutrophils in the microvasculature of the ischaemic and reperfused myocardium. *Eur Heart J* 1993;14 Suppl I:82-86.

188. Strieter RM, Kunkel SL, Elner VM, Martonyi CL, Koch AE, Polverini PJ, Elner SG. Interleukin-8. A corneal factor that induces neovascularization. *Am J Pathol* 1992;141:1279-1284.

189. Koch AE, Polverini PJ, Kunkel SL, Harlow LA, DiPietro LA, Elner VM, Elner SG, Strieter RM. Interleukin-8 as a macrophage-derived mediator of angiogenesis [see comments]. *Science* 1992;258:1798-1801.

190. Boisvert WA, Curtiss LK, Terkeltaub RA. Interleukin-8 and its receptor CXCR2 in atherosclerosis. *Immunol Res* 2000;21:129-137.

191. Schwartz D, Andalibi A, Chaverri-Almada L, Berliner JA, Kirchgessner T, Fang ZT, Tekamp-Olson P, Lusis AJ, Gallegos C, Fogelman AM. Role of the GRO family of chemokines in monocyte adhesion to MM-LDL- stimulated endothelium. *J Clin Invest* 1994;94:1968-1973.

192. Gerszten RE, Garcia-Zepeda EA, Lim YC, Yoshida M, Ding HA, Gimbrone MA, Jr., Luster AD, Luscinskas FW, Rosenzweig A. MCP-1 and IL-8 trigger firm adhesion of monocytes to vascular endothelium under flow conditions. *Nature* 1999;398:718-723.

193. Lee J, Cacalano G, Camerato T, Toy K, Moore MW, Wood WI. Chemokine binding and activities mediated by the mouse IL-8 receptor. *J Immunol* 1995;155:2158-2164.

194. Hamilton TA, Major JA. Oxidized LDL potentiates LPS-induced transcription of the chemokine KC gene. *J Leukoc Biol* 1996;59:940-947.

195. Bozic CR, Kolakowski LF, Jr., Gerard NP, Garcia-Rodriguez C, Uexkull-Guldenband C, Conklyn MJ, Breslow R, Showell HJ, Gerard C. Expression and biologic characterization of the murine chemokine KC. *J Immunol* 1995;154:6048-6057.

196. Lentsch AB, Yoshidome H, Cheadle WG, Miller FN, Edwards MJ. Chemokine involvement in hepatic ischemia/reperfusion injury in mice: roles for macrophage inflammatory protein-2 and KC [corrected and republished article originally printed in Hepatology 1998 Feb;27(2): 507-12]. *Hepatology* 1998;27:1172-1177.

197. Lentsch AB, Yoshidome H, Cheadle WG, Miller FN, Edwards MJ. Chemokine involvement in hepatic ischemia/reperfusion injury in mice: roles for macrophage inflammatory protein-2 and Kupffer cells [published erratum appears in Hepatology 1998 Mar;27(3):889 and corrected and republished in Hepatology 1998 Apr;27(4):1172-7]. *Hepatology* 1998;27:507-512.

198. Thurberg BL, Collins T. The nuclear factor-kappa B/inhibitor of kappa B autoregulatory system and atherosclerosis. *Curr Opin Lipidol* 1998;9:387-396.

199. Gawaz M, Neumann FJ, Dickfeld T, Koch W, Laugwitz KL, Adelsberger H, Langenbrink K, Page S, Neumeier D, Schomig A, Brand K. Activated platelets induce monocyte

chemotactic protein-1 secretion and surface expression of intercellular adhesion molecule-1 on endothelial cells [see comments]. *Circulation* 1998;98:1164-1171.

200. Brand K, Page S, Rogler G, Bartsch A, Brandl R, Knuechel R, Page M, Kaltschmidt C, Baeuerle PA, Neumeier D. Activated transcription factor nuclear factor-kappa B is present in the atherosclerotic lesion. *J Clin Invest* 1996;97:1715-1722.

201. Witztum JL. The oxidation hypothesis of atherosclerosis. *Lancet* 1994;344:793-795.

202. Rajman I, Kendall M, Cramb R. The oxidation hypothesis of atherosclerosis. *Lancet* 1994;344:1363-1364.

203. Haberland ME, Fong D, Cheng L. Malondialdehyde-altered protein occurs in atheroma of Watanabe heritable hyperlipidemic rabbits. *Science* 1988;241:215-218.

204. Palinski W, Rosenfeld ME, Yla-Herttuala S, Gurtner GC, Socher SS, Butler SW, Parthasarathy S, Carew TE, Steinberg D, Witztum JL. Low density lipoprotein undergoes oxidative modification in vivo. *Proc Natl Acad Sci U S A* 1989;86:1372-1376.

205. Boyd HC, Gown AM, Wolfbauer G, Chait A. Direct evidence for a protein recognized by a monoclonal antibody against oxidatively modified LDL in atherosclerotic lesions from a Watanabe heritable hyperlipidemic rabbit. *Am J Pathol* 1989;135:815-825.

206. Yla-Herttuala S, Palinski W, Rosenfeld ME, Parthasarathy S, Carew TE, Butler S, Witztum JL, Steinberg D. Evidence for the presence of oxidatively modified low density lipoprotein in atherosclerotic lesions of rabbit and man. *J Clin Invest* 1989;84:1086-1095.

207. Salonen JT, Yla-Herttuala S, Yamamoto R, Butler S, Korpela H, Salonen R, Nyyssonen K, Palinski W, Witztum JL. Autoantibody against oxidised LDL and progression of carotid atherosclerosis. *Lancet* 1992;339:883-887.

208. Navab M, Berliner JA, Watson AD, Hama SY, Territo MC, Lusis AJ, Shih DM, Van Lenten BJ, Frank JS, Demer LL, Edwards PA, Fogelman AM. The Yin and Yang of oxidation in the development of the fatty streak. A review based on the 1994 George Lyman Duff Memorial Lecture. *Arterioscler Thromb Vasc Biol* 1996;16:831-842.

209. Berliner JA, Territo MC, Sevanian A, Ramin S, Kim JA, Bamshad B, Esterson M, Fogelman AM. Minimally modified low density lipoprotein stimulates monocyte endothelial interactions. *J Clin Invest* 1990;85:1260-1266.

210. Steinberg D, Parthasarathy S, Carew TE, Khoo JC, Witztum JL. Beyond cholesterol. Modifications of low-density lipoprotein that increase its atherogenicity. *N Engl J Med* 1989;320:915-924.

211. Makarov SS. NF-kappaB as a therapeutic target in chronic inflammation: recent advances. *Mol Med Today* 2000;6:441-448.

212. Navab M, Berliner JA, Subbanagounder G, Hama S, Lusis AJ, Castellani LW, Reddy S, Shih D, Shi W, Watson AD, Van Lenten BJ, Vora D, Fogelman AM. HDL and the inflammatory response induced by LDL-derived oxidized phospholipids. *Arterioscler Thromb Vasc Biol* 2001;21:481-488.

213. Brocheriou I, Stengel D, Mattsson-Hulten L, Stankova J, Rola-Pleszczynski M, Koskas F, Wiklund O, Le Charpentier Y, Ninio E. Expression of platelet-activating factor receptor in human carotid atherosclerotic plaques: relevance to progression of atherosclerosis. *Circulation* 2000;102:2569-2575.

214. Leitinger N, Tyner TR, Oslund L, Rizza C, Subbanagounder G, Lee H, Shih PT, Mackman N, Tigyi G, Territo MC, Berliner JA, Vora DK. Structurally similar oxidized phospholipids differentially regulate endothelial binding of monocytes and neutrophils. *Proc Natl Acad Sci U S A* 1999;96:12010-12015.

215. Subbanagounder G, Leitinger N, Schwenke DC, Wong JW, Lee H, Rizza C, Watson AD, Faull KF, Fogelman AM, Berliner JA. Determinants of bioactivity of oxidized phospholipids. Specific oxidized fatty acyl groups at the sn-2 position. *Arterioscler Thromb Vasc Biol* 2000;20:2248-2254.

216. Horkko S, Bird DA, Miller E, Itabe H, Leitinger N, Subbanagounder G, Berliner JA, Friedman P, Dennis EA, Curtiss LK, Palinski W, Witztum JL. Monoclonal autoantibodies specific for oxidized phospholipids or oxidized phospholipid-protein adducts inhibit macrophage uptake of oxidized low-density lipoproteins. *J Clin Invest* 1999;103:117-128.

217. Cyrus T, Witztum JL, Rader DJ, Tangirala R, Fazio S, Linton MF, Funk CD. Disruption of the 12/15-lipoxygenase gene diminishes atherosclerosis in apo E-deficient mice. *J Clin Invest* 1999;103:1597-1604.

218. Harats D, Shaish A, George J, Mulkins M, Kurihara H, Levkovitz H, Sigal E. Overexpression of 15-lipoxygenase in vascular endothelium accelerates early atherosclerosis in LDL receptor-deficient mice. *Arterioscler Thromb Vasc Biol* 2000;20:2100-2105.

219. Yla-Herttuala S, Rosenfeld ME, Parthasarathy S, Glass CK, Sigal E, Witztum JL, Steinberg D. Colocalization of 15-lipoxygenase mRNA and protein with epitopes of oxidized low density lipoprotein in macrophage-rich areas of atherosclerotic lesions. *Proc Natl Acad Sci U S A* 1990;87:6959-6963.

220. Heinecke JW. Mechanisms of oxidative damage of low density lipoprotein in human atherosclerosis. *Curr Opin Lipidol* 1997;8:268-274.

221. Beckmann JS, Ye YZ, Anderson PG, Chen J, Accavitti MA, Tarpey MM, White CR. Extensive nitration of protein tyrosines in human atherosclerosis detected by immunohistochemistry. *Biol Chem Hoppe Seyler* 1994;375:81-88.

222. Daugherty A, Dunn JL, Rateri DL, Heinecke JW. Myeloperoxidase, a catalyst for lipoprotein oxidation, is expressed in human atherosclerotic lesions. *J Clin Invest* 1994;94:437-444.

223. Hazell LJ, Arnold L, Flowers D, Waeg G, Malle E, Stocker R. Presence of hypochlorite-modified proteins in human atherosclerotic lesions. *J Clin Invest* 1996;97:1535-1544.

224. Zingg JM, Ricciarelli R, Azzi A. Scavenger receptors and modified lipoproteins: fatal attractions? *IUBMB Life* 2000;49:397-403.

225. Febbraio M, Podrez EA, Smith JD, Hajjar DP, Hazen SL, Hoff HF, Sharma K, Silverstein RL. Targeted disruption of the class B scavenger receptor CD36 protects against atherosclerotic lesion development in mice. *J Clin Invest* 2000;105:1049-1056.

226. Suzuki H, Kurihara Y, Takeya M, Kamada N, Kataoka M, Jishage K, Ueda O, Sakaguchi H, Higashi T, Suzuki T, Takashima Y, Kawabe Y, Cynshi O, Wada Y, Honda M, Kurihara H, Aburatani H, Doi T, Matsumoto A, Azuma S, Noda T, Toyoda Y, Itakura H, Yazaki Y, Kodama T, . A role for macrophage scavenger receptors in atherosclerosis and susceptibility to infection. *Nature* 1997;386:292-296.

227. De Winther MP, Gijbels MJ, Van Dijk KW, van Gorp PJ, Suzuki H, Kodama T, Frants RR, Havekes LM, Hofker MH. Scavenger receptor deficiency leads to more complex atherosclerotic lesions in APOE3Leiden transgenic mice. *Atherosclerosis* 1999;144:315-321.

228. Li D, Mehta JL. Upregulation of endothelial receptor for oxidized LDL (LOX-1) by oxidized LDL and implications in apoptosis of human coronary artery endothelial cells: evidence from use of antisense LOX-1 mRNA and chemical inhibitors. *Arterioscler Thromb Vasc Biol* 2000;20:1116-1122.

229. Sawamura T, Kume N, Aoyama T, Moriwaki H, Hoshikawa H, Aiba Y, Tanaka T, Miwa S, Katsura Y, Kita T, Masaki T. An endothelial receptor for oxidized low-density lipoprotein. *Nature* 1997;386:73-77.

230. Kume N, Murase T, Moriwaki H, Aoyama T, Sawamura T, Masaki T, Kita T. Inducible expression of lectin-like oxidized LDL receptor-1 in vascular endothelial cells. *Circ Res* 1998;83:322-327.

231. Murase T, Kume N, Korenaga R, Ando J, Sawamura T, Masaki T, Kita T. Fluid shear stress transcriptionally induces lectin-like oxidized LDL receptor-1 in vascular endothelial cells. *Circ Res* 1998;83:328-333.

232. Nagase M, Hirose S, Sawamura T, Masaki T, Fujita T. Enhanced expression of endothelial oxidized low-density lipoprotein receptor (LOX-1) in hypertensive rats. *Biochem Biophys Res Commun* 1997;237:496-498.

233. Chen M, Nagase M, Fujita T, Narumiya S, Masaki T, Sawamura T. Diabetes enhances lectin-like oxidized LDL receptor-1 (LOX-1) expression in the vascular endothelium: possible role of LOX-1 ligand and AGE. *Biochem Biophys Res Commun* 2001;287:962-968.

234. Chen M, Kakutani M, Minami M, Kataoka H, Kume N, Narumiya S, Kita T, Masaki T, Sawamura T. Increased expression of lectin-like oxidized low density lipoprotein receptor-1 in initial atherosclerotic lesions of Watanabe heritable hyperlipidemic rabbits. *Arterioscler Thromb Vasc Biol* 2000;20:1107-1115.

235. Kataoka H, Kume N, Miyamoto S, Minami M, Moriwaki H, Murase T, Sawamura T, Masaki T, Hashimoto N, Kita T. Expression of lectinlike oxidized low-density lipoprotein receptor-1 in human atherosclerotic lesions. *Circulation* 1999;99:3110-3117.

236. Mehta JL, Li D. Identification, regulation and function of a novel lectin-like oxidized low-density lipoprotein receptor. *J Am Coll Cardiol* 2002;39:1429-1435.

237. Giugliano D. Dietary antioxidants for cardiovascular prevention. *Nutr Metab Cardiovasc Dis* 2000;10:38-44.

238. Dieber-Rotheneder M, Puhl H, Waeg G, Striegl G, Esterbauer H. Effect of oral supplementation with D-alpha-tocopherol on the vitamin E content of human low density lipoproteins and resistance to oxidation. *J Lipid Res* 1991;32:1325-1332.

239. Mabile L, Bruckdorfer KR, Rice-Evans C. Moderate supplementation with natural alpha-tocopherol decreases platelet aggregation and low-density lipoprotein oxidation. *Atherosclerosis* 1999;147:177-185.

240. Wu D, Koga T, Martin KR, Meydani M. Effect of vitamin E on human aortic endothelial cell production of chemokines and adhesion to monocytes. *Atherosclerosis* 1999;147:297-307.

241. Erl W, Weber C, Wardemann C, Weber PC. alpha-Tocopheryl succinate inhibits monocytic cell adhesion to endothelial cells by suppressing NF-kappa B mobilization. *Am J Physiol* 1997;273:H634-H640.

242. Panes J, Perry M, Granger DN. Leukocyte-endothelial cell adhesion: avenues for therapeutic intervention. *Br J Pharmacol* 1999;126:537-550.

243. Pratico D, Tangirala RK, Rader DJ, Rokach J, FitzGerald GA. Vitamin E suppresses isoprostane generation in vivo and reduces atherosclerosis in ApoE-deficient mice. *Nat Med* 1998;4:1189-1192.

244. Carr A, Frei B. Does vitamin C act as a pro-oxidant under physiological conditions? *FASEB J* 1999;13:1007-1024.

245. Martin A, Frei B. Both intracellular and extracellular vitamin C inhibit atherogenic modification of LDL by human vascular endothelial cells. *Arterioscler Thromb Vasc Biol* 1997;17:1583-1590.

246. Stocker R, Bowry VW, Frei B. Ubiquinol-10 protects human low density lipoprotein more efficiently against lipid peroxidation than does alpha-tocopherol. *Proc Natl Acad Sci U S A* 1991;88:1646-1650.

247. Frei B, England L, Ames BN. Ascorbate is an outstanding antioxidant in human blood plasma. *Proc Natl Acad Sci U S A* 1989;86:6377-6381.

248. Weber C, Erl W, Weber K, Weber PC. Increased adhesiveness of isolated monocytes to endothelium is prevented by vitamin C intake in smokers. *Circulation* 1996;93:1488-1492.

249. Adams MR, Jessup W, Celermajer DS. Cigarette smoking is associated with increased human monocyte adhesion to endothelial cells: reversibility with oral L-arginine but not vitamin C. *J Am Coll Cardiol* 1997;29:491-497.

250. Mosca L, Rubenfire M, Mandel C, Rock C, Tarshis T, Tsai A, Pearson T. Antioxidant nutrient supplementation reduces the susceptibility of low density lipoprotein to oxidation in patients with coronary artery disease. *J Am Coll Cardiol* 1997;30:392-399.

251. Reaven PD, Khouw A, Beltz WF, Parthasarathy S, Witztum JL. Effect of dietary antioxidant combinations in humans. Protection of LDL by vitamin E but not by beta-carotene. *Arterioscler Thromb* 1993;13:590-600.

252. Reaven PD, Ferguson E, Navab M, Powell FL. Susceptibility of human LDL to oxidative modification. Effects of variations in beta-carotene concentration and oxygen tension. *Arterioscler Thromb* 1994;14:1162-1169.

253. Crawford RS, Kirk EA, Rosenfeld ME, LeBoeuf RC, Chait A. Dietary antioxidants inhibit development of fatty streak lesions in the LDL receptor-deficient mouse. *Arterioscler Thromb Vasc Biol* 1998;18:1506-1513.

254. Thomas SR, Leichtweis SB, Pettersson K, Croft KD, Mori TA, Brown AJ, Stocker R. Dietary cosupplementation with vitamin E and coenzyme Q(10) inhibits atherosclerosis in apolipoprotein E gene knockout mice. *Arterioscler Thromb Vasc Biol* 2001;21:585-593.

255. Rimm EB, Stampfer MJ, Ascherio A, Giovannucci E, Colditz GA, Willett WC. Vitamin E consumption and the risk of coronary heart disease in men. *N Engl J Med* 1993;328:1450-1456.

256. Stampfer MJ, Hennekens CH, Manson JE, Colditz GA, Rosner B, Willett WC. Vitamin E consumption and the risk of coronary disease in women. *N Engl J Med* 1993;328:1444-1449.

257. Gaziano JM, Manson JE, Branch LG, Colditz GA, Willett WC, Buring JE. A prospective study of consumption of carotenoids in fruits and vegetables and decreased cardiovascular mortality in the elderly. *Ann Epidemiol* 1995;5:255-260.

258. Enstrom JE, Kanim LE, Klein MA. Vitamin C intake and mortality among a sample of the United States population. *Epidemiology* 1992;3:194-202.

259. Losonczy KG, Harris TB, Havlik RJ. Vitamin E and vitamin C supplement use and risk of all-cause and coronary heart disease mortality in older persons: the Established Populations for Epidemiologic Studies of the Elderly. *Am J Clin Nutr* 1996;64:190-196.

260. The effect of vitamin E and beta carotene on the incidence of lung cancer and other cancers in male smokers. The Alpha-Tocopherol, Beta Carotene Cancer Prevention Study Group. *N Engl J Med* 1994;330:1029-1035.

261. Lonn EM, Yusuf S. Is there a role for antioxidant vitamins in the prevention of cardiovascular diseases? An update on epidemiological and clinical trials data. *Can J Cardiol* 1997;13:957-965.

262. Omenn GS, Goodman GE, Thornquist MD, Balmes J, Cullen MR, Glass A, Keogh JP, Meyskens FL, Valanis B, Williams JH, Barnhart S, Hammar S. Effects of a combination of beta carotene and vitamin A on lung cancer and cardiovascular disease. *N Engl J Med* 1996;334:1150-1155.

263. Yusuf S, Dagenais G, Pogue J, Bosch J, Sleight P. Vitamin E supplementation and cardiovascular events in high-risk patients. The Heart Outcomes Prevention Evaluation Study Investigators. *N Engl J Med* 2000;342:154-160.

264. Jialal I, Traber M, Devaraj S. Is there a vitamin E paradox? *Curr Opin Lipidol* 2001;12:49-53.

265. Dietary supplementation with n-3 polyunsaturated fatty acids and vitamin E after myocardial infarction: results of the GISSI-Prevenzione trial. Gruppo Italiano per lo Studio della Sopravvivenza nell'Infarto miocardico. *Lancet* 1999;354:447-455.

266. Stephens NG, Parsons A, Schofield PM, Kelly F, Cheeseman K, Mitchinson MJ. Randomised controlled trial of vitamin E in patients with coronary disease: Cambridge Heart Antioxidant Study (CHAOS). *Lancet* 1996;347:781-786.

267. Boaz M, Smetana S, Weinstein T, Matas Z, Gafter U, Iaina A, Knecht A, Weissgarten Y, Brunner D, Fainaru M, Green MS. Secondary prevention with antioxidants of cardiovascular disease in endstage renal disease (SPACE): randomised placebo-controlled trial. *Lancet* 2000;356:1213-1218.

268. Aviram M. Does paraoxonase play a role in susceptibility to cardiovascular disease? *Mol Med Today* 1999;5:381-386.

269. Durrington PN, Mackness B, Mackness MI. Paraoxonase and atherosclerosis. *Arterioscler Thromb Vasc Biol* 2001;21:473-480.

270. Mackness MI, Mackness B, Durrington PN, Fogelman AM, Berliner J, Lusis AJ, Navab M, Shih D, Fonarow GC. Paraoxonase and coronary heart disease. *Curr Opin Lipidol* 1998;9:319-324.

271. Reddy ST, Wadleigh DJ, Grijalva V, Ng C, Hama S, Gangopadhyay A, Shih DM, Lusis AJ, Navab M, Fogelman AM. Human paraoxonase-3 is an HDL-associated enzyme with biological activity similar to paraoxonase-1 protein but is not regulated by oxidized lipids. *Arterioscler Thromb Vasc Biol* 2001;21:542-547.

272. Sanghera DK, Saha N, Aston CE, Kamboh MI. Genetic polymorphism of paraoxonase and the risk of coronary heart disease. *Arterioscler Thromb Vasc Biol* 1997;17:1067-1073.

273. Zama T, Murata M, Matsubara Y, Kawano K, Aoki N, Yoshino H, Watanabe G, Ishikawa K, Ikeda Y. A 192Arg variant of the human paraoxonase (HUMPONA) gene polymorphism is associated with an increased risk for coronary artery disease in the Japanese. *Arterioscler Thromb Vasc Biol* 1997;17:3565-3569.

274. Cao H, Girard-Globa A, Serusclat A, Bernard S, Bondon P, Picard S, Berthezene F, Moulin P. Lack of association between carotid intima-media thickness and paraoxonase gene polymorphism in non-insulin dependent diabetes mellitus. *Atherosclerosis* 1998;138:361-366.

275. Ombres D, Pannitteri G, Montali A, Candeloro A, Seccareccia F, Campagna F, Cantini R, Campa PP, Ricci G, Arca M. The gln-Arg192 polymorphism of human paraoxonase gene is not associated with coronary artery disease in italian patients. *Arterioscler Thromb Vasc Biol* 1998;18:1611-1616.

276. Shih DM, Gu L, Hama S, Xia YR, Navab M, Fogelman AM, Lusis AJ. Genetic-dietary regulation of serum paraoxonase expression and its role in atherogenesis in a mouse model. *J Clin Invest* 1996;97:1630-1639.

277. Shih DM, Gu L, Xia YR, Navab M, Li WF, Hama S, Castellani LW, Furlong CE, Costa LG, Fogelman AM, Lusis AJ. Mice lacking serum paraoxonase are susceptible to organophosphate toxicity and atherosclerosis. *Nature* 1998;394:284-287.

278. Shih DM, Xia YR, Wang XP, Miller E, Castellani LW, Subbanagounder G, Cheroutre H, Faull KF, Berliner JA, Witztum JL, Lusis AJ. Combined serum paraoxonase knockout/apolipoprotein E knockout mice exhibit increased lipoprotein oxidation and atherosclerosis. *J Biol Chem* 2000;275:17527-17535.

279. Feingold KR, Memon RA, Moser AH, Grunfeld C. Paraoxonase activity in the serum and hepatic mRNA levels decrease during the acute phase response. *Atherosclerosis* 1998;139:307-315.

280. Mackness B, Hunt R, Durrington PN, Mackness MI. Increased immunolocalization of paraoxonase, clusterin, and apolipoprotein A-I in the human artery wall with the progression of atherosclerosis. *Arterioscler Thromb Vasc Biol* 1997;17:1233-1238.

281. Navab M, Hama-Levy S, Van Lenten BJ, Fonarow GC, Cardinez CJ, Castellani LW, Brennan ML, Lusis AJ, Fogelman AM, La Du BN. Mildly oxidized LDL induces an increased apolipoprotein J/paraoxonase ratio. *J Clin Invest* 1997;99:2005-2019.

282. Pigott R, Dillon LP, Hemingway IH, Gearing AJ. Soluble forms of E-selectin, ICAM-1 and VCAM-1 are present in the supernatants of cytokine activated cultured endothelial cells. *Biochem Biophys Res Commun* 1992;187:584-589.

283. Leca G, Mansur SE, Bensussan A. Expression of VCAM-1 (CD106) by a subset of TCR gamma delta-bearing lymphocyte clones. Involvement of a metalloprotease in the specific hydrolytic release of the soluble isoform. *J Immunol* 1995;154:1069-1077.

284. Chen A, Engel P, Tedder TF. Structural requirements regulate endoproteolytic release of the L- selectin (CD62L) adhesion receptor from the cell surface of leukocytes. *J Exp Med* 1995;182:519-530.

285. Abe Y, El Masri B, Kimball KT, Pownall H, Reilly CF, Osmundsen K, Smith CW, Ballantyne CM. Soluble cell adhesion molecules in hypertriglyceridemia and potential significance on monocyte adhesion. *Arterioscler Thromb Vasc Biol* 1998;18:723-731.

286. Blann AD, Herrick A, Jayson MI. Altered levels of soluble adhesion molecules in rheumatoid arthritis, vasculitis and systemic sclerosis. *Br J Rheumatol* 1995;34:814-819.

287. Banks RE, Gearing AJ, Hemingway IK, Norfolk DR, Perren TJ, Selby PJ. Circulating intercellular adhesion molecule-1 (ICAM-1), E-selectin and vascular cell adhesion molecule-1 (VCAM-1) in human malignancies. *Br J Cancer* 1993;68:122-124.

288. Lai CK, Wong KC, Chan CH, Ho SS, Chung SY, Haskard DO, Lai KN. Circulating adhesion molecules in tuberculosis. *Clin Exp Immunol* 1993;94:522-526.

289. Ikeda H, Nakayama H, Oda T, Kuwano K, Muraishi A, Sugi K, Koga Y, Toshima H. Soluble form of P-selectin in patients with acute myocardial infarction. *Coron Artery Dis* 1994;5:515-518.

290. Ikeda H, Takajo Y, Ichiki K, Ueno T, Maki S, Noda T, Sugi K, Imaizumi T. Increased soluble form of P-selectin in patients with unstable angina. *Circulation* 1995;92:1693-1696.

291. Frijns CJ, Kappelle LJ, van Gijn J, Nieuwenhuis HK, Sixma JJ, Fijnheer R. Soluble adhesion molecules reflect endothelial cell activation in ischemic stroke and in carotid atherosclerosis. *Stroke* 1997;28:2214-2218.

292. Blann AD, Dobrotova M, Kubisz P, McCollum CN. von Willebrand factor, soluble P-selectin, tissue plasminogen activator and plasminogen activator inhibitor in atherosclerosis. *Thromb Haemost* 1995;74:626-630.

293. Hackman A, Abe Y, Insull W, Jr., Pownall H, Smith L, Dunn K, Gotto AM, Jr., Ballantyne CM. Levels of soluble cell adhesion molecules in patients with dyslipidemia. *Circulation* 1996;93:1334-1338.

294. Shahi CN, Ghaisas NK, Goggins M, Foley B, Crean P, Kelleher D, Walsh M. Elevated levels of circulating soluble adhesion molecules in patients with nonrheumatic aortic stenosis. *Am J Cardiol* 1997;79:980-982.

295. Ghaisas NK, Shahi CN, Foley B, Goggins M, Crean P, Kelly A, Kelleher D, Walsh M. Elevated levels of circulating soluble adhesion molecules in peripheral blood of patients with unstable angina. *Am J Cardiol* 1997;80:617-619.

296. Belch JJ, Shaw JW, Kirk G, McLaren M, Robb R, Maple C, Morse P. The white blood cell adhesion molecule E-selectin predicts restenosis in patients with intermittent claudication undergoing percutaneous transluminal angioplasty. *Circulation* 1997;95:2027-2031.

297. Blann AD, McCollum CN. Circulating endothelial cell/leukocyte adhesion molecules in atherosclerosis. *Thromb Haemost* 1994;72:151-154.

298. Ridker PM, Hennekens CH, Roitman-Johnson B, Stampfer MJ, Allen J. Plasma concentration of soluble intercellular adhesion molecule 1 and risks of future myocardial infarction in apparently healthy men [see comments]. *Lancet* 1998;351:88-92.

299. Peter K, Weirich U, Nordt TK, Ruef J, Bode C. Soluble vascular cell adhesion molecule-1 (VCAM-1) as potential marker of atherosclerosis. *Thromb Haemost* 1999;82 Suppl 1:38-43.

300. Nakai K, Itoh C, Kawazoe K, Miura Y, Sotoyanagi H, Hotta K, Itoh T, Kamata J, Hiramori K. Concentration of soluble vascular cell adhesion molecule-1 (VCAM-1) correlated with expression of VCAM-1 mRNA in the human atherosclerotic aorta. *Coron Artery Dis* 1995;6:497-502.

301. De Caterina R, Basta G, Lazzerini G, Dell'Omo G, Petrucci R, Morale M, Carmassi F, Pedrinelli R. Soluble vascular cell adhesion molecule-1 as a biohumoral correlate of atherosclerosis. *Arterioscler Thromb Vasc Biol* 1997;17:2646-2654.

302. Sampietro T, Tuoni M, Ferdeghini M, Ciardi A, Marraccini P, Prontera C, Sassi G, Taddei M, Bionda A. Plasma cholesterol regulates soluble cell adhesion molecule expression in familial hypercholesterolemia. *Circulation* 1997;96:1381-1385.

303. Davi G, Romano M, Mezzetti A, Procopio A, Iacobelli S, Antidormi T, Bucciarelli T, Alessandrini P, Cuccurullo F, Bittolo BG. Increased levels of soluble P-selectin in hypercholesterolemic patients [see comments]. *Circulation* 1998;97:953-957.

304. Koch AE, Kunkel SL, Harlow LA, Mazarakis DD, Haines GK, Burdick MD, Pope RM, Strieter RM. Macrophage inflammatory protein-1 alpha. A novel chemotactic cytokine for macrophages in rheumatoid arthritis. *J Clin Invest* 1994;93:921-928.

305. Aukrust P, Ueland T, Muller F, Andreassen AK, Nordoy I, Aas H, Kjekshus J, Simonsen S, Froland SS, Gullestad L. Elevated circulating levels of C-C chemokines in patients with congestive heart failure. *Circulation* 1998;97:1136-1143.

306. Koch AE, Kunkel SL, Pearce WH, Shah MR, Parikh D, Evanoff HL, Haines GK, Burdick MD, Strieter RM. Enhanced production of the chemotactic cytokines interleukin-8 and

monocyte chemoattractant protein-1 in human abdominal aortic aneurysms. *Am J Pathol* 1993;142:1423-1431.

307. Cipollone F, Marini M, Fazia M, Pini B, Iezzi A, Reale M, Paloscia L, Materazzo G, D'Annunzio E, Conti P, Chiarelli F, Cuccurullo F, Mezzetti A. Elevated circulating levels of monocyte chemoattractant protein-1 in patients with restenosis after coronary angioplasty. *Arterioscler Thromb Vasc Biol* 2001;21:327-334.

308. Damas JK, Gullestad L, Ueland T, Solum NO, Simonsen S, Froland SS, Aukrust P. CXC-chemokines, a new group of cytokines in congestive heart failure-- possible role of platelets and monocytes [see comments]. *Cardiovasc Res* 2000;45:428-436.

309. Kukielka GL, Youker KA, Michael LH, Kumar AG, Ballantyne CM, Smith CW, Entman ML. Role of early reperfusion in the induction of adhesion molecules and cytokines in previously ischemic myocardium. *Mol Cell Biochem* 1995;147:5-12.

310. Kukielka GL, Smith CW, LaRosa GJ, Manning AM, Mendoza LH, Daly TJ, Hughes BJ, Youker KA, Hawkins HK, Michael LH, . Interleukin-8 gene induction in the myocardium after ischemia and reperfusion in vivo. *J Clin Invest* 1995;95:89-103.

311. Steel DM, Whitehead AS. The major acute phase reactants: C-reactive protein, serum amyloid P component and serum amyloid A protein. *Immunol Today* 1994;15:81-88.

312. Ridker PM, Cushman M, Stampfer MJ, Tracy RP, Hennekens CH. Inflammation, aspirin, and the risk of cardiovascular disease in apparently healthy men. *N Engl J Med* 1997;336:973-979.

313. Ridker PM, Buring JE, Shih J, Matias M, Hennekens CH. Prospective study of C-reactive protein and the risk of future cardiovascular events among apparently healthy women [see comments]. *Circulation* 1998;98:731-733.

314. Ridker PM, Glynn RJ, Hennekens CH. C-reactive protein adds to the predictive value of total and HDL cholesterol in determining risk of first myocardial infarction [see comments]. *Circulation* 1998;97:2007-2011.

315. Uhlar CM, Whitehead AS. Serum amyloid A, the major vertebrate acute-phase reactant. *Eur J Biochem* 1999;265:501-523.

316. Van Lenten BJ, Hama SY, de Beer FC, Stafforini DM, McIntyre TM, Prescott SM, La Du BN, Fogelman AM, Navab M. Anti-inflammatory HDL becomes pro-inflammatory during the acute phase response. Loss of protective effect of HDL against LDL oxidation in aortic wall cell cocultures. *J Clin Invest* 1995;96:2758-2767.

317. Badolato R, Wang JM, Murphy WJ, Lloyd AR, Michiel DF, Bausserman LL, Kelvin DJ, Oppenheim JJ. Serum amyloid A is a chemoattractant: induction of migration, adhesion, and tissue infiltration of monocytes and polymorphonuclear leukocytes. *J Exp Med* 1994;180:203-209.

318. Meek RL, Urieli-Shoval S, Benditt EP. Expression of apolipoprotein serum amyloid A mRNA in human atherosclerotic lesions and cultured vascular cells: implications for serum amyloid A function. *Proc Natl Acad Sci U S A* 1994;91:3186-3190.

319. Liao F, Lusis AJ, Berliner JA, Fogelman AM, Kindy M, de Beer MC, de Beer FC. Serum amyloid A protein family. Differential induction by oxidized lipids in mouse strains. *Arterioscler Thromb* 1994;14:1475-1479.

320. Erren M, Reinecke H, Junker R, Fobker M, Schulte H, Schurek JO, Kropf J, Kerber S, Breithardt G, Assmann G, Cullen P. Systemic inflammatory parameters in patients with atherosclerosis of the coronary and peripheral arteries. *Arterioscler Thromb Vasc Biol* 1999;19:2355-2363.

321. Fyfe AI, Rothenberg LS, deBeer FC, Cantor RM, Rotter JI, Lusis AJ. Association between serum amyloid A proteins and coronary artery disease: evidence from two distinct arteriosclerotic processes. *Circulation* 1997;96:2914-2919.

322. Braeckman L, De Bacquer D, Delanghe J, Claeys L, De Backer G. Associations between haptoglobin polymorphism, lipids, lipoproteins and inflammatory variables. *Atherosclerosis* 1999;143:383-388.

323. Yuan XM, Anders WL, Olsson AG, Brunk UT. Iron in human atheroma and LDL oxidation by macrophages following erythrophagocytosis. *Atherosclerosis* 1996;124:61-73.

324. Gutteridge JM. The antioxidant activity of haptoglobin towards haemoglobin-stimulated lipid peroxidation. *Biochim Biophys Acta* 1987;917:219-223.

325. Delanghe JR, Duprez DA, De Buyzere ML, Bergez BM, Callens BY, Leroux-Roels GG, Clement DL. Haptoglobin polymorphism and complications in established essential arterial hypertension. *J Hypertens* 1993;11:861-867.

326. Delanghe J, Cambier B, Langlois M, De Buyzere M, Neels H, De Bacquer D, Van Cauwelaert P. Haptoglobin polymorphism, a genetic risk factor in coronary artery bypass surgery. *Atherosclerosis* 1997;132:215-219.

327. Stastny J, Fosslien E, Robertson AL, Jr. Human aortic intima protein composition during initial stages of atherogenesis. *Atherosclerosis* 1986;60:131-139.

328. Fiotti N, Giansante C, Ponte E, Delbello C, Calabrese S, Zacchi T, Dobrina A, Guarnieri G. Atherosclerosis and inflammation. Patterns of cytokine regulation in patients with peripheral arterial disease. *Atherosclerosis* 1999;145:51-60.

329. Simonet WS, Bucay N, Pitas RE, Lauer SJ, Taylor JM. Multiple tissue-specific elements control the apolipoprotein E/C-I gene locus in transgenic mice. *J Biol Chem* 1991;266:8651-8654.

330. Harlow E, Lane D. Immunoassay. In: *Antibodies: A Laboratory Manual.* New York: Cold Spring Harbor Laboratory; 1988:533-612.

331. Hennes U, Gross W, Edelmann A. Changes of lipoprotein patterns in hampsters under different metabolic states analysed following separation by micropreparative chromatography on SMART system from multiple micro plasma samplings. *Science Tools* 1992;36:10.

332. Allain CC, Poon LS, Chan CS, Richmond W, Fu PC. Enzymatic determination of total serum cholesterol. *Clin Chem* 1974;20:470-475.

333. Fossati P, Prencipe L. Serum triglycerides determined colorimetrically with an enzyme that produces hydrogen peroxide. *Clin Chem* 1982;28:2077-2080.

334. McGowan MW, Artiss JD, Strandbergh DR, Zak B. A peroxidase-coupled method for the colorimetric determination of serum triglycerides. *Clin Chem* 1983;29:538-542.

335. Paigen B, Morrow A, Holmes PA, Mitchell D, Williams RA. Quantitative assessment of atherosclerotic lesions in mice. *Atherosclerosis* 1987;68:231-240.

336. Birnboim HC, Doly J. A rapid alkaline extraction procedure for screening recombinant plasmid DNA. *Nucleic Acids Res* 1979;7:1513-1523.

337. Birnboim HC. A rapid alkaline extraction method for the isolation of plasmid DNA. *Methods Enzymol* 1983;100:243-255.

338. Rus HG, Vlaicu R, Niculescu F. Interleukin-6 and interleukin-8 protein and gene expression in human arterial atherosclerotic wall. *Atherosclerosis* 1996;127:263-271.

339. Porreca E, Sergi R, Baccante G, Reale M, Orsini L, Febbo CD, Caselli G, Cuccurullo F, Bertini R. Peripheral blood mononuclear cell production of interleukin-8 and IL-8-dependent neutrophil function in hypercholesterolemic patients [see comments]. *Atherosclerosis* 1999;146:345-350.

340. Kostulas N, Kivisakk P, Huang Y, Matusevicius D, Kostulas V, Link H. Ischemic stroke is associated with a systemic increase of blood mononuclear cells expressing interleukin-8 mRNA. *Stroke* 1998;29:462-466.

341. Terkeltaub R, Boisvert WA, Curtiss LK. Chemokines and atherosclerosis. *Curr Opin Lipidol* 1998;9:397-405.

342. Hoch RC, Schraufstatter IU, Cochrane CG. In vivo, in vitro, and molecular aspects of interleukin-8 and the interleukin-8 receptors. *J Lab Clin Med* 1996;128:134-145.

343. Witt DP, Lander AD. Differential binding of chemokines to glycosaminoglycan subpopulations. *Curr Biol* 1994;4:394-400.

344. Wang JM, Su S, Gong W, Oppenheim JJ. Chemokines, receptors, and their role in cardiovascular pathology. *Int J Clin Lab Res* 1998;28:83-90.

345. Sylvester I, Suffredini AF, Boujoukos AJ, Martich GD, Danner RL, Yoshimura T, Leonard EJ. Neutrophil attractant protein-1 and monocyte chemoattractant protein-1 in human serum. Effects of intravenous lipopolysaccharide on free attractants, specific IgG autoantibodies and immune complexes. *J Immunol* 1993;151:3292-3298.

346. Watanabe T, Fan J. Atherosclerosis and inflammation mononuclear cell recruitment and adhesion molecules with reference to the implication of ICAM-1/LFA-1 pathway in atherogenesis. *Int J Cardiol* 1998;66 Suppl 1:S45-S53.

347. Han KH, Tangirala RK, Green SR, Quehenberger O. Chemokine receptor CCR2 expression and monocyte chemoattractant protein- 1-mediated chemotaxis in human monocytes. A regulatory role for plasma LDL. *Arterioscler Thromb Vasc Biol* 1998;18:1983-1991.

348. Rayner K, Van Eersel S, Groot PH, Reape TJ. Localisation of mRNA for JE/MCP-1 and its receptor CCR2 in atherosclerotic lesions of the ApoE knockout mouse. *J Vasc Res* 2000;37:93-102.

349. Kowala MC, Recce R, Beyer S, Gu C, Valentine M. Characterization of atherosclerosis in LDL receptor knockout mice: macrophage accumulation correlates with rapid and sustained expression of aortic MCP-1/JE. *Atherosclerosis* 2000;149:323-330.

350. Reckless J, Rubin EM, Verstuyft JB, Metcalfe JC, Grainger DJ. Monocyte chemoattractant protein-1 but not tumor necrosis factor-alpha is correlated with monocyte infiltration in mouse lipid lesions. *Circulation* 1999;99:2310-2316.

351. Bozic CR, Gerard NP, Uexkull-Guldenband C, Kolakowski LF, Jr., Conklyn MJ, Breslow R, Showell HJ, Gerard C. The murine interleukin 8 type B receptor homologue and its ligands. Expression and biological characterization. *J Biol Chem* 1994;269:29355-29358.

352. Kostulas N, Pelidou SH, Kivisakk P, Kostulas V, Link H. Increased IL-1beta, IL-8, and IL-17 mRNA expression in blood mononuclear cells observed in a prospective ischemic stroke study. *Stroke* 1999;30:2174-2179.

353. Browning DD, Diehl WC, Hsu MH, Schraufstatter IU, Ye RD. Autocrine regulation of interleukin-8 production in human monocytes. *Am J Physiol Lung Cell Mol Physiol* 2000;279:L1129-L1136.

354. Zhou X, Paulsson G, Stemme S, Hansson GK. Hypercholesterolemia is associated with a T helper (Th) 1/Th2 switch of the autoimmune response in atherosclerotic apo E-knockout mice. *J Clin Invest* 1998;101:1717-1725.

355. Blann AD, Seigneur M, Steiner M, Miller JP, McCollum CN. Circulating ICAM-1 and VCAM-1 in peripheral artery disease and hypercholesterolaemia: relationship to the location of atherosclerotic disease, smoking, and in the prediction of adverse events. *Thromb Haemost* 1998;79:1080-1085.

356. Szekanecz Z, Shah MR, Pearce WH, Koch AE. Intercellular adhesion molecule-1 (ICAM-1) expression and soluble ICAM- 1 (sICAM-1) production by cytokine-activated human aortic endothelial cells: a possible role for ICAM-1 and sICAM-1 in atherosclerotic aortic aneurysms. *Clin Exp Immunol* 1994;98:337-343.

357. Rohde LE, Lee RT, Rivero J, Jamacochian M, Arroyo LH, Briggs W, Rifai N, Libby P, Creager MA, Ridker PM. Circulating cell adhesion molecules are correlated with ultrasound- based assessment of carotid atherosclerosis. *Arterioscler Thromb Vasc Biol* 1998;18:1765-1770.

358. Skehel JM, Schneider K, Murphy N, Graham A, Benson GM, Cutler P, Camilleri P. Phenotyping apolipoprotein E*3-leiden transgenic mice by two- dimensional polyacrylamide gel electrophoresis and mass spectrometric identification [In Process Citation]. *Electrophoresis* 2000;21:2540-2545.

359. Lim YK, Jenner A, Ali AB, Wang Y, Hsu SI, Chong SM, Baumman H, Halliwell B, Lim SK. Haptoglobin reduces renal oxidative DNA and tissue damage during phenylhydrazine-induced hemolysis. *Kidney Int* 2000;58:1033-1044.

360. Chomczynski P, Sacchi N. Single-step method of RNA isolation by acid guanidinium thiocyanate- phenol-chloroform extraction. *Anal Biochem* 1987;162:156-159.

361. Lynn EG, Siow YL, O K. Very low-density lipoprotein stimulates the expression of monocyte chemoattractant protein-1 in mesangial cells. *Kidney Int* 2000;57:1472-1483.

362. Han KH, Tangirala RK, Green SR, Quehenberger O. Chemokine receptor CCR2 expression and monocyte chemoattractant protein- 1-mediated chemotaxis in human monocytes. A regulatory role for plasma LDL. *Arterioscler Thromb Vasc Biol* 1998;18:1983-1991.

363. Han KH, Han KO, Green SR, Quehenberger O. Expression of the monocyte chemoattractant protein-1 receptor CCR2 is increased in hypercholesterolemia. Differential effects of plasma lipoproteins on monocyte function. *J Lipid Res* 1999;40:1053-1063.

364. Leeuwenburgh C, Hardy MM, Hazen SL, Wagner P, Oh-ishi S, Steinbrecher UP, Heinecke JW. Reactive nitrogen intermediates promote low density lipoprotein oxidation in human atherosclerotic intima. *J Biol Chem* 1997;272:1433-1436.

365. Heinecke JW. Mass spectrometric quantification of amino acid oxidation products in proteins: insights into pathways that promote LDL oxidation in the human artery wall. *FASEB J* 1999;13:1113-1120.

366. Cushing SD, Berliner JA, Valente AJ, Territo MC, Navab M, Parhami F, Gerrity R, Schwartz CJ, Fogelman AM. Minimally modified low density lipoprotein induces monocyte chemotactic protein 1 in human endothelial cells and smooth muscle cells. *Proc Natl Acad Sci U S A* 1990;87:5134-5138.

367. Parhami F, Fang ZT, Fogelman AM, Andalibi A, Territo MC, Berliner JA. Minimally modified low density lipoprotein-induced inflammatory responses in endothelial cells are mediated by cyclic adenosine monophosphate. *J Clin Invest* 1993;92:471-478.

368. Shi W, Wang NJ, Shih DM, Sun VZ, Wang X, Lusis AJ. Determinants of atherosclerosis susceptibility in the C3H and C57BL/6 mouse model: evidence for involvement of endothelial cells but not blood cells or cholesterol metabolism. *Circ Res* 2000;86:1078-1084.

369. Fuller CJ, Grundy SM, Norkus EP, Jialal I. Effect of ascorbate supplementation on low density lipoprotein oxidation in smokers. *Atherosclerosis* 1996;119:139-150.

370. Jialal I, Grundy SM. Effect of combined supplementation with alpha-tocopherol, ascorbate, and beta carotene on low-density lipoprotein oxidation. *Circulation* 1993;88:2780-2786.

371. Cominacini L, Garbin U, Pasini AF, Davoli A, Campagnola M, Contessi GB, Pastorino AM, Lo C, V. Antioxidants inhibit the expression of intercellular cell adhesion molecule-1 and vascular cell adhesion molecule-1 induced by oxidized LDL on human umbilical vein endothelial cells. *Free Radic Biol Med* 1997;22:117-127.

372. Weber C, Erl W, Pietsch A, Strobel M, Ziegler-Heitbrock HW, Weber PC. Antioxidants inhibit monocyte adhesion by suppressing nuclear factor- kappa B mobilization and induction of vascular cell adhesion molecule-1 in endothelial cells stimulated to generate radicals. *Arterioscler Thromb* 1994;14:1665-1673.

373. Verlangieri AJ, Bush MJ. Effects of d-alpha-tocopherol supplementation on experimentally induced primate atherosclerosis. *J Am Coll Nutr* 1992;11:131-138.

374. Ozer NK, Azzi A. Effect of vitamin E on the development of atherosclerosis. *Toxicology* 2000;148:179-185.

375. Palinski W, Tangirala RK, Miller E, Young SG, Witztum JL. Increased autoantibody titers against epitopes of oxidized LDL in LDL receptor-deficient mice with increased atherosclerosis. *Arterioscler Thromb Vasc Biol* 1995;15:1569-1576.

376. Freigang S, Horkko S, Miller E, Witztum JL, Palinski W. Immunization of LDL receptor-deficient mice with homologous malondialdehyde-modified and native LDL reduces progression of atherosclerosis by mechanisms other than induction of high titers of antibodies to oxidative neoepitopes. *Arterioscler Thromb Vasc Biol* 1998;18:1972-1982.

377. George J, Afek A, Gilburd B, Levkovitz H, Shaish A, Goldberg I, Kopolovic Y, Wick G, Shoenfeld Y, Harats D. Hyperimmunization of apo-E-deficient mice with homologous malondialdehyde low-density lipoprotein suppresses early atherogenesis. *Atherosclerosis* 1998;138:147-152.

378. Tsimikas S, Palinski W, Witztum JL. Circulating autoantibodies to oxidized LDL correlate with arterial accumulation and depletion of oxidized LDL in LDL receptor-deficient mice. *Arterioscler Thromb Vasc Biol* 2001;21:95-100.

379. Terasawa Y, Ladha Z, Leonard SW, Morrow JD, Newland D, Sanan D, Packer L, Traber MG, Farese RV, Jr. Increased atherosclerosis in hyperlipidemic mice deficient in alpha - tocopherol transfer protein and vitamin E. *Proc Natl Acad Sci U S A* 2000;97:13830-13834.

380. Pratico D, Tangirala RK, Horkko S, Witztum JL, Palinski W, FitzGerald GA. Circulating autoantibodies to oxidized cardiolipin correlate with isoprostane F(2alpha)-VI levels and the extent of atherosclerosis in ApoE-deficient mice: modulation by vitamin E. *Blood* 2001;97:459-464.

381. Shaish A, George J, Gilburd B, Keren P, Levkovitz H, Harats D. Dietary beta-carotene and alpha-tocopherol combination does not inhibit atherogenesis in an ApoE-deficient mouse model. *Arterioscler Thromb Vasc Biol* 1999;19:1470-1475.

382. Neuzil J, Christison JK, Iheanacho E, Fragonas JC, Zammit V, Hunt NH, Stocker R. Radical-induced lipoprotein and plasma lipid oxidation in normal and apolipoprotein E gene knockout (apoE-/-) mice: apoE-/- mouse as a model for testing the role of tocopherol-mediated peroxidation in atherogenesis. *J Lipid Res* 1998;39:354-368.

383. Keaney JF, Jr., Gaziano JM, Xu A, Frei B, Curran-Celentano J, Shwaery GT, Loscalzo J, Vita JA. Low-dose alpha-tocopherol improves and high-dose alpha-tocopherol worsens endothelial vasodilator function in cholesterol-fed rabbits. *J Clin Invest* 1994;93:844-851.

384. Blann AD, Seigneur M, Steiner M, Miller JP, McCollum CN. Circulating ICAM-1 and VCAM-1 in peripheral artery disease and hypercholesterolaemia: relationship to the location of atherosclerotic disease, smoking, and in the prediction of adverse events. *Thromb Haemost* 1998;79:1080-1085.

385. Rohde LE, Lee RT, Rivero J, Jamacochian M, Arroyo LH, Briggs W, Rifai N, Libby P, Creager MA, Ridker PM. Circulating cell adhesion molecules are correlated with ultrasound- based assessment of carotid atherosclerosis. *Arterioscler Thromb Vasc Biol* 1998;18:1765-1770.

386. Peter K, Nawroth P, Conradt C, Nordt T, Weiss T, Boehme M, Wunsch A, Allenberg J, Kubler W, Bode C. Circulating vascular cell adhesion molecule-1 correlates with the extent of human atherosclerosis in contrast to circulating intercellular adhesion molecule-1, E-selectin, P-selectin, and thrombomodulin. *Arterioscler Thromb Vasc Biol* 1997;17:505-512.

387. Mulvihill N, Foley JB, Ghaisas N, Murphy R, Crean P, Walsh M. Early temporal expression of soluble cellular adhesion molecules in patients with unstable angina and subendocardial myocardial infarction. *Am J Cardiol* 1999;83:1265-7, A9.

388. Chia MC. The role of adhesion molecules in atherosclerosis. *Crit Rev Clin Lab Sci* 1998;35:573-602.

389. Budnik A, Grewe M, Gyufko K, Krutmann J. Analysis of the production of soluble ICAM-1 molecules by human cells. *Exp Hematol* 1996;24:352-359.

390. Seljeflot I, Arnesen H, Brude IR, Nenseter MS, Drevon CA, Hjermann I. Effects of omega-3 fatty acids and/or antioxidants on endothelial cell markers. *Eur J Clin Invest* 1998;28:629-635.

391. Rovai LE, Herschman HR, Smith JB. The murine neutrophil-chemoattractant chemokines LIX, KC, and MIP-2 have distinct induction kinetics, tissue distributions, and tissue-specific sensitivities to glucocorticoid regulation in endotoxemia. *J Leukoc Biol* 1998;64:494-502.

Appendices

9 Appendices

9.1 Names and addresses of suppliers

Ambion via ams Biotechnology, Oxfordshire, UK.

American Type Culture Collection, VA, USA.

Amersham Pharmacia Biotech, Buckinghamshire, UK.

Bayer Diagnostics, Berkshire, UK.

BioGenex, CA, USA, via Menarini Diagnostics, Berkshire, UK.

Biosource International, CA, USA via Lifescreen Ltd, Hertfordshire, UK.

BDH Laboratory Supplies, Poole, UK.

Boehringer Mannheim now Roche Diagnostics Ltd, East Sussex, UK.

Costar via Merck EuroLabs, Poole, UK.

DAKO Ltd, Cambridgeshire, UK.

Endogen, MA, USA, via TCS Biological Ltd, Buckingham, UK.

European Collection of Cell Cultures, Whiltshire, UK.

Flowgen, Leicestershire, UK.

Hope Farm, The Netherlands.

Invitrogen, Groningen, The Netherlands.

Kodak via Sigma Chemical Company, Poole, UK.

Life Technologies Ltd (GIBCOBRL), Paisley, UK.

NUNC via Life Technologies, Paisley, UK.

NOVEX, San Diego, USA now part of Invitrogen, Groningen, The Netherlands.

Perkin Elmer Applied Biosystems, Warrington UK.

Pierce via Perbio Sciences UK Ltd, Cheshire, UK.

PharMingen, San Diego, USA via Becton Dickinson, UK.

Promega, Southampton, UK.

Qiagen, West Sussex, UK.

Raymond A Lamb, London, UK.

SEBIA via Analytical Technologies, Hampshire, UK.

Serotec, Oxfordshire, UK.

Sigma Chemical Company, Poole, UK.

Special Diet Services, Witham UK.

Stratagene, Cambridge, UK.

Tridelta Development Ltd, EIRE, via Biognosis, East Sussex, UK.

Triple Red Ltd, Oxofordshire, UK.

R&D Systems Europe Ltd, Oxon, UK.

Vector Laboratories Ltd, Peterborough, UK.

WAKO Chemicals Ltd, VA, USA.

9.2 Composition of diet RM1

RAT AND MOUSE NO. 1 MAINTENANCE DIET

SUITABLE SPECIES AND APPLICATIONS:

Rats and mice for long and short term maintenance.

BENEFITS:

- High quality grade human grade soya bean concentrate provides a less variable source of protein.
- Low protein level promotes longer life expectancy, reducing obesity and associated problems in the aged animal.
- Low nutrient levels reduce the risk of undesirable side-effects in toxicity trials being masked.

FEEDING GUIDE:

Ad-lib feeding is recommended

Ingredients	*Percentage composition*
Cereal Products	**88.5%**
Wheat	
Barley	
Wheatfeed	
Proteins	**8.5%**
Ext. Soya Bean Meal	
Whey Powder	
Energy Sources	**0.5%**
Soya Oil	
Supplementation	**2.5%**
Vitamins	
Major Minerals	
Trace Minerals	
Amino Acids	

CALCULATED ANALYSIS OF DIET RM1

NUTRIENTS		
Crude Oil	%	2.6
Crude Protein	%	14.7
Crude Fibre	%	5.3
Ash	%	5.9
N.F.E	%	61.5
Urea	%	
Dig. Crude Oil	%	2.4
Dig. Crude Protein	%	13.3
Tot. Diet Fibre	%	14.5
Pectin	%	1.5
Hemicellulose	%	7.8
Cellulose	%	4.1
Lignin	%	1.1
Starches	%	45.8
Sugars	%	6.5

Energy		
Gross Energy	MJ/kg	14.8
Dig. Energy	MJ/kg	12.1
Met. Energy	MJ/kg	10.9

Fatty Acids		
Myristoleic Acid	%	0.02
Palmitoleic Acid	%	0.10
Oleic Acid	%	0.76
Linoleic Acid	%	0.71
Linolenic Acid	%	0.06
Arachidonic Acid	%	0.13
Clupanodonic Acid	%	
Lauric Acid	%	0.02
Myristic Acid	%	0.14
Palmitic Acid	%	0.32
Stearic Acid	%	0.04

Amino Acids		
Arginine	%	0.95
Lysine	%	0.74
Methionine	%	0.25
Cysteine	%	0.26
Trytophan	%	0.19
Histidine	%	0.36
Threonine	%	0.53
Isoleucine	%	0.60
Leucine	%	1.06
Phenylalanine	%	0.71
Valine	%	0.74
Tyrosine	%	0.53
Taurine	%	
Aspartic Acid	%	0.73
Glutamic Acid	%	3.34
Proline	%	1.26
Serine	%	0.59
Hydroxyproline	%	
Hydroxylysine	%	
Alanine	%	0.16

Major Minerals		
Calcium	%	0.71
Total Phosphorus	%	0.50
Phytate Phosphorus	%	0.21
Available Phosphorus	%	0.29
Sodium	%	0.25
Chlorine	%	0.40
Magnesium	%	0.22
Potassium	%	0.66

Trace Minerals		
Iron	mg/kg	114.0
Copper	mg/kg	11.0
Manganese	mg/kg	66.0
Zinc	mg/kg	18.0
Cobalt	mcg/kg	554.0
Iodine	mcg/kg	1143.0
Selenium	mcg/kg	148.0
Fluorine	mg/kg	17.0

Vitamins		
Retinol	meg/kg	1910.0
Vitamin A	IU/kg	6303.0
Cholecalciferol	mcg/kg	15.0
Vitamin D_3	IU/kg	600.0
α-Tocopherol	mg/kg	69.0
Vitamin E	mg/kg	75.9
Vitamin B_1	mg/kg	8.0
Vitamin B_2	mg/kg	4.4
Vitamin B_6	mg/kg	4.8
Vitamin B_{12}	mg/kg	7.4
Vitamin C	mg/kg	11.0
Vitamin K_3	mg/kg	10.6
Folic Acid	mg/kg	0.07
Nicotinic Acid	mg/kg	57.4
Panthenic Acid	mg/kg	19.6
Choline	mg/kg	1390.0
Inositol	mg/kg	2434.0
Biotin	mcg/kg	264.0
p-Aminobenzoic Acid	mg/kg	
β-Carotene	mg/kg	0.3

Pigments	
Xanthophyll	mg/kg

Note 1. All values calculated to 10% moisture
Note 2. Values are total calculated values
Note 3. 1 mcg Retinol = 3.3 IU Vitamin A activity
Note 4. Total retinol content includes the Retinol equivalent of β-Carotene
Note 5. 1 mcg β-Carotene = 1.6 IU Vitamin A activity
Note 6. 1 mcg Cholecalciferol = 400 IU Vitamin D_3 activity
Note 7. 1 mg α-Tocopherol = 1.1 IU Vitamin E activity
Note 8. 1 MJ = 239.23 Calories

9.3 Restriction enzyme buffers

The composition of Life Technologies restriction enzyme buffers is summarised below. All buffers were supplied at 10x strength and diluted to a final strength of 1x in the reaction mix.

REACT 2 supplied for use with *Pst* I
50 mM Tris-HCl (pH 8.0), 10 mM $MgCl_2$, 50 mM NaCl

REACT 3 supplied for use with *Bam*H I and *Not* I
50 mM Tris-HCl (pH 8.0), 10 mM $MgCl_2$, 100 mM NaCl

9.4 *E.coli* medium composition

9.4.1 LB_{AMP} medium

Medium constituents	Weight (per litre)
Luria broth base	20 g
Sterile distilled water	to a final volume of 1 litre

The medium was autoclaved and allowed to cool before addition of ampicillin to a final concentration of 50 μg/ml.

9.4.2 LB_{AMP} agar

Medium constituents	Weight (per litre)
Luria broth base	20 g
Bacto agar	20 g
Sterile distilled water	to a final volume of 1 litre

The medium was autoclaved and allowed to cool before addition of ampicillin to a final concentration of 50 μg/ml. Aliquots of the medium (25 ml) were poured into 100 mm disposable petri dishes. The plates were stored at 4°C.

9.5 Fixing cryostat sections for *in-situ* hybridisation

Sections were thawed at room temperature (15 mins) in RNase free / autoclaved slide racks. All solutions were prepared in baked RNase free glassware. Ethanol was diluted to desired percentage using DEPC-treated sterile water. Slides were brought

through the following solutions (all at room temperature) in RNase free / autoclaved black boxes in the fume hood:

1. Paraformaldehyde (4% w/v) in DEPC treated PBS for 10 mins. Paraformaldehyde was freshly prepared each day (10 g in 250 ml of DEPC-treated PBS) and was dissolved by heating (50°C) and stirring in the fume hood (2-3 h until the solution was clear).
2. DEPC-treated PBS – 2 x 1 min (change buffer after each slide rack).
3. Acetic anhydride (0.25%, v/v), triethanolamine (0.1 M) and NaCl (0.9%, w/v) for 10 mins (change after each slide rack). Acetic anhydride is very unstable and was therefore added to the autoclaved triethanolamine buffer just 1 min before use.
4. Ethanol (70 %) for 1 min.
5. Ethanol (80 %) for 1 min.
6. Ethanol (95 %) for 1 min.
7. Ethanol (100 %) for 1 min.
8. Chloroform for 10 min.